Impairment of the type I interferon response in HIV-infected macrophages facilitates their infection and killing by the oncolytic virus, MG1

Teslin Stella Sandstrom

Department of Biochemistry, Microbiology and Immunology
Faculty of Medicine
University of Ottawa

Supervisor: Dr. Jonathan B. Angel

Approved by:
Dr. Rebecca Auer
Dr. Ashok Kumar
Dr. Marc-André Langlois

Thesis submitted to the Department of Biochemistry, Microbiology, and Immunology in partial fulfillment of the requirements for the degree of Doctor of Philosophy in Microbiology and Immunology

Declaration

I, Teslin Stella Sandstrom, confirm that the work presented in this thesis is my own. Where information has been derived from other sources, I confirm that this has been indicated in the thesis.

Date: May 27, 2019

Abstract

HIV remains an incurable viral infection and a significant global health concern. Despite the advent of antiretroviral therapy, there are 36.9 million recorded cases of HIV worldwide, with an additional 1.8 million new infections recorded in 2017 alone. An HIV cure is therefore one of several priorities within the field, and will require HIV "reservoir" cells—comprised of latently-HIV infected $CD4^+$ T cells and productively-infected, tissue resident macrophages—to be selectively killed *in vivo.*

HIV reservoir cells are rarely found within the peripheral circulation, residing instead within inaccessible tissue sanctuaries. Consequently, their characterization has been limited to *in vitro* laboratory models. To complicate matters further, a definitive cellular surface marker of HIV infected cells has yet to be identified. Impairment of the type I interferon (IFN1) response has been observed during HIV infection, however, making it a unique intracellular maker of HIV-infected cells. The recent development of oncolytic viruses (OV) designed to selectively kill IFN1-defective cancer cells also suggests that these IFN1 defects possess therapeutic value.

It was therefore hypothesized that the impairment of the IFN1 response in HIV-infected $CD4^+$ cells and macrophages could serve as a target for oncolytic virus-mediated killing. The induction of several antiviral IFN-stimulated proteins, including PKR and ISG15, was inhibited in HIV-infected monocyte-derived macrophages (MDM) following stimulation with IFNα or a synthetic RNA. Consequently, HIV-infected MDM were more susceptible to infection and killing by the oncolytic Maraba virus, MG1. Importantly, MG1-mediated killing required the

presence of replication-competent OV, and could not be potentiated by UV-inactivated MG1 or supernatants from MG1-infected cells. The ability of MG1 to target the HIV reservoir was further confirmed using alveolar macrophages collected from the lungs of cART-suppressed individuals living with HIV.

These findings indicate that IFN1 defects are a feature of HIV infected cells, which can be exploited for selective killing by OV. This project is therefore unique in that it demonstrates that HIV reservoir cells can be eradicated in a targeted manner by exploiting an intracellular marker of HIV infection. As MG1-based cancer therapies are currently being explored in Phase I/II clinical trials, there is potential for this approach to be adapted for use within the HIV cure field.

Dedication

This thesis is dedicated to my Grandparents, Donald Miller, Patricia Miller, and Naida Sandstrom, and in memory of my Grandfather, Ronald Sandstrom. Thank you for your love and support in all things.

Acknowledgements

I would like to begin by extending my sincerest gratitude to my supervisor, Dr. Jonathan Angel, for providing me with the necessary guidance to succeed, as well as the freedom to learn from my failures. Thank you for believing in me even when I lacked the confidence to do so myself. Similarly, I would like to acknowledge the members of my Thesis Advisory Committee; Dr. Rebecca Auer, Dr. Ashok Kumar, and Dr. Marc-André Langlois. Your insightful, supportive, and forthright advice has shaped me into a better scientist and person.

I would also like to wholeheartedly thank the past and present members of the Angel Lab. In particular, Dr. Sandra Côté, Dr. Nischal Ranganath, and Stephanie Burke Schinkel, who provided countless hours of valuable discussion and advice. You have been exemplary role models for scientific conduct and work ethic.

I am also indebted to my parents, Paul and Lorraine, for supporting me in my endeavours, and for teaching me the value of hard work and resilience; my siblings, Emma and Austin, for being there for me when I needed it most; and my friends, Rachel A., Philippe Harvey B., Adam B., Nick C., Alanna F., Brad G., Natalie H., Melanie J., Lindsay O., Kelsey R., Emily R., Steven Nicolas S., and Amy W., for reminding me to take life less seriously and to laugh at myself every once in a while.

Finally, I am grateful to the volunteers and patients who donated samples for the experiments contained within this thesis, as well as the nursing staff at the Ottawa General Hospital for their support in collecting these samples. The work within this thesis was supported by funding from the University of Ottawa, the Government of Ontario, and the Canadian Institutes for Health Research.

Table of Contents

List of Abbreviations

5’ ppp-dsRNA	5’ Triphosphate Double Stranded RNA
ADAR1	Adenosine Deaminase Acting on RNA 1
ADCC	Antibody-Dependent Cellular Cytotoxicity
AGM	African Green Monkey
AICD	Activation-Induced Cell Death
AIDS	Acquired Immunodeficiency Syndrome
AM	Alveolar Macrophage
APC	Allophycocyanin
APOBEC3	Apolipoprotein B mRNA Editing Enzyme, Catalytic Polypeptide-like 3
ART	Antiretroviral Therapy
AZT	3'-Azido-3'-deoxythymidine
BAF	BRG1- or HBRM-Associated Factors
BAL	Bronchoalveolar Lavage
BDCA-2	Blood Dendritic Cell Antigen 2
BET	Bromodomain and Extraterminal (proteins)
BIRC2	Baculoviral IAP Repeat Containing 2
BLT	Bone Marrow, Liver, and Thymus
BSA	Bovine Serum Albumin
BST-2	Bone Marrow Stromal Cell Antigen 2
CA	HIV Capsid Protein
cART	Combination Antiretroviral Therapy
CCL19	Chemokine (C-C Motif) Ligand 19

CCR5	CC-Chemokine Receptor Type 5
CD	Cluster of Differentiation
CDK9	Cyclin-Dependent Kinase 9
cDNA	Complementary DNA
cGAS	Cyclic Guanosine Monophosphate-Adenosine Monophosphate Synthase
CLR	C-type Lectin Receptor
CNS	Central Nervous System
CRISPR	Clustered Regularly Interspaced Short Palindromic Repeats
CXCR4	CXC-chemokine receptor type 4
DAMPs	Danger Associated Molecular Patterns
DC	Dendritic Cell
ddPCR	Digital Droplet PCR
DMEM	Dulbecco's Modified Eagle's medium
dNTP	Deoxynucleotide Triphosphate
dsRNA	Double-Stranded RNA
dUTP	Deoxyuridine Triphosphate
EDTA	Ethylenediaminetetraacetic Acid
EIF2α	Eukaryotic Initiation Factor 2 alpha
EIF4E	Eukaryotic Initiation Factor 4E
EIF4G1	Eukaryotic Initiation Factor 4G1
ELISA	Enzyme-Linked Immunosorbent Assay
Env	HIV Envelope Protein
ESCRT	Endosomal Sorting Complexes Required for Transport

FADD	Fas-Associated Protein with Death Domain
FasL	Fas Ligand
FBS	Fetal Bovine Serum
FLICA	Fluorochrome Inhibitor of Caspases
G	Rhabdoviridae Glycoprotein
GALT	Gut Associated Lymphoid Tissue
GFP	Green Fluorescent Protein
HAND	HIV-Associated Neurodegenerative Disorder
HBSS	Hank's Balanced Salt Solution
HDAC	Histone Deacetylase
HDACi	Histone Deacetylase Inhibitor
HEK Cells	Human Embryonic Kidney Cells
HIV	Human Immunodeficiency Virus
HLA	Human Leukocyte Antigen
HNSCC	Head and Neck Squamous Cell Carcinoma
HSA	Heat Stable Antigen
HSC	Hematopoietic Stem Cell
HSV	Herpes Simplex Virus
Hu-BLT	Humanized Bone Marrow-Liver-Thymus (mice)
IAPs	Inhibitors of Apoptosis
IDU	Injection Drug User
IFI16	IFN-γ-Inducible Protein 16
IFI44	Interferon-Induced Protein 44
IFI44L	Interferon-Induced Protein 44-like

IFN	Interferon
IFN1	Type I Interferon
IFNAR	IFNα/β receptor
IFNAR1	IFNα/β receptor subunit 1
IFNAR2	IFNα/β receptor subunit 2
IL	Interleukin
INT	HIV Integrase
IPS-1	Interferon-β Promoter Stimulator 1
IRAK	Interleukin-1 Receptor Associated Kinase
IRES	Internal Ribosome Entry Site
IRF	Interferon Regulatory Factor
IRFBS	Interferon Regulatory Factor Binding Site
ISG	IFN-stimulated Gene
ISG15	Interferon-stimulated Gene 15
ISGF3	Interferon-stimulated Gene Factor 3
ISRE	Interferon Response Element
JAK	Janus Kinase
LAG-3	Lymphocyte-Activation Gene 3
LDLR	Low Density Lipoprotein Receptor
LGP2	Laboratory of Genetics and Physiology 2
LMW-Poly(I:C)	Low Molecular Weight Polyinosinic-Polycytidylic Acid
LRA	Latency Reversal Agent
LTR	Long Terminal Repeat
M	Rhabdoviridae Matrix Protein

M-CSF	Macrophage Colony Stimulating Factor
MA	HIV Matrix Protein
MAiD	Medical Assistance in Death
MBS Buffer	PBS-5mM EDTA plus 1% BSA
MDA5	Melanoma Differentiation-Associated Gene 5
MDDC	Monocyte-Derived Dendritic Cell
MDM	Monocyte-Derived Macrophage
MG1	Recombinant Maraba Virus
MHC I	Major Histocompatibility Complex I
MOI	Multiplicity of Infection
MoM	Myeloid-Only Mice
Mϕ Media	RPMI-1640, supplemented with PenStrep and 10% heat-inactivated human AB serum
MSM	Men who have sex with men
MTT	3-(4,5-dimethylthiazol-2-yl)-2,5-diphenyltetrazolium bromide
MxB	Human Myxovirus-resistance Protein B
NFAT	Nuclear-Factor of Activated T Cells
NFkB	Nuclear Factor Kappa-light-chain-enhancer of Activated B Cells
NGS	Normal Goat Serum
NHP	Non-Human Primate
NK Cell	Natural Killer Cell
NLR	Nucleotide-binding Oligomerization Domain-like Receptor
NOD-SCID-IL2Rγ^{null}	NSG

NP	HIV Nucleoprotein
OAS1	2’5’ Oligoadenylate Synthetase 1
OV	Oncolytic Virus
PACT	Protein Kinase R Activator
PAMP	Pathogen Associated Molecular Pattern
PBMC	Peripheral Blood Mononuclear Cells
PBS	Phosphate Buffered Saline
PD-1	Programmed Cell Death Protein 1
pDC	Plasmacytoid Dendritic Cell
PE	Phycoerythrin
PE-Cy5	Phycoerythrin-Cyanin5
PE-Cy7	Phycoerythrin-Cyanin7
Pen/Strep	Penicillin, streptomycin
PFA	Paraformaldehyde
PKC	Protein Kinase C
PKR	Protein Kinase R
PLWH	Person(s) Living with HIV
PR	HIV Protease
PRR	Pattern Recognition Receptor
PVDF	Polyvinylidene Fluoride
qPCR	Quantitative PCR
R5-tropic	CCR5 Tropic
RIG-I	Retinoic Acid Inducible Gene I
RIPK1	Receptor-Interacting Serine/Threonine-Protein Kinase 1

RLR	RIG-I-like Receptor
RM	Rhesus Macaque
RP10 medium	RPMI-1640 medium supplemented with 10% FBS, PenStrep, and L-glutamine
RPMI-1640	Roswell Park Memorial Institute 1640 medium
RT	HIV Reverse Transcriptase
SAHA	Suberoylanilide Hydroxamic Acid
SAMHD1	Sterile Alpha Motif Domain and HD Domain-containing Protein 1
SDS	Sodium Dodecyl Sulfate
SFDA	Chinese State Food and Drug Administration
SHIV	SIV/HIV Chimeric Virus
SIV	Simian Immunodeficiency Virus
SM	Seminal Macrophage
Smac	Second Mitochondrial Activator of Caspase
SOCS	Suppressor of Cytokine Signalling
ss	Single Stranded
ssRNA	Single-Stranded RNA
STAT	Signal Transducer and Activator of Transcription
STING	Stimulator of Interferon Genes
SYK	Spleen Tyrosine Kinase
TALENs	Transcription Activator–like Effector Nucleases
TAR	Trans-Activation Response
TBK1	TANK-Binding Kinase
TCR	T Cell Receptor

TGF-β	Transforming Growth Factor Beta
TIGIT	T Cell Immunoreceptor With Ig And ITIM Domains
TLR	Toll-Like Receptor
ToM	T Cell-Only Mice
TRAF6	TNF Receptor Associated Factor 6
TRAIL	TNF-Related Apoptosis-Inducing Ligand
TRBP	Trans-Activation Response RNA Binding Protein
TREX1	Three-Prime Repair Exonuclease 1
TYK2	Tyrosine Kinase 2
UV	Ultra-Violet
V3	Variable Loop 3
VSe1	3,4-dichloro-5-phenyl-2,5-dihydrofuran-2-one
VSV	Vesicular Stomatitis Virus
VSVΔ51	Recombinant Vesicular Stomatitis Virus
X4-tropic	CXCR4 Tropic
XIAP	X-linked Inhibitor of Apoptosis
ZFN	Zinc Finger Nucleases
βTrCP	Beta Transducin Repeat-containing Protein

List of Figures and Illustrations

List of Tables

Chapter 1: Introduction

1.1 A brief history

In the time since the etiological agent of Acquired Immunodeficiency Syndrome (AIDS) was described, scientists, clinicians, and the general public have dedicated considerable effort to the development of a cure. That this effort would be sustained more than 35 years later was likely not a consideration when Barré-Sinoussi et al. and Gallo et al. independently reported and characterized a unique human T-lymphotrophic retrovirus isolated from AIDS patients in 1983 (1,2).

This story begins two years prior in the summer of 1981, when a report detailing the diagnosis of *Pneumocystis* pneumonia in five previously healthy men was published by the Centers for Disease Control (3,4). By December of that year, multiple reports had surfaced describing the development of similar opportunistic infections, as well as Kaposi's Sarcoma, in men who have sex with men (MSM) and injection drug users (IDU) (5-8). In response, the Center for Disease Control released an update detailing the alarming rise in the clinical diagnosis of AIDS among these aforementioned groups, as well as individuals of Haitian origin, and individuals diagnosed with hemophilia A (9).

Although the name "Human Immunodeficiency Virus" (HIV) was not coined until 1986 (10), the confirmation of a viral etiology for AIDS (11,12) sparked a thorough investigation into the potential routes of transmission (13-17), the identification of viral receptor(s) on target cells (18), and potential therapeutic strategies targeting the viral reverse transcriptase (19). Subsequently, implementation of the thymine analogue, 3'-Azido-3'-deoxythymidine (AZT), as a

potent inhibitor of HIV reverse transcriptase (20) led to its approval as the first antiretroviral drug in 1987 (21). The development of numerous antiretrovirals quickly followed, including inhibitors of viral fusion, reverse transcription, integration, and protease activity. Combination antiretroviral therapy (cART) has since become integral in controlling viral load and reducing AIDS-related mortality in people living with HIV (PLWHIV) (22,23). Strict adherence to cART is necessary, however, as treatment interruption has been associated with a rebound of plasma viremia and subsequent immune dysfunction (24).

1.8 million new HIV infections were recorded globally in 2017—the majority of which were caused by HIV-1, subgroup M (which encompasses 11 known subtypes). Although global rates of HIV-1/2 infection have continued to drop steadily since their peak in 1996, this number remains a far cry from the goal of <500,000 infections in 2020 set forth by the Joint United Nations Programme on HIV/AIDS (25). With the appropriate allocation of resources and personnel, and the implementation of culturally-sensitive education programs, a significant reduction in new infections is not out of the question. Even more reassuringly, it is estimated that ~21.7 million out of the total 36.9 million PLWHIV worldwide are receiving treatment (25); a number that continues to increase annually.

Still, the search for an HIV cure continues. Many PLWHIV experience barriers to accessing cART, such as socioeconomic status and the stigmatization of HIV infection (26,27), which has influenced current perceptions of HIV cure research. In several recent surveys of PLWHIV in the United States of America, Australia, and China, for example, HIV cure research was viewed positively, with many participants citing preference for a “sterilizing” approach (in which all infectious virus is removed

from the body), over the likely more attainable “functional” approach (in which a person’s viral load is maintained below detectable levels without cART) (28-30). The need for novel therapeutic strategies intended to eradicate the HIV reservoir is therefore clear, from both the social and clinical perspective.

1.2 HIV infection and pathogenesis

1.2.1 Viral characteristics and lifecycle

HIV is a Baltimore Class VI virus of the family *Retroviridae*, genus *Lentivirus*, which can be further genetically classified into HIV types 1 and 2. For the purposes of this thesis, HIV-1 will be considered exclusively and referenced as “HIV.” The viral envelope of HIV contains a conical nucleocapsid, which harbours two copies of a 9.2kbp, single-stranded (ss), positive-sense (+) RNA genome encoding 16 viral proteins. Each serves a unique role in viral replication, evasion of the cellular antiviral machinery, and subsequent release of viral progeny. These include the capsid (CA), matrix (MA), nucleoprotein (NP), p6, protease (PR), reverse transcriptase (RT), RNaseH, integrase (INT), and gp120/gp41 proteins, as well as six regulatory proteins: Tat, Rev, Nef, Vif, Vpr, and Vpu (31).

Transmission of HIV occurs when infectious viral particles enter the susceptible host and infect CD4-expressing target cells, either via direct entry into the peripheral circulation or across a mucosal membrane (Figure 1). During sexual transmission, for example, HIV may enter the mucosal tissue via microtears within the stratified squamous epithelium of the reproductive tract. Free viral particles are endocytosed by epidermal Langerhans cells, which facilitate the cell-to-cell transfer

of HIV to resident $CD4^+$ T cells, macrophages, and blood-derived dendritic cells (DC) (32,33).

Vaginal Langerhans cells may also contribute to viral persistence within these tissues by supporting productive HIV infection (34), while blood-derived DC can subsequently disseminate surface-bound HIV from the site of infection to lymphoid tissues (35,36). Transcytosis of viral particles across the intestinal epithelium can also aid in the dissemination of HIV to tissue-resident macrophages and $CD4^+$ T cells (37-39). Productive infection of target cells is initiated when the HIV envelope protein, gp120, interacts with the cellular CD4 glycoprotein. This is followed by a series of conformational changes that expose the co-receptor binding site of gp120 as well as the transmembrane gp41. The variable loop 3 (V3) within the co-receptor binding site of gp120 dictates viral tropism, allowing gp120 to interact with the C-C chemokine receptor type 5 (CCR5), C-X-C chemokine receptor type 4 (CXCR4), or both (40). This interaction subsequently facilitates gp41-mediated fusion of the cellular and viral membranes, which releases of the viral nucleocapsid into the cytosol (41).

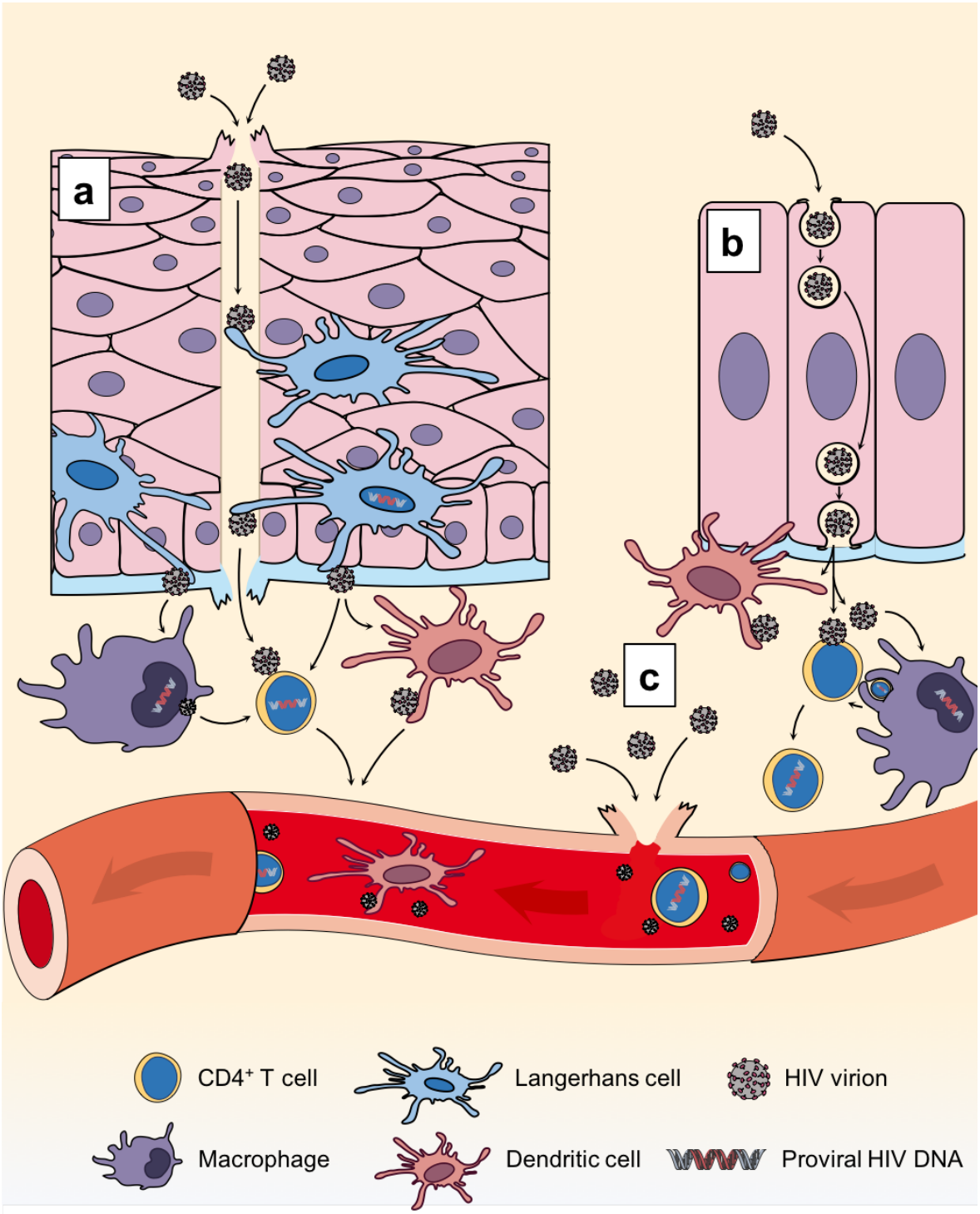
a
b
c
CD4+ T cell
Langerhans cell
HIV virion
Macrophage
Dendritic cell
Proviral HIV DNA

Figure 1: Mechanisms of HIV transmission. a. Microtears facilitate sexual transmission of free and cell-associated (not depicted) HIV through the mucosal epithelium. Here, epidermal Langerhans cells play a key role in facilitating HIV infection of susceptible intra-epithelial $CD4^+$ T cells, macrophages, and DC via cell-to-cell transmission of endocytosed viral particles, or the release of infectious viral progeny following productive infection. Infected cells, or DC carrying surface-bound HIV, can then home to nearby lymphoid tissues by way of the circulatory system, spreading infectious HIV throughout the body. **b.** Similar events follow HIV transmission at the intestinal epithelium, which is facilitated by the transcytosis of viral particles across columnar epithelial cells and the subsequent infection of tissue-resident macrophages and $CD4^+$ T cells. Importantly, tissue resident macrophages (of both the reproductive and gastrointestinal tracts) maintain the viral reservoir within these tissues by phagocytosing HIV-infected $CD4^+$ T cells, harbouring productive HIV infection, and facilitating cell-to-cell transmission of infectious viral progeny to surrounding immune cells. **c.** Finally, HIV transmission may occur via direct inoculation into the peripheral circulation (via a contaminated needle, for example), where $CD4^+$ T cells are the primary target of HIV infection.

The steps that follow in the production of the HIV cDNA are highly regulated and begin with the controlled degradation of the viral nucleocapsid, followed by the initiation of reverse transcription and synthesis of viral cDNA in a step-wise fashion (42). The final double stranded DNA molecule is comprised of a protein-encoding region, flanked by two long-terminal repeats (LTR) at each of the 5' and 3' ends. Following import at the nuclear envelope, these LTR regions are utilized by HIV integrase as it catalyzes cDNA integration within the cellular genome via sequential exonuclease, endonuclease, and ligation processes (43).

The integrated HIV provirus is highly stable and acts as a blueprint for multi-spliced, single-spliced, and full length ss(+)RNA. The production of single and unspliced RNA molecules is dependent on HIV Tat and Rev expression, which initiate viral transcription from the proviral trans-activation response (TAR) element (reviewed in (44)) and mediate the export of viral RNA to the cytosol (reviewed in (45)), respectfully. To complete its lifecycle, HIV structural proteins and two copies of the ss(+)RNA genome assemble into progeny virions at specific micro-domains within the cellular lipid bilayer. Protein translocation and virion assembly are mediated predominantly by cellular proteins, while the association of the viral RNA (in dimer form) with the Gag polypeptide is necessary for its eventual incorporation (46). Once assembled, HIV virions rely on the endosomal sorting complexes required for transport (ESCRT) machinery of the host cell to bud from the cellular membrane and be released into the cellular milieu (47). As a final step in virion maturation, HIV PR mediates the cleavage of Gag and Gag-Pro-Pol polypeptides, yielding an infectious viral particle that is capable of secondary rounds of viral infection (46,48).

1.2.2 Clinical characteristics of HIV infection

HIV infection begins with a short eclipse period of approximately 11 days, during which viral RNA remains undetectable (49). This is followed by Fiebig stages I-V of acute HIV infection; initiated when HIV RNA becomes detectable within the peripheral blood and subsequently defined based on the presence (and amount) of viral proteins and HIV-specific IgM (50). Plasma viral load typically peaks at 10^6-10^7 copies of RNA/ml of blood during stage II, 15-20 days post-infection (50,51). This is accompanied by seroconversion at around 3 weeks post infection within Fiebig stage III, along with the typical development of clinical symptoms such as fever, malaise, fatigue, and swollen lymph nodes, and a substantial drop in $CD4^+$ T cell counts (50,52)

The immune system subsequently controls viral replication, leading to a reduction in viral load and the rebound of $CD4^+$ T cell counts to near-normal levels. So begins the chronic phase of HIV infection, which may last anywhere from 3 to 10 years (although substantially shorter or longer durations have been recorded) (53,54). While this period is typically asymptomatic, immune activation and inflammation persist due to ongoing viral replication and can contribute to damage to the vasculature and increased risk of cardiac arrest (55-57). Still, the immune system is unable to control viral replication indefinitely. This third and final stage of HIV infection—clinically diagnosed as AIDS—is characterized by a $CD4^+$ T cell count of <200 cells/mm^3, the development of opportunistic infections and/or cancers, and if left untreated, death (58).

1.2.3 Immune dysregulation by HIV

Immune dysregulation is a well-known consequence of HIV infection. At the macroscopic level, this manifests as structural changes within lymphoid tissues. The death of $CD4^+$ T cells within the gut-associated lymphoid tissue (GALT), for example, triggers a positive feedback loop of tissue inflammation exacerbated by damage to the intestinal mucosa and exposure of immune cells to pro-inflammatory bacterial signatures (59). Drastic alterations to lymph node architecture (60,61), including fibrosis (62,63) and syncytia formation (64), have also been observed *in vivo* and again may contribute to inappropriate inflammatory signalling and the disruption of T cell homeostasis (65).

On the microscopic level, killing and/or functional inhibition of key immune cells further contributes to immune dysregulation. The main cellular target of HIV is the $CD4^+$ T cell, which both orchestrates and regulates adaptive immune signalling in response to foreign antigen. CD4-expressing myeloid cells, such as tissue resident macrophages, are also infected and consequently are unable to fulfill their role in bridging the innate and adaptive arms of the immune system. The mechanisms by which HIV mediates the massive loss of $CD4^+$ T cell populations and subsequent immunopathogenesis are further described below.

First and foremost is the killing of $CD4^+$ T cells during productive HIV infection. In this context, target cells rapidly succumb to HIV-mediated cytopathogenicity within 1-2 days post-infection (66), due to ionic imbalances, increased cytosolic volume, and ultimately lysis caused by viral fusion and budding events at the cellular membrane (67). Infected cells also undergo cytolytic killing (68,69), natural killer (NK) cell-mediated antibody-dependent cellular cytotoxicity

(ADCC) (70,71), and, during the later stages of chronic infection, the induction of apoptosis following gp41-mediated syncytia formation (72). Finally, unintegrated viral cDNA or RNA products can trigger programmed cell death pathways via the activation of intracellular pattern recognition receptors (PRR). As shown by Dotish et al., the induction of caspase-1-dependent pyroptosis following abortive HIV infection was the predominant mechanism of cell death observed using an *ex vivo* human lymphoid aggregate culture system (73). Still, productively HIV-infected $CD4^+$ T cells are a minority within the total $CD4^+$ T cell pool. Additional investigation has therefore focused on understanding and characterizing the massive bystander death of uninfected cells that occurs *in vivo*.

As reviewed by Alimonte et al., bystander killing during HIV infection is likely to occur via activation-induced cell death (AIDC) in combination with the release of apoptosis-inducing viral proteins from productively infected cells (74). In otherwise healthy individuals, AIDC is an important process that mediates immune tolerance, homeostasis, and clonal contraction of peripheral T cells. Repeated engagement of the T cell receptor (TCR) upregulates the nuclear-factor of activated T cells (NFAT)-dependent expression of Fas(CD95) and Fas-ligand (FasL) (75-78). The interaction of Fas(CD95) and FasL on neighbouring cells promotes the recruitment of FADD (Fas-associated protein with death domain), c-FLIP, and pro-caspase 8 to the intracellular domain of Fas, the proteolytic cleavage of caspase 8, and ultimately apoptosis of the Fas-expressing cell (79-81).

$CD4^+$ T cells isolated from the peripheral blood of PLWHIV have been found to undergo AICD following *in vitro* stimulation (82,83). *In vivo*, the cross-linking of CD4 by gp120, in the absence of appropriate TCR engagement, is believed to

induce AIDC within uninfected $CD4^+$ T cell populations (84-87). Finally, the endocytosis of HIV Tat may also stimulate AICD via upregulation of pro-apoptotic proteins FasL, caspase 8, and Bax, and downregulation of the anti-apoptotic protein Bcl-2 (88-91). Aside from this, gp120-mediated ADCC (92) as well as Nef- or Vpr-induced apoptosis of uninfected $CD4^+$ T cells have been observed *in vitro* (93-95).

Unlike $CD4^+$ T cells, HIV-infected macrophages do not readily succumb to virus-mediated cytopathogenicty. The induction of the anti-apoptotic protein Bcl-xL by HIV Nef (96), Bcl-1 and Mcl-1 by HIV Env (97), and Bcl-2 by HIV Tat (98) have all been demonstrated *in vitro* to subvert the induction of apoptosis in myeloid cells. Nonetheless, HIV-infected macrophages display functional impairments that limit their ability to orchestrate innate immune signalling within various tissues. HIV-infected alveolar macrophages, for example, display limited phagocytic capacity and ability to process internalized pathogens (99-101). A similar observation within gut-associated macrophages has recently been shown to contribute to disease progression within a non-human primate (NHP) model of SIV infection (102). The ability of tissue-resident macrophages to harbour persistent HIV infection, which subsequently impairs the innate immune function of these cells, makes HIV-infected macrophages a particularly relevant cellular reservoir from an HIV cure standpoint.

1.3 Mechanisms of HIV persistence

Replication competent HIV persists within cellular and tissue reservoirs, as evidenced by the isolation of resting $CD4^+$ T cells from the peripheral blood of cART-treated PLWHIV and the subsequent reactivation of these cells to produce infectious

viral progeny *ex vivo* (103,104). The establishment of the viral reservoir itself is believed to be a highly dynamic process, occurring in the early stages of acute HIV infection (104). Recently, Whitney et al. demonstrated the true rapidity of this process after reporting that rhesus macaques treated as early as 3 days post-SIV infection experienced viral rebound following cART-cessation (105). This observation has also been confirmed in humans. As shown by Henrich et al., treatment at approximately 10 days post-infection resulted in prolonged, cART-free remission that eventually cumulated in viral rebound (106). Tissue-resident macrophages may also contribute to ongoing viral replication within the lung, lymph nodes, central nervous system, and reproductive tract (107,108). This is aided by the immune privileged nature of certain tissues such as the testes (109) or lymphoid follicles (110), which facilitate ongoing viral replication without immune clearance.

From an HIV cure standpoint, viral eradication will require all cells containing replication-competent provirus to be killed in a highly targeted manner. Not only this, but reservoir-targeting therapies will be required to penetrate relevant tissues at therapeutically useful concentrations. The identification and characterization of the HIV reservoir, which is primarily comprised of latently-HIV infected $CD4^+$ T cells and productively-infected, tissue resident macrophages, is therefore of particular relevance to the HIV cure field.

1.3.1 HIV Latency within $CD4^+$ T cells

HIV latency is predominantly observed in resting memory $CD4^+$ T cells, and is defined as the presence of a stably integrated HIV provirus without productive viral replication (103,111-113). Latent HIV infection is reversible, and the reactivation of

cells is sufficient to produce infectious viral progeny and viral rebound following cART cessation (111). In the absence of *in vivo* stimulation, however, this cell population is incredibly stable, possessing an estimated half-life of approximately 44 months (114). Attempts to quantify the latent HIV reservoir have revealed that, during cART-treated infection, latently HIV-infected $CD4^+$ T cells are quite rare. Assuming that latently infected cells possess a single copy of integrated HIV provirus (115), recent estimates suggest that the frequency of latent infection is fewer than one copy per million $CD4^+$ T cells (116-118). Presently, the inability to enrich latently infected cells from *ex vivo* samples, due to a lack of phenotypic markers, as well as overall rarity, has hindered our understanding of HIV latency as a whole (119,120). A number of *in vitro* models utilizing primary cells have consequently been established to better understand the cellular and viral characteristics of the latent HIV reservoir (121-124).

The cellular and viral mechanisms involved in latency establishment have been the subject of intense study, but are not yet well-understood. Direct infection of resting $CD4^+$ T cells has been suggested, but remains a highly inefficient process due to the absence of cellular factors and nucleotides required for reverse transcription and nuclear import of viral cDNA (125,126). Alternatively, HIV latency may be established in productively-infected, activated $CD4^+$ T cells, which then revert to a resting state following proviral integration (112,121). In either case, the cellular and viral processes involved in maintaining the HIV provirus in a latent state are similarly complex and several mechanisms have been proposed. These include the limited expression of cellular factors involved in the initiation of viral transcription from the LTR, including NFκB, CDK9, and cyclin T1 (127,128), as well as epigenetic

modifications such as histone deacetylation and nucleosome methylation (127,129). Transcriptional interference due to proximal host gene promoters or convergent transcription has also been observed (130-132).

1.3.2 The establishment and maintenance of HIV infection within macrophages

In studying the kinetics of viral decay following the initiation of cART, Perelson et al. observed a multi-phasic decay curve that suggested the existence of not one, but several independent HIV reservoirs (22,111). The first phase of decay—represented as an initial, rapid drop in peripheral blood viremia—could be explained by the clearance of productively infected $CD4^+$ T lymphocytes, while the infection of long-lived, myeloid lineage cells (macrophages in particular) was found to be responsible for the second (22). Further extrapolation of this data allowed the authors of this study to propose that tissue-resident, HIV-infected macrophages possess a half-life of approximately 2-4 weeks (22).

Igarashi et al. have since investigated the long-lived status of the macrophage HIV reservoir using rhesus macaques infected with a simian immunodeficiency virus/HIV type 1 (SHIV) chimeric virus SHIV(DH12R) (107). In this model, the half-life of macrophages within the spleen, lymph nodes, and gastrointestinal tract were found to contribute to HIV RNA production for an additional 2-5 months following $CD4^+$ T cell depletion. The rate of turnover of productively HIV infected macrophages remains up for debate, however, as two recent studies have shown the half-life of the macrophage HIV reservoir to be closer to that of productively HIV-infected $CD4^+$ T cells. In $CD4^+$ T cell-depleted NHP (133) and humanized myeloid-only mice (MoM) (108), the half-life of productively infected

macrophages within relevant lymphoid tissues was calculated to be within the range of 1-2 days. It is important to note that these recent studies employed animal models which have either been depleted of $CD4^+$ T cells prior to infection (133), or biologically do not support human T cell development (108). The complete absence of $CD4^+$ T cells may therefore contribute to the observed differences in reservoir half-life. Regardless, HIV infected macrophages possess unique cellular characteristics that contribute to their role in HIV persistence *in vivo*.

Unlike $CD4^+$ T cells, latent HIV infection is not believed to be the primary mechanism by which tissue-resident macrophages act as an HIV reservoir. Proviral integration following HIV infection of macrophages is localized to transcriptionally-active regions of the genome (134,135). Moreover, the use of a green fluorescent protein (GFP) expressing virus to establish latent HIV infection *in vitro* showed that fewer than 1% macrophages carrying non-replicating HIV provirus could be reactivated (136). HIV-infected macrophages are therefore more likely to support non-latent infection, established following the differentiation of HIV-infected monocytes to macrophages following extravasation (137), phagocytosis of HIV-infected CD4+ T cells (138,139), or direct infection within mucosal tissues (140).

One of the more notable features of the macrophage reservoir is the ability of these cells to support productive HIV infection, while resisting virus-mediated cytopathogenicity. Swingler et al., have shown that the induction of macrophage colony stimulating factor (M-CSF) by HIV Env protects infected macrophages from TRAIL-mediated apoptosis (97). Additionally, mature monocyte-derived macrophages (MDM) have been found to resist the induction of apoptosis by HIV Vpr by maintaining the expression of anti-apoptotic proteins Bcl-xL and Mcl-1 (141).

The cytolytic eradication of HIV-infected macrophages by $CD8^+$ T cells has also been found to be less efficient than that of infected $CD4^+$ T cells (142). While this study highlighted the ability of macrophages to resist cytolytic killing in a virus-independent manner, the downregulation of MHC I by HIV Nef has been observed and may further contribute the evasion of the cytotoxic T cell response by both HIV-infected macrophages and $CD4^+$ T cells (143,144).

Furthermore, macrophages can house infectious viral particles within cytoplasmic vesicles and facilitate the cell-to-cell transmission of HIV (145,146). This is particularly prevalent within tissues like the genital mucosa and GALT, in which immune cells capable of supporting HIV infection are maintained within close contact. Here, HIV infected macrophages recruit susceptible $CD4^+$ T cells by releasing chemotactic soluble factors (147). Subsequent TCR/MHC II engagement maintains close cellular contact, during which infectious viral particles are transferred via virological synapse from one cell to another (148,149). Intercellular HIV transmission is therefore a mechanism of infection that allows the virus to escape immune sensing and neutralization, as well as facilitate viral spread during cART-treated infection (150-152). It is therefore clear that tissue-resident macrophages form a distinct cellular reservoir of HIV, which can facilitate viral persistence during well-treated HIV infection.

1.4 HIV cure strategies: Past and present

Presently, several strategies have been proposed to either control or completely eradicate the HIV reservoir. These are summarized in brief below, as well as in Figure 2.

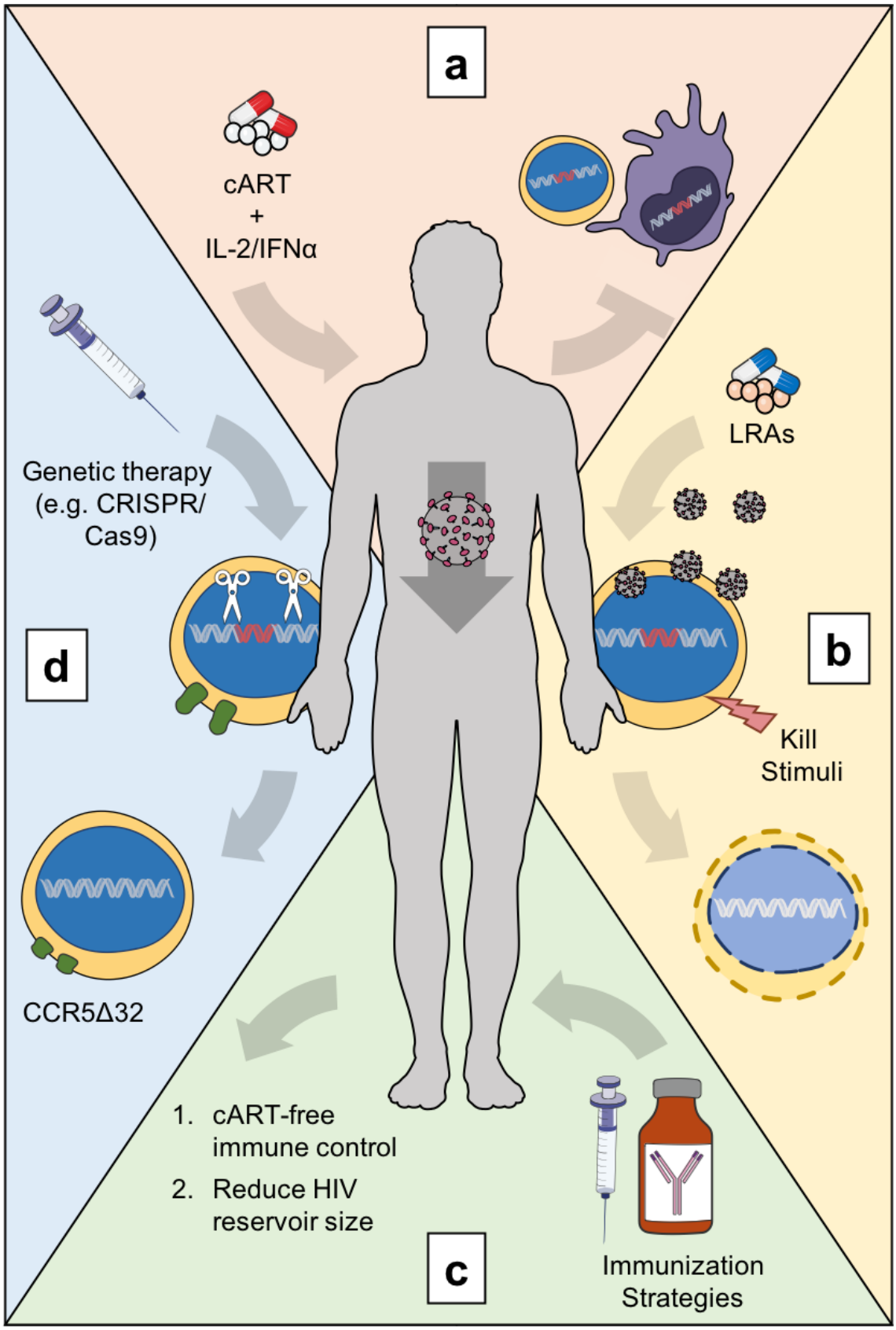
a
cART
+
IL-2/IFNα
LRAs
b
Kill
Stimuli
Genetic therapy
(e.g. CRISPR/
Cas9)
d
CCR5Δ32
1. cART-free
immune control
2. Reduce HIV
reservoir size
c
Immunization
Strategies

Figure 2: Strategies used to control or eradicate the HIV reservoir. a. The combination of cART and IL-2 or IFNα was previously proposed as a strategy by which to retain immune control over viral replication during structured treatment interruption. This strategy was intended to control, rather than eradicate the HIV reservoir. Unfortunately, the existence of infectious HIV within immune privileged tissues has rendered this strategy ineffective. **b.** Latency reversal is a component of the "Shock and Kill" strategy of HIV reservoir eradication. Several LRAs have been tested in the clinical setting, including HDACi (e.g. SAHA), PKC agonists (e.g. Bryostatin-1), BAF inhibitors (e.g. Pyrimethamine), and BET inhibitors (e.g. JQ1). Although latency reversal has been readily observed, this strategy currently lacks a reliable "kill" stimuli that can eradicate HIV-infected cells following reactivation. **c.** Immunotherapy, which includes therapeutic vaccination (intended to enhance T cell responses against conserved viral epitopes) and passive immunization with broadly neutralizing antibodies is largely intended to achieve cART-free immune control over HIV infection. It is also hoped that this strategy will reduce the size of the HIV reservoir by preventing the ongoing infection of HIV reservoir cells within lymphoid and non-lymphoid tissues, as well as promoting the immune-mediated killing of these cells. Although cART-free viremic control has been observed in individuals receiving either broadly neutralizing antibodies or therapeutic vaccination, no change in HIV reservoir size was recorded. The combination of HIV immunotherapy with additional strategies that specifically target HIV reservoir cells may therefore be required. **d.** Gene therapy as an HIV cure strategy has been largely influenced by the Berlin Patient. Presently, genetic editing (rather than stem cell transplant) to achieve an HIV-resistant, CCR5Δ32 homozygous phenotype is being investigated. The use of novel gene editing technologies like CRISPR/Cas9 is also being considered as a means by which to permanently silence proviral HIV DNA, thereby achieving a functional HIV cure.

1.4.1 Antiretroviral therapy

Used alone, cART is (in most instances) sufficient to maintain the viral load of a PLWHIV within the undetectable range. Nonetheless, mathematical modeling has revealed that a lifetime of cART would be required to substantially reduce the size of the latent HIV reservoir, let alone eradicate it (153,154).

The possibility of augmenting cART with immune stimulation was therefore proposed as a means by which to achieve full immune control of HIV infection without antiretroviral therapy. Interleukin 2 (IL-2) (155) and pegylated IFNα2b (156) have both been tested in this context, albeit with the disappointing recurrence of detectable virus during structured treatment interruption. The presence of HIV reservoirs that reside in immune privileged sites and thereby evade immune surveillance has been proposed as an explanation for these findings, as well as those of others who have attempted structured treatment interruption without additional intervention (157,158).

1.4.2 Latency Reversal

The “Shock and Kill” approach to HIV reservoir eradication has been a long-standing goal of the HIV cure field. Cells are first stimulated to reactivate latent provirus (“shock”) using a latency reversal agent (LRA). Subsequently, productively infected cells are eradicated either by virus-induced apoptosis or immune-mediated killing. Initial attempts utilized anti-CD3 monoclonal antibodies in combination with IL-2 to induce non-specific T cell activation and HIV RNA production, but were hindered by toxicity (159,160). Non-T cell activating strategies were therefore

sought, leading to the identification of several small-molecule compounds that could achieve latency reversal (161-163). Among these was the anticonvulsant and histone deacetylase inhibitor (HDACi), valproic acid, which stimulated low-level production of HIV RNA *in vivo*, but did not appreciably reduce the size of the latent reservoir *in vivo* (164,165).

This led to the investigation of the Class I HDACi, suberoylanilide hydroxamic acid (SAHA; Vorinostat) as an LRA. As demonstrated by Archin et al., SAHA potently induced latency reversal *in vitro* and *ex vivo* by facilitating chromatin acetylation and preventing the recruitment of HDAC1 to the HIV LTR region (166). The capacity of SAHA to reactivate latent HIV within resting $CD4^+$ T cells, as well as its overall safety profile, was further confirmed *in vivo* (167). Additional attempts to use SAHA *in vivo* did not demonstrate sufficient latency reversal (168,169), however, and additional *ex vivo* investigation revealed that SAHA was only capable of reactivating a small fraction of provirus-containing $CD4^+$ T cells (170). Furthermore, SAHA treatment was not associated with an appreciable decrease in latent reservoir size (171).

Other LRAs are presently under investigation. Like SAHA, these have been found to induce latency reversal *in vivo* without an appreciable decrease in HIV reservoir size. These include other HDACi, such as Romidepsin (172-174) and Panibinostat (175-177), the aldehyde dehydrogenase inhibitor Disulfiram (178), protein kinase C (PKC) agonists (e.g. Bryostatin-1) (179,180), small molecule inhibitors of the BAF chromatin remodeling complex (e.g. Pyrimethamine) (181), and inhibitors of bromodomain and extraterminal (BET) proteins (e.g. JQ1 or OTX015) (182,183). Other non-HDACi LRAs, like the retinoic acid derivative acitretin, have

been studied *in vitro* with varying success. Although previously shown to reactivate latent provirus and subsequently induce the apoptotic killing of HIV infected $CD4^+$ T cells (184), the efficacy of acitretin as an LRA has since been refuted (185). LRAs may therefore be a useful future component of HIV cure strategies, but will require additional immune-activating or cytotoxic therapies to mediate the selective killing of reactivated HIV reservoir cells. It is also unknown whether these strategies will efficiently target the non-latent reservoir, such as that established in tissue-resident macrophages.

1.4.3 Immunotherapy

The intended outcome of HIV immunotherapy is to achieve immune control over viral replication, as well as reduce the overall size of the HIV reservoir (reviewed in (186,187)). Passive immunization with broadly neutralizing antibodies (e.g. VRC01 or 3BNC117) has been found to significantly reduce plasma viral load in PLWHIV (188,189). These antibodies, which specifically block the CD4 binding site of gp120, can also reduce the cell-to-cell transmission of HIV (190,191). The combination of passive immunization with latency reversal strategies may therefore be a useful approach to prevent the re-seeding of the HIV reservoir.

Several therapeutic HIV vaccines have also been investigated, with immunization against HIV Tat showing particular promise. In two Phase II clinical trials, HIV Tat immunization was sufficient to restore immune cell subsets (in particular $CD4^+$ and $CD8^+$ T cells, as well as NK cells), control HIV viremia, and reduce proviral HIV DNA in peripheral $CD4^+$ T cells (192-194). mRNA-based therapeutic vaccines have also been investigated as a strategy to induce DC-

mediated T cell responses against conserved regions of HIV Gag, Pol, Vif and Nef (195,196). In a recent Phase I clinical trial, the administration of a similar mRNA-based therapeutic vaccine induced T cell responses against conserved regions within HIV Gag, Pol, RT, INT, Vif, and Nef, but had no effect on HIV reservoir size (197). The combination of a therapeutic HIV vaccine with additional HIV reservoir targeting strategies may be a necessary consideration to achieve long-term control of HIV viral load, while reducing the size of the viral reservoir itself.

1.4.4 Gene Therapy

Gene therapy as an HIV cure strategy has gained popularity in recent years, primarily due to a ground-breaking study published in 2009 by Hütter et al. In this study the authors describe an HIV-positive man (referred to as the “Berlin Patient”) who, after undergoing myeloablative chemotherapy, total body irradiation, and two allogenic bone marrow transplants from a homozygous *CCR5Δ32*-donor for the treatment of acute myeloid leukaemia, remained in HIV remission in the absence of cART (198-200). This has inspired several additional attempts to clear the HIV reservoir via allogenic bone marrow transplant. Several of these have resulted in prolonged HIV remission without cART, although viral rebound ultimately did occur (201,202). Concerns regarding patient safety and the development of graft-versus-host disease following transplant remain an additional consideration (203).

With the advancement of genetic editing techniques, several alternatives to allogenic stem-cell transplantation have been proposed. Early work by Sanhadji et al. found that the engineering of cells to express a Tat-inducible IFNβ prevented

their infection by HIV *in vitro*, as well as within an *in vivo* murine model (204). Since then, genetic editing of the *ccr5* locus has been attempted using Zinc Finger Nucleases (ZFN), Transcription Activator–like effector nucleases (TALENs), or Clustered Regularly Interspaced Short Palindromic Repeats (CRISPR)/Cas9 (reviewed in (205)). CRISPR/Cas9 technology has also been used to prevent the expression of HIV Tat and Rev *in vitro* (206), as well as excise large sections of viral DNA yielding a replication incompetent provirus (207). While this latter study represents a significant step forward for gene editing strategies within the HIV cure field, CRISPR/Cas9 technology was not able to completely eradicate replication-competent virus from the tissues of mice engrafted with PBMC from HIV-positive individuals (207). The combination of gene editing with current reservoir targeting strategies will therefore be required if such an approach is to be used as a viable HIV cure strategy.

1.5 Alternative strategies to eradicate the HIV reservoir: Exploiting type I interferon response defects within HIV infected cells

Plasmacytoid dendritic cells (pDC) are the primary producers of type I IFN (IFN1) during viral infection (208,209), and are capable of producing 100-1000 times more IFNα/β than other immune cells following stimulation (210). This remains true in the context of HIV, as increasing levels of IFNα/β (52,211-213) and antiviral IFN-stimulated genes (ISG) (214) have both been observed in PLWHIV. Despite this, the IFN1 response is ineffective in blocking HIV replication and spread *in vivo*. Extensive *in vitro* characterization has revealed that HIV is capable of blocking the IFN1

response at several levels, including the sensing of viral genomic material, the transcriptional upregulation of ISG expression, and the antiviral activity of several ISG themselves. These studies have relied heavily on cell line models of HIV infection. Still, similar IFN1 signalling defects have been observed in primary cell models of productive HIV infection, including peripheral blood mononuclear cells (PBMC), $CD4^+$ T cells, and MDM (Figure 3). The multi-level impairment of IFN1 signalling is therefore a defining feature of HIV infection and can be used to differentiate HIV infected cells at the functional level from their uninfected counterparts. Conversely, the characterization of IFN1 signalling defects in latently HIV-infected primary CD4+ T cells has been precluded by the inability to identify these cells *ex vivo*, as well as within in vitro models of latency. Thus, little is known regarding the status of the IFN1 response within these cells, aside from what has been demonstrated using cell line models of latency (215)

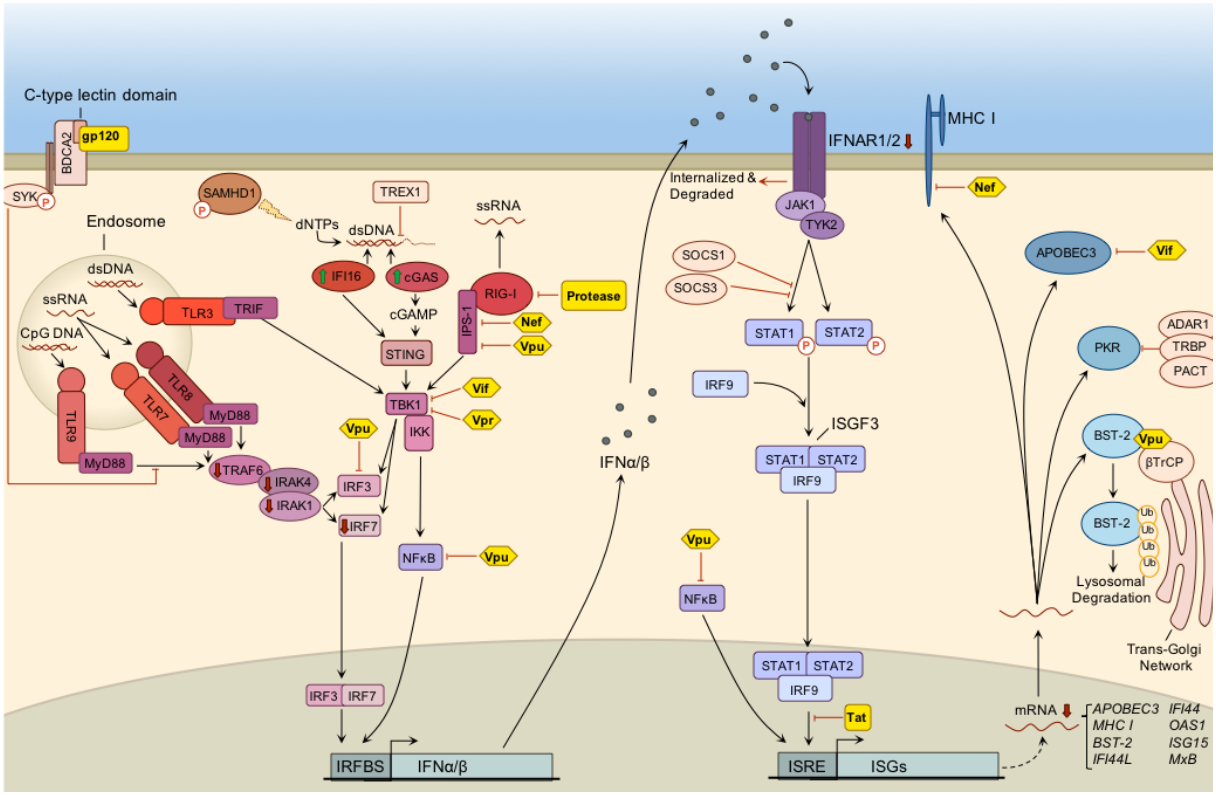
C-type lectin domain
gp120
BDCA2
SYK
Endosome
dsDNA
ssRNA
CpG DNA
TLR3
TRIF
TLR9
TLR8
TLR7
MyD88
MyD88
MyD88
TRAF6
IRAK4
IRAK1
SAMHD1
dNTPs
TREX1
dsDNA
IFI16
cGAS
cGAMP
STING
ssRNA
RIG-I
Protease
IPS-1
Nef
Vpu
TBK1
Vif
Vpr
IKK
Vpu
IRF3
IRF7
NFκB
Vpu
IRF3
IRF7
IRFBS
IFNα/β
IFNα/β
Internalized &
Degraded
IFNAR1/2
JAK1
TYK2
SOCS1
SOCS3
STAT1
STAT2
IRF9
ISGF3
STAT1
STAT2
IRF9
Vpu
NFκB
STAT1
STAT2
IRF9
Tat
ISRE
ISGs
MHC I
Nef
APOBEC3
Vif
PKR
ADAR1
TRBP
PACT
BST-2
Vpu
βTrCP
BST-2
Ub
Ub
Ub
Ub
Lysosomal
Degradation
Trans-Golgi
Network
mRNA
APOBEC3
MHC I
BST-2
IFI44L
IFI44
OAS1
ISG15
MxB

Figure 3: Impairment of the type I IFN response during HIV infection. Type I IFN defects during HIV-1 infection are extensive, affecting viral sensing, downstream signalling cascades, and antiviral ISG expression and activity. Following HIV infection, sensing of viral PAMPS by cellular PRR and activation of various intracellular signalling proteins and transcription factors is required for the induction of IFNα/β expression (**Left**). Secreted IFNα/β may then signal through the IFNAR1/2 heterodimer, triggering ISG induction through binding of the ISGF3 complex to the upstream IFN-stimulated response element (ISRE) (**Centre**). As a result, ISG expression contributes to an intracellular antiviral environment, and thus prevents viral spread (**Right**). Various points of HIV-mediated antagonism of the type I IFN response have been observed using in vitro or ex vivo models of HIV infection. Reported defects range from direct interaction with viral proteins (depicted in yellow; e.g. protease-mediated degradation of RIG-I), indirect upregulation of inhibitory cellular factors (e.g. impairment of PKR by protein complex containing ADAR1, PACT, and TRBP), or transcriptional control. Downregulated mRNA/protein expression is represented using red arrows, whereas upregulated protein expression is represented using green arrows. Additional symbols include phosphorylation (circled "P") and ubiquitination (circled "Ub"); dNTPs, deoxynucleotide triphosphates; dsDNA, double stranded DNA; IRFBS, IRF binding site; ssRNA, single stranded RNA. Figure and caption reprinted with permission from Elsevier Publishers Ltd.: Sandstrom TS, Ranganath N, Angel JB. Impairment of the type I interferon response by HIV-1: Potential targets for HIV eradication. Cytokine Growth Factor Rev. 2017 Apr 24;37:1-16. (Figure 3). Copyright 2017.

1.5.1 Impairment of cytoplasmic virus-sensing machinery during HIV infection

It is the sensing of pathogen-associated molecular patterns (PAMPs) by cellular PRR that initiates IFN1 production during viral infection. These PRR can be grouped into four broad categories—Toll-like receptors (TLRs), retinoic acid inducible gene I (RIG-I)-like receptors (RLRs), nucleotide-binding oligomerization domain (NOD)-like receptors (NLRs), and C-type lectin receptors (CLRs). Several DNA-specific PRR are also involved, including cyclic guanosine monophosphate–adenosine monophosphate synthase (cGAS) and IFN-γ-inducible protein 16 (IFI16) (reviewed in (216)). Given that these proteins are key for the timely induction of the IFN1 response during HIV infection, HIV has evolved several ways to avoid recognition by TLRs, RLRs, cGAS, and IFI16.

1.5.1.1 Involvement and inhibition of Toll-like receptor signalling

Expressed within the cellular endosomal compartment, TLRs 3, 7, 8, and 9 play an important role in the context of viral infection. TLR engagement results in the activation of IFN regulatory factor (IRF) 3 and 7 and subsequent IFN1 production (217,218). The recognition of dsRNA (TLR3) (219), ssRNA (TLR7/8) (220), or unmethylated CpG DNA (TLR9) (221) is therefore an important step in preventing viral spread to neighbouring cells. HIV gp120 has been shown to block TLR9-mediated IFN1 production by pDC via the cross-linking of blood dendritic cell antigen 2 (BDCA-2) and activation of spleen tyrosine kinase (SYK) (222,223). pDC isolated from PLWHIV also produce lower levels of IFNα/β in response to TLR7 or TLR7/8

agonists than pDC from uninfected individuals, although the exact mechanism by which this impairment occurs is unknown (224-226)

1.5.1.2 Involvement and inhibition of RIG-like receptor signalling

Three RLR family members have been identified to date, including the hallmark protein, RIG-I, and melanoma differentiation-associated gene 5 (MDA5). RIG-I and MDA5 recognize non-self dsRNA in a size-dependent manner—MDA5 binds to long dsRNAs, while RIG-I recognizes both the short regions of dsRNA and 5'-triphosphates on uncapped viral RNAs (227,228). In the context of HIV infection, RIG-I is capable of binding to secondary RNA structures found within the HIV genome (such as the TAR element) and inducing the production of IFNα by PBMC and MDM (229). This requires the recruitment of the adaptor protein, interferon-α promoter stimulator 1 (IPS-1, also referred to as MAVS, VISA, or CARDIF) and subsequent activation of IRF3 and 7 (230-232). The third RLR family member, laboratory of genetics and physiology 2 (LGP2), is believed to function as a positive regulator of the innate immune response by enhancing the recognition of dsRNA ligands by MDA5 and RIG-I (233).

Despite the evident antiviral role of MDA5 and LGP2, only RIG-I signalling, as well as subsequent IFN1 induction and ISG expression, has been found to be impaired during HIV infection. As revealed by Solis et al., HIV protease targets RIG-I for lysosomal degradation in productively HIV-infected MDM, preventing further activation of the IFN1 signalling cascade in response to viral RNA (234). This

mechanism of inhibition appeared to be RIG-I-specific, as MDA5 was not targeted by HIV protease in this model (234).

1.5.1.3 Involvement and inhibition of cytoplasmic DNA-sensing proteins

Both cGAS and IFI16 are upregulated during untreated HIV infection (235), and may therefore play a role in the recognition of cytoplasmic viral cDNA, ssDNA, and RNA:DNA hybrids (reviewed in (236)). Similar to the induction of IFN1 following RNA sensing by TLR or RLR, the production of IFN1 following the sensing of viral DNA by cGAS or IFI16 depends on the activation of a cytoplasmic signalling cascade, which is initiated following the recruitment of stimulator of IFN genes (STING) and TANK-binding kinase 1 (TBK1) and cumulates in IRF3 and NFκB activation (237).

Despite their important role in the antiviral innate immune responses, the direct impairment of cGAS or IFI16 has not been observed within HIV-infected primary cells. Evasion may occur indirectly, however, as the HIV capsid has been found to prevent the recognition of HIV cDNA by cGAS during reverse transcription (238). The degradation of HIV DNA by the cytosolic 3'-5' DNase, three-prime repair exonuclease 1 (TREX1), may similarly prevent innate immune sensing of viral DNA, and has been shown to do so in primary MDM, $CD4^+$ T cells, and cervicovaginal tissue explants (239,240). Finally, the inhibition of NFκB activation by HIV Vpu has been shown to block the antiviral function of cGAS in primary $CD4^+$ T cells (241). HIV therefore employs several indirect mechanisms by which to prevent IFN1 signalling in response to viral cDNA produced during reverse transcription.

1.5.2 Impairment of the type I IFN signalling cascade

A large network of signal transduction pathways is activated following viral infection, allowing both the rapid induction of and response to IFN1. This section will therefore provide a brief review of the various adaptor proteins, cellular kinases, and transcription factors that are involved in inducing the IFN1-mediated antiviral response, and how these proteins are impaired during HIV infection.

1.5.2.1 Involvement and inhibition of adaptor proteins

The multi-domain adaptor proteins of the IFN1 response are critical in linking PRR-dependent recognition of viral signatures to the downstream induction of IFNα/β and ISG. RIG-I, for example, relies on IPS-1 to activate downstream cellular kinases responsible for the phosphorylation and nuclear translocation of IRF3 (242,243). During HIV infection, IPS-1 is targeted by Vpu and Nef, preventing the induction of IFN1 by HIV-infected $CD4^+$ T cells (244). Transcriptional downregulation of IPS-1 may also contribute to defective RIG-I signalling in HIV-infected MDM (245). In this study, Sirois et al. also observed transcriptional downregulation of TNF receptor associated factor 6 (TRAF6) (245). As TRAF6 is indispensable for the activation of IRF7 and induction of IFN1 downstream of TLR7 and 9 (246,247), it is possible that MDM also possess impaired TLR signalling during HIV infection.

1.5.2.2 Involvement and inhibition of cytosolic protein kinases

In addition to adaptor proteins, the dysregulation of cytosolic protein kinases can block PRR-mediated signalling during HIV infection. This includes the inhibition

of TBK1 phosphorylation by HIV Vif and Vpr (248), which prevents cGAS and TLR3 mediated signalling (249-251). The downregulation of Interleukin-1 receptor-associated kinase 4 (IRAK4) expression (252) has also been observed in HIV-infected MDM, preventing MyD88-dependent signalling downstream of TLRs 7, 8, and 9 (253-255). At present, the impairment of other cellular kinases and the mechanism of impairment itself have not been characterized using primary cell models of HIV infection. Nonetheless, HIV Tat-mediated promoter occlusion is believed to block IRAK1 expression in HIV-infected CEM $CD4^+$ T cells, suggesting that a similar mechanism of impairment may occur within primary $CD4^+$ T cells or MDM (256).

1.5.2.3 Involvement and Inhibition of transcription factors

The transcription factors IRF3 and 7 are indispensable for the induction of IFN1 expression downstream of PRR engagement (217,218). With the exception of pDC, the cellular IFN1 response is initiated following IRF3 activation and low levels of IFNβ production (257,258). This is followed by autocrine IFN1 signalling, IRF7 induction, and a strong, secondary wave of IFNα/β production (231). Conversely, constitutive expression of IRF7 in pDCs allows the immediate and robust production of IFNα/β during viral infection (259-261).

Reduced IRF7 expression has been observed within pDC isolated from PLWHIV and may contribute to the sub-optimal IFN1 induction observed following TLR stimulation (225,262,263). Similarly, IRF3 expression (264) and phosphorylation (265) is believed to be impaired during HIV infection. Degradation of

IRF3 by HIV Vpu has been suggested (266), although these findings have been refuted by others who have suggested that the weak induction of IFN1 by HIV-infected primary cells is due to Vpu-mediated impairment of NFκB activation (267,268).

1.5.3 Impairment of IFN-stimulated gene expression and function during HIV infection

Although HIV can circumvent innate PRR sensing, elevated IFNα/β and immune activation during acute infection indicate that this process is not fully efficient (211,213). HIV must therefore employ additional strategies to block downstream IFN1 signalling and ISG induction, including antagonism of the IFN1 signalling cascade itself, transcriptional and post-translational regulation of ISG expression, and functional inhibition of key antiviral ISG.

1.5.3.1 Inhibition of the IFNα/β receptor and downstream signalling

Downregulation of subunit 1 of the IFNα/β receptor (IFNAR1) from the cell surface has been observed during HIV infection (269). Binding of IFNα/β to IFNAR1 and subsequent heterodimerization with IFNAR2 is necessary for ISG induction, which is preceded by the phosphorylation of signal transducers and activators of transcription (STAT) 1 and 2, recruitment of IRF9, and assembly of IFN-stimulated gene factor 3 (ISGF3) (235-237). Cells on which IFNAR1 expression is reduced, such as monocytes and monocyte-derived dendritic cells (MDDC) isolated from

PLWHIV, therefore possess an IFN1-insensitive phenotype and do not upregulate ISG expression in response to exogenous IFNα/β stimulation (270).

Aside from this, negative regulation of the cellular IFN1 response has been observed within the downstream IFNAR1/2 signalling cascade. HIV Tat-dependent upregulation of suppressors of cytokine signalling (SOCS) 1 and 3 has been observed in HIV-infected $CD4^+$ T cells and MDM (271,272), preventing STAT1/2 phosphorylation and subsequent ISG induction (273).

1.5.3.2 Transcriptional impairment of IFN-stimulated genes

Transcriptional downregulation has been observed for several ISG during HIV infection. Apolipoprotein B mRNA editing enzyme, catalytic polypeptide-like 3 (APOBEC3), for example, is subject to transcriptional downregulation in PBMCs isolated from HIV-infected individuals (274). Similarly, IFNα-induced expression of 2'5' oligoadenylate synthetase 1 (OAS1), IFN-stimulated gene 15 (ISG15), IFI44, and IFI44L was found to be impaired in HIV-infected MDM (275). While the mechanism of transcriptional inhibition was not explored in either study, others have proposed a role for HIV Tat or Vpu in mediating this process. The association of Tat with host transcriptional activators has been found to block promoter engagement and repress host gene expression (276,277), including that of major histocompatibility complex I (MHC I) (278,279). Additionally, the inhibition of NFκB activation by HIV Vpu has been found to inhibit the transcription of MHC I, bone marrow stromal cell antigen 2 (BST-2), and interferon-induced protein 44-like (IFI44L) in HIV-infected PBMC (280).

1.5.3.3 Functional inhibition of antiviral IFN-stimulated proteins

Hundreds of antiviral ISGs have been identified and are induced in response to HIV. A small number have been investigated using primary cell models of HIV infection, revealing various mechanisms of functional inhibition that may contribute to viral evasion of the innate IFN1 response.

Most commonly, ISG inhibition occurs following interaction with viral proteins. Polyubiquitination of APOBEC3 by HIV Vif, for example, has been observed in $CD4^+$ T cells (281,282), MDM (283), and MDDC (284), resulting in proteosomal degradation (285-287). Similarly, HIV Vpu has been shown to facilitate virion release from infected PBMC by targeting BST-2 (a negative regulator of HIV budding and release) to the lysosomal compartment (256-258). Inhibition of BST-2 by Vpu may also facilitate the cell-to-cell transfer of HIV from MDM to autologous $CD4^+$ T cells, allowing viral spread despite the upregulation of IFN1 signalling during acute HIV infection (288). Moreover, both HIV Vpu and Nef have been shown to redirect MHC I from the surface of HIV-infected $CD4^+$ T cells (289), allowing these cells to evade cytolytic killing. Finally, HIV Tat facilitates the translation of viral proteins by binding to and blocking the autophosphorylation of the dsRNA-binding protein (290-292).

Protein kinase R (PKR) activation and signalling are also inhibited during HIV infection, suggesting that the virus is well-suited to evade translational interference. In addition to the inhibitory function of HIV Tat, elevated levels of viral RNA can also prevent PKR dimerization, autophosphorylation, and activation of the alpha subunit of the eukaryotic translation initiation factor 2α (EIF2α) (293,294). Several cellular dsRNA-binding proteins have also been implicated in PKR inhibition during HIV

infection of primary $CD4^+$ T cells or PBMC. Presently, adenosine deaminase acting on RNA 1 (ADAR1), TAR RNA binding protein (TRBP), and the PKR activator (PACT), have been shown to complex with PKR preventing it's activation in response to viral RNA (295,296).

Additional mechanisms of ISG evasion may result from cell-mediated post-translational modification, as is the case for SAMHD1. Phosphorylation of this protein at Thr592 occurs in activated $CD4^+$ T cells, MDM, and to a certain extent MDDC, and has been found to prevent SAMHD1-mediated HIV restriction in these cell types (297,298). Alternatively, genetic polymorphisms may allow HIV to evade restriction *in vivo*. While myxovirus resistance protein B (MxB) can bind to the HIV capsid and prevent viral uncoating following infection (299), naturally-occurring capsid variants have been shown to evade MxB restriction in HIV-infected MDM (300).

1.6 Oncolytic viruses: a cancer therapeutic with HIV cure potential

Although impairment of the IFN1 response is commonly observed in the context of viral infection, it has also been noted in several other settings. For example, IFN1 signalling defects are characteristic of certain cancers and, as such, have been exploited as a therapeutic target in cancer research. This has subsequently led to the development of genetically engineered oncolytic viruses (OV) that selectively infect and kill IFN1-defective tumor cells (301). The history of the OV field, as well as the development of the IFN1-sensitive OV in this thesis, are discussed below.

1.6.1 A brief history of oncolytic virus research

Reports of cancer regression following natural viral infection have been made since the beginning of the 20th century (302,303). The use of viruses as a novel therapeutic strategy was not the subject to clinical investigation until much later, when Moore et al. demonstrated notable tumor regression in mice infected with Far-Eastern tick-borne encephalitis virus (304-306). As reviewed extensively by Kelly et al., the use of "cancer-killing," oncolytic viruses subsequently gained momentum in the 1950s when several clinical trials began to study the effect of viral infection on both solid and non-solid tumors (307). These studies, which independently employed Hepatitis B virus (308), West Nile virus (referred to as "Egypt 101 virus") (309), Adenovirus (310), or Mumps virus (311) did demonstrate notable tumor/disease regression in a subset of patients. This was at a cost, however, with numerous cases of encephalitis (309), tissue necrosis and hemorrhage (310), and even death (308) reported.

The abandonment (albeit temporary) of OV for therapeutic use was not entirely due to these dissuading findings, however. Rather, it was due to the fallout from an ethically-questionable study published in 1957 (312,313). Under the direction of a prominent name in the field, Chester Southam, healthy volunteers (as well as cancer patients) were implanted with cancerous cell lines in an apparent attempt to investigate the efficacy of viral infection on reducing tumor size *in vivo* (314). Ethical ambiguity aside, subsequent clinical attempts to replicate results obtained in murine models were found to be ineffective or were marred by severe side-effects caused by virulence in immunocompromised patients (307). Thus, OV

research retreated from bedside to bench in an effort to ensure the safety of future study participants, as well as the efficacy of the intervention itself.

It was not until the 1990's that OV were revisited in the clinical setting. With the improvement of gene editing technology, viruses could now be manipulated in order to ensure patient safety (via attenuation), as well as increase specificity for malignant cells. An attenuated Herpes Simplex Virus (HSV1716) was the first OV to return to the clinical trial stage—proving to be both safe and effective against human malignant glioma in a 1995 proof-of-principle clinical trial (315,316). This was followed by the 2006 approval of the genetically modified adenovirus, H101, by the Chinese State Food and Drug Administration (SFDA) for the treatment of head and neck cancers (317,318), and the 2015 approval of the genetically engineered HSV-1, T-VEC, by the US FDA for the treatment of melanoma (319). Present estimates by Lawler et al. indicated that there are approximately 40 ongoing clinical trials to assess the safety and efficacy of OV-based therapies (320). The field of OV research is therefore a growing one, with significant translational potential.

1.6.2 Type I interferon defects in cancer

In addition to mediating the innate antiviral response, IFN1 possess potent anti-proliferative and pro-apoptotic function (321,322). Impairment of the IFN1 response in malignant cells therefore holds biological significance and is readily selected for *in vivo*, as it permits rapid cellular proliferation and survival (323). In cutaneous T cell lymphoma, melanoma, and primary leukemia, for example, STAT1 expression is impaired, rendering these cells unresponsive to exogenous IFN1 (324). Transitional cell carcinoma is similarly unresponsive to exogenous IFN1 due

to downregulation of IRF9 expression (325,326), whereas downregulation of the IFNα/β receptor sensitizes bladder cancer cells to oncolytic virus killing (327). Impaired expression of key transcription factors, such as IRF7 in fibrosarcoma and lung cancer cells due to promoter methylation (328,329), may also cause IFN1-insensitivity.

IFN1 signalling defects in cancer cells may occur as a result of genetic mutation, leading to the under-expression or altered function of key ISG. Early analysis of primary malignant cells from patients diagnosed with acute lymphoblastic leukemia revealed the presence of homozygous deletions within the *ifna* and *ifnb1* genes (330). Germline mutations of the antiviral and pro-apoptotic 2'-5'-oligoadenylate(2-5A)-dependent RNase L have also been identified in prostate cancers, leading to reduced protein expression (331).

The aforementioned defects are not an exhaustive list of all the IFN1 response impairments that have been observed in the context of cancer to date. They do, however, demonstrate that dysregulation of the IFN1 response is a common feature of cancer that can be exploited for therapeutic purposes.

1.6.3 The development of interferon-sensitive oncolytic rhabdoviruses

Several important considerations must be made when developing an OV for therapeutic purposes. First, the virus must not cause severe illness or disease in the patient. Second, pre-existing humoral immunity against the OV has the potential to substantially decrease therapeutic efficacy. Finally, as has been shown for Adenovirus-derived OV, intratumoral injection to avoid neutralization by the host

immune response (332), or immune suppression (333,334), may be required to maintain the oncolytic capabilities of the virus.

To this point, two viruses of the *Rhabdoviridae* family, vesicular stomatitis virus (VSV) and Maraba virus, have recently been found to meet the above criteria, and therefore possess immense therapeutic potential. As a zoonotic virus, VSV infection is typically associated with outbreaks among livestock or laboratory-acquired infection, and is otherwise rare (335,336). Similarly, Maraba virus is predominantly found in Brazilian phlembotomine sand flies (*Lutzomyia* spp.) and human seroconversion has only been recorded on one occasion (337). Potential recipients of a VSV- or Maraba-based oncolytic therapy are therefore unlikely to possess pre-existing immunity to either virus. Human VSV infection is also mild in nature and subject to rapid clinical recovery, supporting the safety profile of these viruses (335,336). Conversely, due to limited data surrounding Maraba virus infection in humans, the pathogenicity of this virus remains unknown. Finally, given that these viruses possess a ssRNA genome, they are limited to cytoplasmic replication and are unlikely to cause genotoxicity *in vivo*.

The use of VSV as an oncolytic agent was first proposed by Stojdl et al. in an attempt to exploit the observed IFN1 defects in malignant cells for therapeutic purposes (338). As hypothesized, intratumoral injection of VSV resulted in notable tumor regression in mice bearing human melanoma xenografts (338), indicating the potential of VSV to act as a potent oncolytic agent in IFN-defective cancer cells. These findings were supported by those of Balachandran et al., who also demonstrated VSV-mediated cytolysis malignant cells *in vivo* (339).

VSV-inoculated mice rapidly succumbed to viral infection, however, suggesting that wild-type VSV was capable of off-target infection of healthy cells (338). It is known that wild-type VSV can block the cellular IFN1 response via its matrix (M) protein (340), which interacts with the nucleoporin Nup98 at the nuclear envelope to prevent cellular mRNA export (341,342). Consequently, mutation of the M protein increases the sensitivity of VSV to IFN1 (343,344). Additional investigation by Stojdl et al. therefore focused on enhancing the selectivity of VSV for IFN1 defective tumors by utilizing VSV variants possessing M protein mutations (301). These studies lead to the identification of VSVΔ51—a VSV variant that, due to the deletion of methionine-51 from the VSV M protein, was attenuated within healthy tissue but remained infectious within IFN1-defective tumor cells (301,345).

More recently, a recombinant Maraba virus possessing two amino acid substitution mutations within the glycoprotein (G) (Q242R) and M (L123W) proteins was identified (346). This virus, referred to as MG1, maintained a similar IFN1-sensitive phenotype as VSVΔ51 but demonstrated enhanced oncolytic potential *in vivo* (346). MG1 has now progressed to Phase I/II clinical trials intended to assess patient safety as well as efficacy in patients diagnosed with non-small cell lung cancer (ClinicalTrials.gov Identifier: NCT02879760) or advanced/metastatic MAGE-A3-expressing solid tumours (ClinicalTrials.gov Identifier: NCT02285816). Reassuringly, few side-effects have been observed following the administration of MG1 to healthy cynomolgous macaques (347).

1.7 Rational

$CD4^+$ T cells and macrophages form unique cellular reservoirs for HIV and must be selectively eradicated to achieve a complete HIV cure. Reliable cellular surface markers of latent and persistent infection have not been identified. Instead, intracellular markers unique to HIV-infected cells—such as type I IFN response defects—may serve as a target for eradication. As summarized in Figure 4, this project intends to use IFN-sensitive oncolytic viruses to eradicate HIV-infected cells, while leaving uninfected cells untouched.

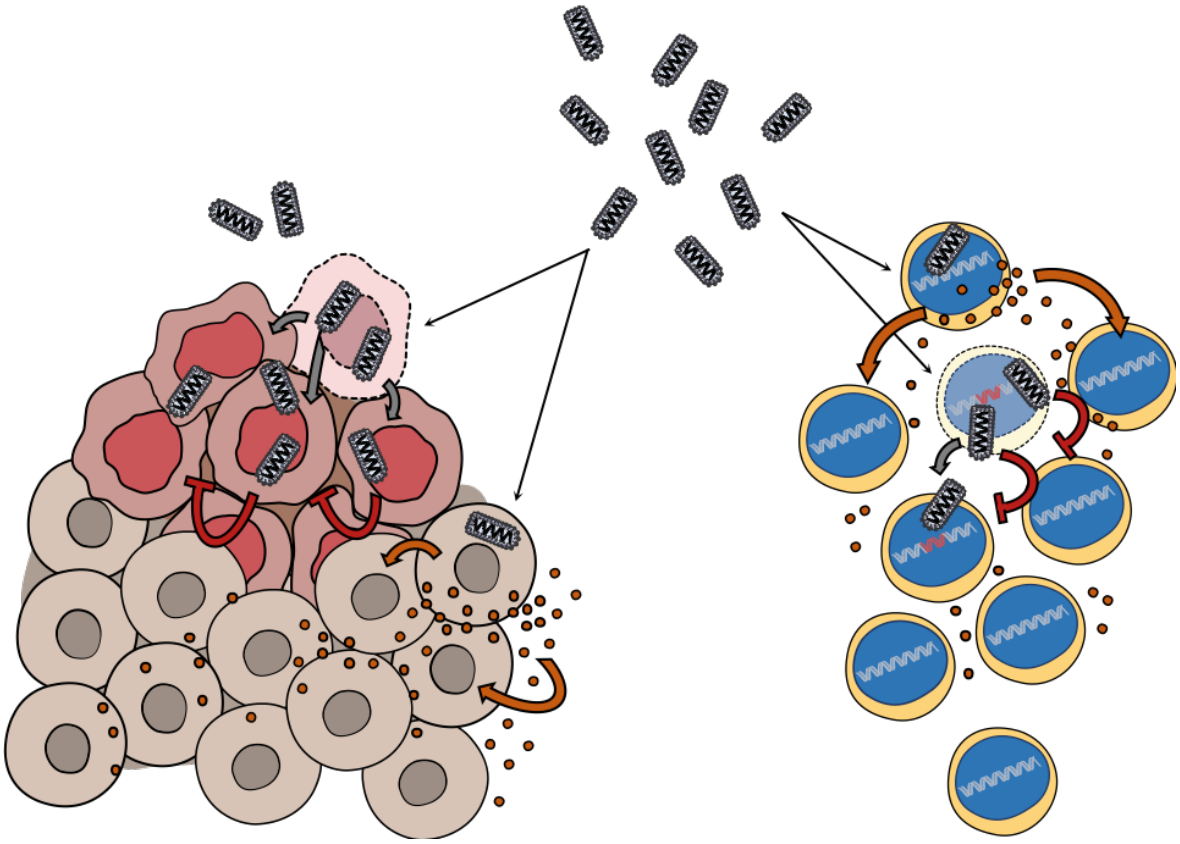

Figure 4: Cells possessing type I IFN defects are selectively killed by oncolytic viruses. Oncolytic virus therapy has been shown to reduce tumor size *in vivo* (left) by selectively infecting and killing malignant cells. The replication of OV within malignant cells facilitates the spread of OV within cancerous tissues. Conversely, non-cancerous cells are capable of producing IFNα/β (orange circles) in response to OV infection, which prevents the spread of OV within healthy tissues. The preferential killing of HIV-infected $CD4^+$ T cells by the OV, MG1, has also been demonstrated *in vitro* (right). It is hypothesized that, like non-cancerous tissues, the induction of a type I IFN response protects HIV-uninfected bystander cells from off-target OV infection and killing.

1.8 Hypothesis

It is hypothesized that the type I IFN response is impaired within cells constituting the HIV reservoir, rendering these cells susceptible to oncolytic virus infection and killing.

1.9 Project aims

The aims of this are as follows: 1. Further our understanding of intracellular signalling defects (particularly those relating to the type I IFN response) that arise within primary, human $CD4^+$ T cells and monocyte-derived macrophages following HIV infection; 2. Investigate the ability of the IFN1-sensitive oncolytic viruses, MG1 and VSVΔ51, to kill HIV-infected cells. Overall, this project will help to inform our current understanding of the HIV reservoir, while providing a framework for the implementation of oncolytic virus-based therapies for non-cancer-related clinical uses. The experimental objectives associated with each chapter are noted below.

Chapter 3: Characterize type I IFN response defects using an *in vitro,* primary $CD4^+$ T cell model of HIV latency.

Chapter 4: Characterize type I IFN response defects using an *in vitro,* primary monocyte-derived macrophage model of HIV persistence.

Chapter 5: Assess the ability of the oncolytic rhabdoviruses, MG1 and VSVΔ51, to target and eradicate HIV-infected monocyte-derived macrophages.

Chapter 6: Assess the *ex vivo* eradication of HIV-infected alveolar macrophages collected from HIV-infected individuals by the oncolytic rhabdovirus, MG1.

Chapter 7: Modulate the ability of MG1 to infect and kill HIV-infected monocyte-derived macrophages.

Chapter 2: Methodology

2.1 Reagents

2.1.1 Media

Gibco® Roswell Park Memorial Institute 1640 medium (RPMI-1640) with and without phenol red indicator, Gibco® Dulbecco's Modified Eagle's medium (DMEM), and Gibco® PBS, pH 7.4 were purchased from Life Technologies (Carlsbad, CA). Reagents for supplementation of media included heat-inactivated fetal bovine serum (FBS), penicillin (100units(U)/mL) and streptomycin (100μg/mL) (PenStrep), and L-glutamine (all from Life Technologies), and heat-inactivated human AB serum (Valley Biomedical, Winchester, Virginia).

2.1.2 Cell Stimulation

Universal type I interferon-α (IFNα) was purchased from PBL Assay Science (Piscataway, NJ). Low molecular weight polyinosinic-polycytidylic acid (LMW-poly(I:C)), 5' triphosphate double stranded RNA (5' ppp-dsRNA), and 5'ppp-free dsRNA negative control were purchased from InvivoGen. Recombinant human Chemokine (C-C motif) ligand 19 (CCL19) was obtained from R&D Systems (Minneapolis, MN) and recombinant human M-CSF (carrier-free) was purchased from Biolegend (Cat # 574802). Raltegravir and Maraviroc (Cat #11580) were obtained from Santa Cruz Biotechnology (Dallas, TX) and the NIH AIDS Reagent Program, Division of AIDS, NIAID, NIH, respectively. Cell activation employed phytohaemagglutinin (PHA) (Sigma-Aldrich) and recombinant human Interleukin-2 (IL-2) (Cell Sciences, Canton, MA).

2.1.3 Transfection

Lipofectamine® 2000 Transfection Reagent was purchased from Invitrogen (Burlington, ON). Gibco™ Opti-MEM™ Reduced Serum Media was purchased from ThermoFisher Scientific. Cells were transfected with increasing concentrations of poly(I:C) or 5'ppp according to the manufacturer's protocol.

2.2 Ethics statement

Experiments relying on the participation of healthy volunteers were approved by The Ottawa Health Science Network Research Ethics Board. Healthy volunteers provided written informed consent to partake in the study. The collection and laboratory use of alveolar macrophages from PLWHIV was approved by the Institutional Review Boards of the MUHC (#15-031), Université du Québec à Montréal (#602) and CHUM-Research Centre (#15-180). All study participants signed a written informed consent.

2.3 Cell culture

2.3.1 Cell Lines

Vero (CCL-81^{TM}) and HEK293T cells (CRL-3216^{TM}) were obtained through American Type Culture Collection (ATCC, Manassas, VA). ACH-2 cells were obtained through the NIH AIDS Reagent Program, Division of AIDS, NIAID, NIH from Dr. Thomas Folks (348,349). Vero and 293T cells were cultured in DMEM with 10% FCS and PenStrep in T75 cell culture flasks (Falcon^{TM}, Fisher Scientific), and routinely split every 2-3 days to maintain the cell monolayer. Upon reaching 80-85%

confluency, cells were detached using TrypLE (Gibco™, ThermoFisher Scientific) and re-seeded at a concentration of 0.1-0.2x10^6 cells/ml, in a total volume of 10ml per T75 flask. ACH-2 cells were cultured in RPMI-1640 medium, supplemented with 10% FCS, PenStrep, and L-Glutamine (2mM), in T75 flasks. Cells were maintained at 0.2x10^5 to 1x10^6cells/ml by passaging every 2-3 days

2.3.2 Isolation of peripheral blood mononuclear cells

Peripheral blood was drawn from healthy donors in sterile 60ml syringes, containing 100U/ml filter-sterilized Heparine Sodium (LEO Pharma Inc., Thornhill, ON). Following collection, 30ml of whole blood was layered over 15ml of Lymphoprep™ density gradient medium (Stemcell Technologies, Vancouver, BC) and centrifuged at 470 x g for 30 minutes (Megafuge 1.0, Heraeus Instruments, Germany) without braking. Buffy coats from individual donors were then collected into 50ml falcon tubes containing 10ml of room-temperature Gibco® 1x Hank's Balanced Salt Solution (HBSS) (Life Technologies) and cells were pelleted by centrifugation (300 x g for 20min). Cell pellets from individual donors were then pooled in one 50ml Falcon Tube, and cells were washed twice more with HBSS (470 x g for 10min). Following the final wash, peripheral blood mononuclear cells (PBMC) were counted by trypan blue exclusion and resuspended at a concentration appropriate for intended isolation protocol, as outlined below.

2.3.3 Isolation of resting $CD4^+$ T cells

Prior to separation, PMBC were resuspended at 5x10^7 cells/ml in the manufacturer's recommended sorting buffer (phosphate buffered saline (PBS), 0.5%

FBS, and 2mM ethylenediaminetetraacetic acid (EDTA, pH 8; Sigma Aldrich). Resting $CD4^+$ T cells were then isolated from PBMC by negative selection using the EasySep™ Human $CD4^+$ T cell Enrichment Kit (StemCell Technologies, Vancouver, BC), in accordance with the manufacturer's protocol. The negative fraction was then counted, and resuspended in sorting buffer at $1x10^8$ cells/ml for the negative selection of resting $CD4^+$ T cells using the EasySep™ Human "Do-It-Yourself" Kit (StemCell Technologies). Selection used the following antibodies: mouse IgG_1 monoclonal anti-CD69 (clone FN50; BD Pharmingen, San Jose, CA) and anti-HLA-DR (Clone L203; R&D Systems). After sorting, cells were counted, resuspended at $2x10^6$ cells/ml in RPMI-1640 medium supplemented with 10% FBS, PenStrep, and L-glutamine (2mM) (RP10 medium) and incubated overnight at 37°C with 5% CO_2. Purity was routinely assessed by flow cytometry immediately post-sort using antibodies against CD4 (clone SK3; BioLegend, San Diego, CA), CD69 (clone 298614; R&D Systems), and HLA-DR (clone L243; BioLegend). The staining protocol for assessing $CD4^+$ T cell purity is described in section 2.7.1.

2.3.4 Isolation of $CD8^+$ T cells

PBMC were resuspended at $1x10^8$ cells/ml in sorting buffer, and $CD8^+$ T cells were isolated in accordance with the manufacturers protocol using the EasySep™ Human CD8 Positive Selection Kit (StemCell Technologies). After sorting, the negative fraction, containing CD8-depleted PBMC, was resuspended at $2x10^6$ cells/ml in RP10 media.

2.3.5 in vitro generation of monocyte-derived macrophages

Monocytes were first separated from healthy donor PBMC by plate adherence. Following isolation, PBMC were resuspended at $6.25x10^6$/ml in warm, serum-free RMPI-1640 with PenStrep. $1.25x10^8$ PBMC were then plated in $150cm^2$ polystyrene tissue culture dishes (Sarstedt, Nümbrecht, Germany), and left to adhere for 2 hours at 37°C. Plates were washed 3 times with endotoxin-free PBS (pH 7.4, Gibco™) to remove non-adherent lymphocytes, and 20ml of of warmed RPMI-1640, supplemented with PenStrep and 10% heat-inactivated human AB serum (Mϕ media), and M-CSF (25u/ml) was added to the plate. Adherent cells were incubated at 37°C with 5% CO_2 for 7 days. At 3 days post-plating, cells were washed twice with warmed endotoxin-free PBS, and 20ml of Mϕ media was added to the plate. On day 8, adherent MDM were washed twice with endotoxin-free PBS, detached using accutase (Millipore-Sigma) and gentle scraping with a Sarstedt cell scraper, and counted by trypan blue exclusion. MDM were then pelleted by centrifugation (300 x g for 10min), resuspended at $2.5x10^5$ cells/ml in Mϕ media, and plated in the appropriate well or dish for further experiments.

2.3.6 Collection of alveolar macrophages from bronchoalveolar lavage fluid

Alveolar macrophages (AM) were isolated from bronchoalveolar lavage (BAL) fluid by plate adherence, as described by Costiniuk et al. (350). Briefly, participants recruited at the McGill University Health Centre (MUHC, Montreal, Canada) were cART-treated PLWHIV, with suppressed plasma viral load for ≥3 years and without respiratory symptoms or active infections. A total of 50-100ml of BAL fluid was

collected during bronchoscopies. BAL cells were pelleted and washed at 180 x g for 10min, then counted by Trypan Blue exclusion. Cells were resuspended in serum-free RPMI 1640 at $5x10^5$ cells/ml and plated in 24 well plates at $2.5x10^5$ cells/well for 2hrs at 37°C. Non-adherent cells were removed by rinsing wells with endotoxin-free PBS, and adherent AM were covered with 500μl of Mϕ media. AM were detached at 37°C for 30min using CellStripper Dissociation Reagent (Corning™, Fisher Scientific), followed by gentle pipetting.

2.3.7 Synthetic RNA Transfection

$CD4^+$ T cells were transfected with 0.5, 1, and 5μg/ml of LMW-poly(I:C) using Lipofectamine® 2000 Transfection Reagent, according to the manufacturer's protocol. MDM were transfected with 1μg/ml 5'ppp-dsRNA or the 5'triphosphate-free dsRNA negative control using Lipofectamine® 2000 Transfection Reagent, according to the manufacturer's protocol. For $CD4^+$ T cells, culture volume was maintained at 1ml using RP10 media plus 10μM Raltegravir and 30U/ml IL-2. For MDM cultures, well volume was maintained at 1ml using Mϕ media for the duration of the transfection.

2.3.8 IFNα stimulation

$CD4^+$ T cells or MDM were stimulated with increasing doses of IFNα at 3 and 6 days post-HIV infection, respectively. For $CD4^+$ T cell cultures, cells were resuspended at $2x10^6$ cells/ml in 500μM RP10 media plus 10μM Raltegravir and 30U/ml IL-2 prior to IFNα stimulation. IFNα was serially diluted in RP10 media and

added directly to wells. The cell suspension was mixed thoroughly by pipetting to ensure an equal distribution of IFNα within the well. For MDM cultures, adherent cells were rinsed with 0.5ml of endotoxin-free PBS, after which total well volume was increased to 1ml using Mϕ media. IFNα was serially diluted in Mϕ media and added directly to the wells. Culture media was mixed by tilting the plate, ensuring an equal distribution of IFNα within the well. Both $CD4^+$ T cells and MDM were incubated at 37°C for 16 hours prior to mRNA isolation or 24 hours prior to flow cytometry analysis.

2.4 Production of virus stocks

2.4.1 HIV Amplification

The HIV NL4.3 plasmid (351) encoding the CXCR4-tropic (X4-tropic) virus was obtained from Dr. Malcolm Martin through the NIH AIDS Reagent Program, Division of AIDS, NIAID, NIH. The HIV NL4.3 BAL-IRES-HSA plasmid, encoding the CCR5-tropic (R5-tropic) virus, was obtained from Dr. Michel J. Tremblay at Université Laval. Both viruses were amplified on HEK293T cells, as follows. Cells were seeded at $2x10^6$ cells/T75 flask and transfected with 20μg of purified plasmid using Lipofectamine™ 2000 and OptiMEM™ I Reduced Serum media, according to the manufacturer's protocol. Mock-infected stocks were made in parallel; instead of plasmid, an equivalent volume of PBS was added to the Lipofectamine™/OptiMEM™ mixture prior to transfection. Transfected cells were incubated at 37°C for 48 hours, after which culture media was collected, centrifuged (460 x g, for 10min), and filtered sequentially through 0.45μm and 0.22μm

polyvinylidene fluoride (PVDF) filters (UltiDent Scientific, St. Laurent, QC). Virus stocks were aliquoted and stored at -80 °C. HIV p24 antigen concentration was measured after one freeze/thaw cycle using the HIV-1 p24 Antigen Capture Kit (Frederick National Laboratory for Cancer Research, Frederick, MD; NIH AIDS Reagent Program), as per manufacturer protocol.

HEK293T-amplified HIV NL4.3 virus was subsequently propagated on CD8-depleted PMBCs. PBMC were first collected from peripheral blood of HIV-uninfected donors, after which $CD8^+$ cells were removed via positive selection (described in detail in section 2.3.4). CD8-depleted PBMC were then resuspended at $2x10^6$ cells/ml in RP10 media, and cultured for 3 days in the presence of PHA (5µg/mL) and IL- 2 (30U/mL). On day 3 of stimulation, $20x10^6$ CD8-depleted PBMC blasts were centrifuged and resuspended in 1ml of RP10 medium (mock infection) or HIV NL4.3 virus stock. Cells were incubated in this volume for 2 hours at 37°C, after which the cell concentration was brought to $2x10^6$ cells/ml using RP10 media. On days 4, 7, and 11 post-infection, $20x10^6$ fresh, activated CD8-depleted PBMC were added as “feeder” cells at a concentration of $2x10^6$ cells/mL in RP10 medium with IL-2 (30U/mL). After 14 days of virus amplification, stocks were harvested as described above.

2.4.2 Oncolytic Virus Amplification

The GFP-expressing recombinant oncolytic viruses, VSVΔ51 and MG1, were obtained from Drs. John Bell and David Stojdl and propagated on Vero cells, as previously described (301,346). Briefly, $2x10^6$ Vero cells were seeded in T75 tissue

culture flasks and grown to confluence at 37°C. Cells were then infected at MOI 0.01 with VSVΔ51 or MG1 in 1ml of serum-free DMEM (with PenStrep) at 37°C for 1hr; mock stocks were created using an equivalent volume of PBS as virus stock. Subsequently, the culture volume was increased to 10ml with DMEM containing PenStrep and 2% FBS, and cells were incubated at 37°C for 24 hours. To harvest the virus, culture supernatants were collected, clarified by centrifugation (300 x g for 10 minutes) and filtered through a 0.2μm pore Nalgene filter (Nalgene Nunc, Rochester, NY). Filtered supernatants were then centrifuged at 30000 x g (Optima L-100 XP, Beckman Coulter, Brea, CA) for 1.5 hours at 4°C, after which the viral pellet was resuspended in PBS, aliquoted, and stored at -80°C.

2.4.3 VSVΔ51 and MG1 titration by standard plaque assay

The titre of VSVΔ51 and MG1 stocks was determined by standard plaque assay on Vero cells with 1% Agarose in DMEM supplemented with PenStrep and 10% FBS (338,352). Mock, VSVΔ51, and MG1 stocks were titred in duplicate by 10-fold serial dilution, starting at a dilution factor of $1x10^7$ and ending at a dilution factor of $0.5x10^9$. At 24 hours post-infection, plaques were visualized by crystal violet staining.

2.4.4 Ultraviolet inactivation of VSVΔ51 and MG1

Ultraviolet-inactivation of oncolytic virus stocks was performed as previously described (353,354). Briefly, virus stocks were diluted to a concentration of $1x10^9$ PFU/mL using endotoxin-free PBS and were UV irradiated at 120mJ/cm^2 for 2

minutes using the Spectrolinker XL-1000 UV crosslinker (Spectronics, Westbury, NY). Virus inactivation was confirmed on Vero cells by flow cytometry at 72 hours post-infection.

2.5 *In vitro* HIV infection

2.5.1 In vitro model of latency in resting CD4$^+$ T cells

HIV latency was established as previously described (122,355). Briefly, resting CD4$^+$ T cells were pelleted (470 x g, 5min), resuspended in RP10 media with 100nM CCL19 at 4x10^6 cells/ml, and incubated at 37°C for 2hr. Next, CD4$^+$ T cells were pelleted (470 x g, 5min) and resuspended in RP10 media at 1x10^7 in preparation for HIV NL4.3 infection. CD4$^+$ T cells were infected by spinoculation (1200xg for 2 hours) at a ratio of 100ng of p24 per 1x10^6 cells. Following spinoculation, cells were washed 3 times with PBS and resuspended at 2x10^6 cells/ml in RP10 media with 25nM CCL19 and 30U/ml IL-2. To allow for sufficient integration of the HIV provirus, CD4$^+$ T cells were incubated at 37°C with 5% CO_2 for 3 days. Infection was confirmed by qPCR (356), as well as p24 ELISA following reactivation.

2.5.2 Confirmation of HIV latency through viral reactivation

To confirm the establishment of HIV latency, *in vitro* infected CD4$^+$ T cells were plated in RP10 media at 1x10^6 cells/ml and either reactivated with 5μg/ml PHA and 30U/ml IL-2, in the presence of 10μM Raltegravir, or left unstimulated (30U/ml IL-2; 10μM Raltegravir, without PHA). CD4$^+$ T cells were then plated in triplicate in a

96 well plate ($2x10^5$ cells/well), and well contents were collected at 2, 4, and 6 days following reactivation. Cells and supernatants were lysed with TritonX (1% final concentration) at 37°C for 1 hour, after which p24 was quantified by ELISA (Section 2.4.2).

2.5.3 HIV infection of MDM

Prior to HIV infection, MDM were washed once with endotoxin-free PBS. HIV NL4.3 BAL-IRES-HSA was added to cells at a ratio of 100ng of p24 per $1x10^6$ MDM, and Mϕ media was added at a volume sufficient to completely cover the cell monolayer. Following an overnight incubation at 37°C with 5% CO_2, the total volume of the well or dish was doubled using Mϕ media. Cells were then incubated for 6 days at 37°C with 5% CO_2, with a 1/2 media change performed at 3dpi. At 6dpi, HIV infection was confirmed by qPCR (356), p24 ELISA, and surface expression of the HIV-encoded murine heat stable antigen (HSA) by flow cytometry (357).

2.5.4 Enrichment of HSA^+ MDM

HSA-expressing MDM were isolated by positive selection using Miltenyi LS columns in combination with the MidiMACS™ magnet (purchased from Miltenyi Biotech). The HSA sorting protocol was previously optimized by the Lab of Dr. Michel Tremblay, as described (357,358). Briefly, HIV NL4.3 BAL-IRES-HSA infected MDM were detached with PBS-5mM EDTA plus 1% BSA (MBS buffer) for 1 hour at 4°C on ice, followed by gentle scraping. Cells were then counted by Trypan Blue exclusion and washed with MBS buffer (300 x g for 5min). MDM were

resuspended in 500μl of cold MBS buffer supplemented with 10% human AB serum and 20% FCS (blocking buffer) to block surface Fc receptors, and incubated at 4°C for 20min. Next, the biotin-conjugated, anti-HSA antibody (eBioscience; clone: M1/69) was added to the cell suspension at 3μg/ml final concentration, and cells were incubated at 4°C for an additional 15min. MDM were then washed twice with MBS buffer (400 x g for 5min) and re-suspended in 500μl blocking buffer. Anti-biotin microbeads (Miltenyi Biotech) were added at a volume of 10μl for every 100μl of cell suspension and cells plus microbeads were then incubated at 4°C for 15min. Cells were washed once with MBS buffer and resuspended in a total volume of 1ml for sorting.

Immediately prior to sorting, cells were washed once and filtered through 40μM cell strainers (Falcon®, Corning). Bulk cells were passed once through a Miltenyi MS column (as per the manufacturer's protocol); the positive fraction was passed through a second column to increase the enrichment of HSA^+ cells. Purity of the HSA^+ and HSA^- fractions were assessed by flow cytometry, as described in section 2.7.1.

2.6 Oncolytic virus infection

2.6.1 in vitro infection

MDM and alveolar macrophages were left uninfected, infected with UV-inactivated MG1 at MOI 10 (calculated based on PFU/ml of infectious stock), or infected with MG1 at 10-fold serial dilutions (MOI 0.1-10) in Mϕ media with 10μM Maraviroc. HIV-infected MDM cultures were infected with VSVΔ51 in a similar

manner. For cells plated in 12 well plates, infections were performed in an initial volume of 0.5ml (volumes were scaled accordingly for larger or smaller well sizes). Following incubation for 2 hours at 37°C, the total well volume was brought up to 1ml using supplemented RMPI 1640. For infections performed in smaller wells, total volumes were scaled down accordingly. At 48hpi, MDM and alveolar macrophages were detached with accutase or CellStripper, respectively, pelleted, and stored at -80°C for quantification of HIV DNA. MG1 infection, frequency of HSA expressing cells, and cell viability were assessed in monocyte-derived macrophage cultures by flow cytometry or MTT assay. In some experiments, MG1 infection was allowed to proceed over 6 days, with cell-free supernatants collected every second day for quantification of HIV p24 antigen release by ELISA.

2.6.2 Supernatant transfer

For supernatant transfer experiments, HIV-uninfected MDM were left uninfected, infected with UV-inactivated OV at MOI 10, or infected with OV MOI 10. In parallel, MDM from the same donor (cultured in 12 well plates) were infected with HIV NL4.3 BAL-IRES-HSA, as described above. At 48hpi, supernatants from OV-infected cells were collected, filtered with Amicon Ultra centrifugal filter units (MWCO 100 kDa) purchased from Millipore Sigma, and stored at -80°C. Removal of infectious OV particles was confirmed on Vero cells by flow cytometry. At 7 days post-HIV infection, filtered supernatants were thawed and added to HIV-infected MDM cultures (1 ml total volume). HIV-infected MDM were infected with OV in parallel (as described in section 2.6.1), to serve as a positive experimental control.

In both cases, Maraviroc was added to a final concentration of 10μM. Both sets of cells were then incubated at 37°C for 2 hours, after which the total well volume was brought up to 2ml using Mϕ media with 10μM Maraviroc. Cells were incubated for an additional 6 days, and cell-free supernatants were collected on days 0, 2, 4, and 6 for quantification of HIV-1 p24 antigen release by ELISA. MDM were pelleted at 6dpi and stored at -80°C for quantification of proviral DNA.

2.7 Flow cytometry

All flow cytometric analysis was performed using the FC500 Beckman Coulter Flow Cytometer (Beckman Coulter) and FCS Express Research Edition 4.0 (De Novo Software, Los Angeles, CA). Prior to staining, MDM were detached using accutase (60min incubation at 37°C) and gentle pipetting. For the assessment of surface and intracellular markers, detached MDM and $CD4^+$ T cells were aliquoted into polypropylene tubes ($1x10^5$ cells/tube) and washed with PBS 1% BSA (460 x g for 5min). All antibodies used in the below experiments are listed in Table 1. All antibodies were titered prior to use in order to identify the optimal volume per test.

Table 1: Antibodies used for flow cytometry

Target	React.	Species	Product Number	Company	Clone	Working Conc. (µg/ml)	Conjugate
CD24 (HSA)	Mouse	Rat	101807	BioLegend	M1/69	3	PE
CD24 (HSA)	Mouse	Rat	101813	BioLegend	M1/69	3	APC
CD24 Isotype	Mouse	Rat	400607	BioLegend	RTK4530	3	PE
CD24 Isotype	Mouse	Rat	400611	BioLegend	RTK4530	3	APC
CD4	Human	Mouse	344612	BioLegend	SK3	5	PE-Cy7
CD69	Human	Mouse	FAB23591 P	R&D Systems	298614	0.25	PE
HLA-ABC (MHC I)	Human	Mouse	15-9983-42	eBioscience	W6/32	0.25	PE-Cy5
HLA-DR	Human	Mouse	307609	BioLegend	L243	1.2	APC
IFNAR1	Human	Mouse	FAB245P	R&D Systems	85228	2.5	PE
IFNAR2	Human	Mamma-lian cell line	130-099-556	Miltenyi	REA124	2	PE
ISG15	Human	Rat	IC8044G	R&D Systems	851701	1	Alexa Fluor® 488
ISG15 Isotype	Human	Rat	IC006G	R&D Systems	54447	2.5	Alexa Fluor® 488
LDLR	Human	Mouse	FAB2148P	R&D Systems	472413	0.25	PE
PKR (1°)	Human, Rat	Mouse	Ab202136	Abcam	6H3A10	10	N/A
PKR (2°)	Mouse	Goat	Ab120782	Abcam	-	20	APC
PKR Isotype	Human	Mouse	Ab91358	Abcam	1F8	20	APC

Abbreviations: APC: Allophycocyanin; CD: cluster of differentiation; Cy5: Cyanine5; Cy7: Cyanine7; HLA: human leukocyte antigen; IFNAR: IFNα/β receptor; ISG: interferon stimulated gene; LDLR: low density lipoprotein receptor. PE: Phycoerythrin; PKR: protein kinase R.

2.7.1 Surface markers

To evaluate the HSA expression on HIV-infected MDM, $1x10^5$ cells were washed with PBS 1% BSA (460 x g for 5min), and re-suspended in 100μl of cold blocking buffer. Cells were incubated at 4°C for 20min, after which the anti-HSA antibody (clone M1/69; BioLegend) or HSA isotype control antibody (Rat IgG2b κ Isotype clone RTK4530; BioLegend) was added at 3μg/ml. Cells were mixed by vortexing, and incubated at 4°C for 15min. Following staining, cells were washed twice and prepared for further staining for either surface or intracellular protein targets, or sorting (as described in section 2.5.4). If no further staining was necessary, cells were fixed in 400μl of pre-warmed 1% paraformaldehyde (PFA; Millipore-Sigma) for 15min at room temperature prior to analysis.

For analysis of surface markers, including the IFNα/β receptor subunit 1 (R&D Systems, clone # 85228), the IFNα/β receptor subunit 2 (Miltenyi, clone REA124), the LDL receptor (LDLR) (R&D Systems, clone # 472413), and MHC I (eBioscience, clone # W6 is/32), $1x10^5$ cells were first resuspended in 100ul of PBS 1% BSA with 10μl of FcR blocking reagent (Miltenyi Biotec) and incubated at 4°C for 15min. Cells were then washed once and resuspended in 100μl PBS 1% BSA. 10μl of the antibody of interest was added, and the cell suspension was incubated at 4°C for 30min. Prior to analysis, cells were washed once with 1ml of PBS 1% BSA, then fixed in 1% PFA.

Resting $CD4^+$ T cell purity was assessed post-sort using antibodies directed against CD4 (clone SK3; BioLegend), CD69 (clone 298614; R&D Systems), and HLA-DR (clone L243; BioLegend). Briefly, cells were pelleted in polypropylene tubes

and resuspended in 100μl PBS 1%BSA. Cells were then stained with the PE/Cy7-conjugated anti-CD4 (5μl), the PE-conjugated anti-CD69 (1μl), and the APC-conjugated anti-HLA-DR (5μl) for 30min at room temperature, protected from light. Prior to analysis, cells were washed with 1ml of PBS 1% BSA, then fixed in 1% PFA.

Annexin-V staining was performed using the eBioscience™ PE/Cy7 Annexin-V Detection Kit (ThermoFisher Scientific), according to the manufacturer's protocol. Cells were stained with 5μl of Annexin-V for 15min at 4°C, washed twice with 1x Annexin-V binding buffer (ThermoFisher Scientific) then fixed using 1% PFA, as described above.

2.7.2 Intracellular markers

For the analysis of intracellular PKR or ISG15 expression, $1x10^5$ cells were fixed in 100μl of pre-warmed 4% PFA for 15min, then washed to remove residual PFA. Intracellular ISG15 expression was evaluated by staining cells with 5μl of the Alexa Fluor®488-conjugated anti-human ISG15 (R&D Systems, Clone # 851701) or 5μl of the isotype-matched control antibody (R&D Systems, Clone # 54447) in 100μl of 0.5% Saponin with 10% NGS for 30 minutes at 4°C. Cells were then washed and resuspended in 400μl of PBS 1% BSA for analysis. In parallel, intracellular PKR expression was evaluated by adding 1μl unconjugated mouse anti-human PKR antibody (Abcam, clone 6H3A10) to cells in 100μl of 0.5% Saponin for 30 minutes at 4°C. Cells were then washed and stained with 4μl of the APC-conjugated goat anti-mouse IgG (Abcam) or 2μl isotype-matched control antibody (1mg/ml; Abcam, clone

1F8) in 100µl of 0.5% Saponin for 30 minutes at 4°C. Cells were washed three times and resuspended in 400ul of PBS 1% BSA for analysis.

Caspase 3/7 activation was assessed using the FLICA™ 660 Caspase-3/7 Kit (BioRad), according to the manufacturer's protocol. Briefly, cells were detached using accutase, pelleted, and $1x10^5$ cells per condition were resuspended in 200ul of RMPI 1640 with 10% human AB serum. FLICA™ 660 working solution was added to a final dilution of 1:60 and cells were incubated at in the dark at 37°C for 60min, with gentle vortexing every 15min. Following incubation, cells were washed twice with 1x apoptosis buffer (BioRad), then fixed, as described above.

2.8 Colourimetric assays

2.8.1 MTT assay

Cell viability following MG1 infection was assessed by Vybrant® MTT Cell Proliferation Assay kit (Invitrogen). The MTT ((3-(4,5-dimethylthiazol-2-yl)-2,5-diphenyltetrazolium bromide)) stock solution was prepared at a final concentration of 12mM, as per the manufacturer's instructions. At 2 days post-MG1 infection, MDM plated in 12 well plates were rinsed with PBS, and 450µl of MTT diluted 1:15 with RPMI without phenol red indicator and supplemented with PenStrep and 10% FCS was added. Cells were incubated for 2 hours at 37°C, at which point the MTT reaction was stopped and viral particles were lysed using a 10% sodium dodecyl sulfate (SDS; Fisher Scientific) solution containing 0.01M HCl (Fisher Scientific). Following lysis, plates were incubated for an additional hour at 37°C. Prior to reading, samples were mixed well by pipetting, and 100µl was aliquoted in

quadruplicate into a 96 well plate. Absorbance was read at 570nm using the Multiskan Ascent 96 Plate Reader (MTX Lab Systems Inc., Bradenton, FL).

2.9 ELISA

2.9.1 p24 ELISA

HIV p24 antigen concentration was measured by ELISA after one freeze/thaw cycle. Cell-free supernatants were lysed for 1 hour at 37°C with 1% Triton-X and p24 antigen expression was quantified by HIV-1 p24 Antigen Capture Kit (Frederick National Laboratory for Cancer Research, Frederick, MD; NIH AIDS Reagent Program) following the manufacturer's protocol. Absorbance was read at 450nm wavelength with a reference wavelength of 540nm using the Multiskan Ascent 96 Plate Reader.

2.9.2 IFNα ELISA

HIV infected and uninfected MDM were transfected with 5'ppp-dsRNA, as described in section 2.3.7. At 24 hours post-transfection, cell culture media was collected and total IFNα was measured using the VeriKine human IFNα ELISA kit (PBL Assay Science, Piscataway, NJ) as per the manufacturer's instructions. Absorbance was read at 450nm wavelength with a reference wavelength of 540nm using the Multiskan Ascent 96 Plate Reader.

2.10 Molecular biology

Primers and probes used in the below experiments are listed in Table 2. This excludes the BioRad PrimePCR™ reagents, as this information is proprietary.

2.10.1 RNA and DNA Extraction

Cell associated-RNA was extracted using the Illustra RNAspin mini kit (GE Healthcare Life Sciences, Mississauga, ON) as per the manufacturer's instructions. RNA integrity was monitored by agarose gel electrophoresis and concentrations were measured using ND-1000 Spectrophotometer (NanoDrop, Wilmington, DE). Genomic DNA extraction for the quantification of HIV proviral DNA was performed via overnight cell lysis, as described by Vandergeeten et al. (356). Briefly, cell pellets were first washed twice with PBS, then resuspended thoroughly in lysis buffer (10mM Tris-HCl, pH 8.0, 50nM KCl, 400ug/mL Proteinase K; Invitrogen) at a concentration of 7500 cells/μl. Tubes were incubated for 16 hours at 55°C in a heating shaker; gentle vortexing was performed every 15min for the first hour of incubation to ensure thorough lysis. If not used immediately, cell pellets were stored at -80°C. All samples were divided into single-use aliquots and stored at -80°C until further use.

2.10.2 Integrated HIV DNA PCR

Two-step nested PCR targeting CD3 and integrated HIV DNA was performed with previously described primer-probe sets (356). In the initial pre-amplification step (Step 1), proviral HIV DNA and CD3 were amplified in triplicate in a 25μl reaction

mix containing 7.5μl of cell lysate, 12.5μl of iQ™ Supermix (BioRad), 0.75μl of the HCD3OUT3', HCD3OUT5', ALU1, and ALU2 primers (300nM each), 0.375μl of the ULF1 primer (150nM), and 1.625μl DNase-free/RNase-free H_2O (Sigma-Aldrich). A 10-fold dilution standard curve using ACH-2 cell lysates (ranging from 300,000 cells to 3 cells) was run in parallel to allow for quantification of proviral copy number. To maintain amplification in an exponential phase, 12-cycle first-round amplification was carried out as described (356) using a T100™ Thermal Cycler (BioRad).

Step 1 PCR products were then prepared for Step 2. In experiments involving *in vitro* HIV-infected MDM, this second amplification was run by qPCR. Step 1 PCR products were first diluted 1:10 using DNase-free/RNase-free water (Sigma-Aldrich). Next, proviral HIV DNA and CD3 were amplified separately in a 20μl reaction mix containing 6.4μl of the diluted Step 1 PCR products, 10μl of SsoAdvanced™ Universal Probes Supermix (BioRad), 3.6μl DNase-free/RNase-free H_2O, and either: 0.25μl of HCD3IN5' and HCD3IN3' (1250nM each) and 0.5μl of CD3 FamZen Probe (200nM) for the CD3 reaction; or, 0.25μl of LambdaT and UR2 (1250nM each) and UHIV FamZen Probe (200nM) for the HIV DNA reaction. The RT-qPCR reaction was then carried out using the CFX Connect™ Real-Time PCR Detection System (BioRad) using the following amplification steps for all reactions: a denaturation step (95°C for 4 minutes), followed by 40 cycles of amplification (95°C for 3s, 60°C for 10s). The inclusion of an ACH-2 standard curve permitted quantification of proviral HIV DNA using CFX Manager 3.1 software (BioRad) and Microsoft Excel.

In experiments using AM, the second amplification step was performed using digital droplet PCR (ddPCR™), as described in (354). Briefly, Step 1 PCR products

were diluted 1:10 (for the measurement of proviral HIV DNA) or 1:1000 (for the measurement of CD3 DNA). Second step reactions were prepared as stated above, except that ddPCR™ Supermix for Probes (No dUTP) (BioRad) was used instead of SsoAdvanced™ Universal Probes Supermix. Using the manufacturer's protocol, the QX200 Droplet Generator (BioRad) was used to aerosolize the reaction mix. Oil droplets were then transferred to a 96-well PCR plate (Eppendorf) and the Step 2 PCR reaction was performed using the C1000 Touch Thermal Cycler (BioRad), as follows: denaturation (95°C for 10min); 50 cycles of amplification (95°C for 30s, 57°C for 1min); droplet stabilization (4°C for 5min and 90°C for 5min). Absolute quantification of proviral HIV DNA and CD3 DNA was performed using the QX200 Droplet Reader (BioRad) and QuantaSoft™ software, version 1.7 (BioRad).

2.10.3 IFN-stimulated gene induction

RNA was converted to cDNA using iScript™ Reverse Transcription Supermix for RT-qPCR (BioRad) and the T100™ Thermal Cycler (BioRad). ISG15, PKR, HLA-B, and GAPDH cDNA was then detected using BioRad's PrimePCR™ SYBR® Green Assay (ISG15 assay ID: qHsaCED0001967; PKR assay ID: qHsaCED0042156; HLA-B assay ID: qHsaCED0037470; GAPDH assay ID: qHsaCED0038674), using the CFX Connect™ Real-Time PCR Detection System (BioRad). All PrimePCR regents (efficiency and melt peak) were validated using pooled cDNA from IFNα stimulated, human MDM, serially diluted 1:10**.** Amplicon purity was confirmed using a 10% agarose gel. If not used immediately, RNA and cDNA were stored at -80°C in single-use aliquots.

Table 2: Primers and probes used for PCR

Target	Primer or probe name	Sequence (5' to 3')	Conc. (nM)
CD3 (Ref. 356)	HCD3OUT5'	ACTGACATGGAACAGGGGAAG	300
	HCD3OUT5'	CCAGCTCTGAAGTAGGGAACATAT	300
	HCD3IN5'	GGCTATCATTCTTCTTCAAGGT	1250
	HCD3IN3'	CCTCTCTTCAGCCATTTAAGTA	1250
	CD3 Probe	FAM-AGCAGAGAA/ZEN/CAGTTAAGAG CCTCCAT/3IABkFQ	200
Integrated HIV DNA (Ref. 356)	ULF1	ATGCCACGTAAGCGAAACTCTGGGTCTCTCTDG TTAGAC	150
	ALU1	TCCCAGCTACTGGGGAGGCTGAGG	300
	ALU2	GCCTCCCAAAGTGCTGGGATTACA	300
	LambdaT	ATGCCACGTAAGCGAAACT	1250
	UR2	CTGAGGGATCTCTAGTTACC	1250
	UHIV FamZen Probe	FAM-CACTCAAGG/ZEN/CAAGCTTTATTGAGGC-3IABkFQ	200

Abbreviations: FAM: 6-carboxyfluorescein group reporter; Q: 6-carboxytetramethylrhodamine group quencher; ZEN: ZEN™ internal quencher; 3IABkFQ: 3'-Iowa Black® FQ

2.11 Artwork

Figures 1, 2, 4, 41, and 42 were created using Smart Servier Medical Art image sets (available from https://smart.servier.com/). Servier Medical Art by Servier is licensed under a Creative Commons Attribution 3.0 Unported License.

2.12 Statistics

Statistics were performed using GraphPad Prism 5.0 software (San Diego, CA), and P values ≤0.05 were considered significant. As determined *a priori*, statistical analyses used included paired t-test, 2way ANOVA with Bonferroni's multiple comparison test, or 1way ANOVA with Bonferroni's multiple comparison test.

Chapter 3: Type I IFN signalling in an *in vitro*, primary CD4$^+$ T cell model of HIV latency

3.1 Introduction

3.1.1 Rational

The establishment of latent HIV infection in resting memory CD4$^+$ T cells—a process in which viral cDNA is integrated into the genome of the infected cell without subsequent production of infectious viral progeny—is a significant barrier impeding current HIV cure strategies (359). Understanding how this latent reservoir is maintained, as well as identifying specific markers or characteristics unique to these cells, is necessary for the development of novel reservoir-clearance strategies. Still, our knowledge of these processes is inadequate and is often based off of similar processes occurring within productively HIV-infected cells.

For example, HIV is known to interfere with the activity of various antiviral proteins, leading to the impairment of the IFN1 response during productive infection (reviewed in (360)). Similar defects have been reported in latently HIV-infected cell line models (215), but have not yet been described *in vitro* using primary cells. The work within this chapter was therefore intended to characterize IFN1 defects within an *in vitro,* primary CD4$^+$ T cell model of HIV latency. The objective of these experiments was to identify a unique intracellular characteristic that could be used to distinguish latently infected cells from their uninfected counterparts.

3.1.2 Memory CD4$^+$ T cells are an important HIV reservoir in vivo

The latent HIV reservoir is comprised primarily of resting memory CD4$^+$ T cells (103,120,359). Although the frequency of these cells *in vivo* is quite low (361), latently HIV-infected CD4$^+$ T cells are incredibly stable, with half-life of ~44 months (114,154), can self-renew via homeostatic proliferation (359,362), and can act as a source of productive viremia during cART interruption (111). Thus, the field of HIV cure research has dedicated substantial effort to understanding how this latent reservoir is established and how it can be eradicated.

Latent infection was previously believed to be a state of complete viral quiescence, in which suppression of the HIV LTR (363,364), activation of cellular transcriptional repressors (365), or epigenetic modifications (366,367) prevented the expression viral transcripts, proteins, and other viral signatures from the stably-integrated HIV provirus (368). Accumulating evidence has suggested that this definition of latency is not entirely correct. Although the majority of latently infected cells are transcriptionally silent, HIV latency may also be maintained as unintegrated cDNA (369,370) or transcriptionally-active provirus (371,372). In alignment with this, viral transcripts have been detected in CD4$^+$ T cells from cART-treated individuals (371,373). Thus, HIV latency is now defined as the presence of a replication-competent provirus (in most cases, a single copy (115)) that is not producing infectious viral progeny, but can be stimulated to do so.

When and how HIV latency is established are additional, pertinent questions when considering the viral reservoir. Studies in non-human primates have shown that the initiation of cART at 3 days post-infection is not sufficient to block reservoir establishment (374). Similarly, the prompt treatment (30 hours following delivery) of

an HIV-exposed infant was not sufficient to prevent eventual viral rebound following the cessation of cART (375,376). While certainly effective in reducing the number and distribution of latently-infected cells, it is now understood that the rapid initiation of cART does not prevent seeding and maintenance of the viral reservoir (376,377). The establishment of HIV latency is therefore a dynamic process occurring in the early stages of infection.

Interestingly, the cells that typically harbour latent HIV provirus would not indicate a process that is dynamic or rapid. True to their name, resting memory $CD4^+$ are not replicating, and are less susceptible to HIV infection, reverse transcription, and integration (378-381). Nonetheless, the establishment of HIV latency in resting memory $CD4^+$ T cells has been demonstrated *in vitro* (382,383). Treatment with cytokines involved in T cell migration has also been shown to enhance nuclear import of viral cDNA, thereby priming resting $CD4^+$ T cells for latent HIV infection (384). Infection of activated $CD4^+$ T cells that are in the process of reverting to a resting state has also been proposed as means by which HIV latency is established within the resting memory $CD4^+$ T cell population (385). It is highly likely that both processes contribute to the establishment of the latent HIV reservoir *in vivo*.

In order to more thoroughly understand the latent HIV reservoir, a number of groups have attempted to define cell surface proteins as unique markers of latently HIV-infected cells (386,387). Unfortunately, these efforts have not yet lead to a reliable means by which to isolate and culture latently HIV-infected cells *ex vivo.* The isolation of cell populations known to be enriched for latent provirus, including those expressing select immune checkpoint molecules, like programmed cell death protein

1 (PD-1), TIGIT (T Cell Immunoreceptor With Ig And ITIM Domains), and Lymphocyte-activation gene 3 (LAG-3) (388), or receptors involved in mucosal homing, like CCR6 (389), may prove more reliable. Still, the relative rarity of these cells *in vivo* (120,390) and their localization to lymphoid tissues in cART-treated individuals (391-395) has necessitated the development of latently HIV-infected cell lines and *in vitro* primary cell models of latency for the ongoing study of the HIV reservoir. The latter, although more time consuming to establish and optimize, are generally preferred given their biological similarity to latently HIV-infected $CD4^+$ T cells found *in vivo*.

3.1.3 In vitro models of HIV latency using primary $CD4^+$ T cells

Several primary cell models of HIV latency have been established and verified *in vitro* for various experimental purposes. For example, two separate latency models using a Δ*env* virus have been developed (121,163), ensuring that viral progeny are limited to a single round of infection. These two models are also similar in that resting $CD4^+$ T cells are polarized to a memory phenotype via TCR stimulation prior to HIV infection, after which they are returned to a resting state. Replication-competent Δ*nef* reporter viruses have also been used (123) to facilitate the detection of infected cells post-stimulation. Due to the use of a modified virus for latency establishment and other cellular manipulations, these models are better suited for the study of latency reversal agents rather than the investigation of defining characteristics of latently HIV-infected cells.

Other models involve the co-culture of resting $CD4^+$ T cells with activated, productively infected autologous $CD4^+$ T cells (124). As a plus, the resulting population of latently HIV-infected cells is quite large in comparison to that generated with other models of latency. As well, the co-culture of cells to induce latency is likely analogous to events *in vivo* (396). Quiescent cells must, however, be isolated from the co-culture after the fact, increasing the risk of contaminating the latent population with productively infected cells.

Finally, certain models focus on the establishment of latency within resting cells using a full-length, replication-competent virus. Although the dynamics of HIV infection within resting $CD4^+$ T cells has been argued, Swiggard et al. have successfully demonstrated the establishment of a small population of latently infected resting $CD4^+$ T cells via spinoculation (382,383). Alternatively, latency can be established in resting $CD4^+$ T cells that have been stimulated with cytokines responsible for cytoskeletal remodeling, motility, and tissue-homing (384). In order to recapitulate tissue microenvironments known to harbour latently HIV-infected cells, Saleh et al. established a latency model in which resting $CD4^+$ T cells were stimulated with the CCR7 ligand, CCL19, prior to infection (122,355). Although the total number of latently infected cells generated in this manner (~29,000 copies of proviral DNA/10^6 cells, or ~2-3%) was less than that observed in the models mentioned above, reactivation of latent provirus could be readily detected. Moreover, proviral reactivation within this latency model was quite similar to that observed within $CD4^+$ T cells from PLWHIV following stimulation via PKC agonists, TCR engagement, transcriptional activators, or HDACi (124).

The Lewin latency model was selected for the experiments addressed within this chapter as it utilizes a full-length virus for the infection of primary cells that have been stimulated in a physiologically-relevant manner. Moreover, the cells used in this model require little manipulation following *in vitro* infection, and exhibit a similar capacity for viral reactivation as that observed in $CD4^+$ T cells isolated from PLWHIV. Thus, this latency model appears to be the best option at present to study the unique characteristics of the latent HIV reservoir. Importantly, these *in vitro* latency models may also be useful to assess similarities between latent and productive HIV infection. In either case, a comprehensive understanding of the latent viral reservoir will be important for the development of reservoir eradication strategies, and ultimately the development of an HIV cure.

3.1.4 Type I IFN signalling defects in HIV-infected $CD4^+$ T cells

As previously discussed in Chapter 1.5, HIV has developed several mechanisms by which to impair the IFN1 response. Many of these depend on the inhibitory characteristics of viral proteins, such as HIV Protease, which targets RIG-I to the lysosomal compartment for degradation (234) or Vpu, which is believed to target IRF3 for caspase-mediated degradation (14). Doehl et al. have demonstrated that IRF3 degradation in HIV-1 infected PBMCs prevented induction of ISG15 (264), a cytoplasmic protein known to inhibit viral budding and release from infected cells (397). Thus, the HIV-1-mediated blockade of antiviral signaling pathways may occur in both a direct and indirect manner.

The assessment of IFN1 signalling in primary $CD4^+$ T cells has been limited to the study of productively infected cells. Not only does this yield a larger population

of infected cells with which to work, but ongoing HIV replication ensures viral protein expression that can be used to differentiate infected and uninfected cells *in vitro*. In this context, HIV-mediated IFN1 response defects have been shown to occur at several points within the IFN1 signalling cascade. Degradation of viral DNA intermediates by TREX1 (239,240) or inhibition of NFκB by HIV Vpu (241,398) prevent the induction of IFNα/β via DNA-sensing proteins like cGAS or IFI16. Similarly, the disruption of key signalling proteins like IPS-1 (244) and STAT1/2 (271), or the downregulation of transcription factors like IRF3 (264), has been found to disrupt cellular antiviral defenses during HIV infection. On top of this, certain ISG, including MHC I (143,289), APOBEC3 (281,282), and SAMHD1 (297,298), are degraded and/or inhibited by HIV accessory proteins, while others are inhibited by cellular proteins upregulated in response to HIV infection. For example, activation of the RNA-sensing protein, PKR is blocked by a complex of three cellular proteins—ADAR1, TRBP, and PACT—facilitating viral protein translation and replication (295,296).

Presently, similar IFN1 signalling defects have not been investigated in primary cell models of HIV latency. Despite an absence of viral replication, transient production of viral RNAs (371) suggest that latently HIV-infected cells may harbour similar IFN1 signalling defects as their productively infected counterparts. Characterization of IFN1 signalling in latently HIV-infected primary $CD4^+$ T cells therefore has important implications for the identification of a definitive intracellular marker and/or target for reservoir clearance strategies.

3.2 Hypothesis

The type I IFN response is impaired in latently HIV-infected $CD4^+$ T cells.

3.3 Results

3.3.1 Establishment of latently HIV-infected $CD4^+$ T cells in vitro

An *in vitro* model of HIV latency was established in resting $CD4^+$ T cells, in adherence to the protocol outlined by Saleh et al. (122,355). The timeline for resting $CD4^+$ T cell isolation, CCL19 stimulation, and HIV NL4.3 infection is outlined in Figure 5. The resting status and purity of enriched lymphocytes was confirmed by flow cytometry, as measured by CD69 and HLA-DR surface expression (Figure 6a,b), the respective markers of early and late activation (399,400). CD69 and HLA-DR antibodies were previously validated using PHA/IL-2 stimulated PBMC (data not shown). Purity of resting $CD4^+$ T cells ($CD4^+/CD69^-/HLA\text{-}DR^-$) was routinely >98%, as shown in Figure 6c.

Latent HIV infection was confirmed at 3dpi (382,401) by the measurement of proviral HIV DNA and *gag* RNA by qPCR, as well as HIV p24 antigen within cell supernatants (354). As previously shown by Ranganath (402), HIV *gag* RNA and p24 was undetectable in unstimulated $CD4^+$ T cells, but was elevated appreciably following reactivation via PHA/IL-2 stimulation. Importantly, PHA/IL-2 stimulation was performed in the presence of the integrase inhibitor, Raltegravir, ensuring that viral signatures were obtained from reactivated provirus rather than unintegrated HIV cDNA (pre-integration latency). Moreover, integrated HIV DNA could be reliably detected at 3dpi.

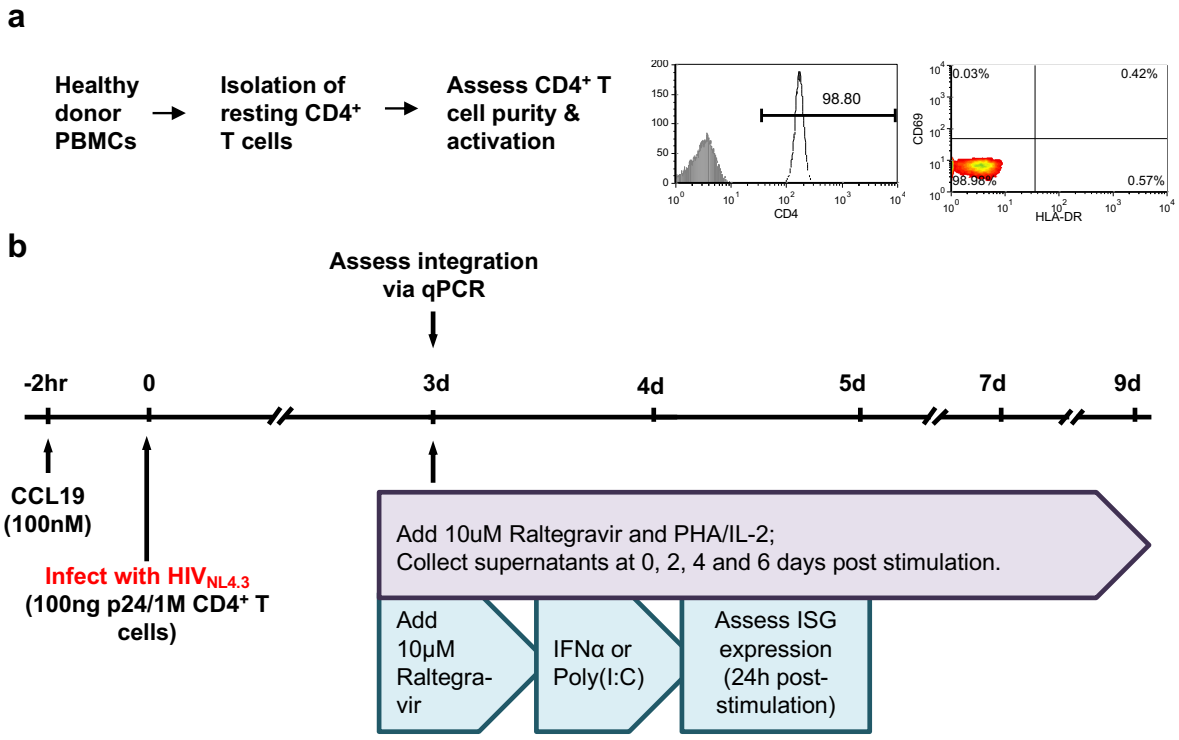
a
Healthy donor PBMCs
Isolation of resting CD4+ T cells
Assess CD4+ T cell purity & activation
98.80
CD4
0.03%
0.42%
98.98%
0.57%
CD69
HLA-DR
b
Assess integration via qPCR
-2hr
0
3d
4d
5d
7d
9d
CCL19 (100nM)
Infect with HIVNL4.3 (100ng p24/1M CD4+ T cells)
Add 10uM Raltegravir and PHA/IL-2;
Collect supernatants at 0, 2, 4 and 6 days post stimulation.
Add 10μM Raltegra-vir
IFNα or Poly(I:C)
Assess ISG expression (24h post-stimulation)

Figure 5: Timeline of resting $CD4^+$ T cell isolation and establishment of latency. a. Timeline describing the enrichment of resting $CD4^+$ T cells from healthy donor PBMCs. **b.** Timeline describing the establishment and verification of HIV latency in CCL19-stimulated, resting $CD4^+$ T cells (purple boxes), as well as the induction of ISG expression in these cells using IFNα or poly(I:C) (green boxes). Note, purple and teal boxes represent separate culture conditions.

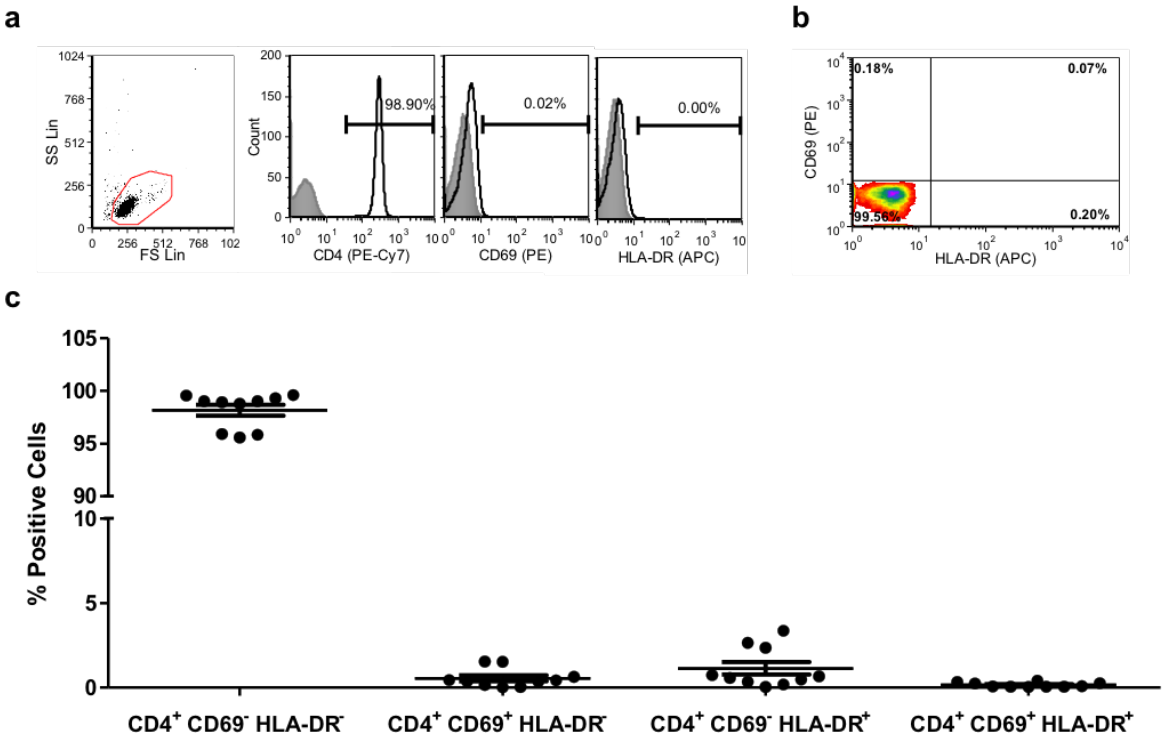
a
b
c
SS Lin
FS Lin
Count
CD4 (PE-Cy7)
CD69 (PE)
HLA-DR (APC)
98.90%
0.02%
0.00%
0.18%
0.07%
99.56%
0.20%
% Positive Cells
CD4+ CD69- HLA-DR-
CD4+ CD69+ HLA-DR-
CD4+ CD69- HLA-DR+
CD4+ CD69+ HLA-DR+

Figure 6: Resting $CD4^+$ T cell purity following magnetic bead enrichment. Representative dot plot demonstrating the gating of intact cells, as well as representative histograms showing $CD4^+$, $CD69^+$, and HLA-DR^+ cells (open, black), as well as unstained controls (filled, grey). **b.** Representative dot plot demonstrating the proportions $CD69^+$ and HLA-DR^+ cells within the $CD4^+$ population. **c.** Cumulative percentages of $CD4^+CD69^-$HLA-DR^- (98.16% ± 0.53), $CD4^+CD69^+$HLA-DR^- (0.55% ± 0.18), $CD4^+CD69^-$HLA-DR^+ (1.14% ± 0.38), and $CD4^+CD69^+$HLA-DR^+ cells (0.16% ± 0.044) (n=10). Data represent mean ± SEM; n values represent separate biological replicates.

3.3.2 Stimulation with IFNα induces ISG expression in mock and latently HIV infected CD4+ T cells

Surface expression of IFNAR1 was first measured by flow cytometry. Both IFNα and IFNβ can trigger downstream ISG induction through the IFNAR1/2 heterodimer. However, elevated levels of IFNAR1 are imperative for IFNα-mediated receptor dimerization and signalling due to the lower affinity of IFNα subtypes for the IFNAR1 subunit (relative to IFNβ) (403,404). As an example of this, downregulation of IFNAR1 on monocytes from PLWHIV desensitized these cells to IFNα stimulation *ex vivo* (270). Latently HIV-infected cell lines, U1 and OM10.1, also express lower levels of IFNAR1 in comparison to their uninfected parental cells, and are similarly less responsive to IFNα stimulation (215). In contrast to these findings, IFNAR1 expression could not be detected on mock or latently HIV infected $CD4^+$ T cells (Figure 7), nor was its expression induced in following IFNα treatment (data not shown). Given that the antibody used in these experiments was previously validated by Ranganath et al. on cell lines (215), it is likely that low IFNAR1 expression is a feature of resting $CD4^+$ T cells and is not a result of poor antibody binding efficiency.

Despite undetectable levels of IFNAR1, the dose-dependent induction of three antiviral ISG; PKR (Figure 8), ISG15 (Figure 9), and MHC I (Figure 10), was observed at 24 hours post-IFNα stimulation in both mock and latently HIV-infected $CD4^+$ T cell cultures.

a

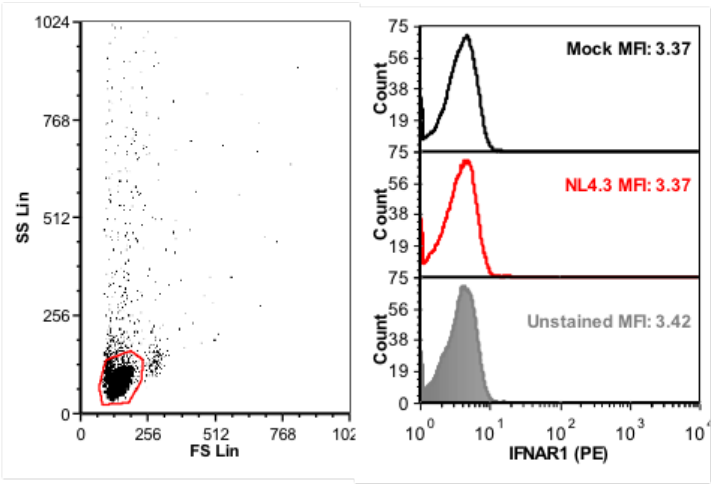
1024
768
512
256
0
SS Lin
0
256
512
768
FS Lin
75
56
38
19
0
Count
Mock MFI: 3.37
NL4.3 MFI: 3.37
Unstained MFI: 3.42
10^0
10^1
10^2
10^3
IFNAR1 (PE)

b

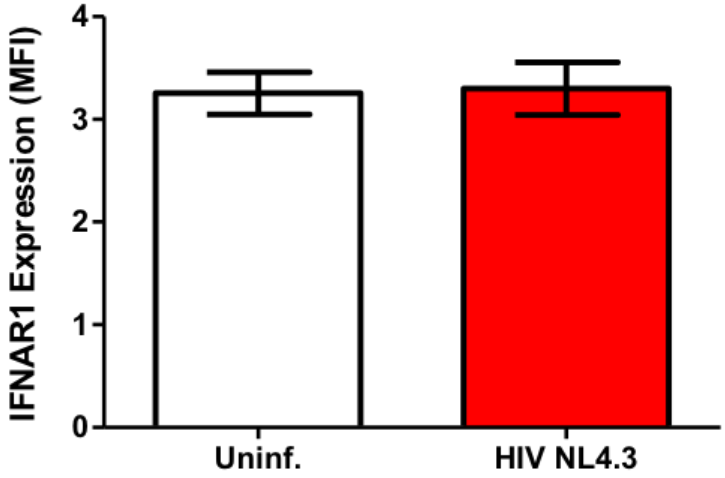
IFNAR1 Expression (MFI)
4
3
2
1
0
Uninf.
HIV NL4.3

Figure 7: Subunit 1 of the IFNα/β receptor (IFNAR1) cannot be detected on uninfected and latently HIV NL4.3-infected CD4$^+$ T cells by flow cytometry. At 3dpi, IFNAR1 surface expression was assessed on mock and latently HIV-NL4.3-infected CD4$^+$ T cells by flow cytometry. **a.** Representative dot plot demonstrating the gating of intact cells, as well as representative histograms showing IFNAR1 expression on mock (black) and HIV-infected (red) cells in comparison to unstained control (grey, filled). **b.** Cumulative IFNAR1 expression as measured by mean fluorescent intensity (n=5). Data represent mean ± SEM; n values represent separate biological replicates.

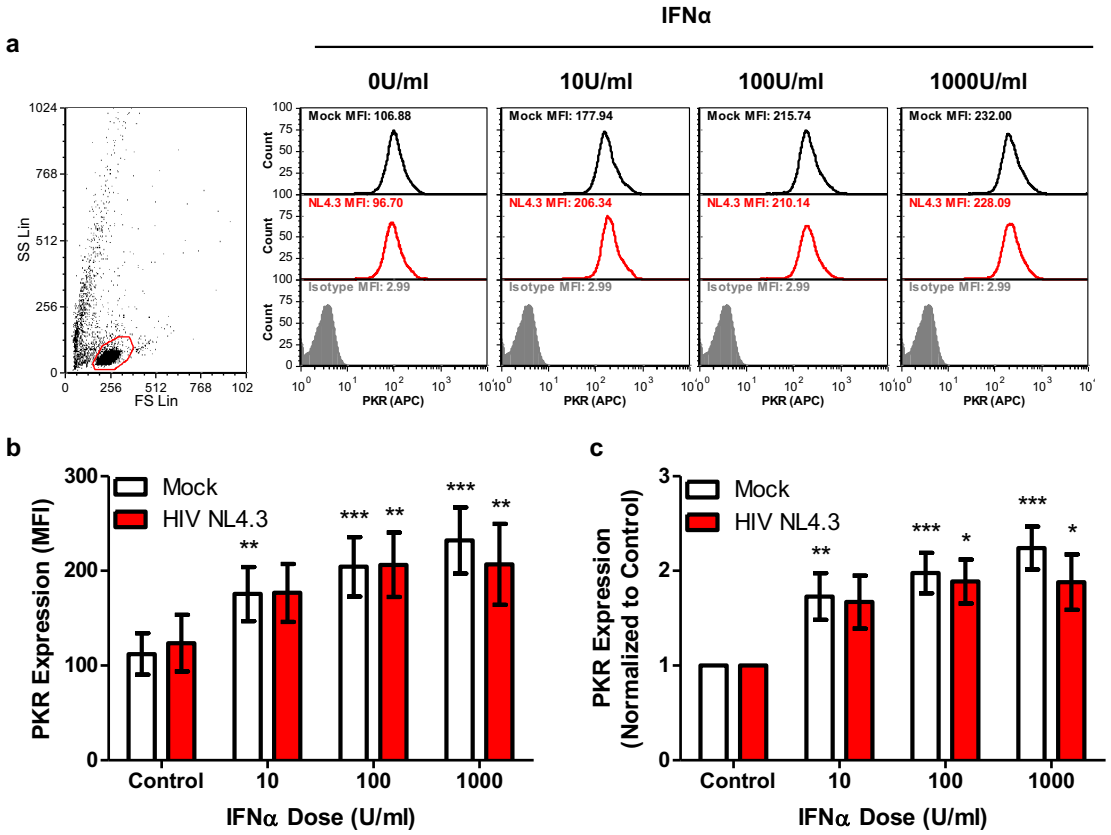
a
IFNα
0U/ml
10U/ml
100U/ml
1000U/ml
SS Lin
FS Lin
Count
Mock MFI: 106.88
Mock MFI: 177.94
Mock MFI: 215.74
Mock MFI: 232.00
NL4.3 MFI: 96.70
NL4.3 MFI: 206.34
NL4.3 MFI: 210.14
NL4.3 MFI: 228.09
Isotype MFI: 2.99
PKR (APC)
b
PKR Expression (MFI)
Mock
HIV NL4.3
Control
10
100
1000
IFNα Dose (U/ml)
c
PKR Expression (Normalized to Control)
IFNα Dose (U/ml)

Figure 8: PKR is induced in uninfected and latently HIV NL4.3-infected CD4$^+$ T cells following treatment with human IFNα. At 3dpi, mock and latently HIV-NL4.3-infected CD4$^+$ T cells were treated with IFNα. At 24 hours post-treatment, intracellular PKR expression was assessed by flow cytometry. **a.** Representative dot plot demonstrating the gating of intact cells, as well as representative histograms showing PKR induction in mock (black) and HIV-infected (red) cells in comparison to PKR isotype control (grey, filled). **b.** Cumulative PKR induction, as measured by mean fluorescent intensity (n=5; $p<0.0001$ and $p=0.0044$ by 1way repeated measures ANOVA for uninfected and NL4.3-infected CD4$^+$ T cells, respectively). **c.** PKR induction, relative to respective control (n=5; $p=0.0001$ and $p=0.0051$ by 1way repeated measures ANOVA for uninfected and NL4.3-infected CD4$^+$ T cells, respectively). *$p<0.05$, **$p<0.01$, ***$p<0.001$ by Bonferroni posttest, compared to unstimulated cells. Data represent mean ± SEM; n values represent separate biological replicates.

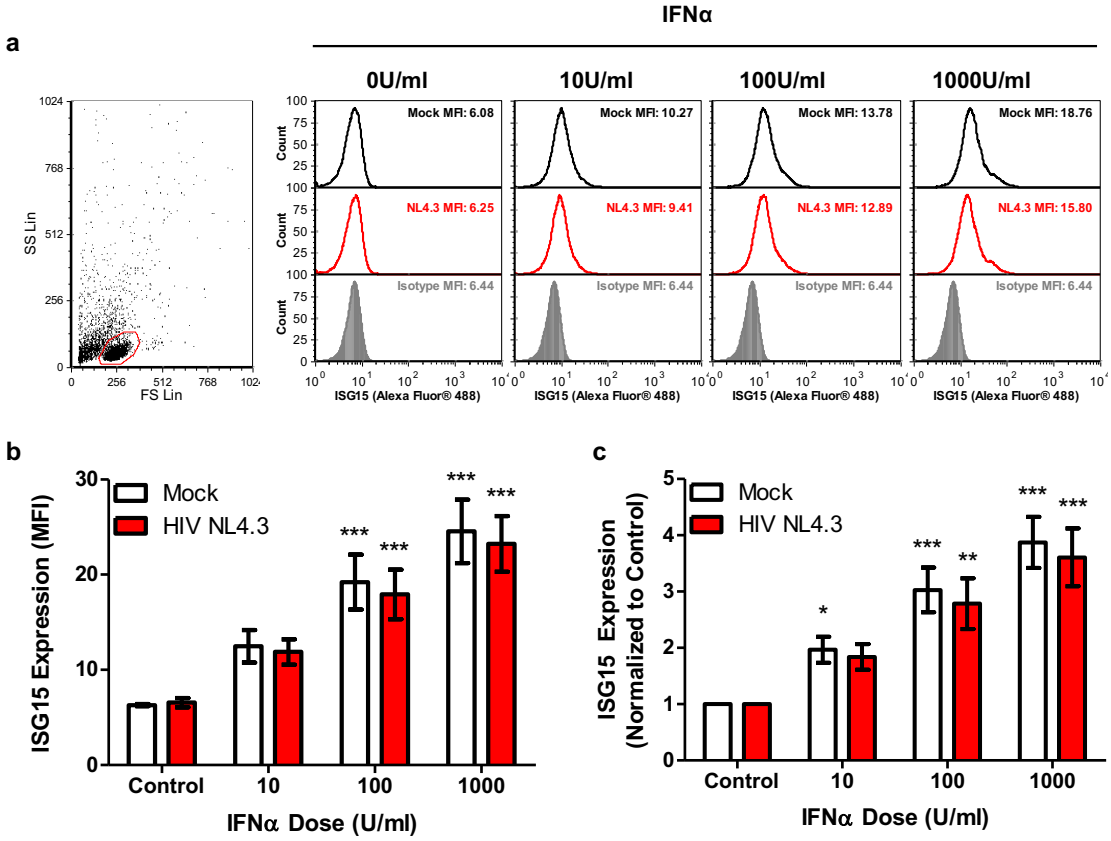
IFNα
a
0U/ml
10U/ml
100U/ml
1000U/ml
SS Lin
FS Lin
Mock MFI: 6.08
Mock MFI: 10.27
Mock MFI: 13.78
Mock MFI: 18.76
NL4.3 MFI: 6.25
NL4.3 MFI: 9.41
NL4.3 MFI: 12.89
NL4.3 MFI: 15.80
Isotype MFI: 6.44
Isotype MFI: 6.44
Isotype MFI: 6.44
Isotype MFI: 6.44
Count
ISG15 (Alexa Fluor® 488)
b
ISG15 Expression (MFI)
Mock
HIV NL4.3
Control
10
100
1000
IFNα Dose (U/ml)
c
ISG15 Expression (Normalized to Control)
Mock
HIV NL4.3
Control
10
100
1000
IFNα Dose (U/ml)

Figure 9: ISG15 is induced in uninfected and latently HIV NL4.3-infected $CD4^+$ T cells following treatment with human IFNα. At 3dpi, mock and latently HIV-NL4.3-infected $CD4^+$ T cells were treated with IFNα. At 24 hours post-treatment, intracellular ISG15 expression was assessed by flow cytometry. **a.** Representative dot plot demonstrating the gating of intact cells, as well as representative histograms showing ISG15 induction in mock (black) and HIV-infected (red) cells in comparison to ISG15 isotype control (grey, filled). **b.** Cumulative ISG15 induction, as measured by mean fluorescent intensity. **c.** ISG15 induction, relative to respective control. n=5; $p<0.0001$ by 1way repeated measures ANOVA, *$p<0.05$, **$p<0.01$, ***$p<0.001$ by with Bonferroni posttest, compared to unstimulated cells. Data represent mean ± SEM; n values represent separate biological replicates.

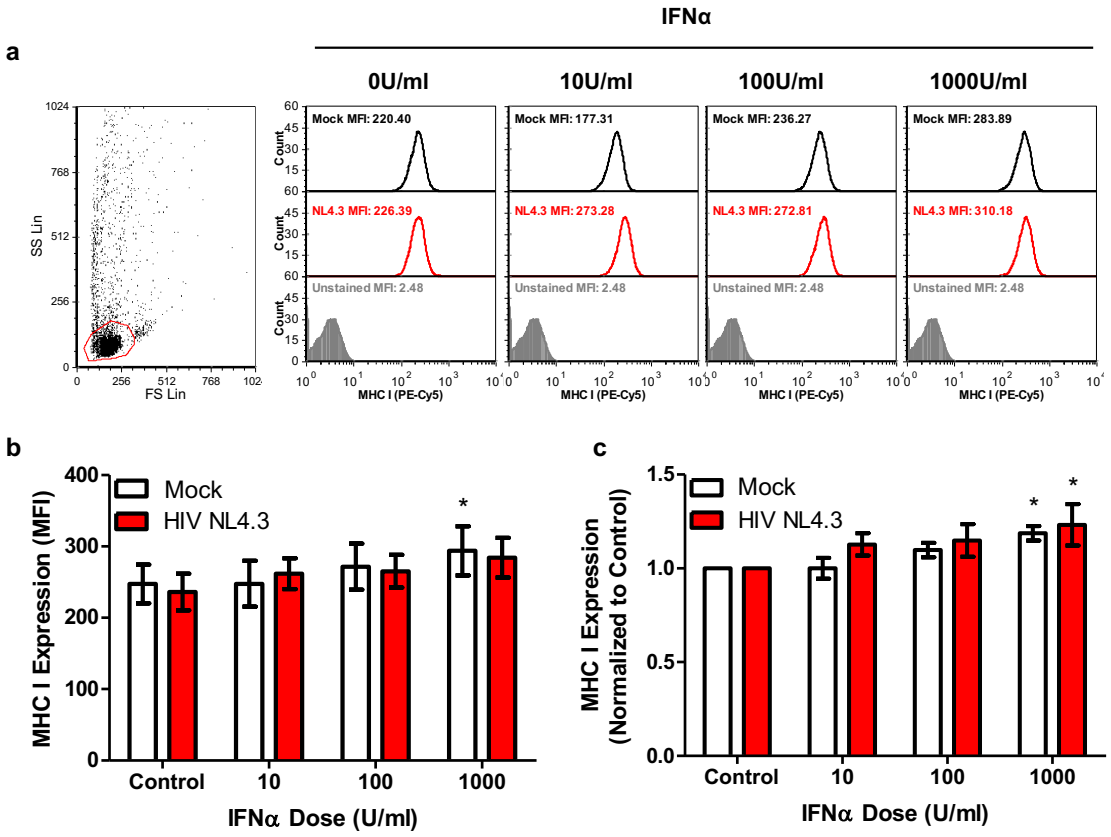
IFNα
a
0U/ml
10U/ml
100U/ml
1000U/ml
SS Lin
FS Lin
Mock MFI: 220.40
NL4.3 MFI: 226.39
Unstained MFI: 2.48
Mock MFI: 177.31
NL4.3 MFI: 273.28
Unstained MFI: 2.48
Mock MFI: 236.27
NL4.3 MFI: 272.81
Unstained MFI: 2.48
Mock MFI: 283.89
NL4.3 MFI: 310.18
Unstained MFI: 2.48
Count
MHC I (PE-Cy5)
b
MHC I Expression (MFI)
Mock
HIV NL4.3
Control
10
100
1000
IFNα Dose (U/ml)
c
MHC I Expression (Normalized to Control)
Mock
HIV NL4.3
Control
10
100
1000
IFNα Dose (U/ml)

Figure 10: MHC I is induced on uninfected and latently HIV NL4.3-infected CD4$^+$ T cells following treatment with human IFNα. At 3dpi, mock and latently HIV-NL4.3-infected CD4$^+$ T cells were treated with IFNα. At 24 hours post-treatment, surface MHC I expression was assessed by flow cytometry. **a.** Representative dot plot demonstrating the gating of intact cells, as well as representative histograms showing MHC I induction on mock (black) and HIV-infected (red) cells in comparison to unstained control (grey, filled). **b.** Cumulative MHC I induction, as measured by mean fluorescent intensity (n=5; p=0.0076 and p=0.06 by 1way repeated measures ANOVA for uninfected and NL4.3-infected CD4$^+$ T cells, respectively). **c.** MHC I induction, relative to respective control (n=5; p=0.013 and p=0.044 by 1way repeated measures ANOVA for uninfected and NL4.3-infected CD4$^+$ T cells, respectively). *p<0.05 by Bonferroni posttest, compared to unstimulated cells. Data represent mean ± SEM; n values represent separate biological replicates.

3.3.3 Transfection with the synthetic RNA, Poly(I:C), induces ISG expression in mock and latently HIV infected CD4$^+$ T cells

Sensing of viral RNAs by cytoplasmic PRR leads to the induction of IFNα/β, as well as the IFN-independent ISG induction. The latter occurs via the phosphorylation of IRF3, which is translocated to the nucleus and interacts with the IFN-stimulated response element within the ISG promoter (230,232,257). Since resting CD4$^+$ T cells did not produce IFNα following transfection with a synthetic dsRNA, low molecular weight (LMW)-poly(I:C) (data not shown), the ability of latently HIV-infected cells to sense and respond to foreign RNA was assessed via measurement of ISG induction. Mock and latently HIV-infected CD4$^+$ T cells were transfected with LMW-poly(I:C), and the induction of PKR and ISG15 was measured by flow cytometry at 24 hours post-transfection. Similar to IFNα-induced ISG expression, the induction of PKR (Figure 11) and ISG15 (Figure 12) by LMW-poly(I:C) did not differ between mock and latently HIV-infected CD4$^+$ T cells.

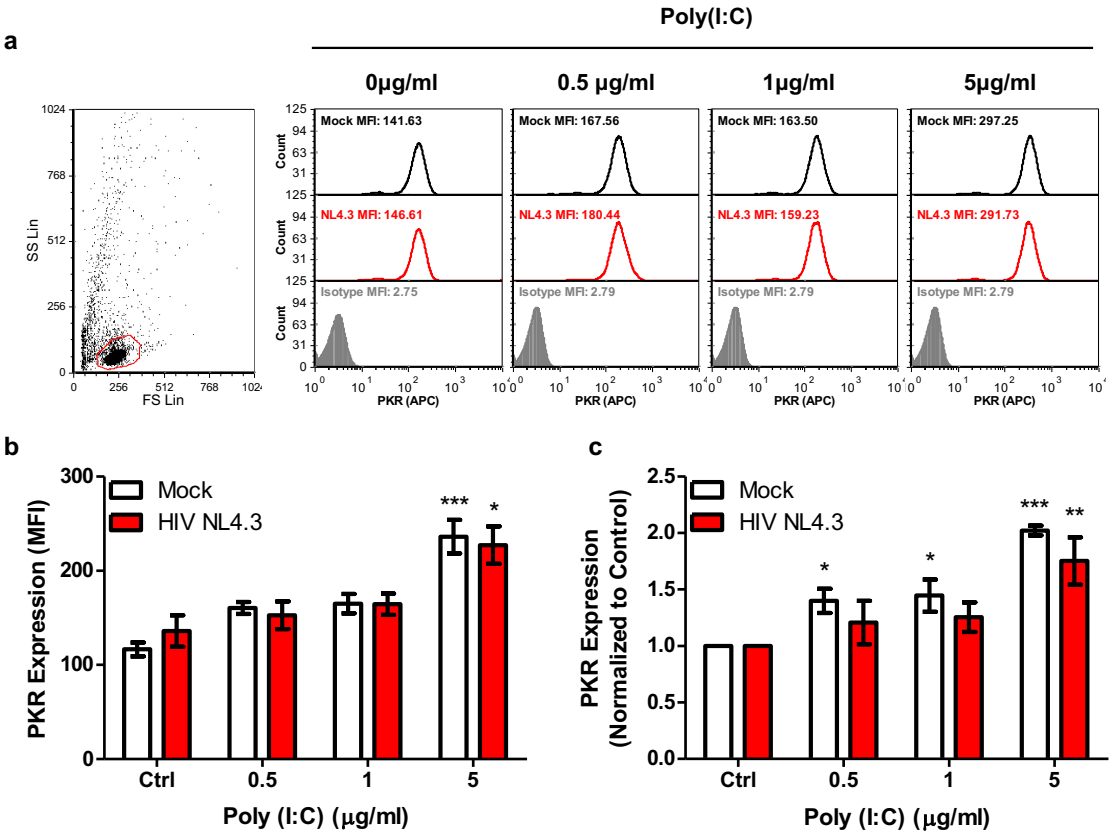
a
Poly(I:C)
0μg/ml
0.5 μg/ml
1μg/ml
5μg/ml
SS Lin
FS Lin
Count
PKR (APC)
Mock MFI: 141.63
NL4.3 MFI: 146.61
Isotype MFI: 2.75
Mock MFI: 167.56
NL4.3 MFI: 180.44
Isotype MFI: 2.79
Mock MFI: 163.50
NL4.3 MFI: 159.23
Isotype MFI: 2.79
Mock MFI: 297.25
NL4.3 MFI: 291.73
Isotype MFI: 2.79
b
PKR Expression (MFI)
Mock
HIV NL4.3
Ctrl
0.5
1
5
Poly (I:C) (μg/ml)
c
PKR Expression (Normalized to Control)
Mock
HIV NL4.3
Ctrl
0.5
1
5
Poly (I:C) (μg/ml)

Figure 11: PKR is induced in uninfected and latently HIV NL4.3-infected CD4$^+$ T cells following transfection with poly(I:C). At 3dpi, mock and latently HIV-NL4.3-infected CD4$^+$ T cells were transfected with the synthetic RNA, poly(I:C). At 24 hours post-transfection, intracellular PKR expression was assessed by flow cytometry. **a.** Representative dot plot demonstrating the gating of intact cells, as well as representative histograms showing PKR induction in mock (black) and HIV-infected (red) cells in comparison to PKR isotype control (grey, filled). **b.** Cumulative PKR induction, as measured by mean fluorescent intensity (n=5; $p<0.0001$ and 0=0.012 for uninfected and NL4.3-infected CD4+ T cells, respectively). **c.** PKR induction, relative to respective control (n=5; $p<0.0001$ and 0=0.0066 for uninfected and NL4.3-infected CD4+ T cells, respectively). *$p<0.05$, **$p<0.01$, ***$p<0.001$ by Bonferroni posttest, compared to unstimulated cells. Data represent mean ± SEM; n values represent separate biological replicates.

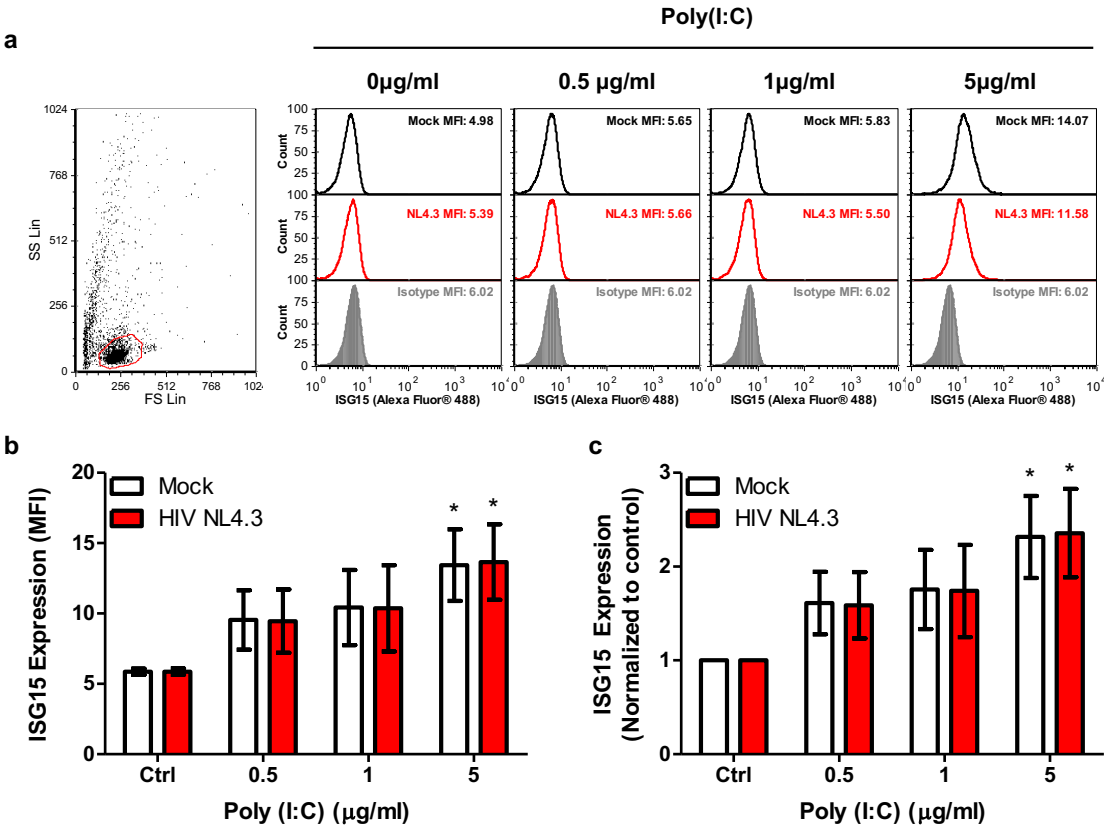
a
Poly(I:C)
0μg/ml
0.5 μg/ml
1μg/ml
5μg/ml
SS Lin
FS Lin
Count
Mock MFI: 4.98
NL4.3 MFI: 5.39
Isotype MFI: 6.02
Mock MFI: 5.65
NL4.3 MFI: 5.66
Isotype MFI: 6.02
Mock MFI: 5.83
NL4.3 MFI: 5.50
Isotype MFI: 6.02
Mock MFI: 14.07
NL4.3 MFI: 11.58
Isotype MFI: 6.02
ISG15 (Alexa Fluor® 488)
b
ISG15 Expression (MFI)
Mock
HIV NL4.3
Ctrl
0.5
1
5
Poly (I:C) (μg/ml)
c
ISG15 Expression (Normalized to control)
Mock
HIV NL4.3
Ctrl
0.5
1
5
Poly (I:C) (μg/ml)

Figure 12: ISG15 is induced in uninfected and latently HIV NL4.3-infected CD4$^+$ T cells following transfection with poly(I:C). At 3dpi, mock and latently HIV-NL4.3-infected CD4$^+$ T cells were transfected with the synthetic RNA, poly(I:C). At 24 hours post-transfection, intracellular ISG15 expression was assessed by flow cytometry. **a.** Representative dot plot demonstrating the gating of intact cells, as well as representative histograms showing ISG15 induction in mock (black) and HIV-infected (red) cells in comparison to ISG15 isotype control (grey, filled). **b.** Cumulative ISG15 induction, as measured by mean fluorescent intensity (n=5; p=0.030 and 0=0.034 for uninfected and NL4.3-infected CD4+ T cells, respectively).. **c.** ISG15 induction, relative to respective control (n=5; p=0.028 and 0=0.033 for uninfected and NL4.3-infected CD4+ T cells, respectively). *p<0.05 by Bonferroni posttest, compared to unstimulated cells. Data represent mean ± SEM; n values represent separate biological replicates.

3.4 Discussion

In summary, this chapter describes the assessment of antiviral ISG induction in an *in vitro,* primary $CD4^+$ T cell model of HIV latency. The status of the IFN1 response in latently HIV-infected cells has, to our knowledge, only been investigated in cell line models of infection (215). These findings therefore represent an interesting observation that holds significance for our understanding of the latent HIV reservoir.

3.4.1 Characterizing IFN1 signalling in an in vitro model of HIV latency

As previously demonstrated by Hardy et al., the downregulation of IFNAR1 expression on the surface of monocytes isolated from PLWHIV inhibited IFN1 signalling in response to IFNα stimulation (270). In this study, IFNAR1 downregulation was hypothesized to have occurred as a result of repeated exposure to infectious viral particles, as well as ongoing inflammatory responses. It was therefore somewhat surprising to see that, despite very low levels of IFNAR1 surface expression, both uninfected and latently HIV-infected primary $CD4^+$ T cells induced the expression of antiviral ISG in response to IFNα-stimulation. Furthermore, *in vitro* exposure to infectious viral particles does not appear to desensitize cells to exogenous IFNα stimulation. This observation could be explained by the low levels of viral infection following spinoculation and the short time-frame (3 days) for infection itself. It is also important to note that IFNAR2 expression was not measured during these experiments. IFNAR1/IFNAR2 heterodimerization is required for the cell to respond appropriately to IFNα, while

IFNβ has been found to trigger IFN1 signalling via IFNAR2 homodimerization (405). Although not currently reported in literature, $CD4^+$ T cells may be capable of upregulating IFNα-induced ISG expression in a similar manner. Alternatively, levels of IFNAR1 on the cell surface may simply be too low to be detected by flow cytometry. Nonetheless, it would appear that the bulk of HIV-exposed and latently HIV-infected cells maintain their ability to respond to exogenous IFNα.

Similarly, transfection with LMW-poly(I:C) induced PKR and ISG15 expression in HIV-infected and uninfected $CD4^+$ T cells. Induction was independent of autocrine and/or paracrine IFN1 signalling, since IFNα secretion was not detected following transfection. pDC are the primary producers of IFNα/β during viral infection *in vivo* (406,407). It is therefore not surprising that IFNα was not detected in cell supernatants. This finding supports previous literature suggesting that the sensing of foreign nucleic acids by cytoplasmic PRR can lead to the direct induction of antiviral ISG (230,232,408). Moreover, it would appear that these PRR and their downstream signalling pathways are intact in latently HIV-infected $CD4^+$ T cell cultures.

Overall, differences in IFN1 signalling between uninfected and latently HIV-infected $CD4^+$ T cells could not be identified using an *in vitro* model of HIV latency. This sheds light on several important considerations and/or pitfalls of such models, including low rates of HIV infection and an inability to enrich HIV-infected cells from the bulk population. Unlike HIV infection of activated $CD4^+$ T cells, primary cell models of latency generate only a small population of HIV-infected cells. In the model used here, for example, only ~0.5-1% of cells contained intact provirus. These numbers are similar to those previously reported by Saleh et al. (122,355),

indicating that low rates of infection are representative of the model itself. When assessed as a bulk population (as was done by flow cytometry in the above experiments), the dominant population of uninfected bystander cells may mask potential IFN1 signalling defects within the much smaller population of latently HIV-infected cells. Moreover, current models do not permit the enrichment of latently HIV-infected cells. Latency requires that the HIV provirus is maintained in a replication-silenced state, rendering the use of a reporter virus to differentiate latently-infected and uninfected cells largely ineffective. To address this, dual-reporter viruses that express a fluorescent reporter molecule independent of the HIV promoter have been used to delineate HIV latency in macrophages (136) and $CD4^+$ T cells (409), and may be of future consideration.

This also brings to question the ability of *in vitro* latency models to accurately represent the *in vivo* latent reservoir. Without a doubt, the ability to establish HIV latency *in vitro,* over a matter of days, affords a powerful model with which to study latency reversal agents or reservoir clearance strategies. In fact, the study of viral reactivation in common latency models revealed that several, including the model used here, had levels of HIV reactivation comparable to those observed in $CD4^+$ T cells from HIV-positive individuals (124). Still, the use of a laboratory-adapted HIV strain—in our case, HIV NL4.3—may not truly recapitulate *in vivo* reservoir characteristics. Transmitted/founder viruses are particularly resistant to IFN1-mediated restriction (410,411), suggesting that reservoirs established during early infection could maintain this IFN1-evasive phenotype. Given that clonal expansion is hypothesized to play an important role in the maintenance of the latent viral reservoir

over time (412,413), progeny cells may harbour a similarly IFN1-evasive latent provirus. Downregulation of IFN1 responses has also been demonstrated in clonally-expanding $CD4^+$ T cells (414), indicating that the cell itself may undergo periods of IFN1-insensitivity, independent of HIV infection. These characteristics cannot be easily mirrored using *in vitro* latency models. Thus, while primary cell models are an excellent tool for the study of LRAs, they demonstrate limited utility for studying molecular characteristics of the latent HIV reservoir.

3.4.2 The relevance of IFN1 signalling defects for HIV reservoir eradication

A thorough understanding of the IFN1 response in latently infected cells has important implications for the development of novel reservoir clearance strategies. As demonstrated in Chapters 4 and 5 of this thesis, and by Ranganath et al. (354,402), IFN1 signalling defects facilitate the infection and killing of HIV-infected cells by the OV, MG1. Identifying the mechanism(s) by which these impairments occur will enable the engineering of OV to be highly specific for HIV-infected cells that harbour these impairments.

Conversely, an intact IFN1 response could be used to eradicate latently infected cells. Li et al. have demonstrated the reactivation and killing of latently HIV-infected cells using the retinoic acid derivative, acitretin (184). In this model, HIV RNA was sensed by RIG-I, which triggered apoptosis in HIV^+ cells (184). Although the utility of acitretin as an LRA has been refuted (185), the link between IFN1 signalling and the induction of programmed cell death is well-established (415-418). Consequently, PRR with links to pro-apoptotic proteins may be an alternative target by which to eradicate LRA-treated HIV-infected cells.

3.5 Future directions

Characterization of the latent HIV reservoir will require the development of a reliable *in vitro* model, in which infected cells can be differentiated from their uninfected counterparts. Without this, the large population of bystander cells will overshadow changes in gene expression or protein induction within the small population of latently-infected cells. A dual-reporter virus has been developed for this purpose (409), and has been used to track latency establishment in primary $CD4^+$ T cells (419). This virus, as well as a similar dual-reporter virus developed by Dahabieh et al. (420), lack *nef* and *env*, ensuring that infection is limited to a single round. It is therefore unlikely that models using these viral constructs will fully recapitulate latency *in vivo*—an important consideration when attempting to characterize latently HIV-infected cells at the molecular level. Still, engineering of a full-length, dual-reporter virus is challenging. The use of single-round reporter viruses may therefore be a necessary interim step for the study of HIV latency.

The identification of a cellular marker of latency is an equally important objective. This will facilitate the study of latently HIV-infected cells *ex vivo*, and ensure that up-and-coming eradication strategies are tested using an appropriate primary cell model. To date, several groups have sought to identify specific cellular biomarkers of HIV latency, such as CD32a and CD2 (386,387). The ability of CD32a to reliably identify latently HIV-infected cells has, however, been recently refuted (421-423). Noto et al. have also shown that lymph node $CD4^+$ T cells expressing PD-1 and CD32 harbour persistent HIV transcription (424). This cellular phenotype

may therefore be more involved in maintaining persistent viral infection of lymphoid tissues than transcriptionally-silent HIV latency, as previously suggested (387).

CD2 as a marker of latently HIV-infected $CD4^+$ T cells has been similarly debated. Tomalka et al. have suggested that CD2 is a marker of activated T cells that are more susceptible to HIV infection, rather than a specific marker of latency (425). Regardless, this study demonstrated that the $CD2^+$-targeting biotherapeutic, Alefacept, enhanced the *ex vivo* killing of HIV-infected $CD4^+$ T cells by NK cells (425). While the search continues for a reliable marker of latently HIV-infected cells, CD2 may therefore remain a valuable target for reservoir clearance strategies.

3.6 Conclusion

In conclusion, ISG induction following IFNα or poly(I:C) stimulation was observed in both an *in vitro*, primary $CD4^+$ T cell model of HIV latency, as well as uninfected cells. HIV-exposed $CD4^+$ T cells therefore remain capable of responding to antiviral stimuli. Whether this is also true of latently HIV-infected $CD4^+$ T cells remains unknown, since this small cell population lacks latency-specific surface markers that would facilitate its identification/enrichment *in vitro*. Still, this finding lends support to the use of an OV-based therapy to eradicate HIV reservoir cells, since an impaired IFN1 response in bystander $CD4^+$ T cells would lead to off-target OV infection and cytopathogenicity. This is in agreement with recently published findings, which indicated that OV are capable of killing latently HIV-infected $CD4^+$ T cells in a highly targeted manner (354).

Chapter 4: Type I IFN defects in HIV-infected monocyte-derived macrophages

4.1 Introduction

4.1.1 Rational

To be of clinical use, HIV cure strategies must target all cell types involved in maintaining HIV persistence *in vivo*. This includes HIV-infected macrophages, which reside within various tissues and support ongoing viral replication (reviewed in (426,427)). Unfortunately, these reservoir cells are not yet identifiable via specific surface markers of either cellular or viral origin. Eradication may therefore require the identification of an intracellular pathway and/or protein unique to HIV-infected myeloid cells. This will also ensure that potential eradication strategies are selective for the HIV reservoir and minimize bystander cell death.

In line with this, the activation of pro-apoptotic proteins has been shown to selectively kill both HIV-infected and SIV-infected macrophages (428). Other cellular signalling pathways known to be targeted by HIV have not yet been investigated in this context, however. The IFN1 response is one such example, which is impaired in HIV-infected myeloid cells (234,245,248,263) and has been exploited for therapeutic purposes in other diseases such as cancer (301,338). Findings within Chapter 4 of this thesis are intended to characterize HIV-mediated IFN1 signalling defects within MDM. Importantly, the model system employed here is novel in that it uses an HIV reporter virus, which facilitates the study of HIV-infected and HIV-uninfected bystander populations. The findings presented here further support the use of a novel oncolytic virus-based therapy for HIV reservoir clearance; the results of which are presented in Chapters 5-7.

4.1.2 Macrophages form an HIV reservoir

Macrophages form a unique, multifaceted cellular reservoir for HIV. As these cells are inherently tissue-resident, HIV-infected macrophages quickly occupy the central nervous system, gastrointestinal and reproductive tracts, lung, and lymph nodes (107,108,429-431), where sub-optimal concentrations of cART permit ongoing viral replication (432-434). Macrophages are also hypothesized to support primarily productive, rather than latent, infection (108,136). Combined with their ability to secrete a number of cytokines involved in T cell and monocyte migration (142,147,435), this can lead to the infection of circulating target cells that have been recruited to lymphoid tissues (147,152,288,436). Here, direct cell-to-cell transfer of viral particles is the predominant mechanism of HIV infection—a process which is ineffectively blocked by antiretroviral drugs (152). Finally, macrophages involved in tissue homeostasis and remodeling may become infected by phagocytosing dead or dying HIV-infected $CD4^+$ T cells (139).

Unlike $CD4^+$ T lymphocytes, HIV-infected macrophages do not succumb to virus-mediated cytopathic effects. Early experiments attributed the survival of HIV-infected macrophages to NFκB activation and the increased expression of several anti-apoptotic proteins (437,438). Resistance to TRAIL-mediated apoptosis is further conferred by the HIV Envelope protein (141). Similarly, HIV Nef orchestrates phosphorylation-mediated inhibition of the pro-apoptotic protein, Bad, by PI3K and PAK (439). Finally, Reynoso et al. showed that HIV infection of MDM protected these cells against oxidative stress via upregulation of cellular telomerase activity (440). The prolonged survival of HIV-infected macrophages within

tissues—estimated to be within the span of several weeks by mathematical and animal models (107,441)—can therefore be attributed to cellular as well as viral characteristics. Not only does this preclude the use of latency-reversal agents for the eradication of HIV (167), but productively infected macrophages may contribute to IFNγ-driven inflammation within lymphoid tissues (142,435). The significant role of these cells in HIV persistence and immunopathogenesis is therefore clear.

4.1.3 Impairment of the type I IFN response in HIV-infected macrophages

HIV-mediated dysregulation of cellular processes is not limited to the induction of pro-survival signals. HIV-infected macrophages display reduced phagocytic capacity (442,443), as well as impaired cytokine production (444) and T cell stimulatory function (445,446). In addition, HIV can potently block innate antiviral signalling pathways involved in the IFN1 response. These impairments range from the degradation of key RNA-sensing proteins like RIG-I (234), to the impaired expression of key antiviral ISG, including OAS1, PKR, and ISG15 (272,275). The release of IFNα/β by HIV-infected macrophages is also reduced, likely due to the dysregulation of toll-like receptor (TLR) or RLR signalling (245,248,252).

It is important to note that many of the above studies measure ISG mRNA, but do not consider antiviral protein expression. Nonetheless, the impairment of innate antiviral signalling appears to be characteristic of HIV-infected macrophages, and likely contributes to the inability of these cells to prevent subsequent rounds of viral infection *in vivo*.

4.2 Hypothesis

The type I IFN response is inhibited in monocyte-derived macrophages during HIV infection.

4.3 Results

4.3.1 An HIV reporter virus facilitates the detection and enrichment of HIV infected monocyte-derived macrophages

IFN1 signalling pathways within HIV-infected, primary human MDM have been studied, revealing impaired pathogen recognition (234,239,240), IFN1 induction (245,248,252), and the expression of key antiviral ISG (272,275). A pitfall of these studies, however, is that the experiments performed fail to differentiate between HIV-infected and HIV-uninfected MDM in culture. Instead, results are obtained using the bulk cell population, which consists primarily of HIV-uninfected cells. To address this, and to allow the description of potential IFN1 signalling differences in HIV-infected and HIV-uninfected MDM, the CCR5-tropic reporter virus was used. Developed in the lab of Dr. Michel Tremblay, HIV NL4.3 BAL-IRES-HSA is a full-length, replication competent virus clone which encodes the murine surface glycoprotein, heat-stable antigen (HSA; CD24) (357).

The timeline of MDM infection and subsequent experiments is shown in (Figure 13). To establish *in vitro* HIV infection in MDM, cells were exposed to HIV NL4.3 BAL-IRES-HSA for 6 days, after which distinct HSA^+ and HSA^- populations could be observed by flow cytometry (Figure 14a). Similar to others (358), HSA^+ MDM continued to release HIV-1 p24 antigen into culture supernatants following

enrichment via immunomagnetic bead separation, whereas HSA^- cells did not (Figure 14b,c). HSA^+ MDM were therefore defined as “HIV-infected,” and HSA^- MDM were defined as “bystander” cells.

An important characteristic of the HIV NL4.3 BAL-IRES-HSA virus is the insertion of an internal ribosome entry site (IRES) between HSA and *nef*. This allows for the expression of a functional Nef protein. As previously demonstrated by Deshiere et al., the expression of a functional Nef protein in MDM infected with HIV NL4.3 BAL-IRES-HSA reduces surface CD4 expression (358). This finding was confirmed by measuring MHC I expression on the surface of infected, HSA^+ MDM, since Nef is known to impair the trafficking of HLA-A and B to the cell surface (143,447,448). In agreement with these previous studies, MHC I expression was significantly lower on HSA^+ MDM than on HSA^- MDM (Figure 15a,b). The insertion of the IRES-HSA construct therefore does not inhibit the expression of a functional HIV Nef following *in vitro* infection of human MDM.

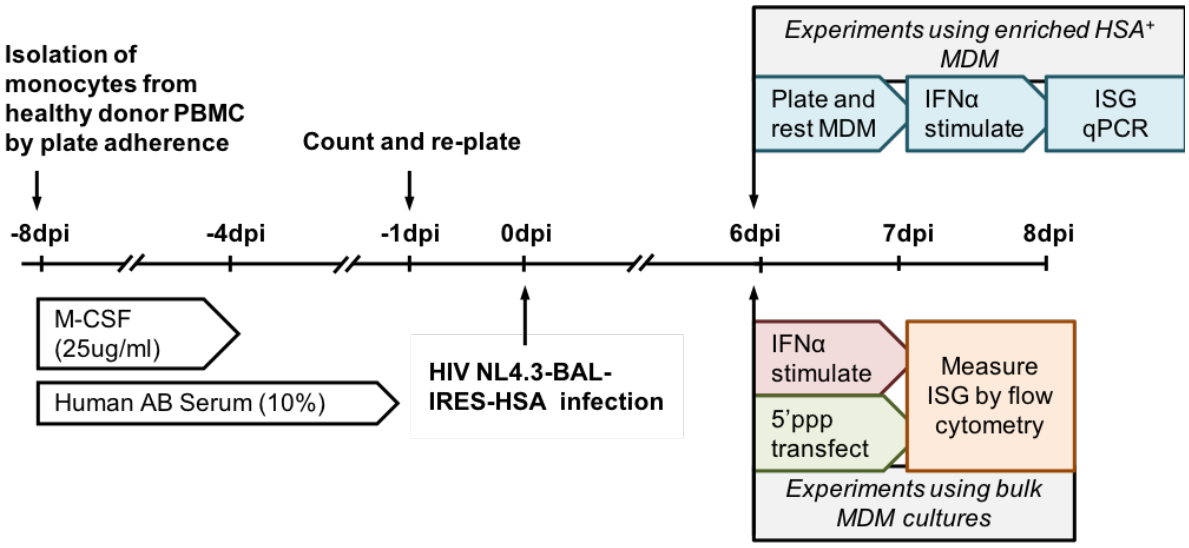
Isolation of monocytes from healthy donor PBMC by plate adherence
Count and re-plate
Experiments using enriched HSA+ MDM
Plate and rest MDM
IFNα stimulate
ISG qPCR
-8dpi
-4dpi
-1dpi
0dpi
6dpi
7dpi
8dpi
M-CSF (25ug/ml)
Human AB Serum (10%)
HIV NL4.3-BAL-IRES-HSA infection
IFNα stimulate
5'ppp transfect
Measure ISG by flow cytometry
Experiments using bulk MDM cultures

Figure 13: Timeline of differentiation and HIV-infection of monocyte-derived macrophages from healthy donor PBMC.

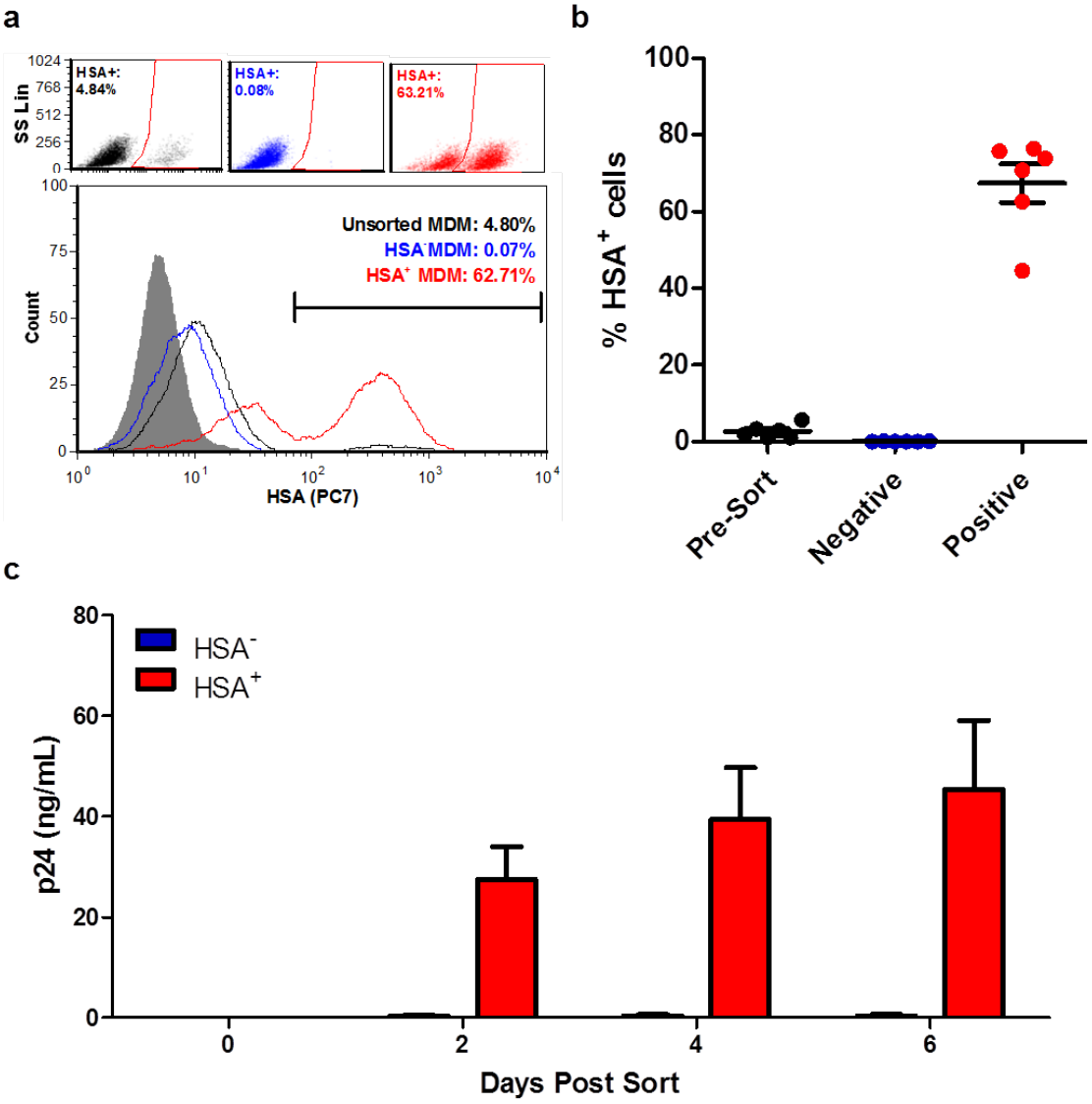
a
HSA+: 4.84%
HSA+: 0.08%
HSA+: 63.21%
SS Lin
Unsorted MDM: 4.80%
HSA- MDM: 0.07%
HSA+ MDM: 62.71%
Count
HSA (PC7)
b
% HSA+ cells
Pre-Sort
Negative
Positive
c
HSA-
HSA+
p24 (ng/mL)
Days Post Sort

Figure 14: Enrichment of HSA^+ MDM. a. Representative histograms showing frequency of HSA^+ MDM pre-sort (black), as well as within the HSA-negative (blue) and HSA-enriched (red) cell fraction. HSA isotype control is shown in grey. **b.** Cumulative purity of HSA-enriched MDM fraction post-sort (n=6). **c.** HIV p24 antigen release by enriched HSA^+ and HSA^- MDM (n=4). Data represent mean ± SEM; n values represent separate biological replicates.

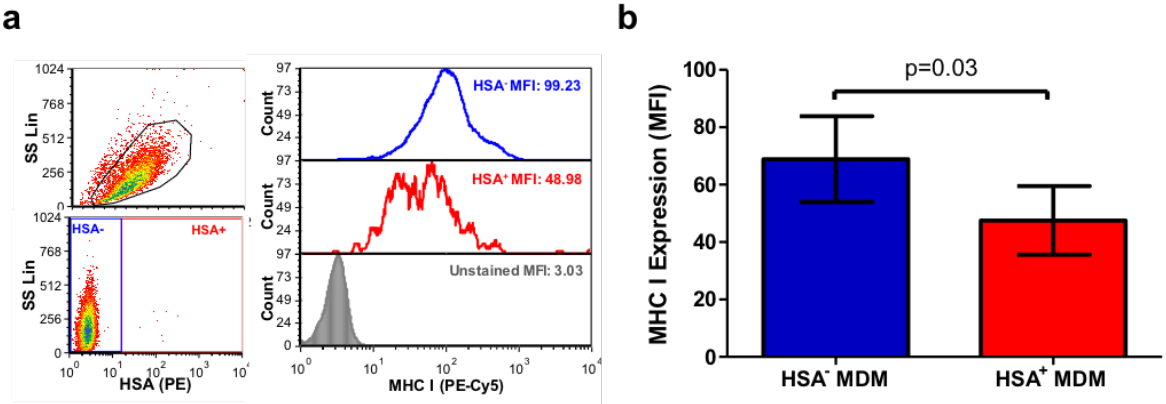
a
b
SS Lin
HSA (PE)
HSA-
HSA+
Count
HSA- MFI: 99.23
HSA+ MFI: 48.98
Unstained MFI: 3.03
MHC I (PE-Cy5)
MHC I Expression (MFI)
p=0.03
HSA- MDM
HSA+ MDM

Figure 15: MHC I expression is reduced on HSA$^+$ MDM in comparison to HSA$^-$ MDM. At 6dpi, MHC I expression was measured on HSA$^-$ and HSA$^+$ MDM flow cytometry. **a.** Representative dot plots and histograms demonstrating the gating strategy employed during data analysis. Cellular debris were excluded (shown in black), after which HSA$^-$ (blue) and HSA$^+$ (red) MDM were gated upon. Histogram peak counts (y-axis) for HSA$^-$ and HSA$^+$ populations were normalized to that of the unstained control for visualization purposes. **b.** Cumulative MHC I expression on HSA$^-$ (blue) and HSA$^+$ (red) MDM (n=6; p=0.03 by paired, one-tailed t-test). Data represent mean ± SEM; n values represent separate biological replicates.

4.3.2 HIV induces IFN-stimulated gene expression within HIV-infected, but not bystander, monocyte-derived macrophages

Next, MDM were assessed for the induction of an IFN1 response at 6 days post-HIV infection. Although no IFNα/β could be detected within cell culture supernatants at this timepoint, the expression of two antiviral ISG, PKR and ISG15, was significantly elevated within HSA^+ MDM (Figure 16). This is in agreement with the findings of Nasr et al., who also observed the direct induction of ISG in HIV-infected MDM without detectable IFNα/β production (449). Importantly, ISG expression did not significantly differ between bystander, HSA^- MDM and control (uninfected) MDM that had not been exposed to HIV. ISG induction following HIV infection is therefore limited to productively infected cells, and is not observed in HSA^- bystander cells.

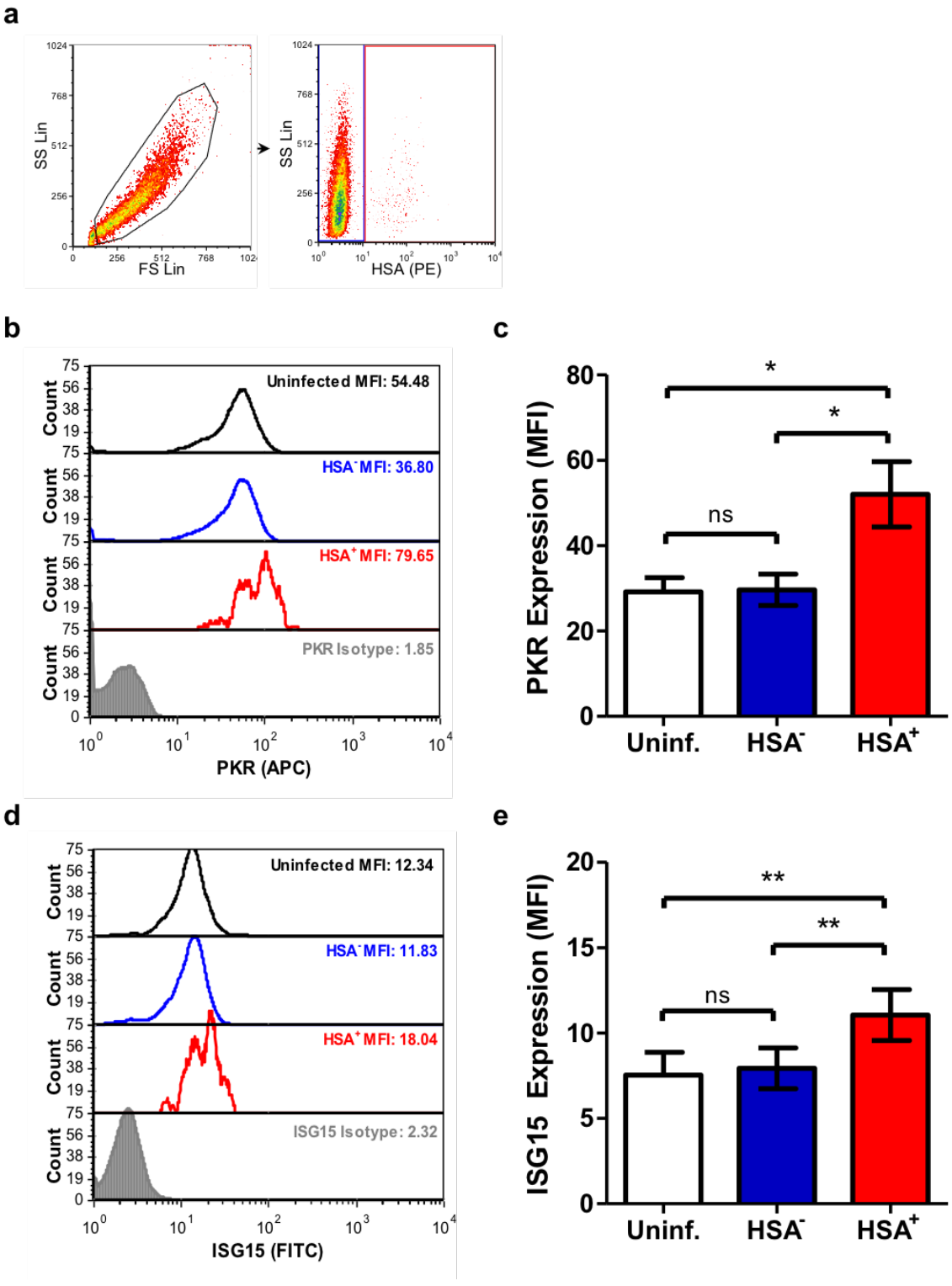
a
SS Lin
FS Lin
HSA (PE)
b
Uninfected MFI: 54.48
HSA⁻ MFI: 36.80
HSA⁺ MFI: 79.65
PKR Isotype: 1.85
Count
PKR (APC)
c
PKR Expression (MFI)
ns
*
*
Uninf.
HSA⁻
HSA⁺
d
Uninfected MFI: 12.34
HSA⁻ MFI: 11.83
HSA⁺ MFI: 18.04
ISG15 Isotype: 2.32
Count
ISG15 (FITC)
e
ISG15 Expression (MFI)
ns
**
**
Uninf.
HSA⁻
HSA⁺

Figure 16: ISG expression is elevated in HSA^+ MDM at baseline, in comparison to HSA^- and uninfected MDM. a. Representative dot plots demonstrating the gating strategy employed during data analysis. Cellular debris were excluded (shown in black), after which HSA^- (blue) and HSA^+ (red) MDM were gated upon. **b.** Representative histogram depicting PKR expression in unstimulated, uninfected (black), HSA^- (blue), and HSA^+ (red) MDM. **c.** Cumulative basal PKR expression in uninfected (black), HSA^- (blue), and HSA^+ (red) MDM (n=6; p=0.0013 by 1way repeated measures ANOVA). **d.** Representative histogram depicting ISG15 expression in uninfected (black), HSA^- (blue), and HSA^+ (red) MDM. **e.** Cumulative basal ISG15 expression in uninfected (black), HSA^- (blue), and HSA^+ (red) MDM (n=7; p=0.0001 by 1way repeated measures ANOVA). Note: histogram peak counts (y-axis) for uninfected, HSA^-, and HSA^+ populations were normalized to that of the isotype control for visualization purposes. *p<0.01, **p<0.001 by Bonferroni multiple comparisons test. Data represent mean ± SEM; n values represent separate biological replicates.

4.3.3 HIV-infected monocyte-derived macrophages are less responsive to exogenous IFNα than bystander cells

Next, the ability of MDM to respond to exogenous IFNα was assessed. Based on prior optimization, 24 hours was selected as the optimal time at which to measure IFNα-induced ISG expression. At this timepoint, cells were detached and the expression of PKR and ISG15 was assessed by flow cytometry. The gating strategy used to assess ISG induction in HSA^+ and HSA^- MDM populations is as shown in Figure 15a.

Although PKR and ISG15 expression remained elevated in HSA^+ MDM in comparison to HSA^- MDM, the induction of both ISG relative to baseline values was significantly lower in HSA^+ cells (Figure 17 and 18). Importantly, PKR induction was similar between HIV-unexposed MDM and HSA^- MDM (Figure 19a), while ISG15 induction was significantly higher in HIV-unexposed MDM (Figure 19b). Prior exposure to infectious HIV virions may therefore desensitize bystander MDM to IFNα stimulation. Productive HIV infection, however, appears to decrease the cell's ability to induce ISG expression. A virus-specific mechanism may therefore be responsible for the observed differences in IFNα-mediated ISG induction between HSA^- and HSA^+ MDM.

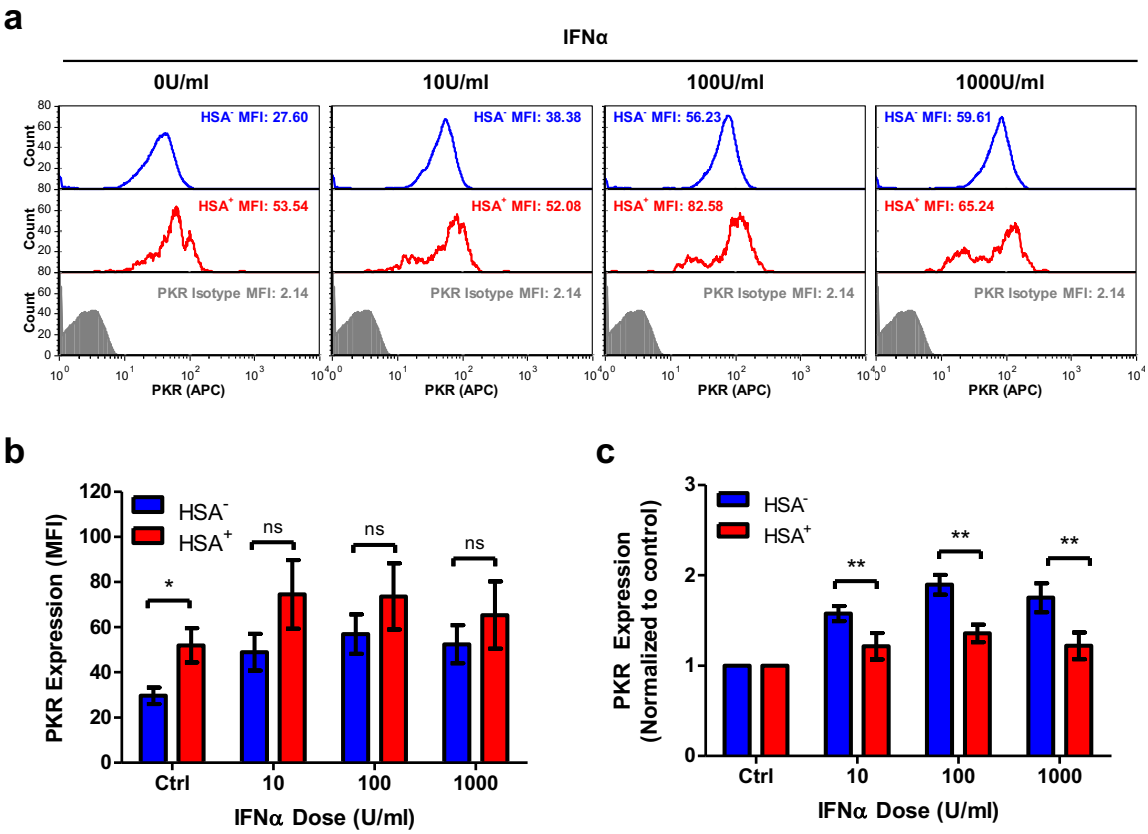
a
IFNα
0U/ml
10U/ml
100U/ml
1000U/ml
HSA- MFI: 27.60
HSA- MFI: 38.38
HSA- MFI: 56.23
HSA- MFI: 59.61
HSA+ MFI: 53.54
HSA+ MFI: 52.08
HSA+ MFI: 82.58
HSA+ MFI: 65.24
PKR Isotype MFI: 2.14
Count
PKR (APC)
b
PKR Expression (MFI)
HSA-
HSA+
ns
*
Ctrl
10
100
1000
IFNα Dose (U/ml)
c
PKR Expression (Normalized to control)
**
IFNα Dose (U/ml)

Figure 17: IFNα-induced PKR expression is lower in HSA^+ MDM relative to HSA^- MDM. At 6dpi, HIV NL4.3 Bal-IRES-HSA-infected MDM were treated with IFNα. At 24 hours post-treatment, intracellular PKR expression was assessed by flow cytometry. **a.** Representative histograms depicting PKR expression with increasing doses of IFNα in HSA^- (blue) and HSA^+ (red) MDM. PKR isotype control is shown as a filled, grey histogram. Histogram peak counts (y-axis) for HSA^- and HSA^+ populations were normalized to that of the isotype control for visualization purposes. **b.** PKR induction in HSA^- (blue) and HSA^+ (red) MDM, as measured by mean fluorescent intensity (n=6; p=0.05 by 2way repeated measures ANOVA). **c.** PKR induction in HSA^- (blue) and HSA^+ (red) MDM, relative to respective unstimulated control (n=6; p=0023 by 2way repeated measures ANOVA). ns=not significant, *p<0.05, **p<0.001 by Bonferroni posttest. Data represent mean ± SEM; n values represent separate biological replicates.

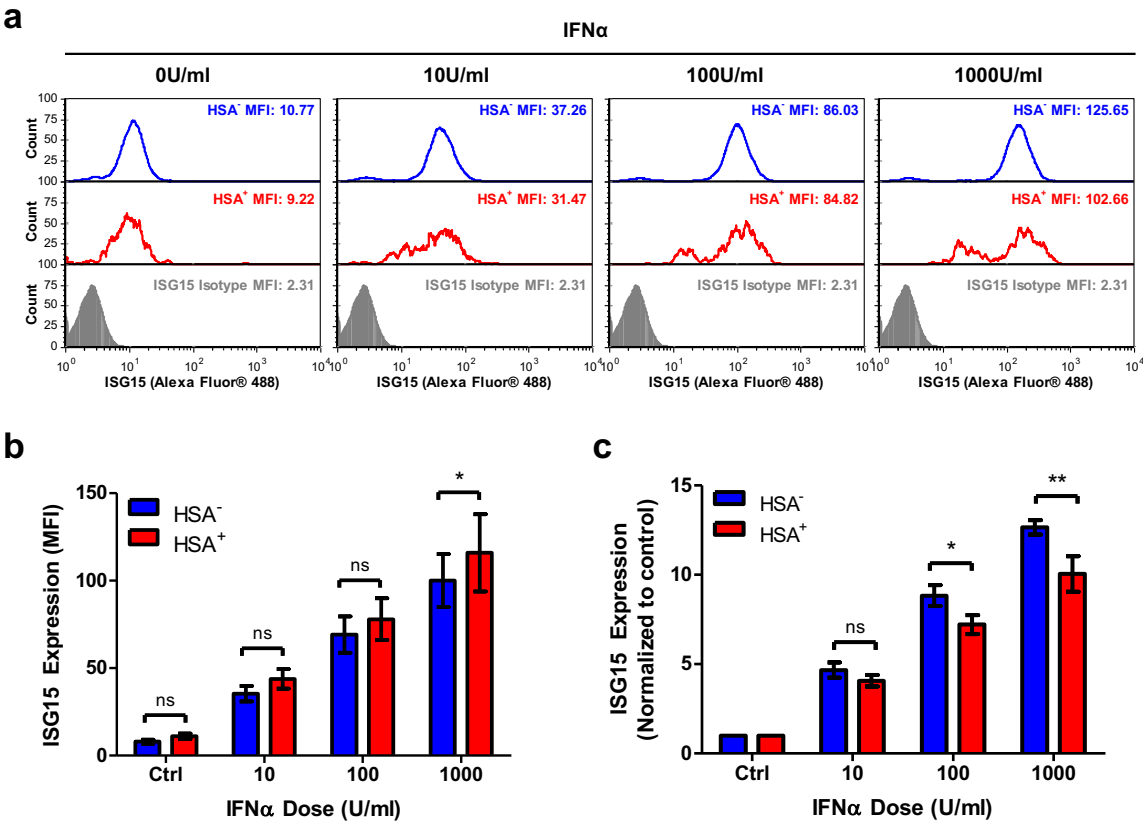
a
IFNα
0U/ml
10U/ml
100U/ml
1000U/ml
HSA- MFI: 10.77
HSA- MFI: 37.26
HSA- MFI: 86.03
HSA- MFI: 125.65
HSA+ MFI: 9.22
HSA+ MFI: 31.47
HSA+ MFI: 84.82
HSA+ MFI: 102.66
ISG15 Isotype MFI: 2.31
Count
ISG15 (Alexa Fluor® 488)
b
ISG15 Expression (MFI)
HSA-
HSA+
ns
*
Ctrl
10
100
1000
IFNα Dose (U/ml)
c
ISG15 Expression (Normalized to control)
**

Figure 18: IFNα-induced ISG15 expression is lower in HSA^+ MDM relative to HSA^- MDM. At 6dpi, HIV NL4.3 Bal-IRES-HSA-infected MDM were treated with IFNα. At 24 hours post-treatment, intracellular ISG15 expression was assessed by flow cytometry. **a.** Representative histograms depicting ISG15 expression with increasing doses of IFNα in HSA^- (blue) and HSA^+ (red) MDM. ISG15 isotype control is shown as a filled, grey histogram. Histogram peak counts (y-axis) for HSA^- and HSA^+ populations were normalized to that of the isotype control for visualization purposes. **b.** ISG15 induction in HSA^- (blue) and HSA^+ (red) MDM, as measured by mean fluorescent intensity (n=7; $p<0.0001$ by 2way repeated measures ANOVA). **c.** ISG15 induction in HSA^- (blue) and HSA^+ (red) MDM, relative to respective, unstimulated control (n=7; $p<0.0001$ by 2way repeated measures ANOVA). ns=not significant, *$p<0.05$, **$p<0.001$ by Bonferroni posttest. Data represent mean ± SEM; n values represent separate biological replicates.

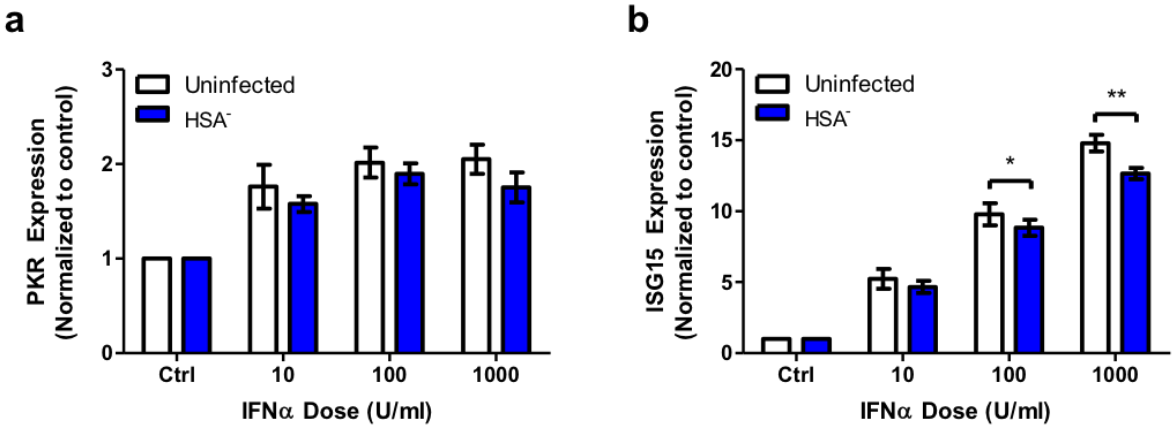
a
PKR Expression
(Normalized to control)
Uninfected
HSA-
0
1
2
3
Ctrl
10
100
1000
IFNα Dose (U/ml)
b
ISG15 Expression
(Normalized to control)
Uninfected
HSA-
0
5
10
15
20
*
**
Ctrl
10
100
1000
IFNα Dose (U/ml)

Figure 19: IFNα-induced ISG induction is similar between uninfected and HSA$^-$ MDM. At 6dpi, uninfected and HIV NL4.3 Bal-IRES-HSA-infected MDM were treated with IFNα. At 24 hours post-treatment, intracellular PKR and ISG15 expression was assessed by flow cytometry. **a.** PKR expression in uninfected (white) and HSA$^-$ (blue) MDM, relative to respective, unstimulated controls (n=6). **b.** ISG15 expression in uninfected (white) and HSA$^-$ (blue) MDM, relative to respective, unstimulated controls (n=7; $p<0.0001$ by 2way repeated measures ANOVA, $^*p<0.05$, $^{**}p<0.001$ by Bonferroni posttest). Data represent mean ± SEM; n values represent separate biological replicates.

IFNAR1 downregulation has been observed during HIV infection, and desensitizes cells to exogenous IFN1 (215,269,270). The possibility that IFNAR1/2 downregulation was responsible for the lower ISG induction observed in HSA^+ MDM was therefore considered. To address this, surface expression of IFNAR1 and IFNAR2 was measured on HSA^+ and HSA^- MDM. No difference in IFNAR1/2 expression could be observed between HIV-unexposed, HSA^-, and HSA^+ MDM (Figure 20a-d). Receptor downregulation therefore does not appear to be the mechanism by which HIV impairs ISG induction within HSA^+ cells.

Impairment of JAK/STAT signalling following IFNAR1/2 engagement may also occur during HIV infection. This impairment is likely mediated by suppressors of cytokine signalling 1 and 3 (SOCS1 and SOCS3), which are upregulated and impair STAT1/2 phosphorylation in HIV-infected $CD4^+$ T cells, monocytes, and MDM (270-273,450). As a result, the formation of ISGF3 by STAT1, STAT2, and IRF9 is prevented, and ISG transcription is downregulated (451,452). To assess whether transcriptional inhibition was responsible for the impaired ISG induction observed in HSA^+ MDM, PKR and ISG15 mRNA was first measured in HIV-unexposed and HIV-infected (comprised of HSA^+ and HSA^- populations) MDM. In agreement with Wie et al. (275), PKR and ISG15 mRNA was significantly lower in HIV-infected MDM at 16 hours post-IFNα stimulation, in comparison to HIV-uninfected cells (Figure 21a,b). Next, PKR and ISG15 mRNA was measured within HSA^+ and HSA^- MDM that had been separated by immunomagnetic bead enrichment (as shown in Figure 14a,b) prior to IFNα stimulation. Relative induction of ISG mRNA did not differ between sorted HSA^+ and HSA^- MDM populations (Figure 22a,b).

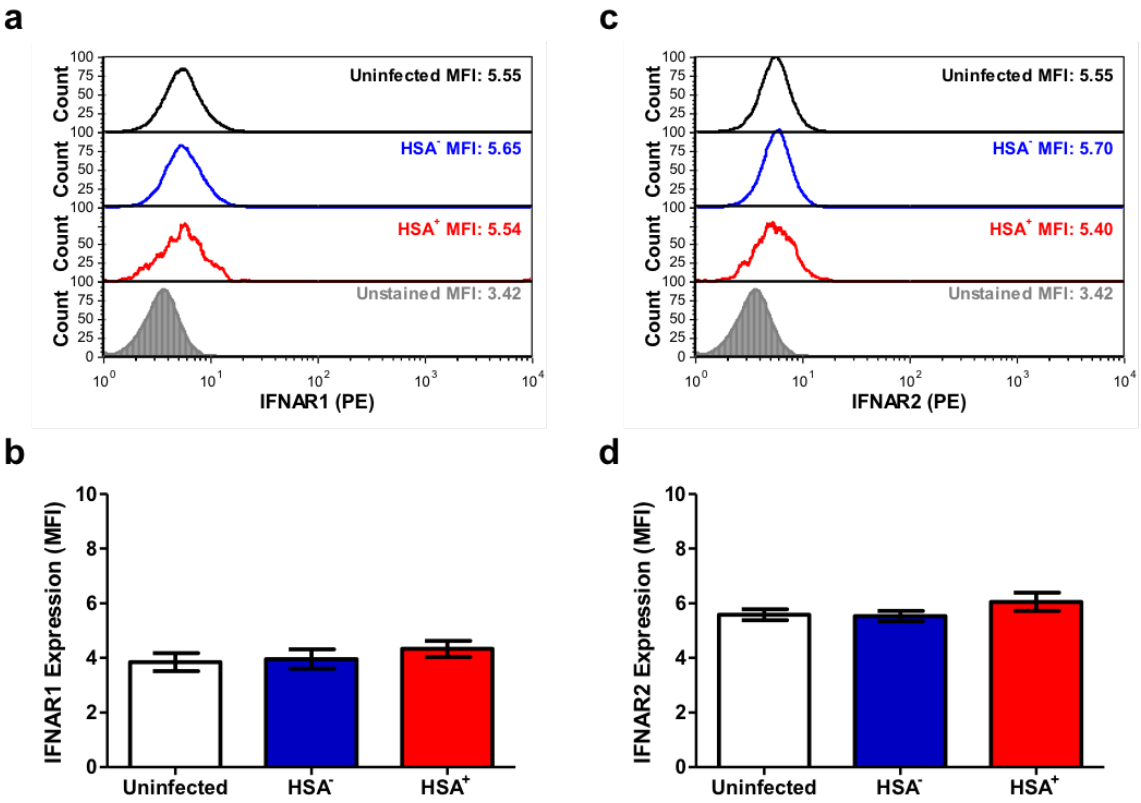
a
c
Uninfected MFI: 5.55
HSA- MFI: 5.65
HSA+ MFI: 5.54
Unstained MFI: 3.42
Count
IFNAR1 (PE)
HSA- MFI: 5.70
HSA+ MFI: 5.40
IFNAR2 (PE)
b
d
IFNAR1 Expression (MFI)
IFNAR2 Expression (MFI)
Uninfected
HSA-
HSA+

Figure 20: IFNAR1/2 expression does not differ between uninfected, HSA$^-$, and HSA$^+$ MDM. a. Representative histograms depicting IFNAR1 expression on uninfected (black), HSA$^-$ (blue), and HSA$^+$ (red) MDM. IFNAR1 unstained control is shown as a filled, grey histogram. **b.** Cumulative IFNAR1 expression on uninfected (white), HSA$^-$ (blue), and HSA$^+$ (red) MDM, as measured by mean fluorescent intensity (n=7). **c.** Representative histograms depicting IFNAR2 expression on uninfected, HSA$^-$, and HSA$^+$ MDM. IFNAR2 unstained control is shown as a filled, grey histogram. **d.** Cumulative IFNAR2 expression on on uninfected, HSA$^-$, and HSA$^+$ MDM, as measured by mean fluorescent intensity (n=7). Note: histogram peak counts (y-axis) for uninfected, HSA$^-$, and HSA$^+$ populations were normalized to that of the unstained control for visualization purposes. Data represent mean ± SEM; n values represent separate biological replicates.

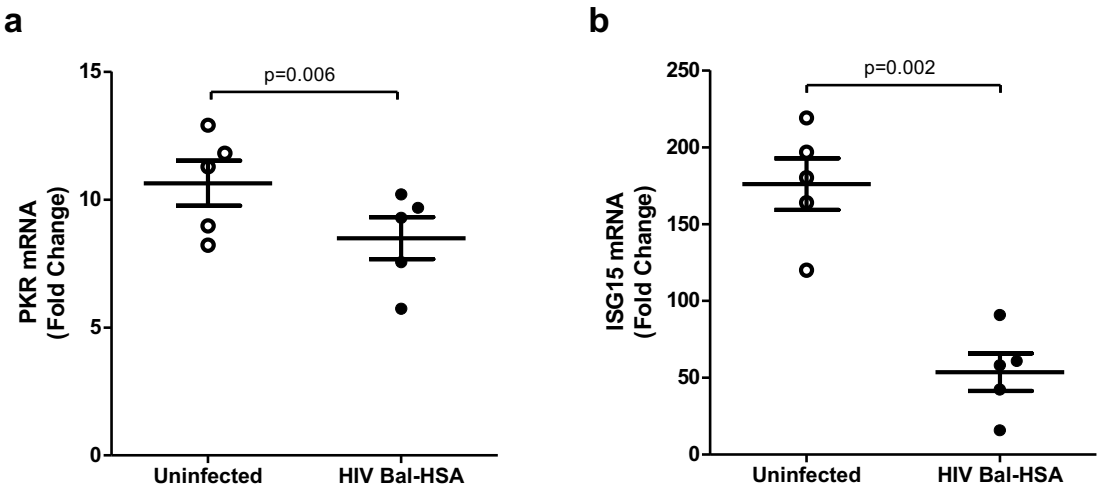
a
p=0.006
PKR mRNA
(Fold Change)
15
10
5
0
Uninfected
HIV Bal-HSA
b
p=0.002
ISG15 mRNA
(Fold Change)
250
200
150
100
50
0
Uninfected
HIV Bal-HSA

Figure 21: PKR and ISG15 expression is reduced at the mRNA level in IFNα-stimulated, HIV-infected MDM. PKR mRNA **(a)** and ISG15 mRNA **(b)** was measured in HIV-infected and HIV-uninfected MDM at 16 hours post-stimulation with 1000U/ml IFNα. ΔΔCts used to calculate fold change were calculated by normalizing Ct values to respective untreated control and GAPDH (n=5). p values were calculated by two-tailed, paired t-test. Data represent mean ± SEM; n values represent separate biological replicates.

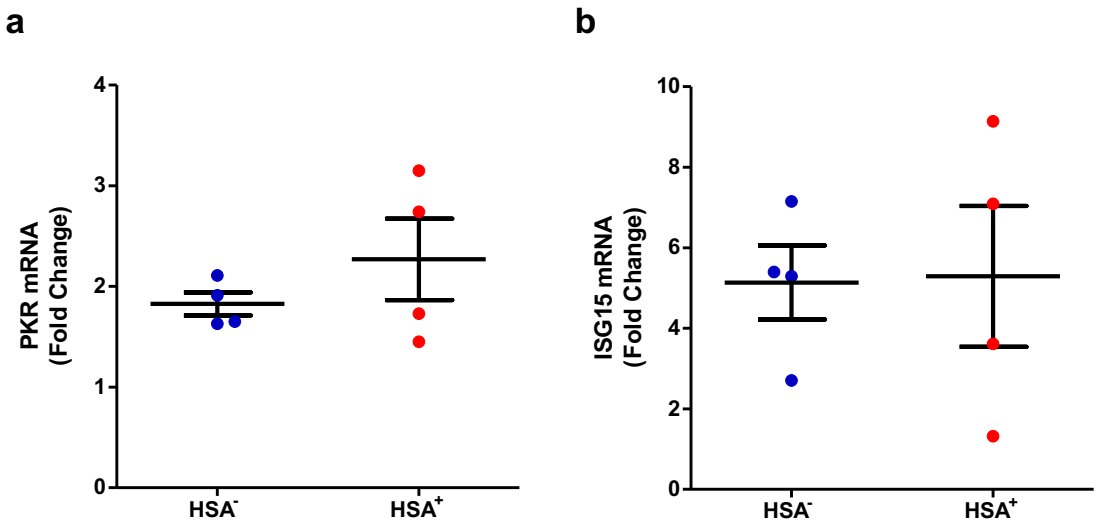
a
PKR mRNA
(Fold Change)
4
3
2
1
0
HSA-
HSA+
b
ISG15 mRNA
(Fold Change)
10
8
6
4
2
0
HSA-
HSA+

Figure 22: ISG expression is induced at the mRNA level in HSA$^+$ and HSA$^-$ MDM following IFNα stimulation. PKR mRNA (**a**) and ISG15 mRNA (**b**) was measured in HSA$^+$ and HSA$^-$ MDM at 16 hours post-stimulation with 1000U/ml IFNα. ΔΔCts used to calculate fold change were calculated by normalizing Ct values to respective untreated control and GAPDH (n=4). Data represent mean ± SEM; n values represent separate biological replicates.

In summary, both HIV-exposed (bystander) and HIV-infected MDM populations were found to be less responsive to IFNα at the transcriptional level relative to HIV-unexposed MDM. While no difference in ISG mRNA was observed between HSA^+ and HSA^- MDM, the relative increase in PKR and ISG15 protein expression was lower in HSA^+ MDM than HSA^- MDM. Differences in ISG induction in HIV-infected MDM may therefore occur at the post-transcriptional level, rather than within the upstream IFN1 signalling cascade.

4.3.4 HIV-infected monocyte-derived macrophages are less responsive to the RIG-I agonist, 5'ppp-dsRNA than bystander cells

To further examine the impairment of ISG15 and PKR expression in HSA^+ MDM, a second pathway for ISG induction was investigated. Recognition of foreign RNA possessing a 5'-triphosphate (5'ppp) by RIG-I induces ISG expression, independent of IFNα/β production (227,232). RIG-I is targeted to the cellular lysosomal compartment by HIV protease, however, preventing HIV-infected MDM from eliciting an appropriate RNA-mediated antiviral response (234).

To investigate whether RNA sensing via RIG-I is intact within HSA^+ MDM, cells were transfected with 1μg/ml 5'ppp-dsRNA, after which PKR and ISG15 expression was assessed by flow cytometry. Although HIV-infected and uninfected MDM produced low levels of IFNα/β following 5'ppp-dsRNA transfection (Figure 23), previous optimization experiments found that ISG mRNA and protein expression were induced at 16 hours and 24 hours post-IFNα stimulation, respectfully. Thus, it is unlikely that the induction of PKR and ISG15 expression observed at 24 hours

post- transfection was a result of IFNα/β production and autocrine IFN1 signalling. The use of an IFNAR1/2 blocking antibody to confirm the direct induction of ISG expression via RIG-I activation was not performed, but remains an important control that should be included in future experiments.

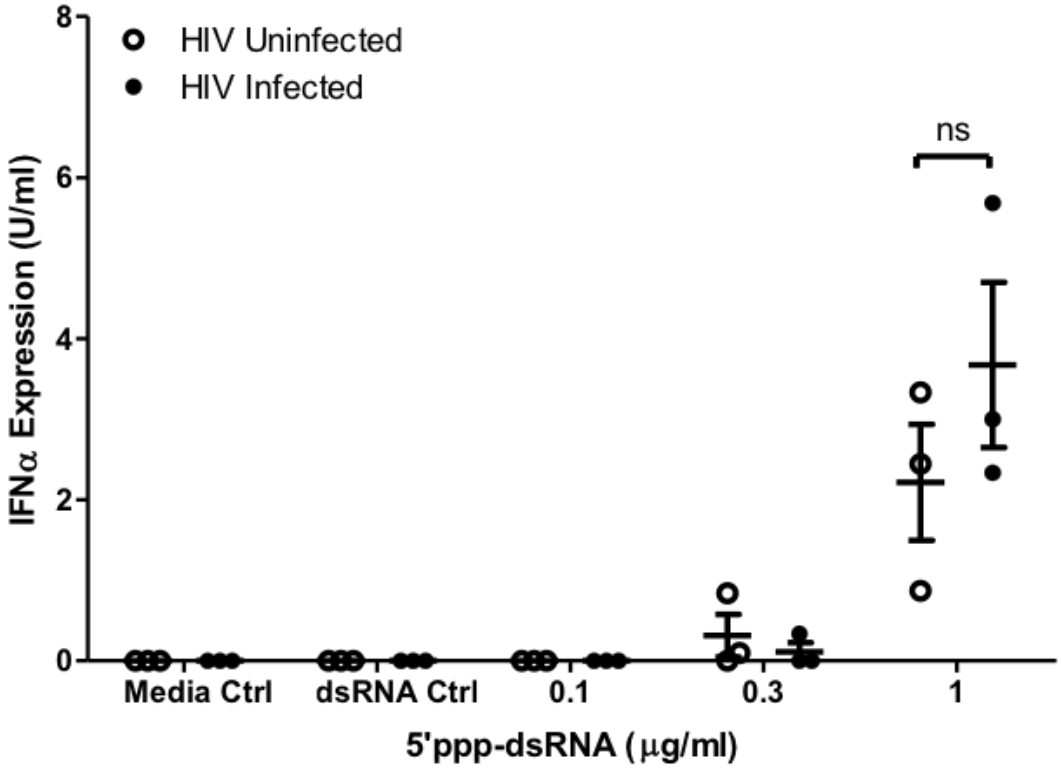
HIV Uninfected
HIV Infected
ns
IFNα Expression (U/ml)
8
6
4
2
0
Media Ctrl
dsRNA Ctrl
0.1
0.3
1
5'ppp-dsRNA (μg/ml)

Figure 23: HIV-infected and uninfected MDM secrete IFNα into culture supernatants. At 6dpi, HIV-infected and uninfected MDM were transfected with 5'ppp-dsRNA, 5'ppp-free dsRNA control, or cultured in the presence of lipofectamine with Opti-Mem reduced serum media (media control). IFNα was quantified by ELISA at 24 hours post-transfection. n=3, $p<0.0001$ by 2way ANOVA, ns=not significant by Bonferroni posttest. Data represent mean ± SEM; n values represent separate biological replicates.

Similar to that seen with IFNα stimulation, PKR and ISG15 expression was elevated in HSA^+ MDM at baseline (Figure 24). While levels of both ISG were increased following 5'ppp-dsRNA transfection, the relative induction of PKR and ISG15 was lower in HSA^+ MDM, in comparison to HSA^- MDM (Figure 25 and 26). Importantly, transfection with a 5'ppp-free dsRNA control did not yield appreciable ISG induction, indicating that 5'ppp-dsRNA does not stimulate ISG expression via another RNA-sensing protein like MDA5 (453). As before, PKR induction was similar between HIV-uninfected and bystander cells (Figure 27a), while ISG15 induction was significantly elevated in HSA^- MDM (Figure 27b). Like the results presented in section 4.3.3, productive HIV infection appears to cause differences in ISG induction between HSA^+ and HSA^- MDM following 5'ppp-dsRNA transfection.

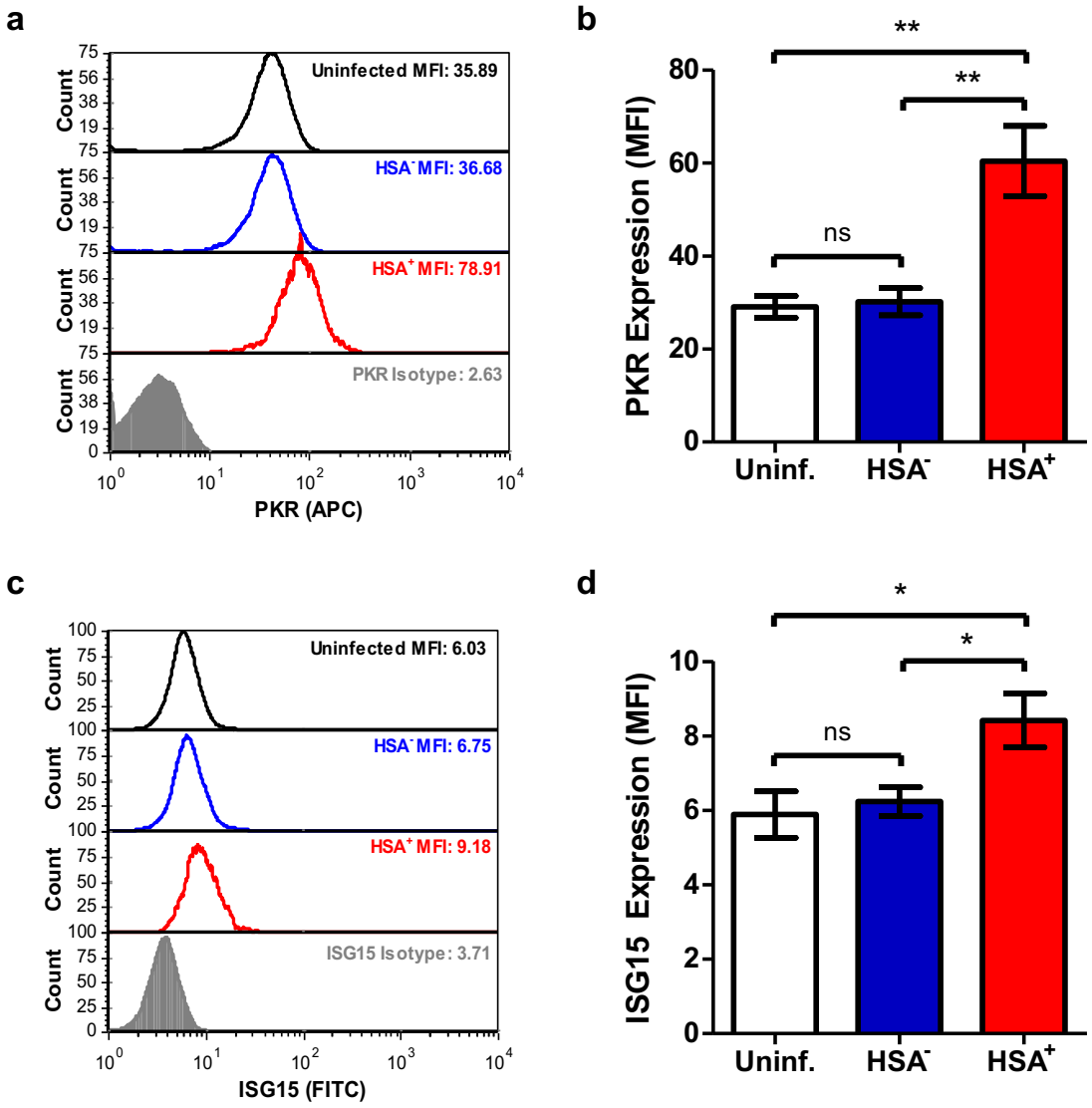
a
Uninfected MFI: 35.89
HSA- MFI: 36.68
HSA+ MFI: 78.91
PKR Isotype: 2.63
Count
PKR (APC)
b
PKR Expression (MFI)
ns
**
**
Uninf.
HSA-
HSA+
c
Uninfected MFI: 6.03
HSA- MFI: 6.75
HSA+ MFI: 9.18
ISG15 Isotype: 3.71
Count
ISG15 (FITC)
d
ISG15 Expression (MFI)
ns
*
*
Uninf.
HSA-
HSA+

Figure 24: ISG expression is elevated in HSA$^+$ MDM at baseline, in comparison to HSA$^-$ and uninfected MDM. a. Representative histogram depicting PKR expression in unstimulated, uninfected (black), HSA$^-$ (blue), and HSA$^+$ (red) MDM. **b.** Cumulative basal PKR expression in uninfected (black), HSA$^-$ (blue), and HSA$^+$ (red) MDM (n=6). **c.** Representative histogram depicting ISG15 expression in uninfected (black), HSA$^-$ (blue), and HSA$^+$ (red) MDM (n=6; $p<0.0001$ by 1way repeated measures ANOVA). **d.** Cumulative basal ISG15 expression in uninfected (black), HSA$^-$ (blue), and HSA$^+$ (red) MDM (n=6; $p=0.0007$ by 1way repeated measures ANOVA). Note: histogram peak counts (y-axis) for uninfected, HSA$^-$, and HSA$^+$ populations were normalized to that of the isotype control for visualization purposes. ns=not significant, *$p<0.01$, **$p<0.001$ by Bonferroni multiple comparisons test. Data represent mean ± SEM; n values represent separate biological replicates.

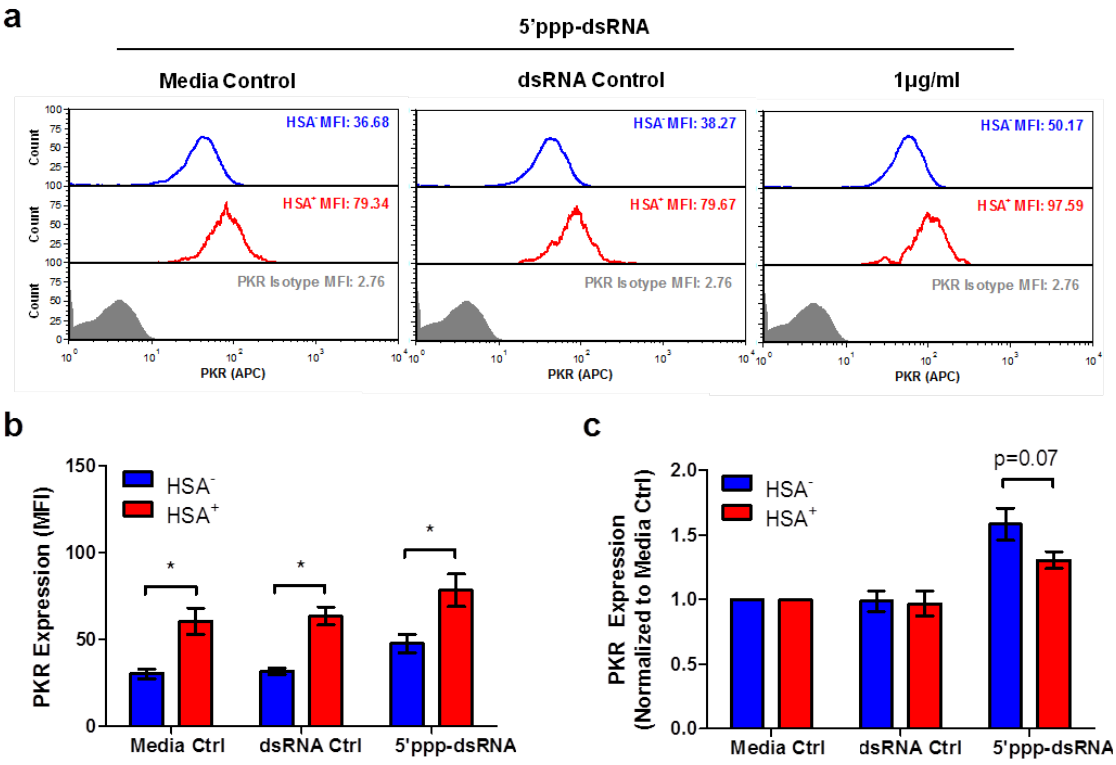
a
5'ppp-dsRNA
Media Control
dsRNA Control
1µg/ml
HSA- MFI: 36.68
HSA+ MFI: 79.34
PKR Isotype MFI: 2.76
HSA- MFI: 38.27
HSA+ MFI: 79.67
PKR Isotype MFI: 2.76
HSA- MFI: 50.17
HSA+ MFI: 97.59
PKR Isotype MFI: 2.76
Count
PKR (APC)
b
PKR Expression (MFI)
HSA-
HSA+
Media Ctrl
dsRNA Ctrl
5'ppp-dsRNA
c
PKR Expression (Normalized to Media Ctrl)
p=0.07
HSA-
HSA+
Media Ctrl
dsRNA Ctrl
5'ppp-dsRNA

Figure 25: PKR induction is lower in HSA^+ MDM relative to HSA^- MDM following 5'ppp-dsRNA transfection. At 6dpi, HIV NL4.3 Bal-IRES-HSA-infected MDM were transfected with 1μg/ml of the 5'ppp-free dsRNA control or 5'ppp-dsRNA, or cultured in the presence of lipofectamine with Opti-Mem reduced serum media (media control). At 24 hours post-transfection, intracellular PKR expression was assessed by flow cytometry. **a.** Representative histograms depicting PKR expression in HSA^- (blue) and HSA^+ (red) MDM. PKR isotype control is shown as a filled, grey histogram. Histogram peak counts (y-axis) for HSA^- and HSA^+ populations were normalized to that of the isotype control for visualization purposes. **b.** PKR expression in HSA^- (blue) and HSA^+ (red) MDM, as measured by mean fluorescent intensity (n=6; p=0.05 by 2way repeated measures ANOVA, *p<0.001, by Bonferroni posttest). **c.** PKR induction in HSA^- (blue) and HSA^+ (red) MDM, relative to respective media control (n=6; p value calculated by paired, two-tailed t-test). Data represent mean ± SEM; n values represent separate biological replicates.

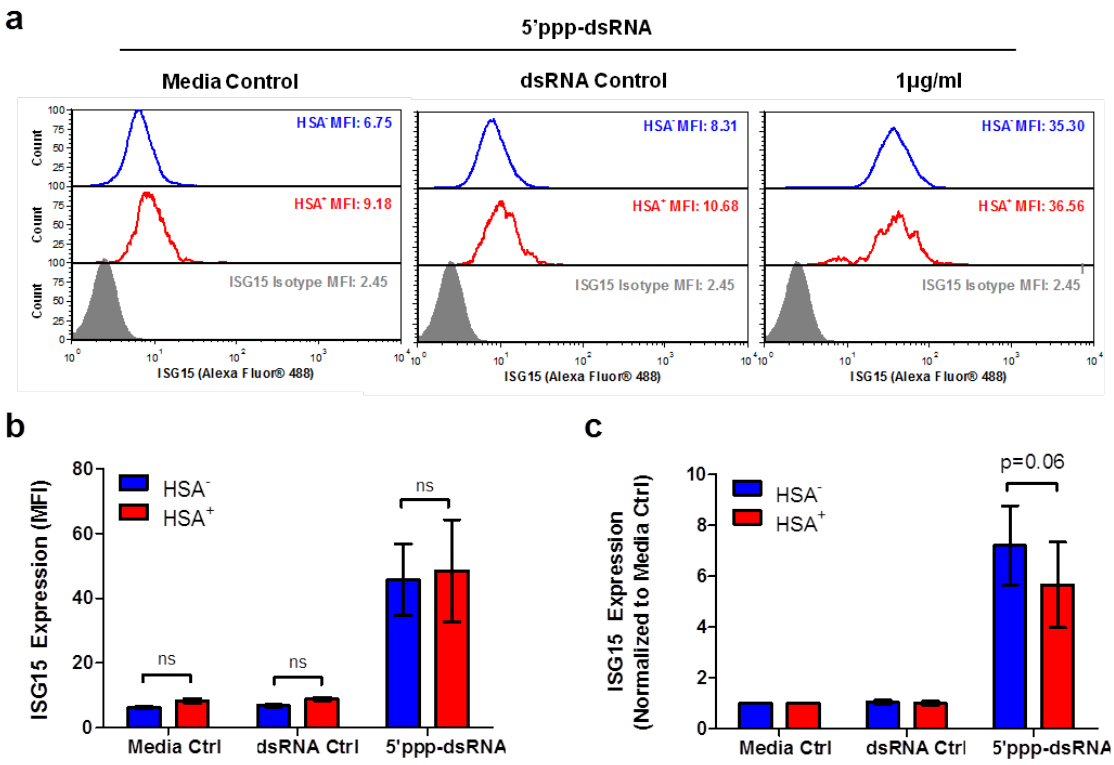
a
5'ppp-dsRNA
Media Control
dsRNA Control
1µg/ml
HSA- MFI: 6.75
HSA+ MFI: 9.18
ISG15 Isotype MFI: 2.45
HSA- MFI: 8.31
HSA+ MFI: 10.68
ISG15 Isotype MFI: 2.45
HSA- MFI: 35.30
HSA+ MFI: 36.56
ISG15 Isotype MFI: 2.45
Count
ISG15 (Alexa Fluor® 488)
b
ISG15 Expression (MFI)
HSA-
HSA+
ns
ns
ns
Media Ctrl
dsRNA Ctrl
5'ppp-dsRNA
c
ISG15 Expression (Normalized to Media Ctrl)
p=0.06
Media Ctrl
dsRNA Ctrl
5'ppp-dsRNA

Figure 26: ISG15 induction is lower in HSA^+ MDM relative to HSA^- MDM following 5'ppp-dsRNA transfection. At 6dpi, HIV NL4.3 Bal-IRES-HSA-infected MDM were transfected with 1µg/ml of the 5'ppp-free dsRNA control or 5'ppp-dsRNA, or cultured in the presence of lipofectamine with Opti-Mem reduced serum media (media control). At 24 hours post-transfection, intracellular ISG15 expression was assessed by flow cytometry. **a.** Representative histograms depicting ISG15 expression in HSA^- (blue) and HSA^+ (red) MDM. ISG15 isotype control is shown as a filled, grey histogram. Histogram peak counts (y-axis) for HSA^- and HSA^+ populations were normalized to that of the isotype control for visualization purposes. **b.** ISG15 expression in HSA^- (blue) and HSA^+ (red) MDM, as measured by mean fluorescent intensity (n=6; p=0.0046 by 2way repeated measures ANOVA, ns=not significant by Bonferroni posttest). **c.** ISG15 induction in HSA^- (blue) and HSA^+ (red) MDM, relative to respective media control (p value calculated by paired, two-tailed t-test). Data represent mean ± SEM; n values represent separate biological replicates.

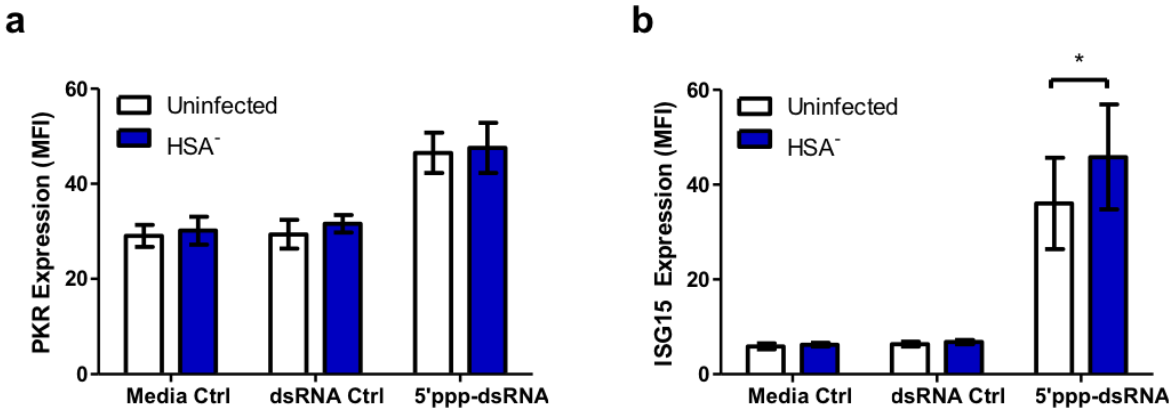
a
PKR Expression (MFI)
60
40
20
0
Uninfected
HSA-
Media Ctrl
dsRNA Ctrl
5'ppp-dsRNA
b
ISG15 Expression (MFI)
60
40
20
0
Uninfected
HSA-
*
Media Ctrl
dsRNA Ctrl
5'ppp-dsRNA

Figure 27: 5'ppp-dsRNA-induced ISG expression is similar between uninfected and HSA$^-$ MDM. At 6dpi, HIV NL4.3 Bal-IRES-HSA-infected MDM were transfected with 1µg/ml of the 5'ppp-free dsRNA control or 5'ppp-dsRNA, or cultured in the presence of lipofectamine with Opti-Mem reduced serum media (media control). At 24 hours post-transfection, intracellular PKR and ISG15 expression was assessed by flow cytometry. **a.** PKR expression in uninfected (white) and HSA$^-$ (blue) MDM, relative to respective media controls (n=6; p=0.0036 by 2way repeated measures ANOVA). **b.** ISG15 expression in uninfected (white) and HSA$^-$ (blue) MDM, relative to respective, unstimulated controls (n=6; p=0.0017 by 2way repeated measures ANOVA, *p<0.01 by Bonferroni posttest). Data represent mean ± SEM; n values represent separate biological replicates.

4.4 Discussion

To summarize, the fold induction of two antiviral proteins, PKR and ISG15, was found to be lower in HIV-infected, HSA^+ MDM than bystander, HSA^- MDM following IFNα stimulation or 5'ppp-dsRNA transfection. Although hundreds of ISG are expressed during the IFN1 response, PKR and ISG15 were chosen as archetypal markers of IFN1 signalling based on previous literature supporting their functionally different antiviral roles in the context of HIV infection. PKR is predominantly involved viral RNA sensing and the inhibition of viral protein translation (292,454), whereas ISG15 blocks HIV virion egress from infected cells (397,455,456). Moreover, inhibition of PKR activation (292,457) and transcriptional downregulation of ISG15 (275,458), have been observed in the context of HIV infection. HIV-mediated inhibition of IFN1 signalling therefore exists at the level of ISG expression, as well as antiviral function.

While these findings represent the first attempt to measure ISG induction in human MDM infected with an established HIV reporter virus, others have previously demonstrated the downregulation of ISG mRNA expression in HIV-infected MDM (275). In agreement with this, HIV-infected MDM cultures (comprised of productively infected and bystander cells) were less responsive to IFNα than their HIV-unexposed counterparts at the transcriptional level (Figure 21). The induction of PKR and ISG15 mRNA was not different in HSA^+ and HSA^- populations isolated via magnetic bead enrichment (Figure 22), however, suggesting that that differences in IFNα-induced ISG expression observed in HSA^+ MDM are unlikely to result from upstream inhibition of the IFN1 response pathway. This is in contrast to previous

studies that have demonstrated the desensitization of peripheral blood mononuclear cells and primary monocytes isolated from PLWHIV to IFN1 following the downregulation of IFNAR1/2 expression (269,270). Alternatively, the impaired activation of key signalling proteins downstream of IFNAR1/2 has been shown to prevent ISG induction in cell line and primary MDM models of HIV infection (271-273). The use of a full-length, replication-competent reporter virus will be an important addition to future experiments that will allow these IFN1 signalling impairments to be characterized within the HIV-infected MDM population, as well as within HIV-uninfected bystander cells.

ISG induction was also measured following transfection of MDM with the RIG-I-specific ligand, 5'ppp-dsRNA (227). RIG-I can sense highly-structured viral RNA during HIV infection, and is therefore a key component of the cellular IFN1 response (229). This PRR is targeted for degradation by HIV protease, blocking the induction of IFN1 and antiviral ISG within HIV-infected macrophages (234). In line with this, the relative induction of PKR and ISG15 from baseline levels was lower in HSA^+ MDM following 5'ppp-dsRNA transfection, in comparison to that observed within HSA^- MDM (Figures 25 and 26, respectfully).

As shown by Yoneyama et al., cells that do not express functional RIG-I do not induce detectable ISG expression following viral infection (459). Given that PKR and ISG15 induction was detectable in HSA^+ MDM, it is unlikely that functional RIG-I was completely ablated in these cells. Rather, impairment of the RIG-I signalling cascade by HIV may partially block or delay IFNα/β-independent ISG induction. Transcriptional downregulation of the RIG-I adaptor protein, mitochondrial IPS-1,

has been shown to block ISG induction in HIV-infected MDM (245). Similarly, the HIV accessory proteins Vif and Vpr can inhibit the phosphorylation of TBK1, preventing ISG expression downstream of RIG-I activation (248). As the expression and/or activation of RIG-I, IPS-1, and TBK1 were not assessed in this model, we cannot explicitly state at which point in the RIG-I signalling cascade this inhibition has occurred. Regardless, these results are consistent with those observed in HSA^+ MDM following IFNα stimulation and confirm that differences in ISG induction exist between HSA^+ and HSA^- MDM.

4.5 Future directions

Going forward, it will be important to identify the mechanism(s) by which ISG induction is downregulated in HIV-infected MDM. This will ideally employ an HSA^+-enriched population to ensure that HSA^- bystander cells do not contaminate the measurement of mRNA and/or protein expression, activation, or interactions. Deshiere et al. recently employed this model to assess the macrophage transcriptome during HIV infection, identifying a number of ISG that were specifically downregulated in HSA^+ MDM (358). Still, transcriptional differences may not fully correlate with protein expression. To this point, Tian et al. previously demonstrated that only 40% of perturbations at the protein level are captured using transcriptome analyses (460). The measurement of ISG using a quantitative proteomics approach will therefore allow specific protein-level differences to be identified between in HSA^+ and HSA^- MDM in future experiments. To date, proteomic analyses of HIV-infected $CD4^+$ T cells and macrophages have identified differential expression of antiviral

ISG, RNA processing machinery, and transcriptional regulators (461,462). Uncovering additional differences may highlight points within the IFN1 signalling network that are inhibited during HIV infection.

Inhibition of ISG induction within HIV-infected MDM can perhaps be explained through one of the following mechanisms. One possibility is the rapid degradation of ISG following translation, which has been observed for several key antiviral proteins, including RIG-I (234), IPS-1 (244), APOBEC3 (287), and possibly IRF3 (265). Although this has not been demonstrated in the context of HIV infection for PKR or ISG15, other viral pathogens such as foot-and-mouth disease virus (463), Rift Valley fever virus (464,465), and certain enteroviruses (466,467) are capable of degrading PKR so as to evade antiviral signalling.

Alternatively, the translation of cellular mRNAs may be blocked during HIV infection. HIV protease, for example, has been shown to degrade EIF4G1 (468,469), while HIV Vpr inhibits the ribosome-directing activity of EIF4E (470). Kleinman et al. have also reported impaired ribosomal RNA (rRNA) transcription and processing, leading to an overall impairment of ribosome biogenesis in HIV-infected $CD4^+$ T cells (471). Finally, the conjugation of ISG15 to PKR in a process similar to ubiquitination can lead to PKR, and ultimately EIF2α, phosphorylation, as well as the inhibition of cellular translation (472). In the above experiments, elevated basal levels of ISG15 and PKR were consistently observed in unstimulated HSA^+ MDM. Although this initial upregulation of these proteins likely occurred as a result of viral infection, the ISGylation of PKR by ISG15 may orchestrate the widespread inhibition of cellular translation at later time points.

Finally, PKR is capable of undergoing autophosphorylation following binding to double-stranded or hairpin RNAs. Subsequent phosphorylation of EIF2α is a well-known mechanism by which cells halt translational processes during viral infection or other instances of cell stress (473,474). Several potential mechanisms therefore exist to explain the differences in ISG induction observed between HSA^+ and HSA^- MDM, which should be investigated in detail as we continue toward the development and testing of novel HIV cure strategies.

4.6 Conclusion

In conclusion, HSA^+ cells appeared to be less responsive to antiviral stimuli than their HSA^- counterparts, suggesting that HIV-infected MDM possess differences in IFN1-mediated antiviral signalling that are not observed in uninfected bystander cells. We hypothesize that the observed differences in ISG induction are mediated by translational inhibition. In support of this hypothesis, HSA^+ MDM expressed elevated levels of PKR at baseline—a key antiviral ISG whose activation blocks subsequent translation of viral and cellular transcripts (473). Going forward, it will be necessary to identify what cellular processes involved in the IFN1 response are being targeted within HIV-infected MDM and which viral proteins (if any) are responsible. Given that aberrant IFN1 signalling forms a unique, intracellular characteristic by which to identify productively HIV-infected MDM, this may be of clinical use during the development of a novel HIV cure strategy.

Chapter 5: Oncolytic viruses target and eliminate HIV-infected monocyte-derived macrophages

5.1 Introduction

5.1.1 Rational

HIV is capable of blocking the antiviral IFN1 response within HIV infected cells, facilitating subsequent rounds of viral replication and persistence *in vivo*. This impairment occurs at several levels, including the desensitization of cells to circulating IFNα/β (270), as well as the transcriptional and translational inhibition of ISG expression (248,275).The functional inhibition of several antiviral proteins like PKR, whose activation is inhibited by cellular and viral proteins, and RIG-I, which is degraded in HIV-infected MDM has also been observed (234,295). Although these defects are clearly undesirable from an immunology standpoint, they are a unique feature of HIV-infected cells and may therefore be used as a therapeutic target.

To this point, IFN1 signalling defects have already been exploited within the field of cancer immunotherapy. Oncolytic rhabdoviruses, engineered to selectively infect and kill IFN1-defective cancer cells have proven effective in eradicating tumour cell lines, as well as reducing tumour mass *in vivo* (301,346,475). Several of these, including the recombinant Maraba virus, MG1, and the related Rhabdovirus, VSV, have progressed to the clinical trial stage and are undergoing evaluation for safety and efficacy (347,476,477). MG1 was recently shown to selectively kill latently HIV-infected primary $CD4^+$ T cells and myeloid cell lines (354), supporting the translation of OV to the HIV cure field. Chapter 5 of this thesis is therefore intended

to investigate the susceptibility of productively HIV-infected MDM to two IFN1-sensitive OV, MG1 and VSVΔ51.

5.1.2 The development and use of IFN-sensitive oncolytic rhabdoviruses, MG1 and VSVΔ51, for the treatment of cancer

Although numerous oncolytic viruses have been developed for the treatment of cancer (reviewed in (307)), the IFN1-sensitive Rhabdoviruses, VSVΔ51 and MG1, are unique. In contrast to other OV, which consist predominantly of human DNA viruses such as adenovirus (478,479) and herpes simplex virus (480), VSVΔ51 and MG1 are insect-born, single-stranded RNA viruses with zoonotic potential.

VSV predominantly infects hoofed livestock, such as pigs, horses, or cows. It may also be transmitted in rare instances to those in close contact with the infected animal or to laboratory workers working with the virus. Although VSV infection is typically non-fatal, it causes the development of painful lesions on the feet and within the mouth and nose; symptoms that are indistinguishable from those caused by the more serious Foot and Mouth Disease virus. Rare instances of human illness are typically self-limiting and characterized by mild flu-like symptoms. The development of encephalitis following VSV infection has been reported, however, highlighting the inherent neurotropic nature of this virus (481).

Closely related to VSV, Maraba virus was first isolated from Brazilian phlebotomine sandflies (specifically, *Lutzomyia* spp) in 1984 (337). Although the prevalence of Maraba infection in humans or livestock has not been readily assessed at present, Travassos da Rosa et al. recorded only one instance of

positive serology among the human sera tested (337). Given that human infection by either Maraba virus or VSV is a rare, the likelihood that an individual will possess pre-existing immunity to these viruses is quite low. Consequently, both VSV and Maraba virus are attractive candidates for future clinical use (345).

An additional attractive feature of *Rhabdoviridae* is their RNA genome, which in addition to restricting viral replication to the cytoplasm (avoiding potential off-target genotoxicity), is easily manipulated. To date, several recombinant VSV strains have been developed that are engineered to express immunostimulatory cytokines, suicide genes, or even other viral proteins for the purpose of immune priming (reviewed in detail in (345)). Attenuation of viral variants is also possible—specifically via the manipulation of the viral M protein, which facilitates the nuclear export of cellular mRNAs and the induction of an IFN1 response by the infected cell (343). Interestingly, while these attenuated VSV variants were unable to infect non-malignant cell lines, cancer cells possessing IFN1 signalling defects were readily targeted and killed (301,338). In particular, the deletion of methionine-51 from the VSV M protein resulted in the enhanced killing of IFN-defective malignant cells and an improved therapeutic index relative to wild-type VSV (301,345). More recently, a recombinant Maraba virus possessing two amino acid substitution mutations within the G (Q242R) and M (L123W) proteins was generated and tested using a panel of malignant cell lines (346). These mutations were chosen specifically based on the work by Sanjuán et al., who previously demonstrated that analogous mutations within the VSV genome increased viral fitness via synergistic epistasis (482). In agreement with this, the recombinant Maraba virus (termed “MG1”) demonstrated

increased cytopathogenicity within IFN1-defective malignant cells, but was effectively blocked from infecting non-malignant cells (346). Finally, both MG1 and VSVΔ51 have been engineered to express green fluorescent protein (GFP), making them a useful tool with which to study OV cytopathogenicity *in vitro.*

VSVΔ51 and MG1 therefore represent two novel OV that infect and kill IFN1-defective malignant cells, but are attenuated in healthy tissues. Although the clinical investigation of VSVΔ51 has been limited so far, an MG1-based vaccine strategy has recently undergone assessment in two first-in-human clinical trials in patients diagnosed with non-small cell lung cancer (ClinicalTrials.gov Identifier: NCT02879760) or advanced/metastatic MAGE-A3-expressing solid tumours (ClinicalTrials.gov Identifier: NCT02285816). The MAGE-A3-expressing MG1 (MG1-MAGEA3) used in these trials is intended to elicit an immune response against MAGE-A3 and facilitate the immune-mediated clearance (rather than direct oncolysis) of MAGE-A3-expressing malignant cells. Although selective OV-mediated oncolysis is not the main objective of these clinical trials, they remain an important step in establishing the safety profile of MG1 in humans. The potential for MG1-MAGEA3 to spread within non-malignant tissues was also investigated within healthy cynomolgous macaques (347). Reassuringly, these animals did not demonstrate adverse side effects, nor was replication competent virus detected in healthy tissues, feces, or urine (347). Off-target infection by MG1 therefore appears to be limited, supporting the continued investigation of this virus in the context of oncolytic virotherapy.

5.1.3 Using a virus-based therapeutic strategy to eradicate HIV-infected cells

Viruses, specifically VSV, have also been proposed for the eradication of HIV infected cells. In 1992, Schubert et al. engineered VSV to express a chimeric CD4/VSV G protein (483), creating a virus that could be targeted towards cells expressing the HIV envelope protein on their surface. These findings were quickly adapted by Schnell et al., who generated a VSV strain expressing CD4 and CXCR4 (VSVΔG-CC4) and tested its efficacy in targeting HIV-infected Jurkat cells (484). Indeed, VSVΔG-CC4 superinfection lead to a potent reduction in both supernatant HIV and detectable HIV-infected cells. CD4 and CXCR4 could therefore be expressed from the VSV genome to generate a virus that effectively targeted cells expressing HIV gp120/gp41 (484). An opposite approach was attempted by Boritz et al., who successfully targeted VSV to CD4-expressing cells by engineering the virus to express a chimeric VSV G-HIV Env (485). More recently, Okuma et al. advanced this idea by generating a CD4/CCR5 expressing VSV strain (VSVΔG-CC5) capable of preferentially infecting primary $CD4^+$ T cells infected with an CCR5-tropic HIV (486). VSVΔG-CC5 was also shown to be effective *in vivo* using a humanized mouse model of HIV infection, lending support to its future use in PLWHIV. An important consideration concerning the use of VSVΔG-CC4 or VSVΔG-CC5 is the requirement for HIV gp120/gp41 to be expressed at appreciable levels. Latently HIV-infected cells, or cells in which the HIV envelope protein has been internalized (487), will not be targeted. For the purposes of eradicating HIV-infected cells using a virus-based therapeutic strategy, it was therefore important to identify and target a unique characteristic of these cells that was not shared by uninfected cells.

Like cancerous cells (discussed in Chapter 1.6.2), a spectrum of IFN1 signalling defects have been observed in the context of HIV infection (discussed in Chapter 1.4). Conversely, uninfected cells remain responsive to both exogenous IFNα/β, as well as intracellular triggers of IFN1 signalling (such as foreign RNA). Given that both VSVΔ51 and MG1 infect and replicate within IFN1-defective malignant cells, it was hypothesized these OV could be used to target and kill HIV-infected cells (488). Indeed, both reactivated and latently HIV-infected cell lines were highly susceptible to OV infection and killing, in comparison to uninfected parental cell lines (354,402,488). These findings were believed to be due to pre-existing IFN1 signalling defects within latently HIV-infected cell lines, exemplified by the inability of these cells to induce ISG expression following IFNα or poly(I:C) stimulation (215). MG1-mediated killing of HIV-infected cells was also observed in an *in vitro* primary $CD4^+$ T cell model of latency, as well as within resting memory $CD4^+$ T cells from PLWHIV (354). In addition to preventing the release of HIV p24 antigen, OV infection reduced detectable HIV DNA, signifying the preferential killing of cells containing HIV provirus (354). Targeting a known intracellular characteristic of HIV-infected cells using OV has therefore formed the foundation on which the work within this chapter is based.

5.2 Hypothesis

HIV-infected MDM are preferentially infected and killed by the oncolytic viruses, MG1 and VSVΔ51.

5.3 Results

5.3.1 HIV-infected macrophages are preferentially infected by OV

To assess whether productively HIV-infected macrophages are preferentially targeted by IFN-sensitive OV, rates of OV infection in HSA^+ and HSA^- MDM were measured by flow cytometry. At 48 hours post-MG1 infection, HSA^+ MDM were found to contain a larger percentage of GFP^+ cells compared to HSA^- cells (Figure 28a,b). A similar result was observed at 48 hours post-VSVΔ51 infection (Figure 28c), despite VSVΔ51 being less infectious than MG1, overall.

Aside from IFN1 signalling defects, preferential OV infection of HSA^+ MDM could result from the elevated surface expression of low-density lipoprotein receptor (LDLR), the cellular receptor employed by MG1 and VSVΔ51 to gain entry to target cells (489-491). To assess whether preferential infection was in fact receptor-mediated, surface expression of LDLR was measured by flow cytometry. Interestingly, LDLR expression was elevated on HSA^+ cells in comparison to the HSA^- population (Figure 29a,b). It is therefore possible that the elevated expression of LDLR on HSA^+ MDM facilitates, in part, preferential OV infection.

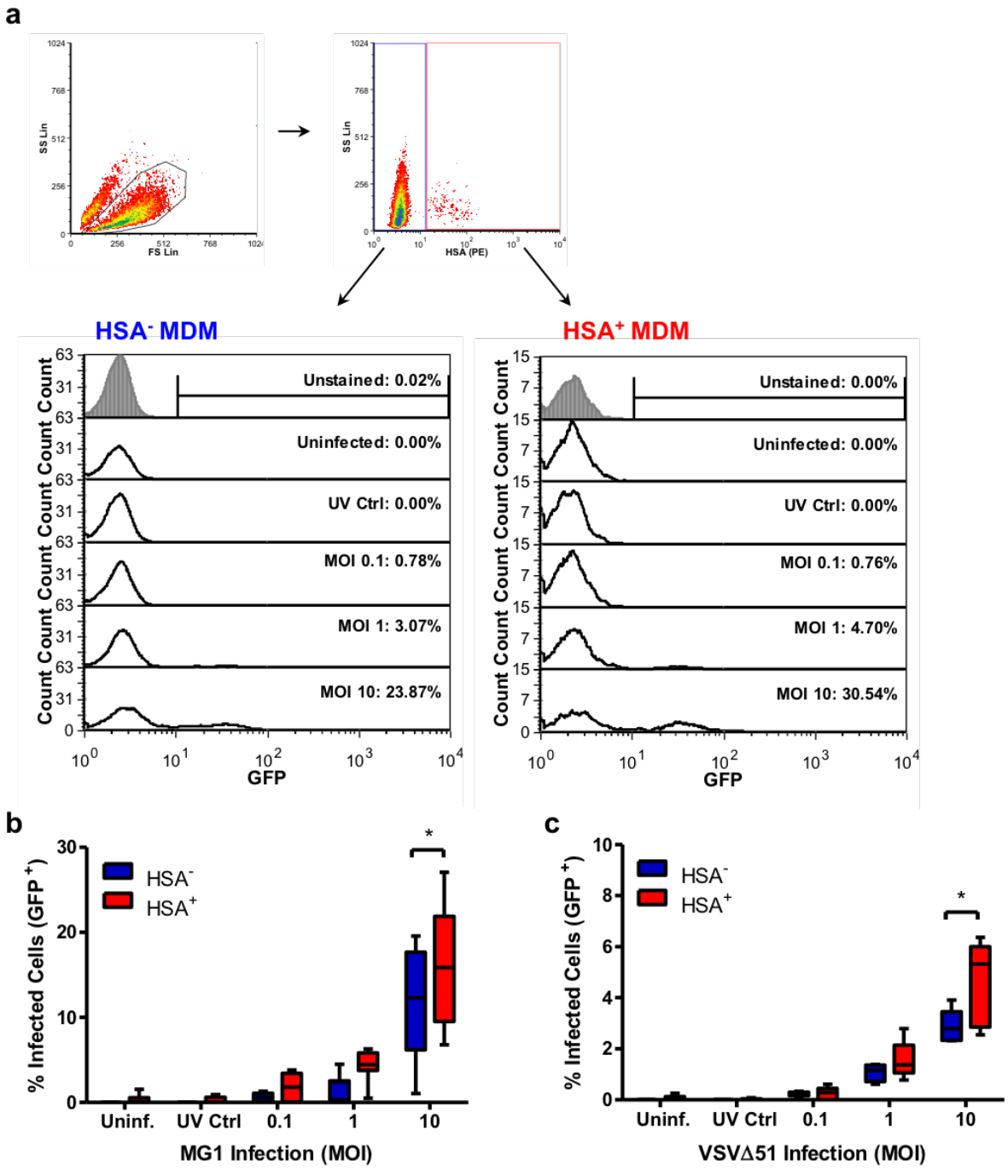
a
SS Lin
FS Lin
HSA (PE)
HSA- MDM
HSA+ MDM
Unstained: 0.02%
Uninfected: 0.00%
UV Ctrl: 0.00%
MOI 0.1: 0.78%
MOI 1: 3.07%
MOI 10: 23.87%
Unstained: 0.00%
Uninfected: 0.00%
UV Ctrl: 0.00%
MOI 0.1: 0.76%
MOI 1: 4.70%
MOI 10: 30.54%
Count
GFP
b
% Infected Cells (GFP+)
HSA-
HSA+
Uninf.
UV Ctrl
0.1
1
10
MG1 Infection (MOI)
c
% Infected Cells (GFP+)
VSVΔ51 Infection (MOI)

Figure 28: HSA^+ MDM are preferentially infected by OV at 48hpi. At 6 days post-HIV infection, MDM cultures were infected with MG1 or VSVΔ51 (MOI 1 or MOI 10), or left uninfected. UV-inactivated MG1 or VSVΔ51 was included as an additional negative control (denoted as "UV Ctrl" above). UV-inactivated viral particles were added to MDM cultures in a ratio of 10:1, as calculated from pre-UV inactivation virus titers. At 48 hours post-OV infection, frequencies of HSA^+ and GFP^+ MDM were measured by flow cytometry. **a.** Example of gating strategy employed during data analysis. Cellular debris was excluded (black gate), after which HSA^- (blue gate) and HSA^+ (red gate) MDM were gated upon. $\%GFP^+$ cells were then measured within HSA^+ and HSA^- populations, as shown using representative histograms. **b.** Frequencies of GFP^+ cells within HSA^+ and HSA^- MDM populations at 48 hours post-MG1 infection (n=7). **c.** Frequencies of GFP^+ cells within HSA^+ and HSA^- MDM populations at 48 hours post-VSVΔ51 infection (n=5). $p<0.0001$ by 2way repeated measures ANOVA, $^*p<0.001$ by Bonferroni posttest. Data represent mean ± SEM; n values represent separate biological replicates.

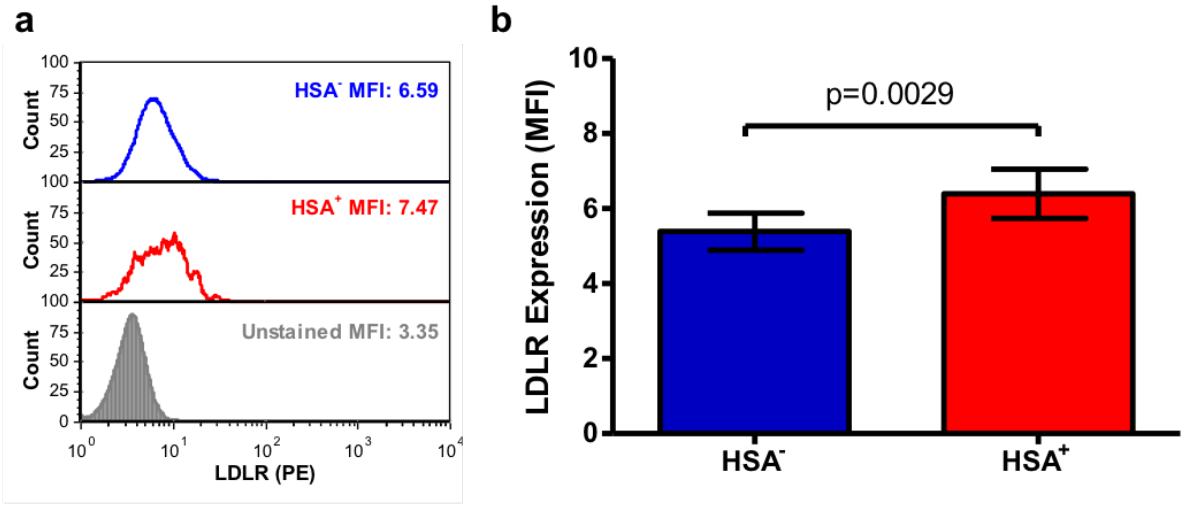
a
HSA- MFI: 6.59
HSA+ MFI: 7.47
Unstained MFI: 3.35
Count
LDLR (PE)
b
p=0.0029
LDLR Expression (MFI)
HSA-
HSA+

Figure 29: Surface expression of the MG1/VSVΔ51 receptor, LDLR, is elevated on HSA$^+$ MDM. At 6 days post-HIV infection, LDLR expression was measured on the surface of HSA$^-$ and HSA$^+$ MDM by flow cytometry. **a.** Representative histograms depicting LDLR expression on HSA$^-$ (blue) and HSA$^+$ (red) MDM. LDLR unstained control is shown as a filled, grey histogram. Histogram peak counts (y-axis) for HSA$^-$ and HSA$^+$ populations were normalized to that of the unstained control for visualization purposes. **b.** Cumulative LDLR expression on HSA$^-$ (blue) and HSA$^+$ (red) MDM (n=7; p=0.029 by paired, two-tailed t-test). Data represent mean ± SEM; n values represent separate biological replicates.

5.3.2 HIV-infected macrophages are preferentially killed by MG1, but not VSVΔ51

For OV to be of therapeutic value, they must kill HIV-infected MDM, while leaving HIV-uninfected cells untouched. The observed frequency of HSA^+ MDM decreased in an MOI-dependent manner at 48 hours post-MG1 infection (Figure 30a,b), as did the accumulation of HIV p24 antigen in cell supernatants (Figure 30c). This was accompanied by an MOI-dependent decrease in proviral HIV DNA (Figure 30d), indicating that HIV-infected MDM were being killed *in vitro*. Importantly, these findings required replication competent MG1, as UV-inactivated virus had no effect on measures of proviral HIV DNA, frequency of HSA^+ MDM, or p24 antigen release.

MG1 infection of HSA^+ MDM could be partially inhibited by pre-treating cells with increasing doses of IFNα (Figure 31a). Infection was completely blocked after pre-treatment with 100U/ml and 1000U/ml IFNα (346). Interestingly, preferential infection of HSA^+ MDM, relative to HSA^- MDM, was maintained following pre-treatment with 10U/ml IFNα. A significant decrease in proviral HIV DNA was also observed in cells pre-treated with 0 or 10U/ml IFNα, but not with 100 and 1000U/ml IFNα (Figure 31b). IFNα is therefore effective in blocking the infection and killing of HIV-infected MDM when used at doses of 100U/ml and higher.

Unlike MG1, VSVΔ51 infection did not result in an MOI-dependent decrease in the frequency of HSA^+ MDM or proviral HIV DNA (Figure 32a,b,d). HIV p24 release into culture supernatants was potently blocked following VSVΔ51 infection but not following exposure to UV-inactivated virus (Figure 32c). The ability of MG1 to selectively kill HIV-infected MDM therefore appears to be characteristic of this specific virus, rather than a quality shared by all IFN-sensitive OV.

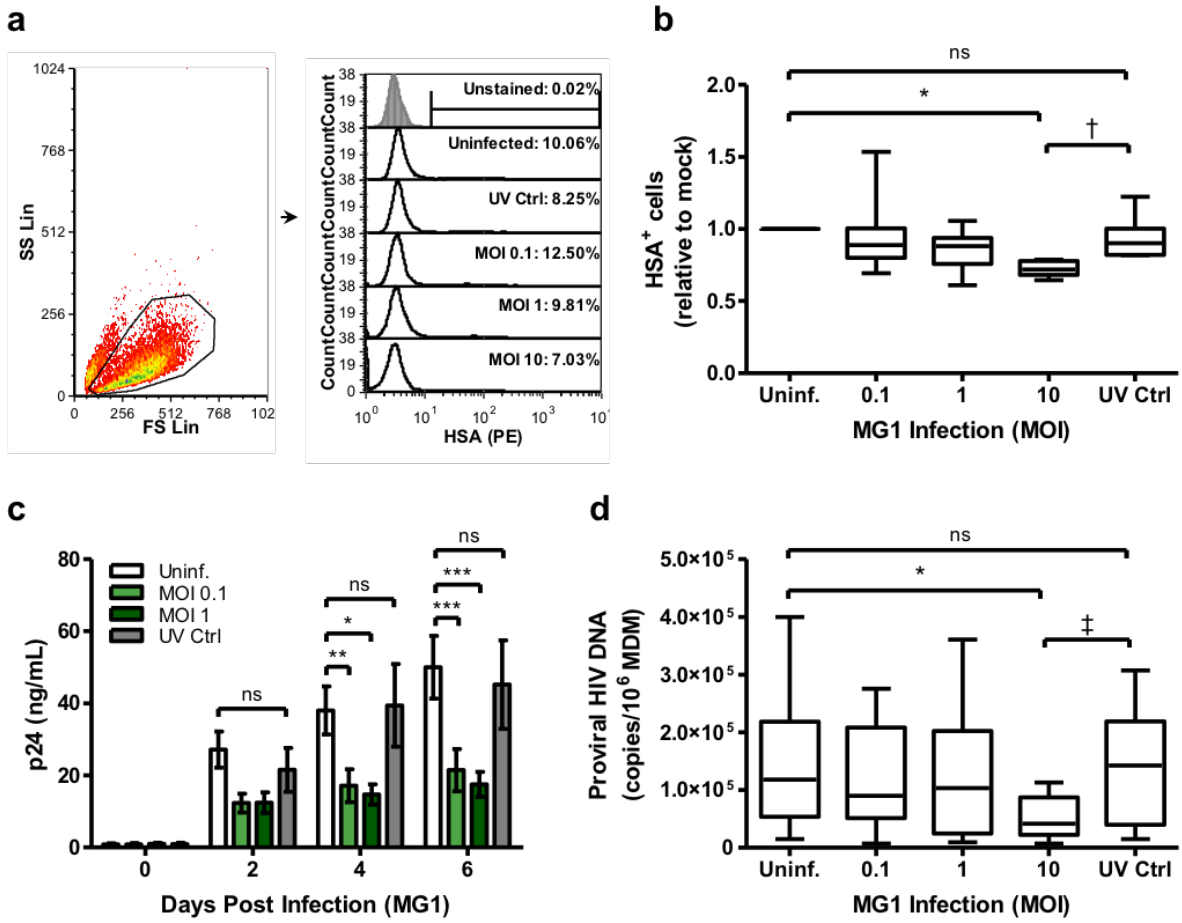
a
SS Lin
FS Lin
Unstained: 0.02%
Uninfected: 10.06%
UV Ctrl: 8.25%
MOI 0.1: 12.50%
MOI 1: 9.81%
MOI 10: 7.03%
HSA (PE)
b
HSA+ cells (relative to mock)
Uninf.
0.1
1
10
UV Ctrl
MG1 Infection (MOI)
c
p24 (ng/mL)
Uninf.
MOI 0.1
MOI 1
UV Ctrl
Days Post Infection (MG1)
d
Proviral HIV DNA (copies/10^6 MDM)
MG1 Infection (MOI)

Figure 30: MG1 selectively kills HIV-infected MDM. At 6 days post-HIV infection, MDM cultures were infected with MG1 (MOI 1 or MOI 10), left uninfected, or treated with UV-inactivated MG1 (UV Ctrl). UV-inactivated viral particles were added to MDM cultures in a ratio of 10:1, as calculated from pre-UV inactivation virus titers. Cells and supernatants were collected for further analysis at 48 hours post-MG1 infection, which included the measurement of HSA^+ MDM by flow cytometry, HIV p24 release by ELISA, and proviral HIV DNA by qPCR. In certain donors, cells were left for 6 days post-MG1 infection in order to measure HIV p24 release over this time period. **a.** Example of gating strategy employed during data analysis. Cellular debris were excluded (black gate) after which $\%HSA^+$ MDM were measured, as shown using representative histograms. **b.** Proportions of HSA^+ MDM, relative to uninfected control, at 48 hours post-MG1 infection (n=7; p=0.012 by 1way ANOVA, ns=not significant, *p<0.01 by Bonferroni posttest; †p=0.004 by unpaired, two-tailed t-test). **c.** HIV p24 accumulation in MDM culture media at 0, 2, 4, and 6 days post-MG1 infection (n=9 for uninfected and MOI 1, n=6 for MOI 0.1, and n=4 for UV Ctrl; p<0.0001 by 2way ANOVA, **p<0.05, *p<0.01, ***p<0.001 by Bonferroni posttest; ns=non-significant by unpaired, two-tailed t-test). **d.** Proviral HIV, as quantified by qPCR, at 48 hours post-MG1 infection (n=10; p=0.0073 by 1way repeated-measure ANOVA, *p<0.01 by Bonferroni posttest; ns=not significant, ‡p=0.005 by paired, two-tailed t-test) Data represent mean ± SEM; n values represent separate biological replicates.

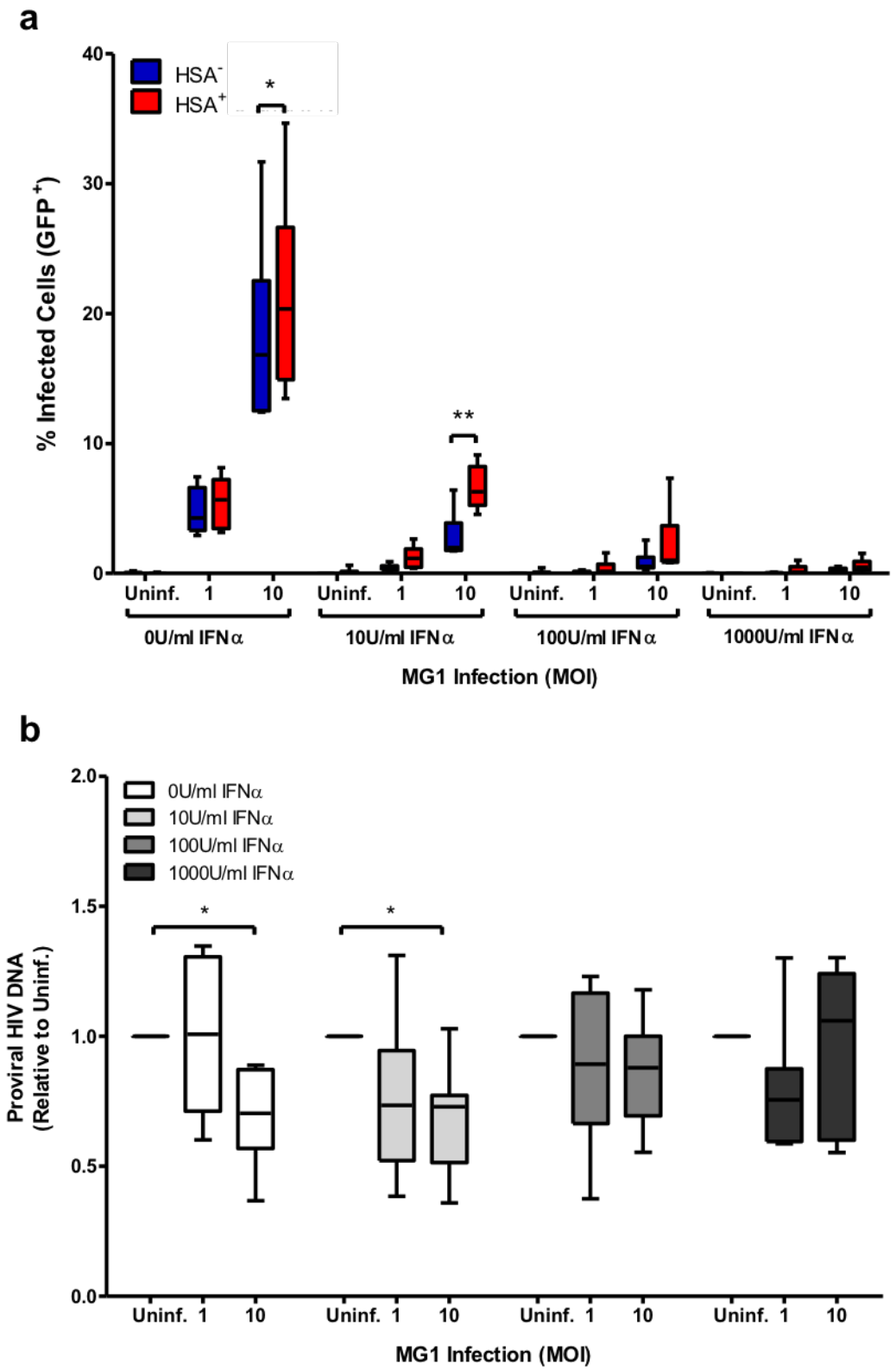
a
HSA-
HSA+
*
**
% Infected Cells (GFP+)
40
30
20
10
0
Uninf. 1 10
0U/ml IFNα
10U/ml IFNα
100U/ml IFNα
1000U/ml IFNα
MG1 Infection (MOI)
b
0U/ml IFNα
10U/ml IFNα
100U/ml IFNα
1000U/ml IFNα
Proviral HIV DNA
(Relative to Uninf.)
2.0
1.5
1.0
0.5
0.0
MG1 Infection (MOI)

Figure 31: IFNα pre-treatment protects HIV-infected MDM from MG1 infection and killing. At 6dpi, HIV-infected MDM cultures were treated with increasing doses of IFNα for 24 hours. Subsequently, MDM were infected with MG1 (MOI 1 and 10), or left uninfected, for 48 hours. To assess infection, %GFP^+ MDM were measured by flow cytometry. Proviral HIV DNA, as measured by qPCR, was used to assess MG1-mediated killing of HIV-infected MDM. **a. %**GFP^+ MDM within HSA^- (blue) and HSA^+ (red) populations at 48 hours post MG1 infection (n=6; $p<0.0001$ by 2way repeated measures ANOVA, $^*p<0.05$, $^{**}p<0.01$ by Bonferroni posttest). **b.** Proviral HIV DNA, relative to respective MG1-uninfected control, at 48 hours post-MG1 infection (n=7; $p=0.018$ and $p=0.028$ by 1way ANOVA for 0U/ml and 10U/ml IFNα, respectfully, not significant by 1way ANOVA for 100U/ml and 1000U/ml IFNα, $^*p<0.05$ by Bonferroni posttest). Data represent mean ± SEM; n values represent separate biological replicates.

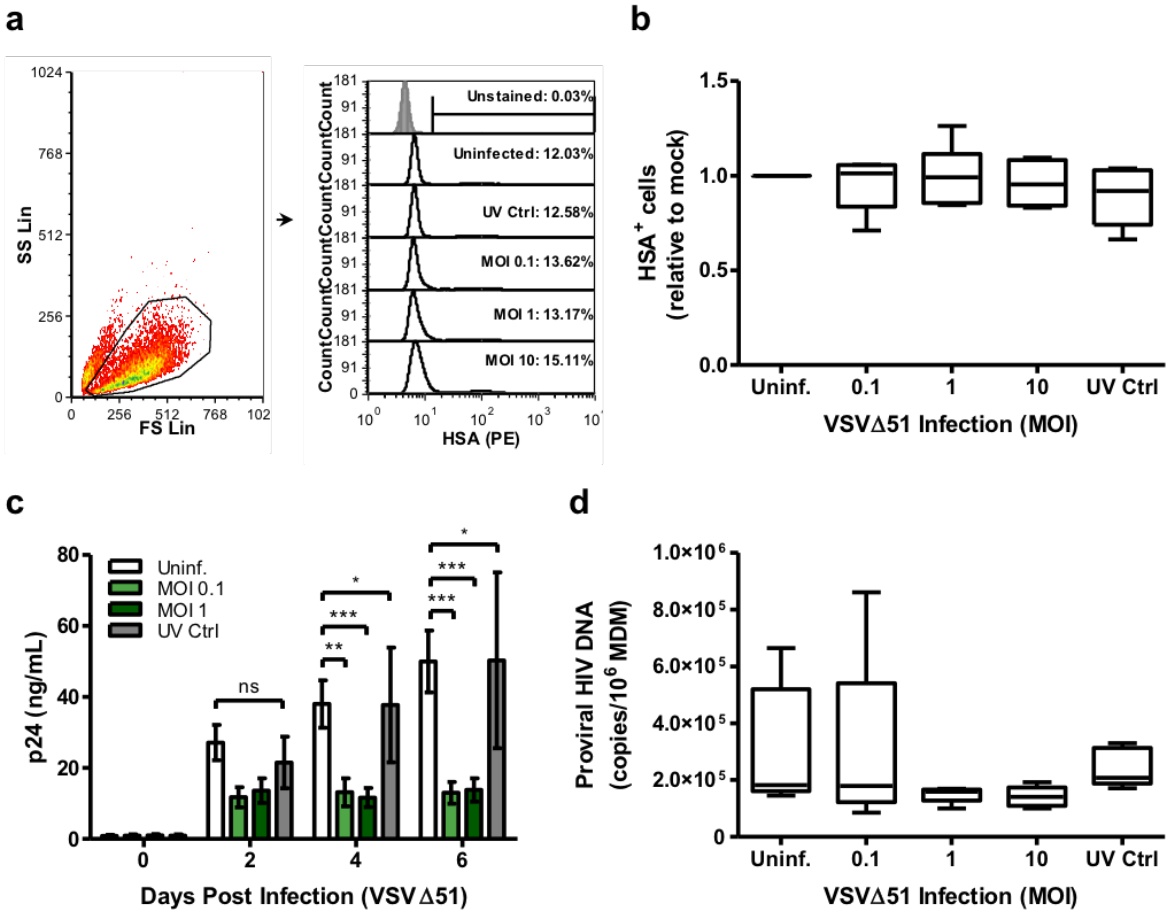
a
SS Lin
FS Lin
HSA (PE)
Unstained: 0.03%
Uninfected: 12.03%
UV Ctrl: 12.58%
MOI 0.1: 13.62%
MOI 1: 13.17%
MOI 10: 15.11%
b
HSA+ cells (relative to mock)
Uninf.
0.1
1
10
UV Ctrl
VSVΔ51 Infection (MOI)
c
p24 (ng/mL)
Uninf.
MOI 0.1
MOI 1
UV Ctrl
ns
Days Post Infection (VSVΔ51)
d
Proviral HIV DNA (copies/10^6 MDM)
VSVΔ51 Infection (MOI)

Figure 32: VSVΔ51 prevents the release of HIV p24 antigen, but does not kill HIV-infected MDM. At 6 days post-HIV infection, MDM cultures were infected with VSVΔ51 (MOI 1 or MOI 10), left uninfected, or treated with UV-inactivated VSVΔ51 (UV Ctrl). UV-inactivated viral particles were added to MDM cultures in a ratio of 10:1, as calculated from pre-UV inactivation virus titers. Cells and supernatants were collected for (further) analysis at 48 hours post-VSVΔ51 infection, which included the measurement of HSA^+ MDM by flow cytometry, HIV p24 release by ELISA, and proviral HIV DNA by qPCR. In certain donors, cells were left for 6 days post-MG1 infection in order to measure HIV p24 release over this time period. **a.** Example of gating strategy employed during data analysis. Cellular debris were excluded (black gate) after which $\%HSA^+$ MDM were measured, as shown using representative histograms. **b.** Proportions of HSA^+ MDM, relative to uninfected control, at 48 hours post-VSVΔ51 infection (n=6). **c.** HIV p24 accumulation in MDM culture media at 0, 2, 4, and 6 days post-VSVΔ51 infection (n=9 for uninfected and MOI 1, n=6 for MOI 0.1, and n=4 for UV Ctrl; $p<0.0001$ by 2way ANOVA, $^{**}p<0.01$, $^{***}p<0.001$ by Bonferroni posttest; ns=non-significant, $^{*}p<0.05$ by unpaired, two-tailed t-test). **d.** Proviral HIV, as quantified by qPCR, at 48 hours post- VSVΔ51 infection (n=5). Data represent mean ± SEM; n values represent separate biological replicates.

5.3.3 MG1-mediated killing of HIV-infected MDM does not depend on apoptotic and/or necroptotic pathways

Given that killing of HIV-infected MDM was observed with MG1, but not VSVΔ51, additional characterization of MG1-mediated killing was warranted. Oncolytic rhabdoviruses, including MG1, have been found to induce apoptosis in a variety of cancerous cell lines and solid tumors (492-496). To investigate whether the same was true for HIV-infected MDM, markers of apoptosis were measured in HSA^+ and HSA^- MDM populations at 8 and 24 hours post-MG1 infection. At both time points, MG1-infected (GFP^+), HSA^+ cells contained a significantly higher percentage of $AnnexinV^+$ cells than the GFP^+/HSA^- population (Figure 33a-c). A greater percentage of caspase $3/7^+$ cells was also observed within the HSA^+/GFP^+ MDM population (Figure 34a-c). MG1 infection therefore induces markers of apoptosis in HIV-infected, but not bystander, MDM.

Notably, GFP^-/HSA^+ MDM were also found to have elevated levels of $AnnexinV^+$ staining and caspase 3/7 activation (Figures 33a and 34a). It is unclear whether these cells had succumbed to indirect bystander killing or had initiated apoptotic cell death in response to MG1 infection, prior to GFP expression. This population was therefore excluded from the aforementioned analysis. Nonetheless, when both GFP^+ and GFP^- populations were considered, HSA^+ MDM had higher frequencies of $AnnexinV^+$ and caspase $3/7^+$ cells at 24 hours post-MG1 infection than HSA^- MDM (measured relative to respective uninfected controls), confirming that MG1-mediated killing occurs preferentially within HIV-infected MDM (Figure 35).

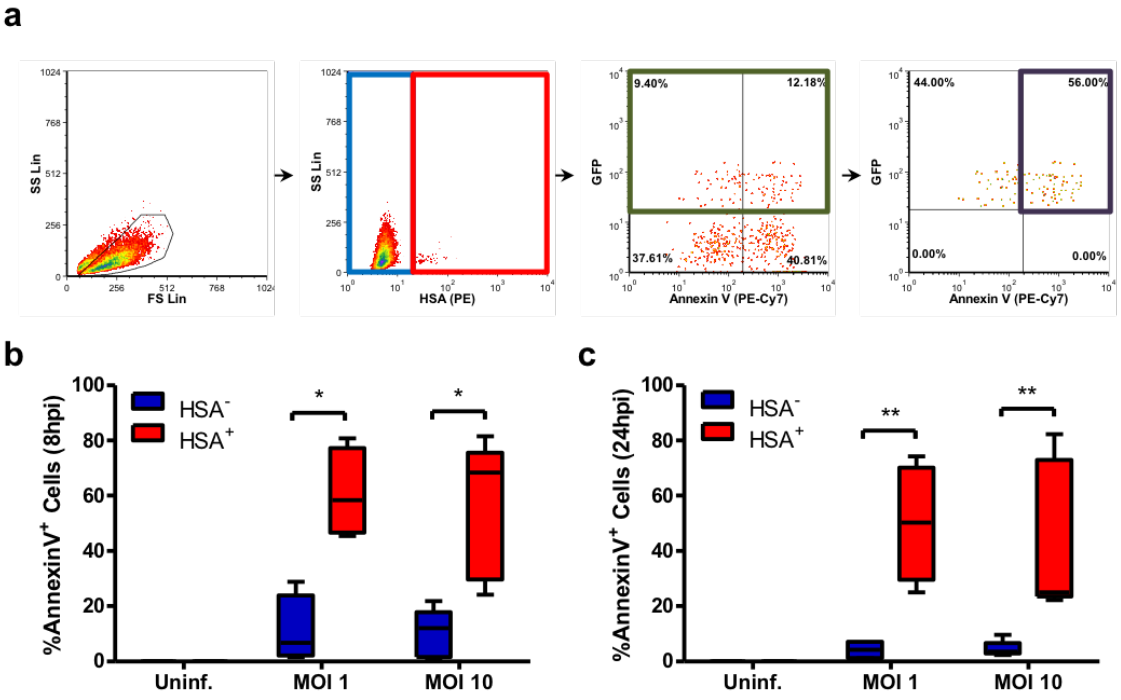
a
SS Lin
FS Lin
HSA (PE)
GFP
Annexin V (PE-Cy7)
9.40%
12.18%
37.61%
40.81%
44.00%
56.00%
0.00%
0.00%
b
%AnnexinV+ Cells (8hpi)
HSA-
HSA+
Uninf.
MOI 1
MOI 10
c
%AnnexinV+ Cells (24hpi)

Figure 33: HSA^+ MDM are AnnexinV-positive at 8 and 24 hours post-MG1 infection. At 6dpi, HIV-infected MDM cultures were infected with MG1 (MOI 1 or MOI 10) or left uninfected. Adherent cells were collected at 8 and 24 hours post-MG1 infection, after which frequencies of $AnnexinV^+$ cells within HSA^- and HSA^+ MDM populations was assessed by flow cytometry. **a.** Example of gating strategy employed during data analysis. Cellular debris were excluded (black gate), after which HSA^- (blue gate) and HSA^+ (red gate) MDM were gated upon. Next, a gate was set on $\%GFP^+$ cells (green) within both the HSA^- and the HSA+ MDM populations, and frequencies of $AnnexinV^+/GFP^+/HSA^-$ or $AnnexinV^+/GFP^+/HSA^+$ MDM were measured (purple). **b.** Frequency of $AnnexinV^+/GFP^+/HSA^-$ (blue) or $AnnexinV^+/GFP^+/HSA^+$ (red) MDM at 8 hours post-MG1 infection (n=5; p=0.0005 by 2way repeated measures ANOVA, *p<0.001 by Bonferroni posttest). **c.** Frequency of $AnnexinV^+/GFP^+/HSA^-$ (blue) or $AnnexinV^+/GFP^+/HSA^+$ (red) MDM at 24 hours post-MG1 infection (n=5; p=0.0037 by 2way repeated measures ANOVA, **p<0.01 by Bonferroni posttest). Data represent mean ± SEM; n values represent separate biological replicates.

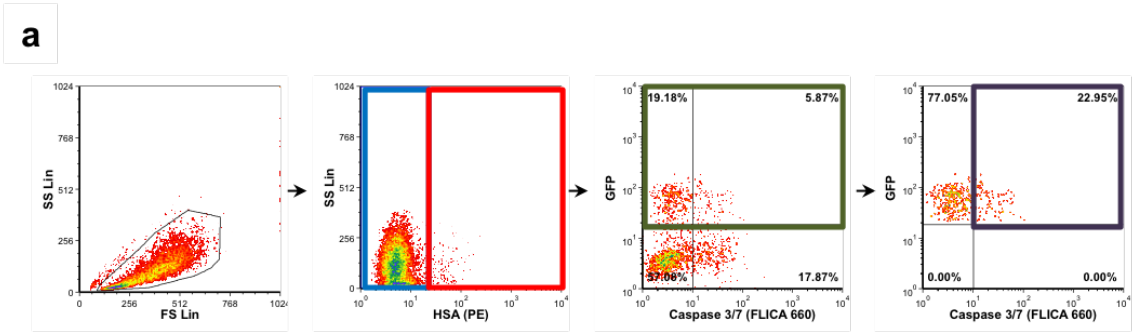
a
SS Lin
FS Lin
HSA (PE)
GFP
Caspase 3/7 (FLICA 660)
19.18%
5.87%
57.08%
17.87%
77.05%
22.95%
0.00%
0.00%

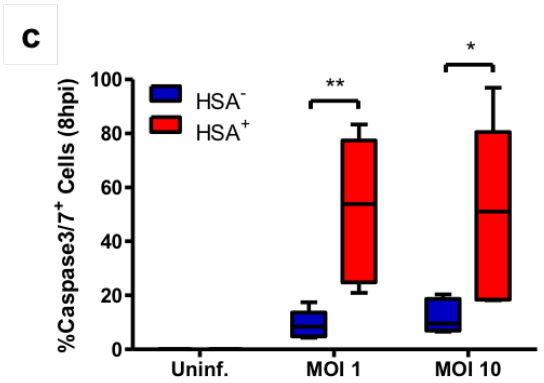
c
%Caspase3/7+ Cells (8hpi)
HSA-
HSA+
Uninf.
MOI 1
MOI 10
**
*

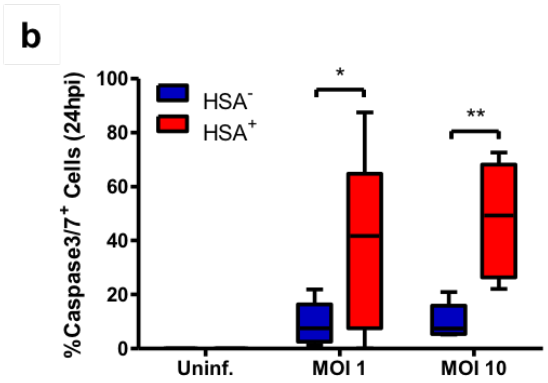
b
%Caspase3/7+ Cells (24hpi)
HSA-
HSA+
Uninf.
MOI 1
MOI 10
*
**

Figure 34: HSA^+ MDM are caspase3/7-positive at 8 and 24 hours post-MG1 infection. At 6dpi, HIV-infected MDM cultures were infected with MG1 (MOI 1 or MOI 10) or left uninfected. Adherent cells were collected at 8 and 24 hours post-MG1 infection, after which frequencies of caspase3/7^+ cells within HSA^- and HSA^+ MDM populations was assessed by flow cytometry. **a.** Example of gating strategy employed during data analysis. Cellular debris were excluded (black gate), after which HSA^- (blue gate) and HSA^+ (red gate) MDM were gated upon. Next, a gate was set on $\%GFP^+$ cells (green) within both the HSA^- and the HSA+ MDM populations, and frequencies of caspase3/7^+/GFP^+/HSA^- or caspase3/7^+/GFP^+/HSA^+ MDM were measured (purple). **b.** Frequency of caspase3/7^+/GFP^+/HSA^- (blue) or caspase3/7^+/GFP^+/HSA^+ (red) MDM at 8 hours post-MG1 infection (n=5; p=0.0035 by 2way repeated measures ANOVA, *p<0.05, **p<0.01 by Bonferroni posttest). **c.** Frequency of caspase3/7^+/GFP^+/HSA^- (blue) or caspase3/7^+/GFP^+/HSA^+ (red) MDM at 24 hours post-MG1 infection (n=5; p=0.014 by 2way repeated measures ANOVA, *p<0.05, **p<0.01 by Bonferroni posttest). Data represent mean ± SEM; n values represent separate biological replicates.

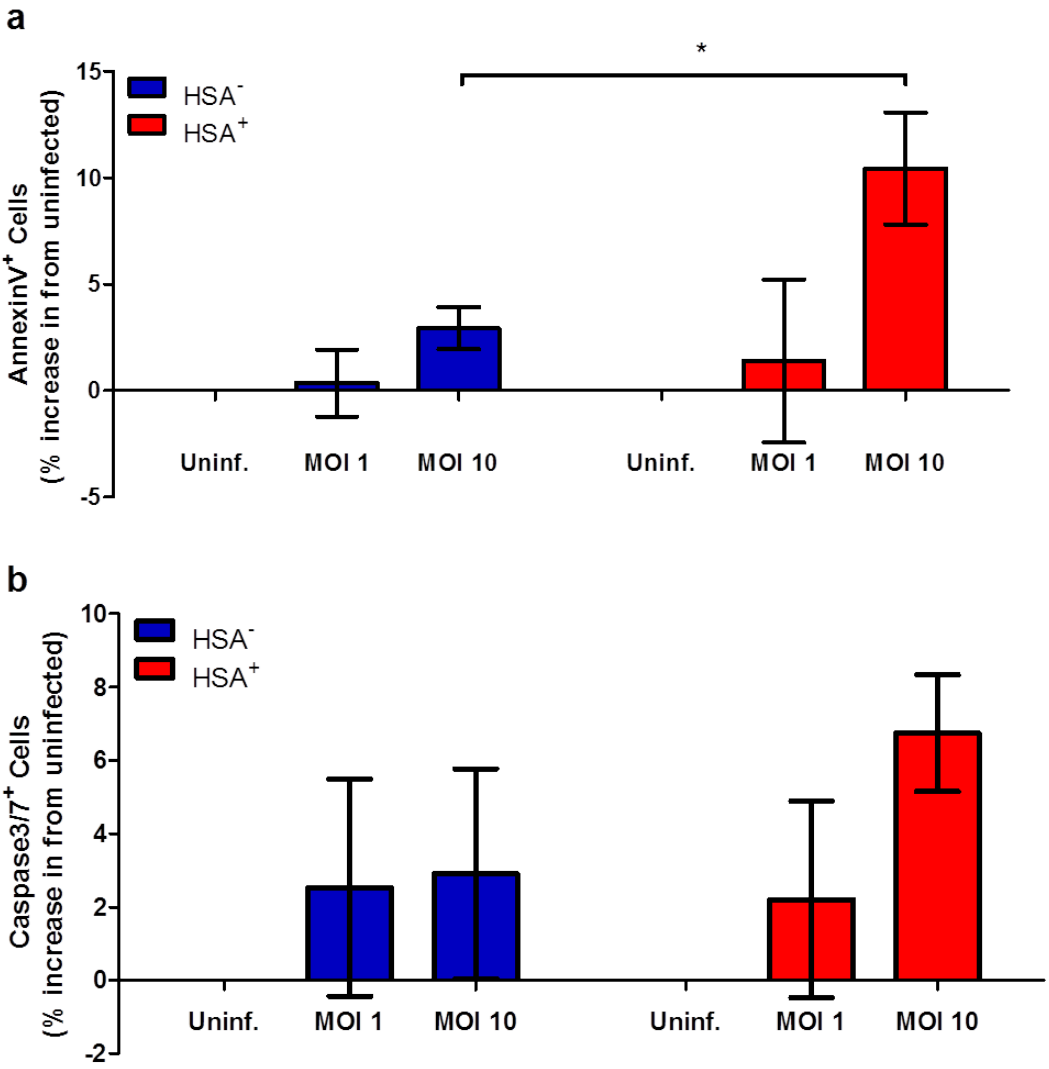
a
*
15
10
5
0
-5
HSA-
HSA+
AnnexinV+ Cells
(% increase in from uninfected)
Uninf.
MOI 1
MOI 10
Uninf.
MOI 1
MOI 10
b
10
8
6
4
2
0
-2
HSA-
HSA+
Caspase3/7+ Cells
(% increase in from uninfected)
Uninf.
MOI 1
MOI 10
Uninf.
MOI 1
MOI 10

Figure 35: HSA^+ MDM contain higher frequencies of AnnexinV- and caspase 3/7-positive cells than HSA^- MDM at 24 hours post-MG1 infection. At 6dpi, HIV-infected MDM cultures were infected with MG1 (MOI 1 or MOI 10) or left uninfected, after which AnnexinV and caspase 3/7 staining was assessed by flow cytometry. **a.** Increase in % $AnnexinV^+$ MDM in HSA^- (blue) or HSA^+ (red) cell populations at 24 hours post-MG1 infection (n=5; p=0.013 by 2way repeated measures ANOVA, *p<0.05 by Bonferroni posttest). **b.** Increase in % caspase $3/7^+$ MDM in HSA^- (blue) or HSA^+ (red) cell populations at 24 hours post-MG1 infection (n=5; not significant by 2way repeated measures ANOVA). Data represent mean ± SEM; n values represent separate biological replicates.

Next, the dependence of MG1-mediated killing on caspase activation was investigated using the pan-caspase inhibitor, ZVAD-FMK. ZVAD-FMK dose was previously optimized using healthy MDM, which were exposed to increasing concentrations of ZVAD-FMK prior to a 2 hour treatment with 10μM camptothecin (data not shown). Unexpectedly, pre-treatment with ZVAD-FMK did not block MG1-mediated killing of HIV-infected MDM. AnnexinV staining on ZVAD-FMK-treated GFP^+/HSA^+ MDM remained elevated relative to that on GFP^+/ HSA^- cells at 24 hours post-MG1 infection (Figure 36a). Moreover, an MG1 MOI-depended reduction in proviral HIV DNA was observed in both ZVAD-FMK-treated and untreated MDM (Figure 36b). ZVAD-FMK has previously been shown to trigger necroptosis in myeloid-lineage cells by permitting the activation of receptor interacting protein 1 (RIPK1) (497-499). In comparison to cells pre-treated with only ZVAD-FMK, the addition of a specific RIPK1 inhibitor, Necrostatin-1 (500), reduced AnnexinV staining on both GFP^+/HSA^+ and GFP^+/HSA^- MDM (Figure 34a). Nonetheless, a significant, MG1-mediated decrease in proviral HIV DNA was observed in cells that had been pre-treated with Necrostatin-1, or combination of Necrostatin-1 and Z-VAD-FMK (Figure 36b). MG1-mediated killing of HIV-infected MDM, therefore, does not appear to depend solely on the induction of programmed cell death pathways such as apoptosis or necroptosis.

a

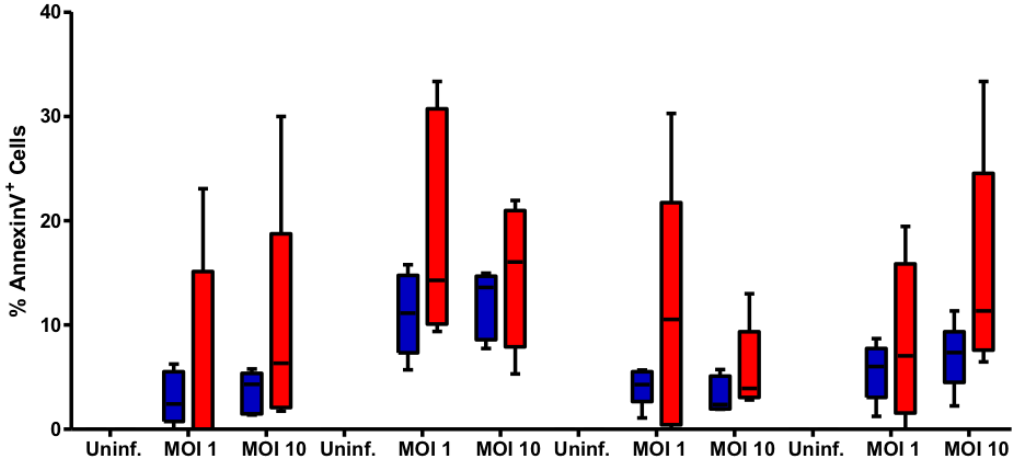

ZVAD-FMK	-	-	-	+	+	+	-	-	-	+	+	+
Necrostatin-1	-	-	-	-	-	-	+	+	+	+	+	+

b

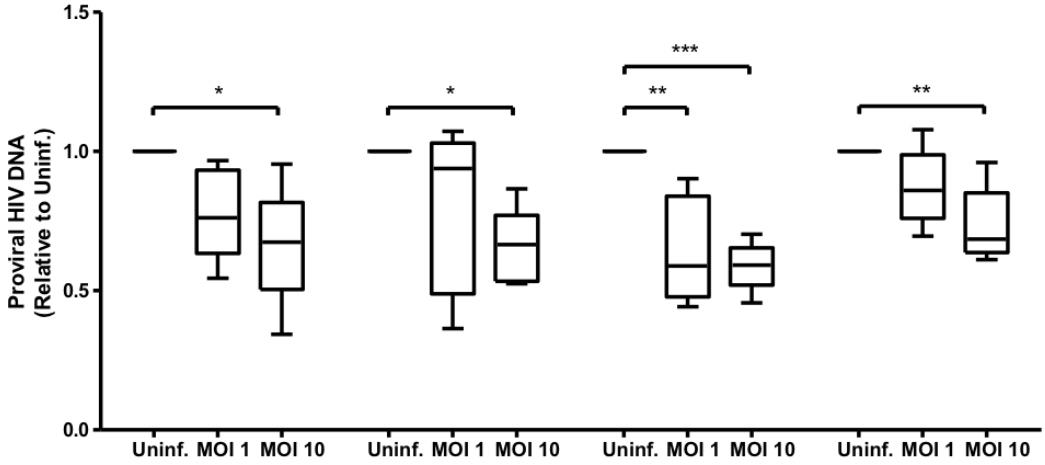

ZVAD-FMK	-	-	-	+	+	+	-	-	-	+	+	+
Necrostatin-1	-	-	-	-	-	-	+	+	+	+	+	+

Figure 36: Inhibitors of caspases or RIPK1 do not prevent MG1-mediated killing of HIV-infected MDM. At 6dpi, HIV-infected MDM cultures were pre-treated with 50μM ZVAD-FMK, 50μM Necrostatin-1, or 50μM of both for 1 hour. An equivalent volume of DMSO was used for the untreated control. Without changing the cell culture media, MDM were infected with MG1 (MOI 1 or MOI 10) or left uninfected. Adherent cells were collected at 24 hours and 48 hours post-MG1 infection for the measurement of AnnexinV$^+$ cells by flow cytometry or proviral HIV DNA by qPCR, respectfully. The gating strategy used to assess AnnexinV$^+$ MDM is as shown in Figure 6a. **a.** AnnexinV$^+$/GFP$^+$/HSA$^-$ and AnnexinV$^+$/GFP$^+$/HSA$^+$ MDM at 24 hours post-MG1 infection. **b.** Proviral HIV DNA at 48 hours post-MG1 infection, relative to MG1-uninfected control. (n=5; p=0.016, p=0.041, p=0.0003, and p=0.0089 by 1way ANOVA for untreated, ZVAD-FMK only, Necrostatin-1 only, and ZVAD-FMK/Necrostatin-1 treated cells, respectfully,*p<0.05, **p<0.01, ***p<0.001 by Bonferroni posttest). Data represent mean ± SEM; n values represent separate biological replicates.

5.3.3 MG1-mediated killing of HIV-infected macrophages requires the presence of infectious virus

Finally, the possibility that MG1 infection could trigger indirect, cytokine-mediated eradication of HIV-infected cells was considered. To address this question, supernatants from MG1-infected, HIV-uninfected MDM were collected and clarified via filtration at 48 hours post-MG1 infection. These virus-free, conditioned supernatants were then added to autologous, HIV-infected MDM (in a 1:2 ratio with fresh media) at 6 days post-HIV infection, with MG1 infection performed in parallel as a positive control. Cells that received conditioned supernatants from MG1-infected MDM showed a small, but significant drop in viability (Figure 37a). As expected, MG1 infection prevented the accumulation of HIV p24 antigen in culture supernatants (Figure 37b) and reduced proviral HIV DNA relative to uninfected control wells (Figure 37c), whereas UV-inactivated MG1 had no effect on HIV p24 release or proviral HIV DNA. The exposure of HIV-infected MDM to filtered supernatants also inhibited p24 antigen release, but no change in proviral HIV DNA was observed relative to untreated control cells (Figure 37b,c). Soluble factors released following MG1 infection are therefore partially responsible for preventing p24 release by HIV-infected cells. The eradication of HIV-infected MDM, conversely, requires the presence of infectious MG1.

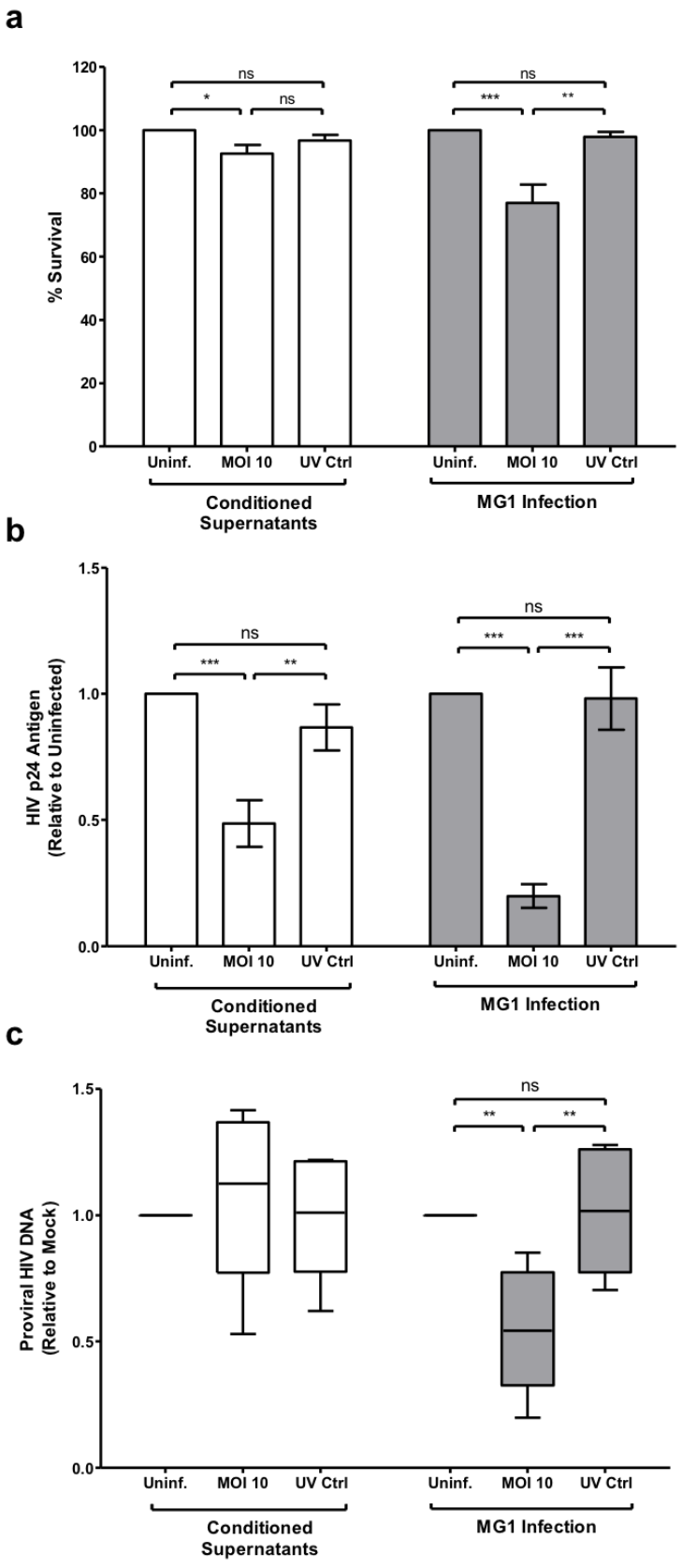
a
% Survival
120
100
80
60
40
20
0
ns
*
ns
ns
***
**
Uninf.
MOI 10
UV Ctrl
Uninf.
MOI 10
UV Ctrl
Conditioned Supernatants
MG1 Infection
b
HIV p24 Antigen (Relative to Uninfected)
1.5
1.0
0.5
0.0
ns
***
**
ns
***
***
Uninf.
MOI 10
UV Ctrl
Uninf.
MOI 10
UV Ctrl
Conditioned Supernatants
MG1 Infection
c
Proviral HIV DNA (Relative to Mock)
1.5
1.0
0.5
0.0
ns
**
**
Uninf.
MOI 10
UV Ctrl
Uninf.
MOI 10
UV Ctrl
Conditioned Supernatants
MG1 Infection

Figure 37: Conditioned supernatants from MG1-infected, HIV-negative MDM block p24 release without the preferential killing of HIV-infected MDM. At 6dpi, HIV-infected MDM cultures were infected with MG1 MOI 10, left uninfected, or treated with UV-inactivated MG1 (UV Ctrl). UV-inactivated viral particles were added to MDM cultures in a ratio of 10:1, as calculated from pre-UV inactivation virus titers. In duplicate, HIV-infected MDM were treated with filtered supernatants collected from autologous HIV-uninfected MDM that had been infected with MG1 MOI 10, left uninfected, or treated with UV-inactivated MG1. At 48 hours post-MG1 infection, cell viability was assessed by MTT or proviral HIV DNA was measured by qPCR. In certain donors, cell supernatants were collected at 0, 2, 4, and 6 days post-MG1 infection for the measurement of HIV p24 release by ELISA. **a.** MDM viability, as measured by MTT assay relative to respective uninfected control, at 48 hours post-MG1 infection or supernatant transfer (n=6; p=0.041 and p=0.0005 by 1way ANOVA for cells treated with conditioned supernatants and MG1 infected cells, respectfully, *p<0.05, **p<0.01, ***p<0.001 by Bonferroni posttest). **b.** HIV p24 antigen in culture supernatants, relative to MG1-uninfected control, at 6 days post-MG1 infection or supernatant transfer (n=6; p=0.0006 and p<0.0001 by 1way ANOVA for cells treated with conditioned supernatants and MG1 infected cells, respectfully, **p<0.01, ***p<0.001 by Bonferroni posttest). **c.** Proviral HIV DNA, measured relative to respective uninfected control, at 48 hours post-MG1 infection or supernatant transfer (n=6; p=0.0012 by 1way ANOVA, **p<0.01 by Bonferroni posttest). Data represent mean ± SEM; n values represent separate biological replicates.

5.4 Discussion

As demonstrated above, HIV-infected MDM showed increased susceptibility to a known OV, MG1, relative to their HIV-uninfected counterparts. We have previously shown HSA^+ MDM to be defective in their ability to upregulate antiviral ISG in response to a synthetic viral RNA mimetic, 5'ppp-dsRNA. HIV-mediated inhibition of the IFN1 response, combined with the higher overall expression of LDLR observed on HSA^+ MDM, may enable their preferential infection by both MG1 and VSVΔ51. Interestingly, only MG1 was capable of mediating preferential killing of HSA^+ MDM—a process that was independent of caspase or RIPK1 activation, but dependent on the presence of infectious viral particles. Although MG1 and VSVΔ51 are both of the *Rhabdoviridae* family, differences in how these viruses were engineered may explain the increased infectivity and cytopathogenicity of MG1. Given that MG1 is currently in clinical trials for the treatment of non-small cell lung cancer and advanced/metastatic solid tumors, expanding its use to PLWHIV may be a feasible future direction.

5.4.1 Different oncolytic viruses vary in their ability to eliminate HIV-infected monocyte-derived macrophages

Consistent with the observations made by Brun et al., MG1 infected and killed target cells with greater efficacy than VSVΔ51 (346). This finding also mirrored that of Ranganath et al., who found that MG1, but not VSVΔ51, was capable of killing latently HIV-infected $CD4^+$ T cells (354,402). Overall, MG1 was more infectious than VSVΔ51 in both HSA^- and HSA^+ MDM (as measured by $\%GFP^+$ cells), which may

partially explain this finding. The ability of MG1 to effectively kill HIV-infected MDM may also be explained by the engineering of the virus itself. While VSVΔ51 and MG1 are highly sensitive to IFN1 due to a single point mutation within the M protein (301), an additional amino acid substitution (Q242R) within the G protein of MG1 enhances its infectivity in tumor cell lines relative to that of the wild-type Maraba virus (346).

How this G protein mutation enhances MG1 infection of malignant cells, and in our case HIV-infected MDM, is currently unknown. Still, it is not surprising that G protein mutagenesis can enhance (501) or attenuate (502) virus infectivity since this protein directly mediates *Rhabdoviridae* tropism, entry, and spread. Mutagenesis of both the M and G proteins of MG1 may therefore work in concert to ensure selectivity for IFN1-deficient cells. For this example, let us assume that the Q242R amino acid substitution within the MG1 G protein enhances viral entry. Regardless of the rate of viral entry, MG1 infection of healthy cells will still elicit an IFN1 response and render these cells refractory to MG1-mediated killing. In IFN1-defective cells, however, enhanced rates of viral entry could outpace residual antiviral defense mechanisms and allow MG1 to establish a productive infection before additional ISG induction occurs. Similar examples of synergistic epistasis have been observed using VSV, with certain pairs of amino acid substitutions increasing viral fitness relative to single mutant or wild-type virus (482). It therefore likely that a similar synergistic relationship between L123W and Q242R has occurred in MG1.

Regardless of the exact synergistic mechanism (if any) underlying the results shown above, MG1 was able to kill HIV-infected MDM while VSVΔ51 was not. This

implies that the killing of HIV-infected cells can be attributed to the unique viral characteristics of MG1, rather than a non-specific cellular response to a second viral infection. Going forward, it will be possible to further engineer MG1 to increase its potency and selectivity for HIV-infected cells *in vivo*, making it an attractive therapeutic option for targeting the HIV reservoir in PLWHIV.

5.4.2 Killing of HIV-infected monocyte-derived macrophages by MG1 occurs independently of programmed cell death pathways

Oncolytic rhabdoviruses MG1 and VSVΔ51 have previously been shown to induce apoptosis in malignant cells (492-496). While caspase activation and increased expression of phosphatidylserine on the outer cell membrane leaflet were elevated on HSA^+ relative to HSA^- MDM (Figures 33-35), the addition of a known pan-caspase inhibitor, ZVAD-FMK, did not block MG1-mediated killing of HIV-infected cells (Figure 36). It therefore appears that the induction of apoptosis is not the primary mechanism of killing following MG1 infection.

Understanding the mechanism behind MG1-induced killing is relevant to its future clinical development. Thus, additional programmed cell death pathways were investigated. Balachandran et al. previously found that the use of ZVAD-FMK could not completely block VSV-mediated killing of the C6 glioblastoma cell line (503). Several cell death pathways may therefore be activated in response to viral infection. Since the activation of caspase 8 has been shown to cleave a key mediator of necroptosis, RIPK1 (498,504), we hypothesized that ZVAD-FMK alone may prime MDM for necroptotic cell death following MG1 infection. Inhibition of

RIPK1 by necrostatin-1 similarly failed to block MG1-mediated killing of HSA^+ MDM, indicating that MG1-mediated cytopathogenicity of HIV-infected cells occurs independently of programmed cell death pathways. The decrease in proviral HIV DNA observed following MG1 infection also occurred in necrostatin-1-treated cells, indicating that HIV-infected MDM continued to succumb to MG1-mediated killing in this experimental condition, whereas bystander MDM remained viable (Figure 36b).

A key difference separating the killing of malignant cells by MG1 from the killing of HIV-infected cells by MG1 is the fact that latter have already sustained one viral infection. Ongoing HIV replication may inhibit the cell's ability to mount an appropriate antiviral response, facilitating selective infection by MG1. Although HIV possesses several means by which to limit homologous superinfection, these barriers typically involve the downregulation of HIV-specific cell surface receptors (487) and would therefore not impact *Rhabdoviridae* infection. Interestingly, HIV is capable of blocking pro-apoptotic pathways within target cells in order to facilitate its own persistence *in vivo* (505). In combination with the results obtained following treatment of HIV-infected MDM with ZVAD-FMK, this suggests that cell death following MG1 superinfection is not dependent on apoptosis. Similarly, HIV protease is capable of degrading RIPK1 leading to the hypothesized suppression of necroptosis in HIV-infected cells (506).

The potential role of other cell death pathways, such are autophagic cell death (507), must therefore be considered. Two proteins involved in mediating cell stress responses, PKR and GCN2, are implicated in this process (508). We have previously shown HIV-infected MDM to possess elevated levels of PKR at baseline (Chapter 4, Figures 16 & 24), suggesting that the activation of this protein in

combination with the metabolic stress placed on the cell due to ongoing viral replication may trigger autophagic cell death. The HIV accessory protein Nef has, however, been found to block the late-stage maturation of the autophagosome and prevent autophagic death of infected cells (509). Alternatively, caspase 1-mediated pyroptosis has been demonstrated in HIV-infected $CD4^+$ T cells (73), and in melanoma cells infected by the oncolytic HSV-2 mutant, DeltaPK (510). Cells undergoing pyroptosis sustain cell membrane damage, leading to the release of danger-associated molecular patterns (DAMPs) and the expression of “eat me” signals required for clearance by phagocytic cells such as macrophages (511,512). Thus, MG1 infection may potentiate this process in HIV-infected MDM, leading to their elimination.

At present, the exact mechanism by which MG1 mediates the killing of HIV-infected MDM remains uncharacterized. Understanding the cellular pathways involved in potentiating or inhibiting MG1-mediating killing in HIV-infected cells will certainly form an important future direction with direct relevance to the clinical development of OV-based therapies. Nonetheless, we can be confident that the presence of replication competent MG1 and the expression of viral proteins are key to this process.

5.4.3 Killing of HIV-infected monocyte-derived macrophages and inhibition of HIV replication occur by different pathways following MG1 infection

The field of oncolytic virotherapy has explored several additional strategies to achieve targeted killing of cancer cells while maintaining patient safety. UV-inactivated viral particles, for instance, effectively eradicate acute myeloid leukemia

cells (513). As discussed above and shown in Figure 29, UV-inactivated MG1 did not kill HIV-infected MDM, nor did it have any impact on HIV p24 release.

The induction of a pro-inflammatory cytokine response following OV infection may also facilitate the indirect eradication of malignant cells. VSV infection of primary PBMC and glial cells, for example, has been shown to induce the secretion of TNFα, IL-6, IFNγ, and IFNα/β, (514,515). It is believed that the release of these cytokines in tumour-bearing mice infected by VSV results in the recruitment of neutrophils to the tumor bed, which is followed by a loss of blood flow to the tumour, acute ischemia, and the apoptosis of malignant cells (516). TNFα and IFNγ have also been shown to induce cell death in HIV infected cell lines (517), as well as block viral replication within HIV-infected macrophages (283,518). The induction of a similar pro-inflammatory cytokine response by MG1-infected MDM was therefore considered as a possible mechanism of MG1-mediated killing. While IFNα/β could not be detected in cell supernatants following MG1 infection of MDM, both conditioned media (following filtration to remove infectious viral particles) and MG1 infection significantly reduced HIV p24 antigen release from HIV-infected cells. Moreover, no difference in proviral HIV DNA was observed following supernatant transfer (despite a small but significant decrease in cell viability). Soluble factors released following MG1 infection therefore appear to block HIV replication without selectively killing HIV-infected cells. The characterization of the soluble factors released following MG1 infection may be an important consideration, since several pro-inflammatory cytokines (including IFNα, IFNγ, and TNFα) have been found to block HIV replication at the pre- or post-integration stage (283,518-520). MG1-

mediated killing of HIV-infected MDM may therefore elicit a pro-inflammatory response that can prevent subsequent rounds of HIV replication and re-seeding of the HIV reservoir.

5.5 Future directions

As noted by Batenchuk et al., the treatment of immunocompromised patients with a replication-competent oncolytic virus is concerning from a patient safety standpoint (513). Similar to the use of OV for cancer therapy, this concern may be avoided in the context of HIV infection by using a recombinant OV that is unable to infect healthy cells. Fortunately, potential neurotoxicity by VSV (521,522) or MG1 (346,347) is ameliorated via mutation of the viral M protein. These attenuated viruses are therefore only capable of establishing productive infection within cells that lack a robust IFN1 response (301,346). Given that low concentrations of IFNα were sufficient to protect IFN1-sensitive, HIV-uninfected MDM but not HIV-infected MDM it may be possible to further limit MG1-mediated killing of HIV-uninfected cells by engineering the virus to express IFNα. Westcott et al. have previously shown that an IFNα2-expressing VSV displayed enhanced selectivity for head and neck squamous cell carcinoma (HNSCC) cells over non-cancerous cells (523). VSV expressing IFNβ (VSV-IFNβ) has also been tested in murine models of metastatic lung disease, non-small cell lung cancer, and mesothelioma with positive results (476,524,525). Consequently, VSV-IFNβ is currently under investigation in several Phase I clinical trials (reviewed in detail in (526)). Alternatively, elevated levels of IFN1 within tissues harbouring HIV reservoir cells may prevent effective MG1-

mediated killing, as was observed in Figure 31 when doses of 100U/ml and 1000U/ml IFNα were used. Still, it is difficult to accurately quantify tissue IFNα/β levels *ex vivo*. The limitations that persistent IFN1 signalling may pose for the use of therapeutic OV in PLWHIV are therefore an important consideration that will be better assessed *in vivo*.

Limiting cytotoxicity to HIV-infected cells may also be achieved via direct modification of the MG1 genome. As previously suggested by Ranganath (402) insertion of a HIV protease cleavage site in between the G and L genes of MG1 will result in a viral variant that requires the presence of HIV protease to complete its replication cycle and generate infectious viral progeny. This strategy, however, necessitates productive HIV replication and appropriate expression of HIV protease. Alternatively, re-targeting VSV for CD4-expressing cells can be achieved by engineering the virus to express a chimeric VSV G-HIV gp160 (gp160G) (485). This approach has since been investigated as means by which to treat adult T cell leukemia, with notable success (and safety) in animal models of the disease (527). A similar strategy may allow CD4-expressing, HIV-infected target cells to killed by MG1 in a highly specific manner. In this scenario, HIV-uninfected $CD4^+$ cells may still be infected, but will be capable of preventing productive MG1 infection via upregulation of IFN1. The development of an MG1 variant engineered to target HIV-infected cells specifically therefore remains an important future direction, which is currently under investigation by our group. Going forward, MG1 will be investigated as an HIV-reservoir targeting therapy using humanized mouse models, as well as

within a proof-of-concept clinical trial in PLWHIV. The translation of an MG1-based HIV cure strategy to *in vivo* study is discussed further within Chapter 8.4.

5.6 Conclusion

In conclusion, HIV-infected MDM were found to be selectively infected and killed by the IFN1-sensitive oncolytic Rhabdovirus, MG1. Pre-treatment with low doses of IFNα failed to prevent MG1-mediated killing, highlighting the role of defective IFN1 signalling pathways in facilitating the eradication of HIV-infected cells. Moreover, this process required the presence of infectious MG1 and was not mediated solely by a proinflammatory cytokine response or programmed cell death pathways such as apoptosis or necroptosis. It will be necessary to characterize the mechanism of MG1-mediated killing, especially since a related, IFN1-sensitive OV, VSVΔ51, was not found to selectively kill HIV-infected MDM. This knowledge will inform our *in vivo* use of MG1—for example, in humanized mouse models of HIV infection—and provide further opportunity to modify MG1 to be better able to target and eradicate HIV-infected reservoir cells. Given that MG1 is now in clinical trials for the treatment of metastatic solid tumors and non-small cell lung cancer (ClinicalTrials.gov Identifier: NCT02285816 and NCT02879760), a proof of concept clinical trial in PLWHIV may also be warranted.

Chapter 6: Assessing MG1-mediated killing of HIV-infected alveolar macrophages

6.1 Introduction

6.1.1 Rational

MG1-mediated killing of HIV-infected cells has been shown using promyeloid cell line models of latent HIV infection (354) and *in vitro* HIV-infected MDM (Chapter 5.3.2). Primary macrophages isolated from PLWHIV form an additional tool with which to investigate the capacity for MG1 to eradicate the myeloid HIV reservoir. Unlike $CD4^+$ T cells, however, the isolation, culture, and study of these cells is technically challenging. HIV-infected macrophages do not circulate within the peripheral blood, residing instead within tissues such as the gastrointestinal tract (528,529), brain (429,530,531), and spleen (108). Isolation of these cells relies on tissue collection via biopsy, which is invasive and yields very few cells with which to perform downstream *ex vivo* studies. Furthermore, MDM from PLWHIV is not a reliable model as circulating monocytes are resistant to HIV infection *in vivo* (532-534). A unique solution to this problem is the use of alveolar macrophages (AM), which are reservoirs for HIV during well-treated infection and can be easily isolated via BAL. We therefore chose to use AM for the *ex vivo* study of MG1 infection and killing of HIV-infected cells, since AM form a rare source of primary HIV-infected macrophages that can be isolated from PLWHIV.

6.1.2 Role of alveolar macrophages *in vivo*

AM form the first line of defense within the lung and play a key role in the removal of bacteria, viruses, and cellular debris. Proximal to alveolar epithelial cells within the alveolar lumen, AM possess immense phagocytic capacity that limits dendritic cell activation and lung inflammation following exposure to inhaled pathogens (535). Release of immunosuppressive factors like transforming growth factor beta (TGF-β) and interleukin-10 (IL-10) by AM further promotes immune tolerance in infiltrating $CD4^+$ T cells (536-538). Together, this maintains airway structure and prevents respiratory failure and mortality during lung infection (539).

Given their important role in tissue homeostasis and protection, AM comprise the largest population of immune cells within the lung (>90%) (539,540). Like other tissue resident macrophage subsets, AM are derived predominantly from embryonic yolk sac erythro-myeloid progenitors, and are believed to undergo active replication to maintain their presence within the lung (541,542). Evidence of this has been shown in lung transplant recipients—donor AM are maintained within the recipient rather than being replaced by recipient-derived cells (543,544). Other precursor cells can further contribute to the AM population over time, including fetal liver and bone marrow-derived monocytes (542,545). The latter play a particularly important role in re-establishing the AM population and tissue homeostasis following lung inflammation or infection (542,546).

6.1.3 Alveolar macrophages as a target for HIV infection and persistence

The ability of HIV to infiltrate the lung was first described in 1986 (547,548). *Ex vivo* culture of alveolar macrophages from PLWHIV resulted in the production of infectious viral particles by these cells (548). Analysis of lung biopsy tissue further revealed that cells possessing both lymphoid and myeloid phenotypes contained HIV RNA (547). Given that pulmonary infections were (and remain) quite common in PLWHIV (reviewed in (549)), the impairment of AM function following HIV infection was suspected. Indeed, subsequent studies demonstrated that HIV-infected AM possessed a reduced phagocytic capacity for certain bacterial pathogens (99,443); an effect which can be exacerbated by smoking (550).

AM possess a half-life of approximately 30 days (551,552) and do not succumb to HIV-mediated cytopathogenicity (548). The role of these cells as a significant tissue-resident reservoir for HIV has therefore been recently proposed (reviewed in (553)). The detection of proviral DNA in the lungs of cART-controlled individuals (443,554,555) and non-human primates (556) lends further support to this hypothesis, as does evidence supporting the maintenance of AM populations via a combination of local proliferation and monocyte infiltration (542,545,546). The latter provide a continuously renewing source of target cells to support subsequent rounds of viral replication. HIV-infected $CD4^+$ T cells are also present in appreciable numbers within the lung (350,554), and may be phagocytosed by AM resulting in their infection (139,557). AM therefore comprise an important viral reservoir *in vivo*, which is relevant to HIV cure research and form a valuable *ex vivo* model of HIV-infection in primary macrophages.

6.2 Hypothesis

HIV-infected alveolar macrophages isolated from PLWHIV will be eradicated by the oncolytic rhabdovirus, MG1.

6.3 Results

6.3.1 The oncolytic rhabdovirus, MG1, kills HIV-infected alveolar macrophages

AM were collected by BAL from HIV-positive donors on suppressive cART for ≥3 years at the time of collection. Relevant patient details are described in Table 3. Adherent BAL cells were infected at MOI 1 or 10 with MG1, and at 48 hours post-MG1 infection, proviral HIV DNA was measured by digital droplet PCR. As expected (553), copies of proviral HIV DNA were variable between donors at baseline. No difference in proviral DNA was observed at MG1 MOI 1, although infection at MOI 10 resulted in a slight decrease in proviral HIV DNA within the AM of most individuals (Figure 38). In fact, a decrease in proviral HIV DNA, relative to baseline levels, was observed in 7 out of 10 AM cultures following infection with MG1 MOI 10 (Figure 39a). Conversely, infection at MG1 MOI 10 did not reduce proviral HIV DNA in AM isolated from the remaining 3 donors (Figure 39b). Exact proviral DNA copy numbers for all donors are found in Table 4.

Table 3: Patient clinical characteristics

Pt Code	Age	Tobacco (Ever; Current)	MJ*	Sex	ARVs at time of bronch.	CD4 (cells/µl)	Time from sero-conversion (years)	Duration of suppressed PBVL (years)
Pt34	52	No; No	No	F	Truvada; Atazanavir; Ritonavir	621	19	7
Pt35	62	No; No	Yes	M	Triumeq	899	28	9
Pt37	58	No; No	No	M	Truvada; Isentress	537	22	10
Pt38	57	Yes; Yes	Yes	M	Atripla	396	32	10
Pt39	58	Yes; No	Yes	M	Stribild	269	20	8
Pt40	54	Yes; Yes	Yes	F	Reyataz; Complera; Raltegravir	360	24	6
Pt41	58	Yes; No	Yes	M	Raltegravir; Etravirine; Ritonavir; Darunavir	412	31	11
Pt42	51	No; No	No	M	Atripla	541	18	8
Pt43	52	No; No	No	M	Stribild	448	10	10
Pt44	58	Yes; Yes	Yes	M	Darunavir; Ritonavir; Abacavir/ Lamivudine	1135	22	10
Pt45	57	No; No	No	M	Ritonavir; Darunavir; Maraviroc; Abacavir	1007	8	7
Pt46	59	No; No	No	M	Triumeq	580	13	12

Abbreviations: MJ = marijuana; M = male; F = female; ARV = antiretroviral therapy; bronch. = bronchoscopy; PBVL = peripheral blood viral load
* Marijuana use in the last 6 months

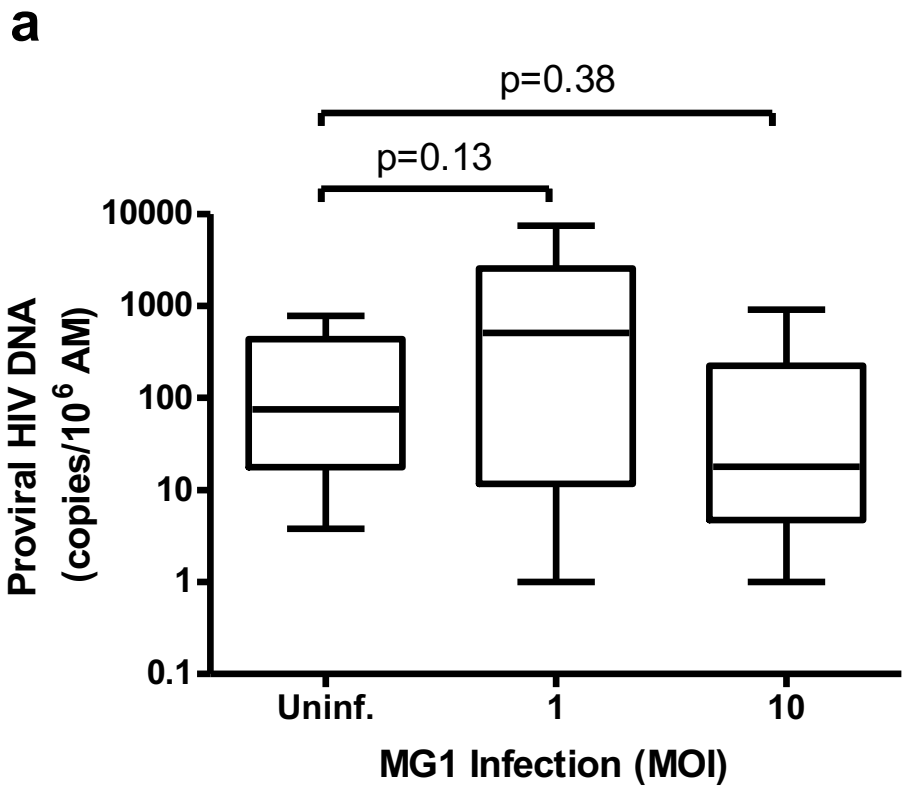
a
p=0.38
p=0.13
10000
1000
100
10
1
0.1
Proviral HIV DNA
(copies/10^6 AM)
Uninf.
1
10
MG1 Infection (MOI)

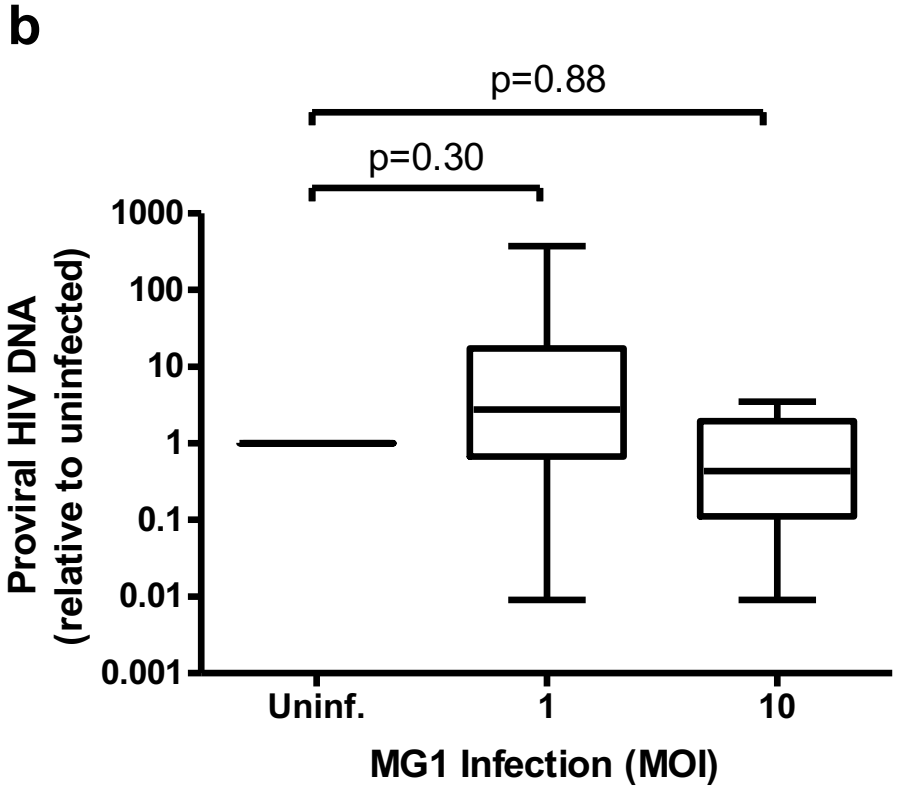
b
p=0.88
p=0.30
1000
100
10
1
0.1
0.01
0.001
Proviral HIV DNA
(relative to uninfected)
Uninf.
1
10
MG1 Infection (MOI)

Figure 38: MG1-mediated killing of HIV-infected alveolar macrophages is enhanced at MG1 MOI 10. Following collection by BAL, AM were allowed to adhere for 2 hours at 37°C. Subsequently, non-adherent cells were removed by washing, and remaining AM were infected with MG1. Cell pellets were collected at 48 hours post-infection, and proviral HIV DNA was measured by ddPCR. **a.** Total copies of proviral HIV DNA following infection with MG1 MOI 1 and 10 at 48 hours post-MG1 infection. **b**. Proviral HIV DNA, relative to respective uninfected controls, at 48 hours post-MG1 infection. Samples in which proviral HIV DNA was below 1 copy per well were excluded. (n=9; p values calculated by two-tailed, paired t-test). Data represent mean ± SEM; n values represent separate biological replicates.

a

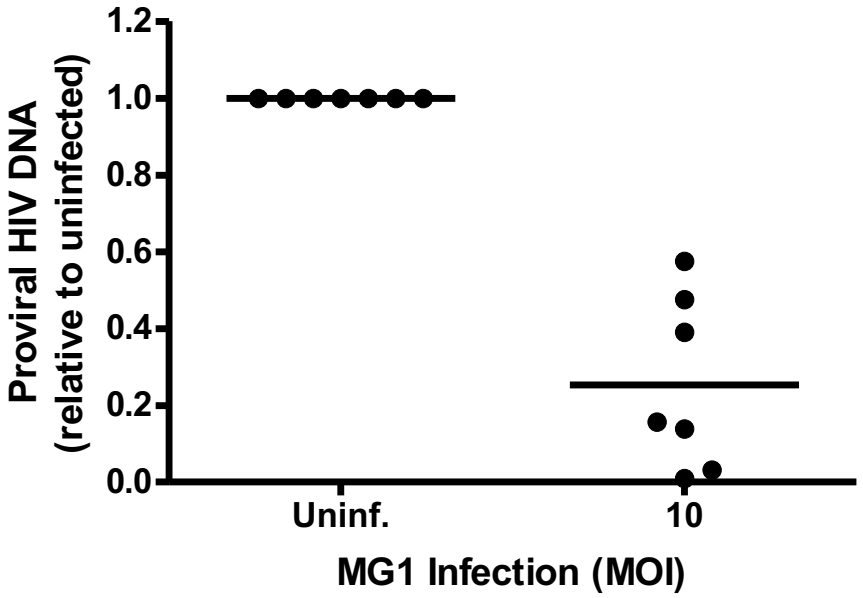
1.2
1.0
0.8
0.6
0.4
0.2
0.0
Proviral HIV DNA
(relative to uninfected)
Uninf.
10
MG1 Infection (MOI)

b

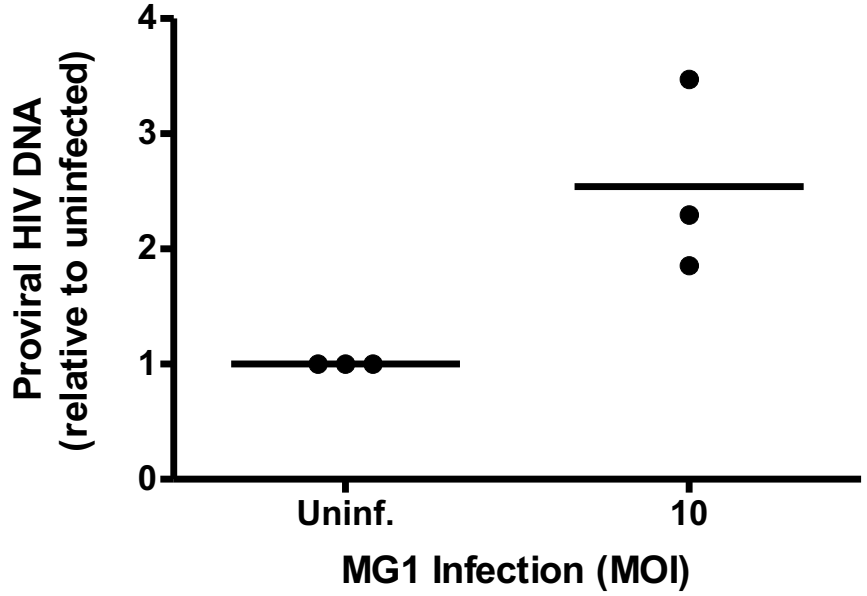
4
3
2
1
0
Proviral HIV DNA
(relative to uninfected)
Uninf.
10
MG1 Infection (MOI)

Figure 39: Patient alveolar macrophages can be grouped into "responder" and "non-responder" populations based on the relative change in proviral HIV DNA levels observed following MG1 infection. a. In responder AM, a substantial decrease in proviral HIV DNA (relative to respective uninfected control), was observed at 48 hours post-MG1 MOI 10 infection (n=7). **a.** In non-responder AM, no decrease in proviral HIV DNA (relative to respective uninfected control), was observed at 48 hours post-MG1 MOI 10 infection (n=3). Experiments in which proviral HIV DNA was found to be <1 copy in the control well were excluded.

Table 4: Total copies of proviral HIV DNA

	Copies per 10^6 alveolar macrophages		
Pt Code	**Uninf.**	**MOI 1**	**MOI 10**
Pt34*	1.35	1.65	9.02
Pt35	781.28	2159.72	371.79
Pt37	54.9	ND	ND
Pt38*	ND	ND	ND
Pt39	20.88	29.12	ND
Pt40	20.15	7507.14	7.87
Pt41	3.8	12.09	13.19
Pt42	399.37	11.43	916.93
Pt43	163.18	511.45	22.65
Pt44	547.2	720.76	85.47
Pt45	95.41	2975.91	177.12
Pt46	10.49	NA	6.03

Abbreviations: ND = not detectable; NA = not available
* Patient values excluded from overall analysis

6.4 Discussion

AM are an accessible source of tissue-resident macrophages that harbour replication competent HIV and act as a viral reservoir in cART-treated individuals (443,554,558). We have shown here that the IFN1-sensitive oncolytic virus, MG1, is capable of killing HIV-infected alveolar macrophages isolated from cART-treated individuals, as measured by a decrease in copies of proviral DNA per 10^6 cells at MG1 MOI 10. Low cell numbers were typically obtained from the BAL fluid, prohibiting further experiments to directly measure cell death and frequency of MG1 infection. Still, the measurement of proviral DNA following pharmacological intervention is frequently used as a reliable indication that HIV-infected cells are being killed (175,559,560). We are therefore confident that the decrease in proviral DNA observed represents the MG1-mediated killing of HIV infected AM.

It is also important to note the inter-donor variability in MG1-mediated killing (as shown in Figure 39). There are several possible explanations for this, which although not investigated here, remain important considerations for the use of MG1 as a reservoir-clearance strategy. First are the culture conditions employed during AM isolation from BAL fluid. Transient activation of AM has been observed immediately post-isolation by plate adherence, characterized by the release of TNFα, CXCL8, and IL-6 (561,562). Typically associated with classical macrophage activation and polarization to an M1 state (563,564), these cytokines and chemokines may induce an infection-resistant phenotype, as has been observed using human cytomegalovirus (565) and influenza virus (566,567). The AM used in

the above experiments may therefore have been less susceptible to MG1 infection, which was performed immediately following the 2 hours adherence step.

Polarization of AM to an M1 phenotype as a result of bacterial infection of the lung (563,568) or smoking (569) has also been observed. Although efforts were made to recruit otherwise healthy patients without a history smoking (tobacco or cannabis), this does not fully ensure that AM obtained via BAL were not polarized from an M0 state prior to subsequent experiments. Still, no correlation between patient clinical characteristics (such as smoking) and the selective eradication of HIV-infected AM by MG1 was observed. *In vivo* polarization of certain donor AM is therefore more likely to have resulted in a reduced susceptibility of these cells to MG1 infection and killing.

Similarly, the status of IFN1 signalling within HIV-infected AM is likely to affect the cytopathogenicity of MG1 infection. Rather than pDC, AM are the primary IFNα producers within the lung (570). The upregulation of type I IFN and numerous ISG has also been observed within the lungs of SIV-infected macaques (571,572). Although the ability of HIV to impair IFN1 signalling within infected AM remains unknown, the production of IFNα/β by HIV-uninfected AM following MG1 infection may protect HIV-infected AM from MG1-mediated killing *ex vivo*. MG1 MOI 1 had little to no effect on proviral HIV DNA, suggesting that the induction of type I IFN signalling at this MOI could be sufficient to block MG1 infection and killing.

Regardless of individual patient considerations, the eradication of HIV using MG1 will require the oncolytic virus to effectively infiltrate affected tissues and/or organs *in vivo*. In support of this, MG1 genomes have been detected in the spleen

and lymph nodes of rhesus macaques following intravenous viral challenge (347). Although the presence of MG1 in the lungs of these animals was not assessed, VSV infection within the lungs of intranasally-challenge mice has also been observed, and was enhanced in $PKR^{-/-}$ animals (573). MG1 genomes have also been detected within the lungs of cats following intramuscular injection (574). The detection of replication-competent MG1 within the lungs of HIV-infected humanized mice will form an important future direction, as discussed in Chapter 8.4.

6.5 Future directions

Given that AM form an invaluable source of primary, tissue-resident macrophages, it will be necessary to further study the cellular characteristics that could influence MG1 infection. As discussed above, AM polarization to an M1 state is observed following bacterial or viral infection, as well as in the lungs of individuals who smoke (564,569). This reduces the susceptibility of these cells to subsequent viral infections, including HIV (518,519), and triggers a pro-inflammatory immune response within the tissue. This observation is relevant for the therapeutic implementation of OV-based therapies, since M1-like tumor-associated macrophages were found to impair the killing of breast cancer cells by VSV through the activation of JAK/STAT signalling and ISG expression (575,576). M1 macrophages may also be more resistant to apoptotic cell death following viral infection (566). Describing the status of AM polarization within the HIV-infected lung will therefore inform the clinical use of oncolytic viruses—allowing this therapeutic approach to be tailored to the individual patient. Additionally, assessing how

polarization affects MG1 infection and/or killing of HIV-infected AM will form an important research question with implications in both HIV cure research and the ongoing evaluation of MG1 for the treatment of non-small cell lung cancer (347).

6.6 Conclusion

This finding has important implications in the search for an HIV cure, since it is the first evidence that an oncolytic virus, MG1, can effectively kill HIV-infected, tissue-resident macrophages *ex vivo*. Prior to this, investigation of MG1-mediated eradication of HIV-infected myeloid cells had been limited to cell line models of HIV latency (354) or primary, *in vitro* HIV-infected MDM; neither of which truly recapitulates the *in vivo* macrophage reservoir. The ability to use primary, tissue-resident macrophages in this context, as well as for HIV cure research as a whole, is therefore of great benefit. 2 Further experiments will be required to assess the effect of AM polarization on MG1 infection and killing, as well as measure the capacity for MG1 to eradicate the lung HIV reservoir *in vivo.* The latter will necessitate the use of relevant animal models, such as humanized mice or non-human primates, or the establishment of a proof of concept clinical trial in PLWHIV. These future directions are discussed further in Chapter 8.4. If successful, additional engineering of MG1 to enhance tissue localization and specificity for HIV-infected cells will likely be required.

Chapter 7: Modulating infection and killing of HIV-infected monocyte-derived macrophages by MG1

7.1 Introduction

7.1.1 Rational

It is unlikely that the use of OV as a monotherapy for the cure of HIV will be entirely effective. Tissues such as the lymph nodes, central nervous system (CNS), and reproductive tract are often inaccessible from a therapeutic standpoint, and harbour both latently and productively HIV-infected cells of diverse phenotypes (reviewed in (577)). Ensuring that OV are able to reach relevant target tissues at appropriate concentrations will therefore require a method of administration that avoids OV neutralization. In addition, devising potential combination therapies that will enhance OV infection and/or killing of HIV-infected cells will be desirable. As reviewed by Martin and Bell, combination therapies using anti-PD-1 antibodies, HDACi, and second mitochondrial activator of caspase (Smac)-mimetic compounds have shown promise in the context of cancer treatment (578). The data within Chapter 7 therefore represents a preliminary investigation of the class I HDACi, SAHA as an experimental combination strategy intended to increase MG1-mediated killing of HIV-infected macrophages.

The specific PKR inhibitor, C16, was also investigated as a means by which to modulate the effects of MG1 on HIV-infected MDM. Although not currently under investigation in the context of HIV infection or cancer therapy, PKR plays a key protective role against *Rhabdoviridae* infection and is induced as part of the IFN1 response (573). PKR induction was shown to be inhibited in HSA^+ MDM in Chapter

4 of this thesis, suggesting that additional functional impairment of PKR may prime HIV-infected MDM for MG1 infection and killing.

7.1.2 Combination strategies used to enhance oncolytic virus efficacy in cancer research

Enhancing the oncolytic nature of MG1 by pharmacological means has yet to be attempted in the clinical setting. Nonetheless, other combination strategies are currently under investigation in the form of two Phase I/II clinical trials. The first (ClinicalTrials.gov Identifier: NCT02285816) is intended for the treatment of MAGE-A3-expressing solid tumors using a replication-deficient MAGE-A3 expressing Adenovirus (prime) followed by a MG1-MAGE-A3 boost. This prime-boost strategy is intended to increase immune cell homing to the tumor site, as well as generate a humoral immune response against the specific tumor-associated antigen (347). The use of MG1-MAGEA3 in combination with the immune checkpoint inhibitor, pembrolizumab, is also being investigated for the treatment of metastatic melanoma or cutaneous squamous cell skin carcinoma (ClinicalTrials.gov Identifier: NCT02879760). In this case, pembrolizumab binds to PD-1 on $CD8^+$ T cells, preventing immune exhaustion and facilitating the lysis of malignant cells (579).

Pharmacological agents for the enhancement of MG1 infection and killing remain attractive from a therapeutic standpoint. In a recent screen of over 12 thousand small molecules, Diallo et al. identified a panel of fifteen candidate molecules that appreciably sensitized cancerous cells to VSVΔ51 infection and killing. One molecule in particular, 3,4-dichloro-5-phenyl-2,5-dihydrofuran-2-one (VSe1), proved particularly potent and effectively synergized with VSVΔ51 *in vivo*,

as well as in human tumor explants (580). Interestingly, VSe1 inhibited the induction of antiviral ISG following OV infection; a mechanism of oncolytic synergy that has previously been shown using two HDACi, SAHA and trichostatin A (580,581).

Finally, Smac-mimetics have been recently investigated as a means by which to potentiate OV-mediated killing. These molecules bind to and inhibit cellular inhibitors of apoptosis (IAPs), thereby facilitating apoptotic cell death in treated cells (582,583). Importantly, several Smac-mimetics are currently under clinical investigation for cancer therapy given their ability to induce selective killing of malignant cells (Clinical trial identifiers NCT02890069 and NCT02587962). Using mice bearing tumors derived from the mammary carcinoma cell line, EMT6, Beug et al. demonstrated that Smac-mimetics enhanced bystander killing of tumor cells by VSVΔ51 (495). This response was predominantly mediated by inflammatory cytokines (including IFNα/β) produced by macrophages in response to OV infection. The combination of Smac-mimetics with a TNF-α-expressing VSVΔ51 further potentiated tumor regression (584). Smac-mimetics have also been shown to promote the polarization of tumor-associated macrophages to a proinflammatory M1 phenotype, leading to the accumulation of $CD8^+$ T cells within murine EMT6 tumors and subsequent tumor regression (585).

7.1.3 Translation of cancer therapies to the field of HIV research

Cancer and HIV infection share several notable similarities. Both are characterized by immune dysfunction, exhaustion, and the persistence of functionally-altered cells that can evade treatment and cause subsequent pathology

in the affected individual (586,587). Co-opting cancer therapies for the treatment of HIV is therefore a common occurrence that has led to notable breakthroughs in the field of HIV research.

For example, PD-1 expression on HIV-specific $CD8^+$ T cells prevents the eradication of infected cells and is correlated with disease progression (588-590). PD-1 expression is lower on $CD8^+$ T cells from long-term non-progressors than normal progressors, indicating that a functional $CD8^+$ T cell response is key for immune control in HIV infection. As such, PD-1 and other immune checkpoint inhibitors such as T cell immunoreceptor with immunoglobulin and ITIM domains (TIGIT) (591), are attractive therapeutic targets. The anti-PD-1 antibody Pebrolizumab has undergone evaluation in PLWHIV who have been diagnosed with non-small cell lung cancer (592), Kaposi's Sarcoma (593), as well as a number of other relapsed or refractory neoplasms (ClinicalTrials.gov Identifier: NCT02595866). Currently, pembrolizumab is being investigated as a mechanism by which to restore immune function in cART-treated PLWHIV who, despite controlled viremia, maintain low $CD4^+$ T cell counts (ClinicalTrials.gov Identifier: NCT03367754).

Aside from restoring immune function, several groups have sought to identify a therapeutic strategy that is effective in eradicating HIV reservoir cells. These approaches have focused predominantly on the "shock and kill' strategy, in which latently HIV-infected cells are reactivated and subsequently eliminated via the host immune system (594). In particular, Archin et al. have pioneered the use of SAHA as a novel LRA (166,167), given its ability to selectively inhibit a number of class I HDACs that normally repress HIV transcription from the latent provirus (595). Although SAHA alone has not proven effective in reducing the size of the HIV

reservoir *in vivo* (167,168), it and other LRAs remain clinically relevant. Notably, recent work by Cummins et al. showed that priming $CD4^+$ T cells isolated from PLWHIV with a BCL-2 antagonist enhanced the killing of HIV-infected cells following subsequent latency reversal (596). Additionally, Hattori et al. successfully demonstrated the apoptotic killing of HIV-infected cell lines and $CD4^+$ T cells isolated from PLWHIV using various LRAs (including SAHA and the PKC activator, PEP005) in combination with the Smac-mimetic, birinapant (597). Similar combination strategies using SAHA may therefore be feasible in the context of an OV-based therapeutic approach. In fact, the ability of SAHA to synergize with MG1 and enhance OV-mediated killing latently HIV-infected, promyeloid cell lines, U1 and OM10.1, has previously been demonstrated by Ranganath (402).

7.2 Hypothesis

Enhancement of MG1 infection via therapeutic means will lead to better killing of HIV-infected monocyte-derived macrophages *in vitro*.

7.3 Results

7.3.1 The histone deacetylase inhibitor, suberanilohydroxamic acid, maintains selective killing of HIV-infected cells without altering IFN responsiveness or enhancing rates of MG1 infection

SAHA has been demonstrated to enhance viral infection of healthy cells by inhibiting ISG induction at the transcriptional level (581). As such, SAHA and other HDACi have been suggested as a means by which to supplement OV-based cancer

therapy (598). To assess whether treatment with SAHA prevented ISG induction in primary MDM, cells were cultured overnight in the presence of 2.5μM SAHA followed by stimulation with 1000U/ml IFNα. At 16 hours post-stimulation, PKR, ISG15, and HLA-B mRNA were measured by qPCR. Contrary to prior findings, however, SAHA pre-stimulation did not alter IFNα-induced ISG expression within healthy MDM (Figure 40).

SAHA pre-stimulation has been shown to enhance infection and killing of HIV-infected pro-myeloid cell lines by VSVΔ51 and MG1 (402). To assess whether this was also true of HIV-infected MDM, cells were stimulated overnight with 2.5μM SAHA then infected with MG1 at MOI 1 and 10. SAHA did not significantly enhance MG1 infection in either HSA^- or HSA^+ MDM at 24 hours post-infection (Figure 41a), nor did it enhance preferential MG1-mediated killing of HIV-infected MDM relative to unstimulated control wells (Figure 41b). The HDACi SAHA was therefore ineffective in further sensitizing HIV-infected MDM to MG1-mediated killing. Although it is possible that higher doses of SAHA could enhance MG1 infection and killing, stimulation with concentrations greater than 2.5μM resulted in a notable decrease in cell viability during optimization experiments. For this reason, higher concentrations were not investigated in this context.

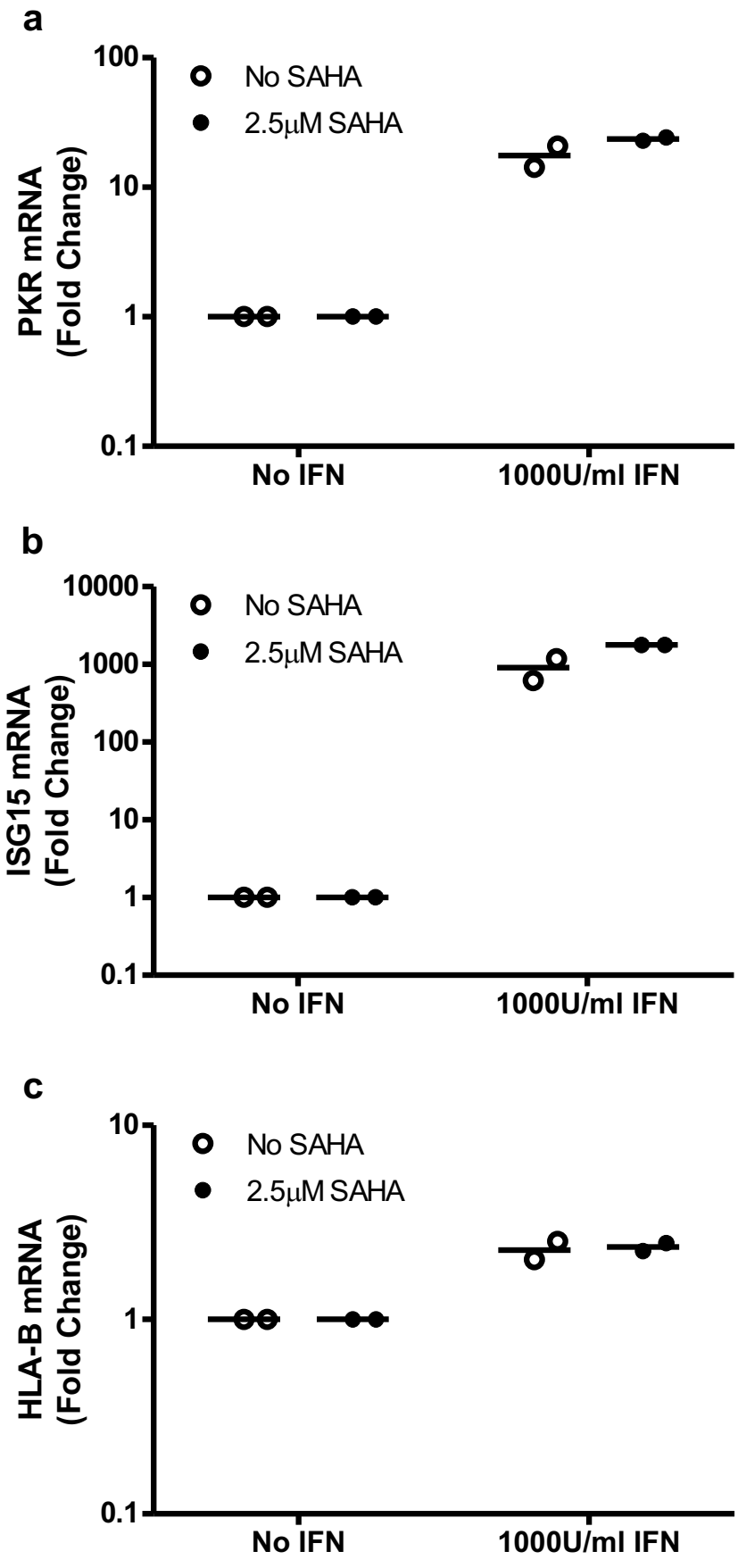
a
100
10
1
0.1
PKR mRNA
(Fold Change)
No SAHA
2.5μM SAHA
No IFN
1000U/ml IFN
b
10000
1000
100
10
1
0.1
ISG15 mRNA
(Fold Change)
No SAHA
2.5μM SAHA
No IFN
1000U/ml IFN
c
10
1
0.1
HLA-B mRNA
(Fold Change)
No SAHA
2.5μM SAHA
No IFN
1000U/ml IFN

Figure 40: SAHA does not impair IFNα-induced ISG expression in healthy, SAHA-treated MDM. HIV-uninfected MDM were cultured overnight in media containing 2.5μM SAHA, or left untreated. Without changing the cell culture media, MDM were then left unstimulated or stimulated with 1000U/ml IFNα for 16 hours. To assess whether SAHA pre-treatment affected IFNα responsiveness, mRNA levels of PKR (**a**), ISG15 (**b**), and HLA-B (**c**) were measured by qPCR. ΔΔCts used to calculate fold change were calculated by normalizing Ct values to respective untreated control and GAPDH (n=2); n values represent separate biological replicates.

a

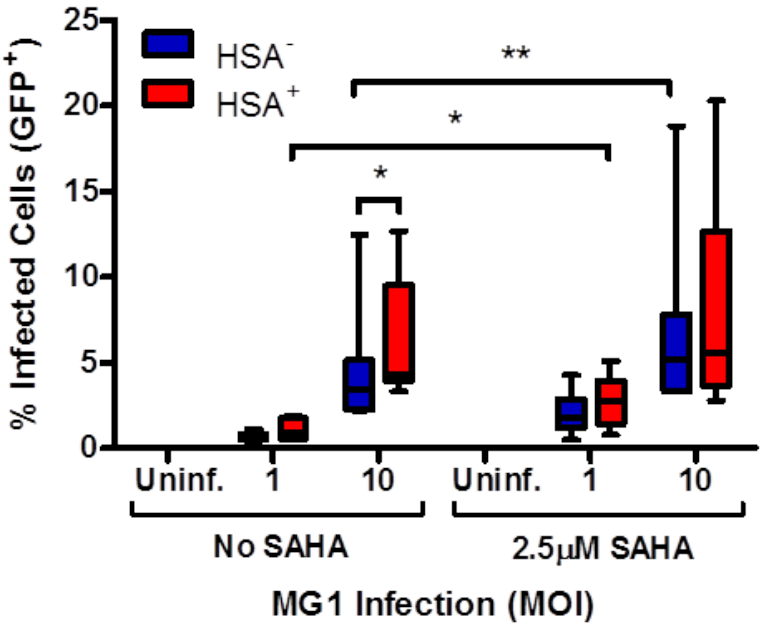
HSA-
HSA+
% Infected Cells (GFP+)
25
20
15
10
5
0
**
*
*
Uninf.
1
10
Uninf.
1
10
No SAHA
2.5μM SAHA
MG1 Infection (MOI)

b

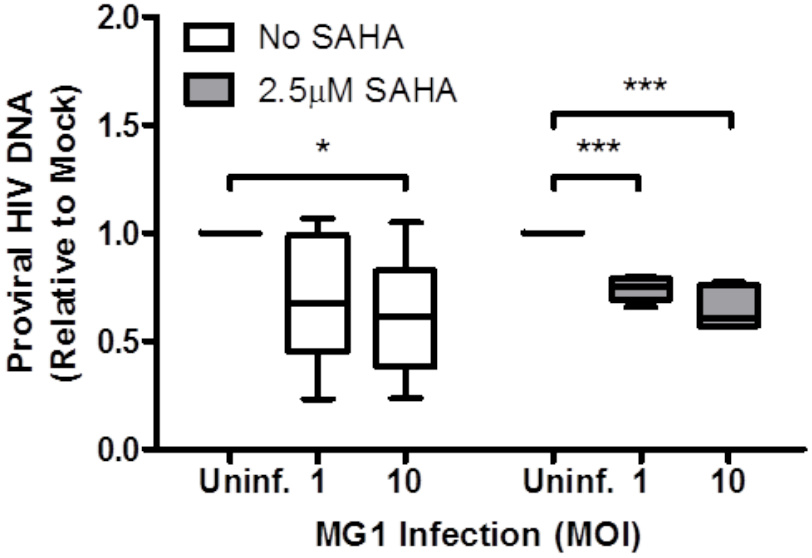
No SAHA
2.5μM SAHA
Proviral HIV DNA
(Relative to Mock)
2.0
1.5
1.0
0.5
0.0
***
***
*
Uninf.
1
10
Uninf.
1
10
MG1 Infection (MOI)

Figure 41: The HDACi, SAHA, does not enhance MG1-mediated killing of HIV-infected MDM. At 6 days post-HIV infection, MDM cultures were cultured overnight in media containing 2.5μM SAHA, left untreated. Without changing the cell culture media, MDM were then infected with MG1 (MOI 1 and 10), or left uninfected, for 48 hours. To assess infection, %GFP^+ MDM were measured by flow cytometry. Proviral HIV DNA, as measured by qPCR, was used to assess MG1-mediated killing of HIV-infected MDM. **a. %**GFP^+ MDM within HSA^- (blue) and HSA^+ (red) populations at 48 hours post MG1 infection (n=7; p=0.0006 by 2way repeated measures ANOVA, *p<0.05, **p<0.01 by Bonferroni posttest). **b.** Proviral HIV DNA, relative to respective MG1-uninfected control, at 48 hours post-MG1 infection (n=6; p=0.03 and p<0.0001 by 1way ANOVA for No SAHA and 2.5μM SAHA, respectfully, *p<0.05, ***p<0.0001 by Bonferroni posttest). Data represent mean ± SEM; n values represent separate biological replicates.

7.3.2 The PKR inhibitor, C16, enhances both infection and killing of HIV-infected cells by MG1

Inhibition of the RNA-sensing, antiviral protein, PKR, was next assessed in the context of MG1 infection. PKR-deficient mice are highly susceptible to VSV infection (573), suggesting that specific PKR inhibition may enhance MG1-mediated killing of HIV-infected MDM. In order to block the kinase activity of PKR (thereby preventing a downstream, antiviral translational blockade), cells were treated for 1 hour prior to MG1 infection with 2.5μM of the specific PKR inhibitor, C16 (599).

At 48 hours post-MG1 infection, %GFP^+ MDM and proviral HIV DNA were measured by flow cytometry and qPCR, respectively. As shown in Figure 42a, the selective infection of HSA^+ MDM (relative to HSA^- MDM) was maintained following C16 treatment. C16 also significantly enhanced MG1 infection of both HSA^+ and HSA^- MDM, relative to unstimulated cells. MG1-mediated killing of HIV infected cells was also maintained following C16 pre-treatment, although killing was not significantly greater than that observed within unstimulated cells (Figure 42b). Given that enhanced rates of infection, without notable differences in the killing of HIV-infected cells were observed, it is likely that C16 pre-treatment lead to the off-target killing of HIV-uninfected cells. This is not unexpected, considering the important role played by PKR in the context of viral infection, and highlights the importance of maintaining an intact IFN1 response in bystander cells when attempting to enhance the OV-mediated killing of the HIV reservoir.

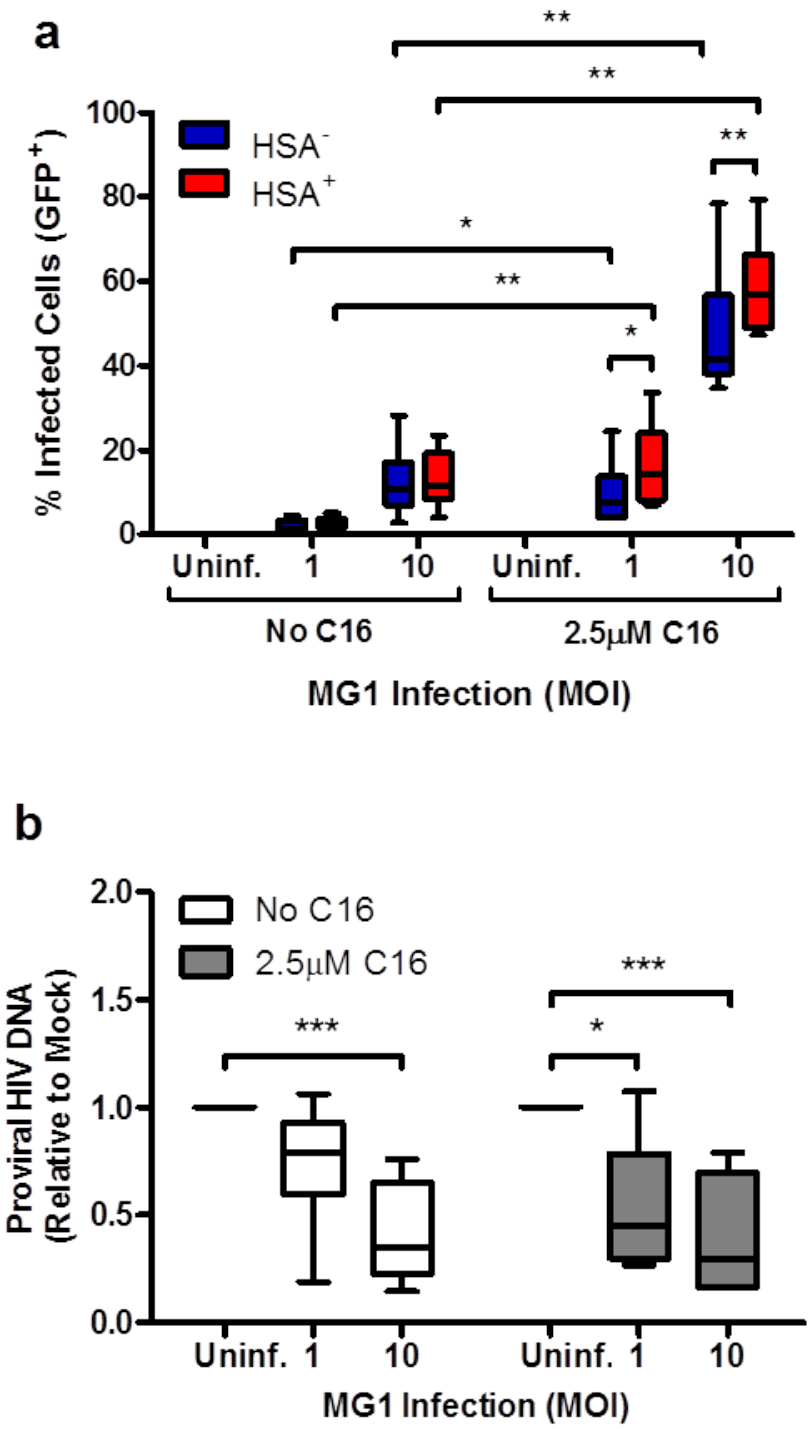
a
**
**
**
*
**
*
100
80
60
40
20
0
% Infected Cells (GFP+)
HSA-
HSA+
Uninf.
1
10
Uninf.
1
10
No C16
2.5μM C16
MG1 Infection (MOI)
b
2.0
1.5
1.0
0.5
0.0
Proviral HIV DNA (Relative to Mock)
No C16
2.5μM C16
***
***
*
Uninf.
1
10
Uninf.
1
10
MG1 Infection (MOI)

Figure 42: MG1 infection and, but not killing, of HIV-infected MDM is increased by the specific PKR inhibitor, C16. At 6 days post-HIV infection, MDM cultures were treated with 2.5μM C16 for 1 hour or left untreated. Without changing the cell culture media, MDM were then infected with MG1 (MOI 1 and 10), or left uninfected, for 48 hours. To assess infection, %GFP^+ MDM were measured by flow cytometry. Proviral HIV DNA, as measured by qPCR, was used to assess MG1-mediated killing of HIV-infected MDM. **a. %**GFP^+ MDM within HSA^- (blue) and HSA^+ (red) populations at 48 hours post MG1 infection (n=6; $p<0.0001$ by 2way repeated measures ANOVA, *$p<0.05$, **$p<0.001$ by Bonferroni posttest). **b.** Proviral HIV DNA, relative to respective MG1-uninfected control, at 48 hours post-MG1 infection (n=6; $p=0.0012$ and $p=0.0013$ by 1way ANOVA for No C16 and 2.5μM C16, respectfully, *$p<0.05$, ***$p<0.01$ by Bonferroni posttest). Data represent mean ± SEM; n values represent separate biological replicates.

7.4 Discussion

Therapeutic strategies intended to reactivate latent HIV infection or induce an HIV-specific immune response will likely accompany MG1 for the treatment and eradication of the HIV reservoir. Combination therapy to enhance OV-mediated killing of malignant cells are currently under investigation for the treatment of cancer. Experiments within Chapter 7 of this thesis were therefore intended to first investigate the use of one such strategy—the class I HDACi, SAHA—to enhance MG1-mediated killing of HIV-infected MDM. A small molecule inhibitor of PKR was subsequently investigated as a means to enhance MG1-infection *in vitro*. The implications of these observations are further discussed below.

7.4.1 Enhancing the rates of MG1 infection in primary cells is not sufficient to enhance selective killing of HIV-infected monocyte-derived macrophage

Previous members of the lab have shown that SAHA pre-treatment reactivated latent provirus and enhanced MG1 infection of latently HIV-infected, but not uninfected, pro-myeloid cell lines (402). Given that this work was not conducted in a primary cell model of HIV infection, we were curious as to whether SAHA could similarly increase rates of MG1 infection in productively HIV-infected MDM.

HDACi are currently under investigation as a combination approach to enhance the efficacy of OV-based therapies for the treatment of cancer. It is hypothesized that impairment of ISG expression is responsible for this enhancement (600). Unlike these previous reports, pre-treatment with 2.5μM SAHA did not prevent IFNα-induced PKR, ISG15, and HLA-B expression. It is important to note

that ISG induction was measured following IFNα stimulation, but not MG1 infection, or transfection with a synthetic RNA (e.g. 5'ppp-dsRNA). SAHA pre-treatment also did not enhance rates of MG1 infection in HSA^- or HSA^+ MDM, or the selective killing of HIV-infected MDM. Although Shulak et al. have shown that treatment with SAHA prior to VSV infection inhibited ISG induction while stimulating NF-κB activation and programmed cell death in prostate cancer cell lines (601), this mechanism does not appear to apply to HIV-infected MDM. These results indicate that SAHA pre-treatment is not sufficient to enhance MG1-mediated eradication of productively HIV-infected macrophages. Alternative combination strategies should therefore be investigated.

7.4.2 Inhibition of the cytoplasmic RNA sensing protein, PKR, enhances selective MG1 infection, but not killing, of HIV-infected MDM

The RNA-sensing protein, PKR, plays an important role in innate antiviral immunity. Upon binding to regions of double-stranded RNA, PKR undergoes dimerization and autophosphorylation (293,473). Subsequently, PKR initiates a potent block of cellular and viral translation by phosphorylating EIF2α. In the context of HIV infection, PKR activation is inhibited by both viral (290,602,603) and cellular (295,296) proteins, facilitating viral replication and spread. PKR also plays an important antiviral role against other RNA viruses, including those of the *Rhabdoviridae* family. Mice deficient in PKR rapidly succumbed to VSV following intranasal inoculation (573). Despite this established antiviral role, the over-

expression of PKR has also been shown to trigger apoptosis in VSV-infected cells (415,604), which could be reversed via the functional inhibition (604).

In agreement with Stojdl et al. (573), treatment with the Imidazolo-oxindole PKR inhibitor, C16, increased rates of MG1 infection in both HSA^- and HSA^+ MDM. It would therefore appear that the inhibition of PKR primed HSA^+ and HSA^- MDM for MG1 infection by inhibiting a key antiviral signalling pathway. RNA-sensing pathways, such as that mediated by RIG-I, have already been shown to be impaired HIV-infected cells (234,605-607). It is therefore not surprising that the further inhibition of cellular RNA-response pathways using C16 increased the sensitivity of HSA^+ MDM to MG1 infection. Despite this, C16 pre-treatment did not enhance MG1-mediated killing of HIV-infected MDM relative to the untreated control wells. This is likely because the inhibition of PKR by C16 was not limited to HIV-infected MDM, resulting in the off-target killing of HSA^- bystander MDM. Although additional investigation will be required to understand the implications of these findings, prior experiments demonstrated that HSA^- MDM were better able to induce ISG expression following transfection with a synthetic dsRNA (Chapter 4.3.4). Devising a means by which to selectively increase the expression and activation of other antiviral ISG in HIV-uninfected bystander cells may therefore be a useful strategy to compensate for PKR inhibition and enhance the preferential killing of HIV-infected MDM by MG1 following C16 pre-treatment.

C16 has been found to possess anti-inflammatory and neuroprotective properties *in vivo,* highlighting its therapeutic potential (608-610). While its use in the field of OV therapy has not yet been investigated in detail, the inhibition of PKR using a non-specific inhibitor, sunitinib, enhanced VSV infection and killing of tumor

cells *in vitro* (611). Co-administration of sunitinib and VSV also resulted in notable tumor regression and increased survival in tumor-bearing mice (611). Thus, the targeted inhibition of antiviral PRR in HIV-infected cells may be a relevant future direction in the development of an OV-based combination therapy.

7.5 Future directions

Although the results presented within this chapter suggest that MG1 infection can be modulated via additional therapeutic intervention, neither SAHA nor C16 appreciably enhanced MG1-mediated killing of HIV-infected MDM. The identification of a reliable combination therapy that facilitates the eradication of HIV-infected MDM while leaving uninfected cells untouched therefore remains a pertinent future direction. Therapeutic strategies like SAHA, which have been used to enhance OV infection and killing (601), have also been investigated *in vitro* for the eradication of latently HIV-infected $CD4^+$ T cells (167,597,612). Additional strategies, including the retinoic acid derivative acitretin (184), the BCL2 antagonist venetoclax (613), and a competitive inhibitor of glycolysis, 2-deoxy glucose (2-DG) (614) have also been found to potentiate the killing of latently HIV-infected $CD4^+$ T cells *in vitro*. Still, these studies have neglected to test these strategies other relevant HIV reservoir cells, including HIV-infected macrophages. Compounds such as Smac mimetics, which have been investigated in the context of both HIV infection and oncolytic virotherapy, may therefore be a promising lead.

As discussed above, Smac mimetics have been investigated as a potential strategy by which to enhanced the tumor-killing capabilities of OV *in vivo*

(495,584,585). Similarly, several IAP antagonists have been shown to act as a reliable “kill” strategy following HIV reactivation from latency (597). For example, the Smac mimetics GDC-0152, embelin, and birinapant have been shown to potentiate the killing of HIV-infected $CD4^+$ T cells by degrading the anti-apoptotic proteins X-linked inhibitor of apoptosis (XIAP), and baculoviral IAP repeat containing 2 (BIRC2) (615). BIRC2 is similarly involved in the survival of HIV-infected macrophages, and can be targeted by the Smac mimetic, AEG40730, to facilitate the eradication of these cells (141). Assessing whether Smac mimetics can enhance killing of HIV-infected MDM by MG1, without off-target killing of uninfected cells, will therefore be an interesting future direction with direct clinical applications.

7.6 Conclusion

In conclusion, two pharmacological agents known to inhibit the IFN1 response demonstrated varying abilities to potentiate MG1-mediated infection and killing of HIV-infected MDM. Contrary to previous findings in malignant or HIV-infected cell lines (402,601), SAHA pre-treatment did not enhance MG1 infection or killing of HIV-infected MDM. Although suggested to inhibit the IFN1 response in malignant cells (600), healthy MDM remained responsive to IFNα in the presence of SAHA. It is therefore unlikely that the IFN1 response within HIV-infected MDM is further inhibited by SAHA pre-treatment, preventing the enhanced killing of these cells by MG1. Conversely, treatment of MDM with the PKR inhibitor C16 increased rates of MG1 infection in both HSA^- and HSA^+ MD, without significantly reducing proviral HIV DNA relative to untreated, MG1-infected MDM. Increasing the overall

frequency of MG1 infection by specifically inhibiting an antiviral, RNA-sensing protein is therefore not sufficient to increase preferential OV-mediated killing of HIV-infected cells—likely due to increased bystander killing of bystander MDM. The identification of additional pharmacological agents capable of exploiting pre-existing IFN1 defects unique to HIV infected cells will form an important future direction of this work. Additionally, the investigation of Smac mimetics and their ability to synergize with MG1 for the eradication of HV infected cells is an important future direction that will allow both the latent HIV reservoir (597,615), and productively HIV infected cells (141), to be targeted appropriately *in vivo*.

Chapter 8: Discussion and Future Directions

8.1 Type I interferon defects in HIV-infected macrophages facilitate oncolytic virus infection and killing

Based on the previous work of C. Costiniuk (488) and N. Ranganath (402), it was hypothesized that cells that comprise the HIV reservoir could be selectively infected and killed by the IFN-sensitive oncolytic Rhabdoviruses, MG1 and VSVΔ51. The purpose of this thesis was therefore twofold—to identify and characterize defects within the IFN1 response in primary, HIV-infected cells, and to assess the ability of OV to selectively eradicate HIV-infected MDM *in vitro*.

The status of the IFN1 response during HIV infection was first investigated using a primary $CD4^+$ T cell model of HIV latency. In Chapter 3 of this thesis, it was shown that these cells were capable of inducing the expression of PKR, ISG15, and MHC I following stimulation with IFNα or transfection with a LMW-poly(I:C). The magnitude of this induction was similar to that of uninfected $CD4^+$ T cells, suggesting that IFN signalling defects do not persist during latent HIV infection. Still, to correctly interpret this result one must consider the relative number of latently infected cells generated in this manner. Similar to Saleh et al., we found that latently infected cells (defined as $CD4^+$ T cells containing an intact provirus) comprised only ~0.5-1% of the total cell population (122,355,402). Given that upwards of 99% of $CD4^+$ T cells used in this model were uninfected, it is likely that the ISG induction observed could be attributed to this population, and not the small proportion of HIV-infected cells.

To reliably investigate the IFN1 response during HIV latency, it will be necessary to physically enrich this small population of $CD4^+$ T cells (for example, via

magnetic bead sorting). Unfortunately, the identification of a cellular marker of HIV latency remains elusive (387,422). Still, *in vitro* models of HIV latency are useful in the context of HIV eradication strategies—including OV. As evidence of this, Ranganath et al. recently showed that latently HIV-infected $CD4^+$ T cells could be selectively killed by MG1 (354). Given the selectivity of MG1 for IFN1-defective cells (346), it can be postulated that latently HIV-infected $CD4^+$ T cells are impaired in their ability to elicit an appropriate IFN1 response during OV infection. For this reason, future models of latent HIV infection utilizing a known reporter virus, such as the HSA-expressing HIV NL4.3 BAL-IRES-HSA (357), or dual-reporter viruses that facilitate differentiation between productive and latent infection (409,419,420) will be paramount for the successful study of this viral reservoir.

Unlike $CD4^+$ T cells, HIV-infected macrophages support ongoing viral replication and consequently, have been found to possess IFN1 response impairments at various levels (234,245,272,275). To investigate whether these impairments were truly characteristic of HIV-infected MDM, the HSA-expressing HIV NL4.3 BAL-IRES-HSA was used to establish an *in vitro* model of HIV-infected MDM. Chapter 4 of this thesis was therefore dedicated to the measurement of IFNα- or 5'ppp-dsRNA-induced ISG expression within HIV-infected (HSA^+) and bystander (HSA^-) MDM.

Although ISG expression was upregulated within HSA^+ MDM at baseline, the relative induction of PKR and ISG15 was lower in HSA^+ MDM than in HSA^- MDM following IFNα stimulation or 5'ppp-dsRNA transfection. This was not a result of impaired IFNAR1/2 expression, nor was it due to impairment of ISG transcription.

Rather, these results suggest post-transcriptional inhibition, leading to differences in ISG protein levels. This hypothesis is supported by previous studies citing HIV-mediated inhibition of cellular translational machinery (468-471), but has not yet been studied in this exact model of HIV infection. Similarly, potential functional impairment of key ISG, such as PKR (295,616), was not investigated in this context. Investigation of whether ISG expressed within HIV-infected MDM retain their antiviral role remains an important future objective that necessitates further refinement of the HSA-enrichment protocol employed.

The fact that 5'ppp-dsRNA-induced ISG expression was lower in magnitude within HSA^+ MDM suggested that HIV-infected MDM were less capable of eliciting an antiviral response following a secondary viral infection. The data presented in Chapter 5 supports this hypothesis, showing that HIV-infected MDM are preferentially infected by the IFN1-sensitive OV, MG1 and VSVΔ51. Preferential killing of HIV-infected MDM was, however, only observed in the context of MG1 infection indicating that these related OV possess different cytopathic potential. The killing of HIV-infected MDM was not observed when UV-inactivated OV or clarified supernatants from MG1-infected MDM were applied to the cells, demonstrating that MG1-mediated eradication of the HIV reservoir will require the delivery of replication competent OV. These results are visually summarized in Figure 43.

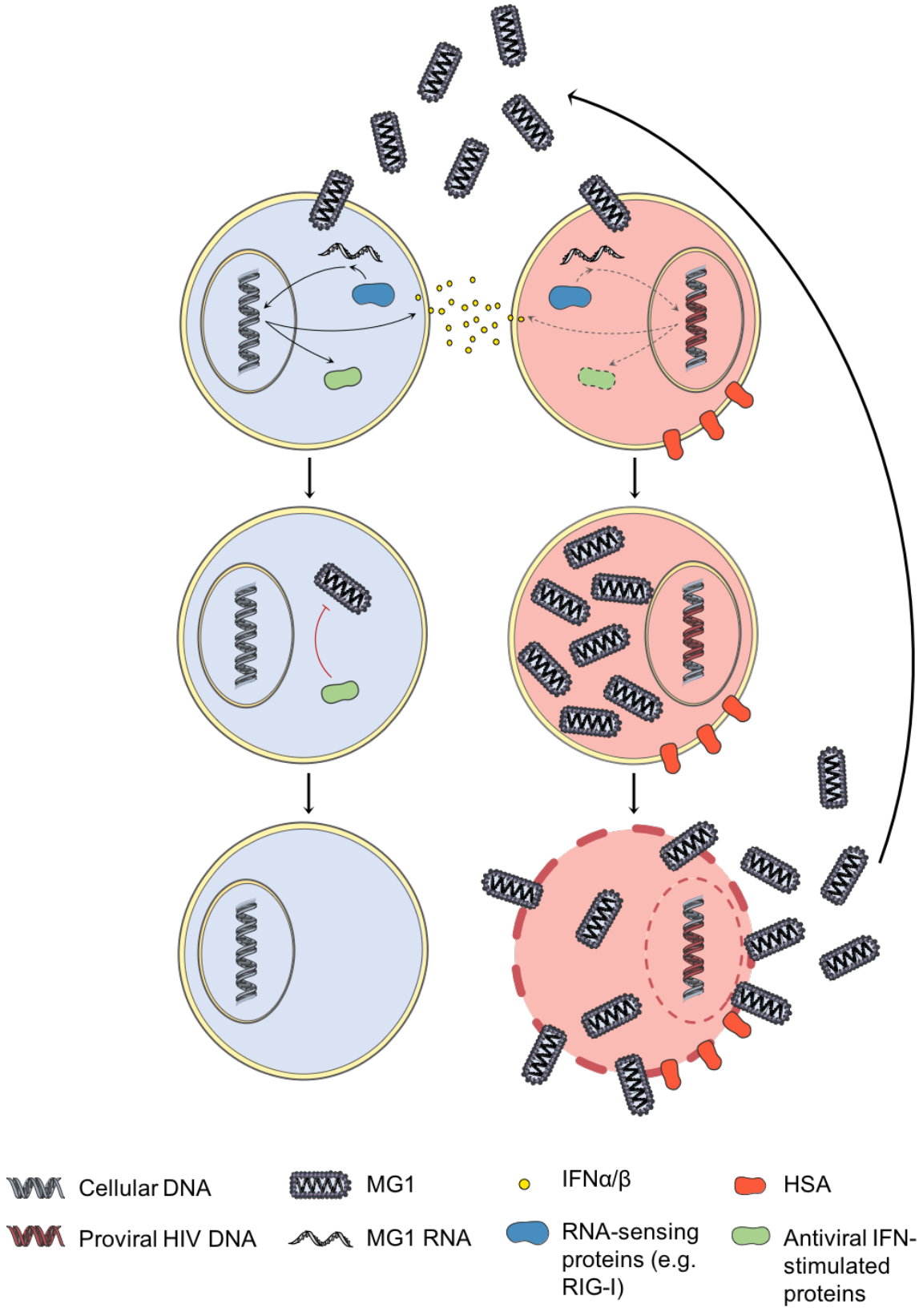
Cellular DNA
Proviral HIV DNA
MG1
MG1 RNA
IFNα/β
RNA-sensing proteins (e.g. RIG-I)
HSA
Antiviral IFN-stimulated proteins

Figure 43: MG1 infects and kills HIV-infected cells that possess IFN1 signalling defects. HIV-uninfected bystander cells (blue; left-hand side) induce IFN1 production and ISG expression in response to MG1 infection, which blocks further MG1 replication and cytopathogenicity. Conversely, HIV-infected MDM (red; right-hand side) are impaired in their ability to induce ISG expression in response to foreign RNA, facilitating MG1 replication and cell death.

Next, the experiments within Chapter 6 of this thesis sought to assess MG1-mediated killing in primary, tissue-resident macrophages. Specifically, AM from PLWHIV were collected by BAL and infected with MG1 *ex vivo*, after which proviral HIV DNA was measured. Although the killing of HIV-infected AM by MG1 was observed in the majority of individuals, the HIV-infected AM of a small number of participants remained refractory to MG1-mediated killing. The polarization of AM to a pro-inflammatory, infection-resistant phenotype has been associated with certain patient clinical characteristics, such as smoking (569), or *ex vivo* manipulation (561,562). Experiments investigating AM phenotype and/or baseline IFN1 response pathways were precluded by the small numbers of cells obtained via BAL. Still, this information may be useful in determining what characteristics will facilitate the effective treatment of PLWHIV using an OV-based therapy.

The therapeutic enhancement of OV for the treatment of cancer is currently under investigation, and includes the use of HDACi (580,581) and Smac-mimetics (495,584). The use of the HDACi, SAHA, and the PKR-inhibitor, C16, to enhance MG1-mediated killing of HIV-infected MDM was therefore investigated within Chapter 7. Contrary to the findings of N. Ranganath, who found that the treatment of HIV-infected pro-myeloid cell lines enhanced MG1 killing (402), SAHA pre-treatment did not significantly enhance the cytopathic effects of MG1 in HIV-infected primary MDM. Conversely, the PKR inhibitor, C16, significantly enhanced MG1-mediated infection of both bystander and HIV-infected cells (although preferential infection of HSA^+ cells was maintained). This is not surprising, considering that PKR is a key RNA-sensing protein shown to be required for the induction of an antiviral response during VSV infection (573). What is interesting, however, is that these findings

suggest that the activation of PKR by viral RNA is not completely inhibited in HIV-infected MDM. If PKR activation was, in fact, completely blocked by HIV infection, we would expect to see no difference in MG1 infection in cells pre-treated with C16. Previously published data demonstrating the inhibition of PKR phosphorylation by HIV Tat or cellular factors may reveal a mechanism of IFN1 signalling impairment that is specific to the cell line or virus strain used (295,602,603,616). Still, we cannot rule out the possibility that PKR is subject to incomplete inhibition in HIV-infected macrophages. This would explain both the preferential infection of HSA^+ MDM at baseline, and the substantial increase in GFP^+HSA^+ MDM in C16 treated cells. Although increasing MG1 infection of C16-treated, HSA^+ MDM should also increase MG1-mediated killing of these cells, no significant difference in proviral HIV DNA was observed between C16-treated and untreated conditions. This suggests that off-target MG1-mediated killing of HIV-uninfected bystander cells is also enhanced by C16 pre-treatment—a hypothesis that is supported by the significant increase in MG1 infection observed within C16-treated HSA^- cells.

8.2 *Ex vivo* study of the HIV reservoir: relevance for HIV cure research

The ability to accurately locate and monitor HIV reservoir cells within the body has become an increasingly pertinent goal in the field of HIV cure research. Tissues from SIV or SHIV-infected NHP have allowed the viral reservoir to be studied during various stages of infection (374,434,617,618). Still, NHP models are not a complete substitute for the study of HIV infection in humans due to notable differences in both viral pathogenesis and host immune function. It is therefore important to consider

new methods by which to access and study various anatomical HIV reservoirs, as well as the HIV-infected cells contained within.

8.2.1 Novel strategies for characterizing the HIV reservoir in humans

Measurement of HIV reservoir size has, to date, relied on substitute measures such as proviral HIV copy number within the peripheral blood. Although tissues such as cerebrospinal fluid (619), lymphoid tissues, adipose tissue, and lower gastrointestinal tract (via biopsy) (389,395,620), and lungs (via bronchoalveolar lavage) (553), remain accessible for additional study, patients may view the procedures required to access these tissues to be invasive or uncomfortable. Moreover, deep-tissue HIV reservoirs like the brain, reproductive tract, spleen, and GALT (434) are largely neglected due to the obvious risks associated with tissue collection.

To address this, post-mortem tissue collection from consenting PLWHIV has been proposed (555,621). This has led to the establishment several biorepositories in the United States, including The National NeuroAIDS Tissue Consortium (622), the National Neurological AIDS Bank program (623,624), and the AIDS and Cancer Specimen Resource (625), which have facilitated the sampling of diverse anatomical sites and HIV reservoir characterization within cART-treated individuals. Still, there are certain pitfalls that are associated with post-mortem tissue collection and storage. Ante-mortem clinical information, such as cART adherence, $CD4^+$ T cell count, and viral load, is often unavailable for the donors of these tissues, which can complicate estimates of HIV reservoir size and distribution (577,624). Concurrent illnesses, particularly those contributing to the cause of death, could also have an

unforeseen impact on qualitative and quantitative aspects of the HIV reservoir. Finally, delays in tissue collection due to the unexpected death of a participant, or other external factors, are problematic when measuring viral RNA or DNA (555).

These pitfalls in post-mortem tissue collection have led to the recent proposal of the "Last Gift" model by Gianella et al. at the University of California, San Diego (624). This model seeks to recruit PLWHIV who have been diagnosed with non-AIDS related advanced illnesses, collect (while alive) clinically relevant samples such as blood, stool, or biopsies, record additional clinical information, including current cART, and finally, collect and store relevant tissues upon death. This initiative takes advantage of California's End of Life Option Act law, which permits medical assistance in death (MAiD) for terminally ill individuals with a prognosis of <6 months. The use of post-mortem tissues in HIV research has in fact been recently explored by our group at the Ottawa Hospital Research Institute, as well as collaborators in Montreal and Edmonton (626). The recent legalization of MAiD in Canada suggests that a similar model of post-mortem tissue collection could be implemented locally. This would allow the autopsy to be coordinated in a manner that is sensitive to the participant's chosen time of death, while avoiding delays that could compromise the quality of the tissue itself.

8.2.2 Strategies for the ex vivo study of HIV reservoir cells

The ability to study HIV-infected $CD4^+$ T cells and tissue-resident macrophages *ex vivo* is required for assessing the efficacy of any HIV cure strategy. As outlined in Chapter 3, the identification of cell surface molecules for the isolation of latently HIV-infected cells has proven to be a challenge. Immune checkpoint

molecules, like PD-1, TIGIT, and LAG-3 (388), receptors involved in mucosal homing (e.g. CCR6) (389), surface adhesion molecules (e.g. CD2) (386), and most recently, the Fc receptor CD32a (386,387) have been suggested to act as markers of HIV latency. Additional studies have revealed that these markers enrich for, but do not exclusively identify, latently HIV-infected $CD4^+$ T cells (29-33). Latently HIV-infected cells are also located predominantly within the lymphoid tissues of cART-treated individuals and, as such, are rarely found within the peripheral circulation (391-395). The search for a reliable surface marker of latently HIV-infected cells that can be used to enrich small proportions of cells from the peripheral blood of PLWHIV is therefore ongoing.

The study of the macrophage HIV reservoir requires additional consideration, in that tissue-resident macrophages are typically long-lived populations originating from the fetal yolk sac (as opposed to bone marrow-derived monocytes) (541,627,628). A notable exception to this are the macrophages found surrounding the GI tract, whose homeostasis is believed to maintained predominantly by infiltrating bone marrow-derived monocytes (629-632). Circulating monocytes may also contribute to tissue resident macrophage populations following inflammation or with age (542,633,634), but the half-life of these cells remains relatively short (632,635,636). Due to these attributes, it is highly likely that fetal macrophage populations facilitate HIV persistence within the myeloid cell compartment *in vivo*, as opposed to infiltrating monocyte-derived macrophages.

Tissue-resident macrophages are adherent in nature and are therefore difficult to isolated from tissue sections. This has limited the *ex vivo* study of tissue resident macrophages to AM within the lung, since these cells can be collected by

BAL with relative ease. Additional strategies to work with these cells *ex vivo* must therefore be explored. One such option is the collection and culture of macrophages isolated from semen (seminal macrophages; SM). Ganor et al. previously identified urethral macrophages as a primary target for HIV transmission using a human tissue explant model (140,637). Subsequently, Matusali et al. demonstrated that macrophages containing SIV RNA and DNA could persist within the urethral tissue of cART-treated macaques (638). This, combined with the detection of HIV genomic material within SM collected from PLWHIV (639,640), the observation of HIV-infected macrophages within the stroma and lumen of the seminal vesicles (640), and most recently, the identification of viral signatures within several other male reproductive organs (including the testes, epididymis, and vas deferens of SIV-infected macaques) (641) implicate macrophages within the male reproductive tract as HIV reservoir cells. Although the number of SM that can be isolated from semen are limited (430,639), these cells form an invaluable source of primary, tissue-resident macrophages that can be accessed in a non-invasive manner.

In addition to the isolation of viable, tissue-resident macrophages from BAL fluid or semen, *in situ* hybridization techniques like RNAscope can facilitate the detection and phenotypic analysis of HIV RNA^+ and HIV DNA^+ cells within fixed tissue sections (642). This approach allows for the frequency of HIV-infected cells to be accurately quantified, and has been used to provide estimates of reservoir size within human lymph node and rectum biopsies (434). RNAscope has recently been employed by the Canadian HIV Cure Enterprise Team for the identification of HIV infected macrophages within organs/tissues collected following MAiD (626). This

technology will be integral to future experiments that intend to estimate the HIV reservoir size and location without relying on single cell isolation and culture *ex vivo*.

8.3 Further development of oncolytic viruses for the treatment of HIV

The thorough identification and characterization of cells comprising the HIV reservoir is necessary for the continuing development of an OV-based HIV cure strategy. As discussed within Chapter 5.5 of this thesis, several strategies to enhance the specificity of OV for cells that make up the HIV reservoir have been considered. These are primarily focused on viral engineering, and include: the expression of IFNα or IFNβ by OV, which will limit viral infection and killing to IFN1-defective cells; the engineering of OV to express a chimeric VSV G-HIV Env protein, which will limit MG1 infection to CD4-expressing cells; and the insertion of an HIV protease cleavage site between the G and L genes of MG1, which will limit MG1 infection to productively HIV-infected cells that contain a functional HIV protease. On top of this, it will be necessary to ensure that MG1 is capable of reaching lymphoid and non-lymphoid tissue reservoirs. As has been shown in cancer research, neutralization by complement or the humoral immune response may reduce the systemic delivery of OV (643,644). By extension, similar immune responses are likely to impair HIV reservoir eradication by OV, indicating that the development of a delivery system capable of circumventing humoral neutralization will be a necessary future direction. The delivery of MG1 to the brain, which remains separate from the circulation via the blood-brain barrier, will also necessitate specific consideration.

8.3.1 Building a “Trojan Horse”

Several groups have independently proposed the “Trojan Horse” approach as a means by which to avoid OV neutralization and enhance systemic delivery. This technique relies on carrier cells, which are loaded with virus *ex vivo* and re-administered to the tumor-bearing animal. OV carrier cells, used alone or in combination with adoptive T cell therapy, can facilitate tumor clearance by VSVΔ51 in murine models (644,645). Importantly, tumor regression was also observed in pre-immunized mice, indicating protection from humoral neutralization (644).

This technique has been further developed by Roy et al., who demonstrated the successful delivery of VSVΔ51 to murine tumors (and subsequent tumor regression) using *Drosophila* S2 cells (646). These cells support persistent VSVΔ51 infection, display low immunogenicity *in vivo,* and successfully deliver infectious viral particles to the tumour bed while avoiding virus neutralization. Systemic delivery of virus to the lungs, spleen, and liver was also observed (646). Although this off-target delivery may be undesirable for the treatment of cancer, the ability to target OV to various HIV reservoir tissues will be highly beneficial should this technique be employed in the context of an HIV cure. Finally, *Drosophila* S2 cells supported the expression of transgenes that aided in VSVΔ51-mediated killing of tumor cells (646). The ability to engineer these cells to express certain tissue-homing markers, such as $\alpha 4\beta 7$ involved in lymphocyte homing to the gut (647,648), may facilitate their targeted delivery to HIV reservoir sites *in vivo*.

8.3.2 Special considerations for the HIV reservoir within the brain

HIV is believed to enter the brain via $CD14^{+}CD16^{+}$ monocytes, which differentiate into macrophages once across the blood-brain barrier (137,649). Viral replication within perivascular macrophages, microglia, and (to a certain extent) astrocytes contributes to the development of HIV-associated neurodegenerative disorder (HAND), which remains a common concern among cART-suppressed PLWHIV (530,650-652). A system by which to achieve targeted delivery of OV to the brain is therefore required.

Given the inherent neurotropism of VSV, avoiding neurotoxicity associated with the therapeutic use of this virus has been a significant focus of the OV field. Conversely, the neurotropism of Maraba virus is not well-established in humans. In mice, the M and G protein mutations of MG1 prevented significant neurotoxicity at therapeutic doses (346). Still, elevated viral titers were discovered in the brains of mice receiving high doses of MG1, indicating that this virus retains some neurotropic potential (346). Several other groups have attempted to exploit the neurotropic nature of certain OV for the treatment of brain tumors. For example, Dey et al. found that CXCR4-expressing neuronal stem cells loaded with an oncolytic adenovirus successfully treated brain tumors in a murine model of glioma (653). Wollmann et al. have also demonstrated the impressive tumor-targeting capabilities of a Lassa-Vesicular stomatitis chimeric virus, which could successfully cross the blood brain barrier and reduce tumor size in mice, without causing neurotoxicity (654).

Similar strategies may be adopted for the targeted delivery of OV to the brain in the context of HIV infection. In humans, HIV infection of the brain results in the upregulation of chemoattractant molecules, such as CCL2, which subsequently

recruit immune cells to the brain (655-658). This includes HIV-infected monocytes, whose diapedesis across the blood-brain barrier in response to CCL2 is mediated by the expression of ALCAM, JAM-A, CD99, and PECAM-1 on the cell surface (658). As discussed in section 8.3.1, *Drosophila* S2 cells can express various surface markers, and can be loaded with OV to achieve targeted delivery to certain tissues. The engineering of these cells to express ALCAM, JAM-A, CD99, and PECAM-1, as well as the CCL2 receptor, CCR2, may facilitate the homing of MG1-loaded S2 cells to the blood-brain barrier. Elevated levels of CCL2 have also been shown to increase the overall permeability of the blood-brain barrier (659,660), which would further promote the migration of cell-associated or free MG1 into the brain.

The potential inflammatory response caused by MG1 infection and killing of HIV-infected cells within the brain remains an important consideration. While MG1-associated neurotoxicity has not been observed within healthy NHP (347), pre-existing inflammation within the brains and CNS of SIV-infected rhesus macaques may increase the risk for adverse neuroinflammatory events following the therapeutic administration of MG1 (661,662). The pre-clinical assessment of MG1 in HIV-infected humanized mice or SIV-infected NHP should therefore include measurements of neurotoxicity and inflammation associated with MG1 replication within neuronal tissues. Similarly, potential neurotoxicity should also be closely monitored when assessing MG1 as an HIV cure strategy during future proof-of-principle clinical trials in PLWHIV (discussed further in section 8.4.3).

8.4 Translating oncolytic viruses from bench to bedside

In addition to the thorough assessment of patient safety, it will be important to consider the potential environmental risk posed by MG1 in the event that it returns to its natural arthropod host. Since the environment impact of such an event remains unknown at present, Koppers-Lalic et al. consider the environmental risk of MG1 to be high (663). Still, an IFNβ-expressing VSV was recently found to be non-pathogenic in pigs (a common livestock reservoir of VSV), indicating that the modification of these viruses to enhance selectivity for tumour cells may not cause significant environmental impact (664). This, combined with the relatively innocuous nature of VSV and MG1 infection observed within NHP models (347,665,666), have supported the recent translation of MG1 to Phase I/II clinical trials for the treatment of cancer. Nonetheless, the impact of MG1 on HIV reservoir size must also be assessed using appropriate pre-clinical models before it is evaluated in a proof-of-principle clinical trial in humans. The pros and cons of humanized mice and NHP for the study of HIV cure strategies have been reviewed in (667), and are listed in Figure 44.

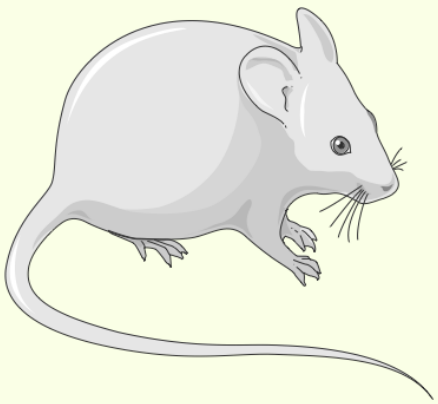

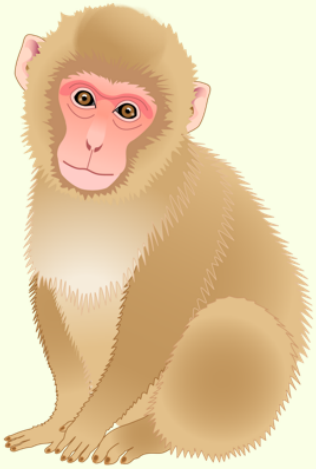

Humanized Mice (Hu-BLT)	Non-human Primates
Pros: ▪ Low maintenance (relative to NHP) ▪ Mimics the human immune system ▪ Allows infection with HIV ▪ HIV reservoir is similar to that established in humans (including tissue colonization) ▪ Viral load can be controlled by ART ▪ Depletion of specific arms of the immune system is possible	**Pros:** ▪ Similar anatomy/physiology as humans ▪ Similar disease progression as humans ▪ HIV reservoir is similar to that established in humans (including tissue colonization) ▪ Large size permits frequent sample collection ▪ Depletion of specific arms of the immune system is possible
Cons: ▪ Anatomically/physiologically different than humans ▪ The production of Hu-BLT mice requires surgical methods using human fetal tissues (subject to restriction) ▪ Complete immune reconstitution takes 5-7 months ▪ The development of graft versus host disease occurs in ~6 months ▪ Cannot be bred ▪ Sample collection is limited by small size	**Cons:** ▪ High maintenance costs and space requirements (relative to humanized mice) ▪ Requires infection using SIV or SHIV, rather than HIV ➢ SIV are naturally resistant to non-nucleoside reverse transcriptase inhibitors ➢ SIV expresses Vpx and is therefore capable of antagonizing the viral restriction factor SAMHD1

Figure 44: Comparison between murine and non-human primate models for HIV cure research. While humanized mice permit the study of HIV pathogenesis using a human immune system, their small size, as well as the time and materials required for establishment, remain significant drawbacks. Conversely, NHP support the study of SIV or SHIV infection in a physiologically-similar, but non-human, model. While these differences remain a pitfall in the use of NHP for the study of HIV cure strategies, disease progression and reservoir establishment in NHP is similar to that in humans. Moreover, their large size facilitates repeated sampling and the collection of tissue post-mortem. The above is a graphical depiction of Table 1 found in: Policicchio BB, Pandrea I,Apetrei C. Animal Models for HIV Cure Research. Front Immunol.2016 Jan 28;7:12.

8.4.1 Humanized mice

Mice possessing a human immune system are a likely first step in the preclinical investigation of the reservoir-targeting abilities of MG1. As a more cost- and space-efficient option than NHP, several humanized mouse models have been developed for the study of HIV cure strategies. For our purposes, humanized bone marrow-liver-thymus (Hu-BLT) mice will be considered. In this model, fetal thymus sections are engrafted under the renal capsule of NOD-SCID-IL2Rγ^{null} (NSG) mice following sub-lethal irradiation, resulting in the establishment of a surrogate thymic organ. Human CD34^{+} hematopoietic stem cells (HSC) isolated from the fetal liver are injected in parallel, and migrate to the bone marrow to promote the establishment of human hematopoietic lineages. The reconstitution of human immune cells within lymphoid and mucosal tissues, as well as the ability of these cells to elicit an adaptive immune response to foreign antigen make Hu-BLT mice a viable option for the study of HIV pathogenesis in a small animal model (668-670).

Latently HIV-infected CD4^{+} T cells and HIV-infected tissue resident macrophages have been detected in Hu-BLT mice following HIV infection, indicating that relevant viral reservoirs are established and maintained (669). This has allowed for several HIV cure strategies to be assessed, including the “Shock and Kill” approach using LRAs (671). An alternative therapeutic approach, in which latent provirus is transcriptionally silenced via inhibition of HIV Tat (referred to as the “Block and Lock” approach), has also been investigated (672). In these studies, therapeutic efficacy was assessed by measurements of peripheral viral load, as well as the detection and quantification of tissue HIV DNA and RNA. For our purposes,

similar measures of HIV reservoir size will be feasible following the administration of MG1 to HIV-infected, cART-treated Hu-BLT mice. It will also be possible to measure peripheral viral load via repeated blood collection, allowing viral rebound (or lack thereof) to be assessed following cART cessation.

The establishment of Hu-BLT mice can also be tailored to allow for specific viral reservoirs to be studied separately. Hu-BLT mice that explicitly express human T cells (T cell-only mice; ToM) or human myeloid cells (MoM) are two such examples, which have been developed to assess the individual contribution of T cells and myeloid cells to HIV persistence *in vivo* (108,673). Similar models may prove useful for the therapeutic evaluation of MG1, since it is unknown whether this OV will preferentially target one cellular HIV reservoir over another.

8.4.2 Non-human primates

NHP, such as rhesus (Indian or Chinese subspecies), cynomologus, and pigtail macaques are widely used in HIV research. In addition to their physiological and anatomical similarities to humans, the immune response and fluctuation in viral load observed following SIV/SHIV infection closely matches that of human HIV infection (674). In comparison, the humoral immune response observed in HIV-infected humanized mice occurs over several months (675). Reservoir establishment in lymphoid tissues is also observed in SIV-infected macaques which, similar to humans, contributes to viral rebound following the cessation of cART (374).

For these reasons, SIV-infected NHP models have been immensely beneficial for our understanding of HIV transmission and pathogenesis (reviewed in

(676)), as well as the ongoing development of an HIV vaccine (677,678). NHP have also been of use within the field of oncolytic virotherapy. The safety profile of VSV-rIFNβ and MG1-MAGEA3 have been assessed in healthy macaques; data which has been used to establish the safe starting dose for both OV in clinical trials (347,679). Using a SIV-infected NHP model, it will be possible to accurately measure changes in HIV reservoir size following the therapeutic administration of MG1, as well as gain clinically-relevant insight into the potential toxicity associated with an OV-based HIV cure strategy.

8.4.3 Proof-of-principle clinical trial

Ultimately, the ability of MG1 to reduce the size of the viral reservoir must be assessed in PLWHIV. This will likely take the form of a proof-of-principle clinical trial, in which both the safety profile and pharmacokinetics of MG1 will be assessed in cART-treated individuals. Importantly, the safety data acquired from one Phase I study of MG1-MAGEA3 (NCT02285816) has revealed the development of clinical symptoms (e.g. nausea, fatigue, headache) in several participants (680). These findings will be considered when establishing the safe starting dose of MG1 in future clinical assessment. Proxy measures of HIV reservoir size prior to and following treatment of MG1, such as the frequency of peripheral $CD4^+$ T cells containing HIV provirus, may lend additional support for the bench-to-bedside translation of MG1.

8.5 Conclusion

The data contained within this thesis has been generated in order to address the hypothesis that impairment of the IFN1 response within HIV reservoir cells serves as an intracellular target for infection and killing by IFN-sensitive oncolytic viruses. The characterization of the HIV reservoir—specifically that within latently HIV-infected $CD4^+$ T cells and persistently HIV-infected tissue resident macrophages—is a highly relevant topic of study within the HIV cure field. Not only will this inform our understanding of HIV reservoir establishment and persistence, but it will allow for the development of targeted therapeutic strategies intended for reservoir clearance.

Using a reporter HIV strain, it was found that ISG induction was impaired at the post-transcriptional level in HIV-infected MDM. HIV-infected MDM were also more susceptible to infection and killing by the IFN1-sensitive OV, MG1, indicating a role for these defects in facilitating the selective killing of HIV-infected MDM *in vitro*. Similar observations of selective MG1-mediated killing of HIV-infected cells were observed *ex vivo* using AM from PLWHIV. Although additional models by which to assess the eradication of HIV infected primary macrophages by MG1 are required (for example, human SM), these results remain promising. Investigation of MG1 within a humanized mouse model of HIV infection may provide additional insight with regard to the capability of OV to infiltrate both lymphoid and non-lymphoid tissues, and subsequently eradicate the HIV reservoir. This, combined with the recent investigation of MG1 dissemination within healthy NHP (347), and the translation of MG1 to clinical trials support the investigation of this OV in a proof-of-principle clinical trial intended to assess safety and impact on reservoir size.

Oncolytic virotherapy has the potential to influence a new direction for HIV cure research that exploits intracellular, rather than extracellular, signatures of HIV infection. For this reason, we are optimistic that this project not only represents a collaborative opportunity between the fields of HIV and cancer research, but may lead to the development of a unique and versatile strategy for an HIV cure.

References

1. Barré-Sinoussi F, Chermann JC, Rey F, Nugeyre MT, Chamaret S, Gruest J, et al. Isolation of a T-lymphotropic retrovirus from a patient at risk for acquired immune deficiency syndrome (AIDS). Science. 1983 May 20;220(4599):868–71.

2. Gallo RC, Sarin PS, Gelmann EP, Robert-Guroff M, Richardson E, Kalyanaraman VS, et al. Isolation of human T-cell leukemia virus in acquired immune deficiency syndrome (AIDS). Science. 1983 May 20;220(4599):865–7.

3. Centers for Disease Control (CDC). Pneumocystis pneumonia--Los Angeles. MMWR Morb Mortal Wkly Rep. 1981 Jun 5;30(21):250–2.

4. Gottlieb MS. Pneumocystis pneumonia--Los Angeles. 1981. Vol. 96, American journal of public health. 2006. 2 p.

5. Durack DT. Opportunistic infections and Kaposi's sarcoma in homosexual men. N Engl J Med. 1981 Dec 10;305(24):1465–7.

6. Gottlieb MS, Schroff R, Schanker HM, Weisman JD, Fan PT, Wolf RA, et al. Pneumocystis carinii pneumonia and mucosal candidiasis in previously healthy homosexual men: evidence of a new acquired cellular immunodeficiency. N Engl J Med. 1981 Dec 10;305(24):1425–31.

7. Masur H, Michelis MA, Greene JB, Onorato I, Stouwe RA, Holzman RS, et al. An outbreak of community-acquired Pneumocystis carinii pneumonia: initial manifestation of cellular immune dysfunction. N Engl J Med. 1981 Dec 10;305(24):1431–8.

8. Siegal FP, Lopez C, Hammer GS, Brown AE, Kornfeld SJ, Gold J, et al. Severe acquired immunodeficiency in male homosexuals, manifested by chronic perianal ulcerative herpes simplex lesions. N Engl J Med. 1981 Dec 10;305(24):1439–44.

9. Centers for Disease Control (CDC). Update on acquired immune deficiency syndrome (AIDS)--United States. MMWR Morb Mortal Wkly Rep. 1982 Sep 24;31(37):507–8–513–4.

10. Coffin J, Haase A, Levy JA, Montagnier L, Oroszlan S, Teich N, et al. What to call the AIDS virus? Nature. 1986 May;321(6065):10.

11. Barré-Sinoussi F, Mathur-Wagh U, Rey F, Brun-Vezinet F, Yancovitz SR, Rouzioux C, et al. Isolation of lymphadenopathy-associated virus (LAV) and detection of LAV antibodies from US patients with AIDS. JAMA. 1985 Mar;253(12):1737–9.

12. Goedert JJ, Gallo RC. Epidemiological evidence that HTLV-III is the AIDS agent. Eur J Epidemiol. 1985 Sep;1(3):155–9.

13. Ammann AJ, Cowan MJ, Wara DW, Weintrub P, Dritz S, Goldman H, et al. Acquired immunodeficiency in an infant: possible transmission by means of blood products. Lancet. 1983 Apr 30;1(8331):956–8.

14. Zagury D, Bernard J, Leibowitch J, Safai B, Groopman JE, Feldman M, et al. HTLV-III in cells cultured from semen of two patients with AIDS. Science. 1984 Oct 26;226(4673):449–51.

15. Thiry L, Sprecher-Goldberger S, Jonckheer T, Levy J, Van de Perre P, Henrivaux P, et al. Isolation of AIDS virus from cell-free breast milk of three healthy virus carriers. Lancet. 1985 Oct 19;2(8460):891–2.

16. Feorino PM, Jaffe HW, Palmer E, Peterman TA, Francis DP, Kalyanaraman VS, et al. Transfusion-associated acquired immunodeficiency syndrome. Evidence for persistent infection in blood donors. N Engl J Med. 1985 May 16;312(20):1293–6.

17. Vogt MW, Witt DJ, Craven DE, Byington R, Crawford DF, Schooley RT, et al. Isolation of HTLV-III/LAV from cervical secretions of women at risk for AIDS. Lancet. 1986 Mar 8;1(8480):525–7.

18. Klatzmann D, Champagne E, Chamaret S, Gruest J, Guetard D, Hercend T, et al. T-lymphocyte T4 molecule behaves as the receptor for human retrovirus LAV. Nature. 1984 Jan;312(5996):767–8.

19. Chandra P, Vogel A, Gerber T. Inhibitors of retroviral DNA polymerase: their implication in the treatment of AIDS. Cancer Res. 1985 Sep;45(9 Suppl):4677s–4684s.

20. Mitsuya H, Weinhold KJ, Furman PA, St Clair MH, Lehrman SN, Gallo RC, et al. 3“-Azido-3-”deoxythymidine (BW A509U): an antiviral agent that inhibits the infectivity and cytopathic effect of human T-lymphotropic virus type III/lymphadenopathy-associated virus in vitro. Proc Natl Acad Sci U S A. National Academy of Sciences; 1985 Oct;82(20):7096–100.

21. Brook I. Approval of zidovudine (AZT) for acquired immunodeficiency syndrome. A challenge to the medical and pharmaceutical communities. JAMA. 1987 Sep 18;258(11):1517.

22. Perelson AS, Perelson AS, Essunger P, Essunger P, Cao Y, Cao Y, et al. Decay characteristics of HIV-1-infected compartments during combination therapy. Nature. 1997 May 8;387(6629):188–91.

23. Wlodawer A. Rational approach to AIDS drug design through structural biology. Annu Rev Med. 2002;53(1):595–614.

24. Chun T-W, Justement JS, Murray D, Hallahan CW, Maenza J, Collier AC, et al. Rebound of plasma viremia following cessation of antiretroviral therapy despite profoundly low levels of HIV reservoir: implications for eradication. AIDS. 2010 Nov 27;24(18):2803–8.

25. UNAIDS. UNAIDS Data 2018. 2018 Jul 26;:1–376.

26. Dutta A, Wirtz AL, Baral S, Beyrer C, Cleghorn FR. Key harm reduction interventions and their impact on the reduction of risky behavior and HIV incidence among people who inject drugs in low-income and middle-income countries. Current Opinion in HIV and AIDS. 2012 Jul;7(4):362–8.

27. Dombrowski JC, Simoni JM, Katz DA, Golden MR. Barriers to HIV Care and Treatment Among Participants in a Public Health HIV Care Relinkage Program. AIDS Patient Care and STDs. 2015 May;29(5):279–87.

28. Power J, Westle A, Dowsett GW, Lucke J, Tucker JD, Sugarman J, et al. Perceptions of HIV cure research among people living with HIV in Australia. Newman PA, editor. PLoS One. 2018;13(8):e0202647.

29. Sylla L, Evans D, Taylor J, Gilbertson A, Palm D, Auerbach JD, et al. If We Build It, Will They Come? Perceptions of HIV Cure-Related Research by People Living with HIV in Four U.S. Cities: A Qualitative Focus Group Study. AIDS Res Hum Retroviruses. 2018 Jan;34(1):56–66.

30. Zhang A, Pan X, Wu F, Zhao Y, Hu F, Li L, et al. What Would an HIV Cure Mean to You? Qualitative Analysis from a Crowdsourcing Contest in Guangzhou, China. AIDS Res Hum Retroviruses. 2018 Jan;34(1):80–7.

31. German Advisory Committee Blood (Arbeitskreis Blut), Subgroup 'Assessment of Pathogens Transmissible by Blood'. Human Immunodeficiency Virus (HIV). Transfus Med Hemother. 2016 May;43(3):203–22.

32. Hladik F, Sakchalathorn P, Ballweber L, Lentz G, Fialkow M, Eschenbach D, et al. Initial events in establishing vaginal entry and infection by human immunodeficiency virus type-1. Immunity. 2007 Feb;26(2):257–70.

33. Shen R, Richter HE, Smith PD. Early HIV-1 target cells in human vaginal and ectocervical mucosa. Am J Reprod Immunol. 2011 Mar;65(3):261–7.

34. Pena-Cruz V, Agosto LM, Akiyama H, Olson A, Moreau Y, Larrieux J-R, et al. HIV-1 replicates and persists in vaginal epithelial dendritic cells. J Clin Invest. 2018 Aug 1;128(8):3439–44.

35. Geijtenbeek TBH, van Duijnhoven GCF, van Vliet SJ, Krieger E, Vriend G, Figdor CG, et al. Identification of different binding sites in the dendritic cell-

specific receptor DC-SIGN for intercellular adhesion molecule 3 and HIV-1. J Biol Chem. 2002 Mar 29;277(13):11314–20.

36. Yu Kimata MT, Cella M, Biggins JE, Rorex C, White R, Hicks S, et al. Capture and transfer of simian immunodeficiency virus by macaque dendritic cells is enhanced by DC-SIGN. J Virol. 2002 Dec;76(23):11827–36.

37. Hocini H, Bomsel M. Infectious human immunodeficiency virus can rapidly penetrate a tight human epithelial barrier by transcytosis in a process impaired by mucosal immunoglobulins. J Infect Dis. 1999 May;179 Suppl 3(s3):S448–53.

38. Meng G, Wei X, Wu X, Sellers MT, Decker JM, Moldoveanu Z, et al. Primary intestinal epithelial cells selectively transfer R5 HIV-1 to CCR5+ cells. Nat Med. Nature Publishing Group; 2002 Feb;8(2):150–6.

39. Berges BK, Akkina SR, Folkvord JM, Connick E, Akkina R. Mucosal transmission of R5 and X4 tropic HIV-1 via vaginal and rectal routes in humanized Rag2-/- gammac -/- (RAG-hu) mice. Virology. 2008 Apr 10;373(2):342–51.

40. Moulard M, Lortat-Jacob H, Mondor I, Roca G, Wyatt R, Sodroski J, et al. Selective interactions of polyanions with basic surfaces on human immunodeficiency virus type 1 gp120. J Virol. 2000 Feb;74(4):1948–60.

41. Freed EO, Myers DJ, Risser R. Characterization of the fusion domain of the human immunodeficiency virus type 1 envelope glycoprotein gp41. Proc Natl Acad Sci USA. 1990 Jun;87(12):4650–4.

42. Piekna-Przybylska D, Bambara RA. Requirements for efficient minus strand strong-stop DNA transfer in human immunodeficiency virus 1. RNA Biol. 2011 Mar;8(2):230–6.

43. Brin E, Leis J. HIV-1 integrase interaction with U3 and U5 terminal sequences in vitro defined using substrates with random sequences. J Biol Chem. 2002 May 24;277(21):18357–64.

44. Jeang KT, Xiao H, Rich EA. Multifaceted activities of the HIV-1 transactivator of transcription, Tat. J Biol Chem. 1999 Oct 8;274(41):28837–40.

45. Blissenbach M, Grewe B, Hoffmann B, Brandt S, Uberla K. Nuclear RNA export and packaging functions of HIV-1 Rev revisited. J Virol. 2010 Jul;84(13):6598–604.

46. Sundquist WI, Kräusslich H-G. HIV-1 assembly, budding, and maturation. Cold Spring Harb Perspect Med. 2012 Jul;2(7):a006924–4.

47. Usami Y, Popov S, Popova E, Inoue M, Weissenhorn W, G Göttlinger H. The ESCRT pathway and HIV-1 budding. Biochem Soc Trans. 2009 Feb;37(Pt 1):181–4.

48. Coffin JM, Hughes SH, Varmus HE, Swanstrom R, Wills JW. Synthesis, Assembly, and Processing of Viral Proteins. Cold Spring Harbor (NY): Cold Spring Harbor Laboratory Press; 1997.

49. Kahn JO, Walker BD. Acute human immunodeficiency virus type 1 infection. N Engl J Med. 1998 Jul 2;339(1):33–9.

50. Fiebig EW, Wright DJ, Rawal BD, Garrett PE, Schumacher RT, Peddada L, et al. Dynamics of HIV viremia and antibody seroconversion in plasma donors. AIDS. AIDS; 2003 Sep;17(13):1871–9.

51. Lindback S, Karlsson AC, Mittler J, AIDS AB, 2000. Viral dynamics in primary HIV-1 infection. Karolinska Institutet Primary HIV Infection Study Group. AIDS. 2000 Oct 20;14(15):2283–91.

52. Stacey AR, Norris PJ, Qin L, Haygreen EA, Taylor E, Heitman J, et al. Induction of a striking systemic cytokine cascade prior to peak viremia in acute human immunodeficiency virus type 1 infection, in contrast to more modest and delayed responses in acute hepatitis B and C virus infections. J Virol. 2009 Apr;83(8):3719–33.

53. Audigé A, Taffé P, Rickenbach M, Battegay M, Vernazza P, Nadal D, et al. Low postseroconversion CD4 count and rapid decrease of CD4 density identify HIV+ fast progressors. AIDS Res Hum Retroviruses. 2010 Sep;26(9):997–1005.

54. Kumar P. Long term non-progressor (LTNP) HIV infection. Indian J Med Res. Wolters Kluwer -- Medknow Publications; 2013 Sep;138(3):291–3.

55. Craddock C, Pasvol G, Bull R, Protheroe A, Hopkin J. Cardiorespiratory arrest and autonomic neuropathy in AIDS. Lancet. 1987 Jul 4;2(8549):16–8.

56. Reilly JM, Cunnion RE, Anderson DW, O'Leary TJ, Simmons JT, Lane HC, et al. Frequency of myocarditis, left ventricular dysfunction and ventricular tachycardia in the acquired immune deficiency syndrome. Am J Cardiol. 1988 Oct 1;62(10 Pt 1):789–93.

57. Nishimura C, Polesskaya O, Dewhurst S, Silva JN. Quantification of Cerebral Vascular Architecture using Two-photon Microscopy in a Mouse Model of HIV-induced Neuroinflammation. J Vis Exp. 2016 Jan 12;(107):e53582.

58. Welch K, Morse A, Adult Spectrum of Disease Project in New Orleans. The clinical profile of end-stage AIDS in the era of highly active antiretroviral therapy. AIDS Patient Care and STDs. 2002 Feb;16(2):75–81.

59. Sankaran S, George MD, Reay E, Guadalupe M, Flamm J, Prindiville T, et al. Rapid onset of intestinal epithelial barrier dysfunction in primary human immunodeficiency virus infection is driven by an imbalance between immune response and mucosal repair and regeneration. J Virol. 2008 Jan;82(1):538–45.

60. Metroka CE, Cunningham-Rundles S, Sonnabend JA, Fernandez RD, Mouradian J. Generalized Lymphadenopathy in Homosexual Men. In: Diseases of the Lymphatic System. New York, NY: Springer, New York, NY; 1984. pp. 296–305.

61. Tindall B, Barker S, Donovan B, Barnes T, Roberts J, Kronenberg C, et al. Characterization of the Acute Clinical Illness Associated With Human Immunodeficiency Virus Infection. Arch Intern Med. American Medical Association; 1988 Apr 1;148(4):945–9.

62. Schacker TW, Nguyen PL, Beilman GJ, Wolinsky S, Larson M, Reilly C, et al. Collagen deposition in HIV-1 infected lymphatic tissues and T cell homeostasis. J Clin Invest. American Society for Clinical Investigation; 2002 Oct;110(8):1133–9.

63. Sanchez JL, Hunt PW, Reilly CS, Hatano H, Beilman GJ, Khoruts A, et al. Lymphoid fibrosis occurs in long-term nonprogressors and persists with antiretroviral therapy but may be reversible with curative interventions. J Infect Dis. 2015 Apr 1;211(7):1068–75.

64. Murooka TT, Sharaf RR, Mempel TR. Large Syncytia in Lymph Nodes Induced by CCR5-Tropic HIV-1. AIDS Res Hum Retroviruses. Mary Ann Liebert, Inc. 140 Huguenot Street, 3rd Floor New Rochelle, NY 10801 USA; 2015 May;31(5):471–2.

65. Zeng M, Southern PJ, Reilly CS, Beilman GJ, Chipman JG, Schacker TW, et al. Lymphoid tissue damage in HIV-1 infection depletes naïve T cells and limits T cell reconstitution after antiretroviral therapy. Silvestri G, editor. PLoS Pathog. 2012 Jan;8(1):e1002437.

66. Ho DD, Neumann AU, Perelson AS, Chen W, Leonard JM, Markowitz M. Rapid turnover of plasma virions and CD4 lymphocytes in HIV-1 infection. Nature. 1995 Jan 12;373(6510):123–6.

67. Costin JM. Cytopathic Mechanisms of HIV-1. Virol J. 2007;4(1):100.

68. Klenerman P, Phillips RE, Rinaldo CR, Wahl LM, Ogg G, May RM, et al. Cytotoxic T lymphocytes and viral turnover in HIV type 1 infection. Proc Natl Acad Sci USA. National Academy of Sciences; 1996 Dec 24;93(26):15323–8.

69. Althaus CL, De Boer RJ. Implications of CTL-Mediated Killing of HIV-Infected Cells during the Non-Productive Stage of Infection. Dieli F, editor. PLoS ONE. Public Library of Science; 2011 Feb 7;6(2):e16468.

70. Smalls-Mantey A, Doria-Rose N, Klein R, Patamawenu A, Migueles SA, Ko S-Y, et al. Antibody-dependent cellular cytotoxicity against primary HIV-infected CD4+ T cells is directly associated with the magnitude of surface IgG binding. J Virol. 2012 Jul 27.

71. Smalls-Mantey A, Connors M, Sattentau QJ. Comparative Efficiency of HIV-1-Infected T Cell Killing by NK Cells, Monocytes and Neutrophils. Paxton WA, editor. PLoS ONE. 2013 Sep 10;8(9):e74858.

72. Spijkerman I, de Wolf F, Langendam M, Schuitmaker H, Coutinho R. Emergence of syncytium-inducing human immunodeficiency virus type 1 variants coincides with a transient increase in viral RNA level and is an independent predictor for progression to AIDS. J Infect Dis. 1998 Aug;178(2):397–403.

73. Doitsh G, Galloway NLK, Geng X, Yang Z, Monroe KM, Zepeda O, et al. Cell death by pyroptosis drives CD4 T-cell depletion in HIV-1 infection. Nature. 2014 Jan 23;505(7484):509–14.

74. Alimonti JB. Mechanisms of CD4+ T lymphocyte cell death in human immunodeficiency virus infection and AIDS. J Gen Virol. 2003 Jul;84(Pt 7):1649–61.

75. Brunner T, Mogil RJ, LaFace D, Yoo NJ, Mahboubi A, Echeverri F, et al. Cell-autonomous Fas (CD95)/Fas-ligand interaction mediates activation-induced apoptosis in T-cell hybridomas. Nature. 1995 Feb 2;373(6513):441–4.

76. Ju ST, Panka DJ, Cui H, Ettinger R, el-Khatib M, Sherr DH, et al. Fas(CD95)/FasL interactions required for programmed cell death after T-cell activation. Nature. 1995 Feb 2;373(6513):444–8.

77. Latinis KM, Carr LL, Peterson EJ, Norian LA, Eliason SL, Koretzky GA. Regulation of CD95 (Fas) ligand expression by TCR-mediated signaling events. J Immunol. 1997 May 15;158(10):4602–11.

78. Latinis KM, Norian LA, Eliason SL, Koretzky GA. Two NFAT transcription factor binding sites participate in the regulation of CD95 (Fas) ligand expression in activated human T cells. J Biol Chem. 1997 Dec 12;272(50):31427–34.

79. Muzio M, Chinnaiyan AM, Kischkel FC, O'Rourke K, Shevchenko A, Ni J, et al. FLICE, A Novel FADD-Homologous ICE/CED-3–like Protease, Is

Recruited to the CD95 (Fas/APO-1) Death-Inducing Signaling Complex. Cell. Cell Press; 1996 Jun 14;85(6):817–27.

80. Sprick MR, Rieser E, Stahl H, Wilde AG, Weigand MA, Walczak H. Caspase-10 is recruited to and activated at the native TRAIL and CD95 death-inducing signalling complexes in a FADD-dependent manner but can not functionally substitute caspase-8. EMBO J. EMBO Press; 2002 Sep 2;21(17):4520–30.

81. Lavrik IN, Mock T, Golks A, Hoffmann JC, Baumann S, Krammer PH. CD95 stimulation results in the formation of a novel death effector domain protein-containing complex. J Biol Chem. 2008 Sep 26;283(39):26401–8.

82. Groux H, Torpier G, Monté D, Mouton Y, Capron A, Ameisen JC. Activation-induced death by apoptosis in CD4+ T cells from human immunodeficiency virus-infected asymptomatic individuals. J Exp Med. 1992 Feb 1;175(2):331–40.

83. Meyaard L, Otto SA, Jonker RR, Mijnster MJ, Keet RP, Miedema F. Programmed death of T cells in HIV-1 infection. Science. 1992 Jul 10;257(5067):217–9.

84. Algeciras A, Dockrell DH, Lynch DH, Paya CV. CD4 Regulates Susceptibility to Fas ligand– and Tumor Necrosis Factor–mediated Apoptosis. J Exp Med. Rockefeller University Press; 1998 Mar 2;187(5):711–20.

85. Badley AD, Dockrell DH, Algeciras A, Ziesmer S, Landay A, Lederman MM, et al. In vivo analysis of Fas/FasL interactions in HIV-infected patients. J Clin Invest. American Society for Clinical Investigation; 1998 Jul 1;102(1):79–87.

86. Dockrell DH, Badley AD, Algeciras-Schimnich A, Simpson M, Schut R, Lynch DH, et al. Activation-Induced CD4+ T Cell Death in HIV-Positive Individuals Correlates with Fas Susceptibility, CD4+ T Cell Count, and HIV Plasma Viral Copy Number. AIDS Res Hum Retroviruses. Mary Ann Liebert, Inc; 1999 Nov;15(17):1509–18.

87. Somma F, Tuosto L, Montani MSG, Di Somma MM, Cundari E, Piccolella E. Engagement of CD4 Before TCR Triggering Regulates Both Bax- and Fas (CD95)-Mediated Apoptosis. J Immunol. 2000 May 15;164(10):5078–87.

88. Li CJ, Friedman DJ, Wang C, Metelev V, Pardee AB. Induction of apoptosis in uninfected lymphocytes by HIV-1 Tat protein. Science. 1995 Apr 21;268(5209):429–31.

89. Westendorp MO, Frank R, Ochsenbauer C, Stricker K, Dhein J, Walczak H, et al. Sensitization of T cells to CD95-mediated apoptosis by HIV-1 Tat and gp120. Nature. 1995 Jun 8;375(6531):497–500.

90. Sastry KJ, Marin MC, Nehete PN, McConnell K, el-Naggar AK, McDonnell TJ. Expression of human immunodeficiency virus type I tat results in down-regulation of bcl-2 and induction of apoptosis in hematopoietic cells. Oncogene. 1996 Aug 1;13(3):487–93.

91. Vendeville A, Rayne F, Bonhoure A, Bettache N, Montcourrier P, Beaumelle B. HIV-1 Tat enters T cells using coated pits before translocating from acidified endosomes and eliciting biological responses. Mol Biol Cell. 2004 May;15(5):2347–60.

92. Richard J, Veillette M, Ding S, Zoubchenok D, Alsahafi N, Coutu M, et al. Small CD4 Mimetics Prevent HIV-1 Uninfected Bystander CD4 + T Cell Killing Mediated by Antibody-dependent Cell-mediated Cytotoxicity. EBioMedicine. 2016 Jan;3:122–34.

93. Stewart SA, Poon B, Song JY, Chen IS. Human immunodeficiency virus type 1 vpr induces apoptosis through caspase activation. J Virol. American Society for Microbiology (ASM); 2000 Apr;74(7):3105–11.

94. James CO, Huang M-B, Khan M, Garcia-Barrio M, Powell MD, Bond VC. Extracellular Nef protein targets CD4+ T cells for apoptosis by interacting with CXCR4 surface receptors. J Virol. 2004 Mar;78(6):3099–109.

95. Lenassi M, Cagney G, Liao M, Vaupotic T, Bartholomeeusen K, Cheng Y, et al. HIV Nef is secreted in exosomes and triggers apoptosis in bystander CD4+ T cells. Traffic. 2010 Jan;11(1):110–22.

96. Choi H-J, Smithgall TE. HIV-1 Nef promotes survival of TF-1 macrophages by inducing Bcl-XL expression in an extracellular signal-regulated kinase-dependent manner. J Biol Chem. 2004 Dec 3;279(49):51688–96.

97. Swingler S, Mann AM, Zhou J, Swingler C, Stevenson M. Apoptotic killing of HIV-1-infected macrophages is subverted by the viral envelope glycoprotein. PLoS Pathog. 2007 Sep 7;3(9):1281–90.

98. Zheng L, Yang Y, Guocai L, Pauza CD, Salvato MS. HIV Tat protein increases Bcl-2 expression in monocytes which inhibits monocyte apoptosis induced by tumor necrosis factor-alpha-related apoptosis-induced ligand. Intervirology. 2007;50(3):224–8.

99. Koziel H, Eichbaum Q, Kruskal BA, Pinkston P, Rogers RA, Armstrong MY, et al. Reduced binding and phagocytosis of Pneumocystis carinii by alveolar macrophages from persons infected with HIV-1 correlates with mannose receptor downregulation. Journal of Clinical Investigation. American Society for Clinical Investigation; 1998 Oct 1;102(7):1332–44.

100. Ieong MH, Reardon CC, Levitz SM, Kornfeld H. Human immunodeficiency virus type 1 infection of alveolar macrophages impairs their innate fungicidal activity. Am J Respir Crit Care Med. 2000 Sep;162(3 Pt 1):966–70.

101. Jambo KC, Banda DH, Kankwatira AM, Sukumar N, Allain TJ, Heyderman RS, et al. Small alveolar macrophages are infected preferentially by HIV and exhibit impaired phagocytic function. Mucosal Immunol. 2014 Sep;7(5):1116–26.

102. Swan ZD, Bouwer AL, Wonderlich ER, Barratt-Boyes SM. Persistent accumulation of gut macrophages with impaired phagocytic function correlates with SIV disease progression in macaques. Eur J Immunol. 2017 Nov;47(11):1925–35.

103. Chun TW, Finzi D, Margolick J, Chadwick K, Schwartz D, Siliciano RF. In vivo fate of HIV-1-infected T cells: quantitative analysis of the transition to stable latency. Nat Med. 1995 Dec;1(12):1284–90.

104. Chun TW, Engel D, Berrey MM, Shea T, Corey L, Fauci AS. Early establishment of a pool of latently infected, resting CD4(+) T cells during primary HIV-1 infection. Proc Natl Acad Sci USA. National Academy of Sciences; 1998 Jul 21;95(15):8869–73.

105. Whitney JB, Lim S-Y, Osuna CE, Kublin JL, Chen E, Yoon G, et al. Prevention of SIVmac251 reservoir seeding in rhesus monkeys by early antiretroviral therapy. Nat Commun. 2018 Dec 21;9(1):5429.

106. Henrich TJ, Hatano H, Bacon O, Hogan LE, Rutishauser R, Hill A, et al. HIV-1 persistence following extremely early initiation of antiretroviral therapy (ART) during acute HIV-1 infection: An observational study. Bekker L-G, editor. PLoS Med. 2017 Nov;14(11):e1002417.

107. Igarashi T, Brown CR, Endo Y, Buckler-White A, Plishka R, Bischofberger N, et al. Macrophage are the principal reservoir and sustain high virus loads in rhesus macaques after the depletion of CD4+ T cells by a highly pathogenic simian immunodeficiency virus/HIV type 1 chimera (SHIV): Implications for HIV-1 infections of humans. Proc Natl Acad Sci U S A. National Acad Sciences; 2001 Jan 16;98(2):658–63.

108. Honeycutt JB, Thayer WO, Baker CE, Ribeiro RM, Lada SM, Cao Y, et al. HIV persistence in tissue macrophages of humanized myeloid-only mice during antiretroviral therapy. Nat Med. 2017 May;23(5):638–43.

109. Jenabian M-A, Costiniuk CT, Mehraj V, Ghazawi FM, Fromentin R, Brousseau J, et al. Immune tolerance properties of the testicular tissue as a viral sanctuary site in ART-treated HIV-infected adults. AIDS. 2016 Nov 28;30(18):2777–86.

110. Connick E, Mattila T, Folkvord JM, Schlichtemeier R, Meditz AL, Ray MG, et al. CTL fail to accumulate at sites of HIV-1 replication in lymphoid tissue. J Immunol. 2007 Jun 1;178(11):6975–83.

111. Blankson JN, Persaud D, Siliciano RF. The challenge of viral reservoirs in HIV-1 infection. Annu Rev Med. 2002;53:557–93.

112. Siliciano RF, Greene WC. HIV latency. Cold Spring Harb Perspect Med. 2011 Sep;1(1):a007096.

113. Jaafoura S, de Goër de Herve MG, Hernandez-Vargas EA, Hendel-Chavez H, Abdoh M, Mateo MC, et al. Progressive contraction of the latent HIV reservoir around a core of less-differentiated $CD4^+$ memory T Cells. Nat Commun. 2014;5:5407.

114. Finzi D, Blankson J, Siliciano JD, Margolick JB, Chadwick K, Pierson T, et al. Latent infection of CD4+ T cells provides a mechanism for lifelong persistence of HIV-1, even in patients on effective combination therapy. Nat Med. 1999 May;5(5):512–7.

115. Josefsson L, King MS, Makitalo B, Brännström J, Shao W, Maldarelli F, et al. Majority of CD4+ T cells from peripheral blood of HIV-1-infected individuals contain only one HIV DNA molecule. Proc Natl Acad Sci U S A. 2011 Jul 5;108(27):11199–204.

116. Eriksson S, Graf EH, Dahl V, Strain MC, Yukl SA, Lysenko ES, et al. Comparative analysis of measures of viral reservoirs in HIV-1 eradication studies. Douek DC, editor. PLoS Pathog. Public Library of Science; 2013 Feb;9(2):e1003174.

117. Crooks AM, Bateson R, Cope AB, Dahl NP, Griggs MK, Kuruc JD, et al. Precise Quantitation of the Latent HIV-1 Reservoir: Implications for Eradication Strategies. J Infect Dis. Oxford University Press; 2015 Nov 1;212(9):1361–5.

118. Poon AFY, Prodger JL, Lynch BA, Lai J, Reynolds SJ, Kasule J, et al. Quantitation of the latent HIV-1 reservoir from the sequence diversity in viral outgrowth assays. Retrovirology. 2018 Jul 5;15(1):47.

119. Chun TW, Stuyver L, Mizell SB, Ehler LA, Mican JA, Baseler M, et al. Presence of an inducible HIV-1 latent reservoir during highly active antiretroviral therapy. Proc Natl Acad Sci U S A. 1997 Nov 25;94(24):13193–7.

120. Finzi D, Finzi D, Hermankova M, Hermankova M, Pierson T, Pierson T, et al. Identification of a reservoir for HIV-1 in patients on highly active antiretroviral therapy. Science. 1997 Nov 14;278(5341):1295–300.

121. Bosque A, Planelles V. Induction of HIV-1 latency and reactivation in primary memory CD4+ T cells. Blood. 2009 Jan 1;113(1):58–65.

122. Saleh S, Wightman F, Ramanayake S, Alexander M, Kumar N, Khoury G, et al. Expression and reactivation of HIV in a chemokine induced model of HIV latency in primary resting CD4+ T cells. Retrovirology. BioMed Central Ltd; 2011;8(1):80.

123. Lassen KG, Hebbeler AM, Bhattacharyya D, Lobritz MA, Greene WC. A flexible model of HIV-1 latency permitting evaluation of many primary CD4 T-cell reservoirs. Lassen KG, Hebbeler AM, Bhattacharyya D, Lobritz MA, Greene WC, editors. PLoS One. 2012 Jan 24;7(1):e30176–6.

124. Spina CA, Anderson J, Archin NM, Bosque A, Chan J, Famiglietti M, et al. An in-depth comparison of latent HIV-1 reactivation in multiple cell model systems and resting CD4+ T cells from aviremic patients. Emerman M, editor. PLoS Pathog [Internet]. Public Library of Science; 2013;9(12):e1003834. Available from: http://eutils.ncbi.nlm.nih.gov/entrez/eutils/elink.fcgi?dbfrom=pubmed&id=24385908&retmode=ref&cmd=prlinks

125. Zack JA, Arrigo SJ, Weitsman SR, Go AS, Haislip A, Chen IS. HIV-1 entry into quiescent primary lymphocytes: molecular analysis reveals a labile, latent viral structure. Cell. 1990 Apr 20;61(2):213–22.

126. Zhou Y, Zhang H, Siliciano JD, Siliciano RF. Kinetics of Human Immunodeficiency Virus Type 1 Decay following Entry into Resting CD4+ T Cells. J Virol. 2005 Jan 28;79(4):2199–210.

127. Williams SA, Chen L-F, Kwon H, Ruiz-Jarabo CM, Verdin E, Greene WC. NF-kappaB p50 promotes HIV latency through HDAC recruitment and repression of transcriptional initiation. EMBO J. 2006 Jan 11;25(1):139–49.

128. Sung T-L, Rice A. Effects of prostratin on Cyclin T1/P-TEFb function and the gene expression profile in primary resting CD4+ T cells. Retrovirology. 2006 Oct 2;3:66.

129. Blazkova J, Murray D, Justement JS, Funk EK, Nelson AK, Moir S, et al. Paucity of HIV DNA methylation in latently infected, resting CD4+ T cells from infected individuals receiving antiretroviral therapy. J Virol. 2012 May;86(9):5390–2.

130. Greger IH, Demarchi F, Giacca M, Proudfoot NJ. Transcriptional interference perturbs the binding of Sp1 to the HIV-1 promoter. Nucleic Acids Res. 1998 Mar 1;26(5):1294–301.

131. Lewinski MK, Yamashita M, Emerman M, Ciuffi A, Marshall H, Crawford G, et al. Retroviral DNA integration: viral and cellular determinants of target-site selection. PLoS Pathog. 2006 Jun;2(6):e60.

132. Lenasi T, Contreras X, Peterlin BM. Transcriptional interference antagonizes proviral gene expression to promote HIV latency. Cell Host Microbe. 2008 Aug 14;4(2):123–33.

133. Micci L, Alvarez X, Iriele RI, Ortiz AM, Ryan ES, McGary CS, et al. CD4 depletion in SIV-infected macaques results in macrophage and microglia infection with rapid turnover of infected cells. Douek DC, editor. PLoS Pathog. 2014 Oct;10(10):e1004467.

134. Mack KD, Jin X, Yu S, Wei R, Kapp L, Green C, et al. HIV insertions within and proximal to host cell genes are a common finding in tissues containing high levels of HIV DNA and macrophage-associated p24 antigen expression. JAIDS Journal of Acquired Immune Deficiency Syndromes. 2003 Jul 1;33(3):308–20.

135. Barr SD, Ciuffi A, Leipzig J, Shinn P, Ecker JR, Bushman FD. HIV integration site selection: targeting in macrophages and the effects of different routes of viral entry. Mol Ther. 2006 Aug;14(2):218–25.

136. Brown A, Zhang H, Lopez P, Pardo CA, Gartner S. In vitro modeling of the HIV-macrophage reservoir. Journal of Leukocyte Biology. Society for Leukocyte Biology; 2006 Nov;80(5):1127–35.

137. Veenstra M, León-Rivera R, Li M, Gama L, Clements JE, Berman JW. Mechanisms of CNS Viral Seeding by HIV+ CD14+ CD16+ Monocytes: Establishment and Reseeding of Viral Reservoirs Contributing to HIV-Associated Neurocognitive Disorders. MBio. 2017 Oct 24;8(5):961.

138. Groot F, Russell RA, Baxter AE, Welsch S, Duncan CJ, Willberg C, et al. Efficient macrophage infection by phagocytosis of dying HIV-1 -infected CD4+T cells. Retrovirology. 2011 Oct 3;8(S2):O31.

139. Baxter AE, Russell RA, Duncan CJA, Moore MD, Willberg CB, Pablos JL, et al. Macrophage Infection via Selective Capture of HIV-1-Infected CD4(+) T Cells. Cell Host Microbe. 2014 Dec 10;16(6):711–21.

140. Ganor Y, Zhou Z, Bodo J, Tudor D, Leibowitch J, Mathez D, et al. The adult penile urethra is a novel entry site for HIV-1 that preferentially targets resident urethral macrophages. Mucosal Immunol. Nature Publishing Group; 2013 Jul;6(4):776–86.

141. Busca A, Saxena M, Kumar A. Critical Role for Antiapoptotic Bcl-xL and Mcl-1 in Human Macrophage Survival and Cellular IAP1/2 (cIAP1/2) in

Resistance to HIV-Vpr-induced Apoptosis. J Biol Chem. 2012 Apr 27;287(18):15118–33.

142. Clayton KL, Clayton KL, Collins DR, Collins DR, Lengieza J, Ghebremichael M, et al. Resistance of HIV-infected macrophages to CD8+ T lymphocyte-mediated killing drives activation of the immune system. Nat Immunol. 2018 May;19(5):475–86.

143. Collins KL, Chen BK, Kalams SA, Walker BD, Baltimore D. HIV-1 Nef protein protects infected primary cells against killing by cytotoxic T lymphocytes. Nature. Nature Publishing Group; 1998 Jan 22;391(6665):397–401.

144. Brown A, Gartner S, Kawano T, Benoit N, Cheng-Mayer C. HLA-A2 down-regulation on primary human macrophages infected with an M-tropic EGFP-tagged HIV-1 reporter virus. J Leukoc Biol. John Wiley & Sons, Ltd; 2005 Sep;78(3):675–85.

145. Orenstein JM, Meltzer MS, Phipps T, Gendelman HE. Cytoplasmic assembly and accumulation of human immunodeficiency virus types 1 and 2 in recombinant human colony-stimulating factor-1-treated human monocytes: an ultrastructural study. J Virol. 1988 Aug;62(8):2578–86.

146. Pelchen-Matthews A, Kramer B, Marsh M. Infectious HIV-1 assembles in late endosomes in primary macrophages. J Cell Biol. Rockefeller Univ Press; 2003 Aug 4;162(3):443–55.

147. Foley JF, Yu C-R, Solow R, Yacobucci M, Peden KWC, Farber JM. Roles for CXC chemokine ligands 10 and 11 in recruiting CD4+ T cells to HIV-1-infected monocyte-derived macrophages, dendritic cells, and lymph nodes. J Immunol. 2005 Apr 15;174(8):4892–900.

148. Jolly C, Sattentau Q. Retroviral spread by induction of virological synapses. Traffic. 2004 Sep;5(9):643–50.

149. Groot F, Welsch S, Sattentau Q. Efficient HIV-1 transmission from macrophages to T cells across transient virological synapses. Blood. 2008 May 1;111(9):4660–3.

150. Abela IA, Berlinger L, Schanz M, Reynell L, Günthard HF, Rusert P, et al. Cell-cell transmission enables HIV-1 to evade inhibition by potent CD4bs directed antibodies. PLoS Pathog. 2012;8(4):e1002634.

151. Koppensteiner H, Banning C, Schneider C, Hohenberg H, Schindler M. Macrophage internal HIV-1 is protected from neutralizing antibodies. J Virol. 2012 Mar;86(5):2826–36.

152. Duncan CJA, Russell RA, Sattentau QJ. High multiplicity HIV-1 cell-to-cell transmission from macrophages to CD4+ T cells limits antiretroviral efficacy. AIDS. 2013 Sep 10;27(14):2201–6.

153. Siliciano JD, Margolick JB, Chadwick K, medicine TPN, 1999. Latent infection of CD4+ T cells provides a mechanism for lifelong persistence of HIV-1, even in patients on effective combination therapy. Nat Med. 1999 May;5(5):512–7.

154. Siliciano JD, Kajdas J, Finzi D, Quinn TC, Chadwick K, Margolick JB, et al. Long-term follow-up studies confirm the stability of the latent reservoir for HIV-1 in resting CD4+ T cells. Nat Med. 2003 May 18;9(6):727–8.

155. Sued O, Ambrosioni J, Nicolás D, Manzardo C, Agüero F, Claramonte X, et al. Structured Treatment Interruptions and Low Doses of IL-2 in Patients with Primary HIV Infection. Inflammatory, Virological and Immunological Outcomes. Landay A, editor. PLoS ONE. 2015;10(7):e0131651.

156. Goujard C, Emilie D, Roussillon C, Godot V, Rouzioux C, Venet A, et al. Continuous versus intermittent treatment strategies during primary HIV-1 infection: the randomized ANRS INTERPRIM Trial. AIDS. 2012 Sep 24;26(15):1895–905.

157. Oxenius A, Price DA, Günthard HF, Dawson SJ, Fagard C, Perrin L, et al. Stimulation of HIV-specific cellular immunity by structured treatment interruption fails to enhance viral control in chronic HIV infection. Proc Natl Acad Sci U S A. 2002 Oct 15;99(21):13747–52.

158. Mancini E, Castiglione F, Bernaschi M, de Luca A, Sloot PMA. HIV reservoirs and immune surveillance evasion cause the failure of structured treatment interruptions: a computational study. Brusic V, editor. PLoS ONE. 2012;7(4):e36108.

159. Prins JM, Jurriaans S, van Praag RM, Blaak H, van Rij R, Schellekens PT, et al. Immuno-activation with anti-CD3 and recombinant human IL-2 in HIV-1-infected patients on potent antiretroviral therapy. AIDS. 1999 Dec 3;13(17):2405–10.

160. van Praag RM, Prins JM, Roos MT, Schellekens PT, Berge ten IJ, Yong SL, et al. OKT3 and IL-2 treatment for purging of the latent HIV-1 reservoir in vivo results in selective long-lasting CD4+ T cell depletion. J Clin Immunol. 2001 May;21(3):218–26.

161. Van Lint C, Emiliani S, Ott M, Verdin E. Transcriptional activation and chromatin remodeling of the HIV-1 promoter in response to histone acetylation. EMBO J. 1996 Mar 1;15(5):1112–20.

162. Quivy V, Adam E, Collette Y, Demonte D, Chariot A, Vanhulle C, et al. Synergistic activation of human immunodeficiency virus type 1 promoter activity by NF-kappaB and inhibitors of deacetylases: potential perspectives for the development of therapeutic strategies. J Virol. 2002 Nov;76(21):11091–103.

163. Yang H-C, Xing S, Shan L, O'Connell K, Dinoso J, Shen A, et al. Small-molecule screening using a human primary cell model of HIV latency identifies compounds that reverse latency without cellular activation. J Clin Invest. 2009 Nov 1;119(11):3473–86.

164. Lehrman G, Hogue IB, Palmer S, Jennings C, Spina CA, Wiegand A, et al. Depletion of latent HIV-1 infection in vivo: a proof-of-concept study. Lancet. 2005 Aug;366(9485):549–55.

165. Archin NM, Eron JJ, Palmer S, Hartmann-Duff A, Martinson JA, Wiegand A, et al. Valproic acid without intensified antiviral therapy has limited impact on persistent HIV infection of resting CD4+ T cells. AIDS. 2008 Jun 19;22(10):1131–5.

166. Archin NM, Espeseth A, Parker D, Cheema M, Hazuda D, Margolis DM. Expression of latent HIV induced by the potent HDAC inhibitor suberoylanilide hydroxamic acid. AIDS Res Hum Retroviruses. 2009 Feb;25(2):207–12.

167. Archin NM, Liberty AL, Kashuba AD, Choudhary SK, Kuruc JD, Crooks AM, et al. Administration of vorinostat disrupts HIV-1 latency in patients on antiretroviral therapy. Nature. 2012 Jul 25;487(7408):482–5.

168. Archin NM, Bateson R, Tripathy MK, Crooks AM, Yang K-H, Dahl NP, et al. HIV-1 expression within resting CD4+ T cells after multiple doses of vorinostat. J Infect Dis. 2014 Sep 1;210(5):728–35.

169. Elliott JH, Wightman F, Solomon A, Ghneim K, Ahlers J, Cameron MJ, et al. Activation of HIV transcription with short-course vorinostat in HIV-infected patients on suppressive antiretroviral therapy. Cullen BR, editor. PLoS Pathog. Public Library of Science; 2014 Oct;10(10):e1004473.

170. Cillo AR, Sobolewski MD, Bosch RJ, Fyne E, Piatak M, Coffin JM, et al. Quantification of HIV-1 latency reversal in resting CD4+ T cells from patients on suppressive antiretroviral therapy. Proc Natl Acad Sci U S A. 2014 May 13;111(19):7078–83.

171. Archin NM, Kirchherr JL, Sung JA, Clutton G, Sholtis K, Xu Y, et al. Interval dosing with the HDAC inhibitor vorinostat effectively reverses HIV latency. J Clin Invest. 2017 Aug 1;127(8):3126–35.

172. Søgaard OS, Graversen ME, Leth S, Olesen R, Brinkmann CR, Nissen SK, et al. The Depsipeptide Romidepsin Reverses HIV-1 Latency In Vivo. Siliciano RF, editor. PLoS Pathog. 2015 Sep;11(9):e1005142.

173. Leth S, Schleimann MH, Nissen SK, Højen JF, Olesen R, Graversen ME, et al. Combined effect of Vacc-4x, recombinant human granulocyte macrophage colony-stimulating factor vaccination, and romidepsin on the HIV-1 reservoir (REDUC): a single-arm, phase 1B/2A trial. The Lancet HIV. 2016 Oct;3(10):e463–72.

174. Tapia G, Højen JF, Ökvist M, Olesen R, Leth S, Nissen SK, et al. Sequential Vacc-4x and romidepsin during combination antiretroviral therapy (cART): Immune responses to Vacc-4x regions on p24 and changes in HIV reservoirs. J Infect. 2017 Dec;75(6):555–71.

175. Rasmussen TA, Tolstrup M, Brinkmann CR, Olesen R, Erikstrup C, Solomon A, et al. Panobinostat, a histone deacetylase inhibitor, for latent-virus reactivation in HIV-infected patients on suppressive antiretroviral therapy: a phase 1/2, single group, clinical trial. Lancet HIV. 2014 Oct;1(1):e13–21.

176. Barton K, Hiener B, Winckelmann A, Rasmussen TA, Shao W, Byth K, et al. Broad activation of latent HIV-1 in vivo. Nat Commun. Nature Publishing Group; 2016 Sep 8;7(1):12731.

177. Tsai P, Wu G, Baker CE, Thayer WO, Spagnuolo RA, Sanchez R, et al. In vivo analysis of the effect of panobinostat on cell-associated HIV RNA and DNA levels and latent HIV infection. Retrovirology. 2016 May 21;13(1):15109.

178. Spivak AM, Andrade A, Eisele E, Hoh R, Bacchetti P, Bumpus NN, et al. A pilot study assessing the safety and latency-reversing activity of disulfiram in HIV-1-infected adults on antiretroviral therapy. Clin Infect Dis. 2014 Mar;58(6):883–90.

179. Martínez-Bonet M, Clemente MI, Álvarez S, Díaz L, García-Alonso D, Muñoz E, et al. Antiretroviral drugs do not interfere with bryostatin-mediated HIV-1 latency reversal. Antiviral Res. 2015 Nov;123:163–71.

180. Gutiérrez C, Serrano-Villar S, Madrid-Elena N, Pérez-Elías MJ, Martín ME, Barbas C, et al. Bryostatin-1 for latent virus reactivation in HIV-infected patients on antiretroviral therapy. AIDS. 2016 Jun 1;30(9):1385–92.

181. Stoszko M, De Crignis E, Rokx C, Khalid MM, Lungu C, Palstra R-J, et al. Small Molecule Inhibitors of BAF; A Promising Family of Compounds in HIV-1 Latency Reversal. EBioMedicine. 2016 Jan;3:108–21.

182. Boehm D, Calvanese V, Dar RD, Xing S, Schroeder S, Martins L, et al. BET bromodomain-targeting compounds reactivate HIV from latency via a Tat-

independent mechanism. Cell Cycle. Taylor & Francis; 2013 Feb 1;12(3):452–62.

183. Lu P, Qu X, Shen Y, Jiang Z, Wang P, Zeng H, et al. The BET inhibitor OTX015 reactivates latent HIV-1 through P-TEFb. Sci Rep. Nature Publishing Group; 2016 Apr 12;6(1):24100.

184. Li P, Kaiser P, Lampiris HW, Kim P, Yukl SA, Havlir DV, et al. Stimulating the RIG-I pathway to kill cells in the latent HIV reservoir following viral reactivation. Nat Med. 2016 Jul;22(7):807–11.

185. Garcia-Vidal E, Castellví M, Pujantell M, Badia R, Jou A, Gomez L, et al. Evaluation of the Innate Immune Modulator Acitretin as a Strategy To Clear the HIV Reservoir. Antimicrob Agents Chemother. 2017 Nov;61(11):1.

186. García F, León A, Gatell JM, Plana M, Gallart T. Therapeutic vaccines against HIV infection. Hum Vaccin Immunother. Taylor & Francis; 2012 May;8(5):569–81.

187. Gray GE, Laher F, Lazarus E, Ensoli B, Corey L. Approaches to preventative and therapeutic HIV vaccines. Current Opinion in Virology. 2016 Apr;17:104–9.

188. Caskey M, Klein F, Lorenzi JCC, Seaman MS, West AP, Buckley N, et al. Viraemia suppressed in HIV-1-infected humans by broadly neutralizing antibody 3BNC117. Nature. 2015 Jun 25;522(7557):487–91.

189. Lynch RM, Boritz E, Coates EE, DeZure A, Madden P, Costner P, et al. Virologic effects of broadly neutralizing antibody VRC01 administration during chronic HIV-1 infection. Sci Transl Med. 2015 Dec 23;7(319):319ra206–6.

190. Gombos RB, Kolodkin-Gal D, Eslamizar L, Owuor JO, Mazzola E, Gonzalez AM, et al. Inhibitory Effect of Individual or Combinations of Broadly Neutralizing Antibodies and Antiviral Reagents against Cell-Free and Cell-to-Cell HIV-1 Transmission. Silvestri G, editor. J Virol. American Society for Microbiology Journals; 2015 Aug;89(15):7813–28.

191. Scott YM, Park SY, Dezzutti CS. Broadly Neutralizing Anti-HIV Antibodies Prevent HIV Infection of Mucosal Tissue Ex Vivo. Antimicrob Agents Chemother. 2016 Feb;60(2):904–12.

192. Ensoli F, Cafaro A, Casabianca A, Tripiciano A, Bellino S, Longo O, et al. HIV-1 Tat immunization restores immune homeostasis and attacks the HAART-resistant blood HIV DNA: results of a randomized phase II exploratory clinical trial. Retrovirology. BioMed Central; 2015 Apr 29;12(1):33.

193. Cafaro A, Tripiciano A, Sgadari C, Bellino S, Picconi O, Longo O, et al. Development of a novel AIDS vaccine: the HIV-1 transactivator of transcription protein vaccine. Expert Opin Biol Ther. 2015;15 Suppl 1(sup1):S13–29.

194. Ensoli B, Nchabeleng M, Ensoli F, Tripiciano A, Bellino S, Picconi O, et al. HIV-Tat immunization induces cross-clade neutralizing antibodies and CD4(+) T cell increases in antiretroviral-treated South African volunteers: a randomized phase II clinical trial. Retrovirology. 2016 Jun 9;13(1):34.

195. Mothe B, Hu X, Llano A, Rosati M, Olvera A, Kulkarni V, et al. A human immune data-informed vaccine concept elicits strong and broad T-cell specificities associated with HIV-1 control in mice and macaques. J Transl Med. 2015 Feb 15;13(1):60.

196. Guardo AC, Joe PT, Miralles L, Bargalló ME, Mothe B, Krasniqi A, et al. Preclinical evaluation of an mRNA HIV vaccine combining rationally selected antigenic sequences and adjuvant signals (HTI-TriMix). AIDS. 2017 Jan 28;31(3):321–32.

197. Leal L, Guardo AC, Morón-López S, Salgado M, Mothe B, Heirman C, et al. Phase I clinical trial of an intranodally administered mRNA-based therapeutic vaccine against HIV-1 infection. AIDS. 2018 Nov 13;32(17):2533–45.

198. Hütter G, Nowak D, Mossner M, Ganepola S, Müssig A, Allers K, et al. Long-term control of HIV by CCR5 Delta32/Delta32 stem-cell transplantation. 2009 Feb 12;360(7):692–8.

199. Allers K, Hütter G, Hofmann J, Loddenkemper C, Rieger K, Thiel E, et al. Evidence for the cure of HIV infection by CCR5Δ32/Δ32 stem cell transplantation. Blood. 2011 Mar 10;117(10):2791–9.

200. Yukl SA, Boritz E, Busch M, Bentsen C, Chun T-W, Douek D, et al. Challenges in detecting HIV persistence during potentially curative interventions: a study of the Berlin patient. PLoS Pathog. 2013;9(5):e1003347.

201. Henrich TJ, Hanhauser E, Marty FM, Sirignano MN, Keating S, Lee T-H, et al. Antiretroviral-free HIV-1 remission and viral rebound after allogeneic stem cell transplantation: report of 2 cases. Ann Intern Med. 2014 Sep 2;161(5):319–27.

202. Cummins NW, Rizza S, Litzow MR, Hua S, Lee GQ, Einkauf K, et al. Extensive virologic and immunologic characterization in an HIV-infected individual following allogeneic stem cell transplant and analytic cessation of antiretroviral therapy: A case study. Lewin SR, editor. PLoS Med. 2017 Nov;14(11):e1002461.

203. Rothenberger M, Wagner JE, Haase A, Richman D, Grzywacz B, Strain M, et al. Transplantation of CCR5Δ32 Homozygous Umbilical Cord Blood in a Child With Acute Lymphoblastic Leukemia and Perinatally Acquired HIV Infection. Open Forum Infect Dis. 2018 May;5(5):ofy090.

204. Sanhadji K, Leissner P, Firouzi R, Pelloquin F, Kehrli L, Marigliano M, et al. Experimental gene therapy: the transfer of Tat-inducible interferon genes protects human cells against HIV-1 challenge in vitro and in vivo in severe combined immunodeficient mice. AIDS. 1997 Jul;11(8):977–86.

205. Allen AG, Chung C-H, Atkins A, Dampier W, Khalili K, Nonnemacher MR, et al. Gene Editing of HIV-1 Co-receptors to Prevent and/or Cure Virus Infection. Front Microbiol. 2018;9:2940.

206. Ophinni Y, Inoue M, Kotaki T, Kameoka M. CRISPR/Cas9 system targeting regulatory genes of HIV-1 inhibits viral replication in infected T-cell cultures. Sci Rep. Nature Publishing Group; 2018 May 17;8(1):7784.

207. Bella R, Kaminski R, Mancuso P, Young W-B, Chen C, Sariyer R, et al. Removal of HIV DNA by CRISPR from Patient Blood Engrafts in Humanized Mice. Mol Ther Nucleic Acids. 2018 Sep 7;12:275–82.

208. Fitzgerald-Bocarsly P. Human natural interferon-α producing cells. Pharmacology & Therapeutics. 1993 Jan;60(1):39–62.

209. Kadowaki N, Liu Y-J. Natural type I interferon-producing cells as a link between innate and adaptive immunity. HIM. 2002 Jan 1;63(12):1126–32.

210. Siegal FP, Kadowaki N, Shodell M, Fitzgerald-Bocarsly PA, Shah K, Ho S, et al. The nature of the principal type 1 interferon-producing cells in human blood. Science. 1999 Jun 11;284(5421):1835–7.

211. Hardy GAD, Sieg S, Rodriguez B, Anthony D, Asaad R, Jiang W, et al. Interferon-α Is the Primary Plasma Type-I IFN in HIV-1 Infection and Correlates with Immune Activation and Disease Markers. Gray CM, editor. PLoS One. 2013 Feb 20;8(2):e56527.

212. Hosmalin A, Lebon P. Type I interferon production in HIV-infected patients. Journal of Leukocyte Biology. Society for Leukocyte Biology; 2006 Nov;80(5):984–93.

213. Sydow von M, Sönnerborg A, Gaines H, Strannegård O. Interferon-alpha and tumor necrosis factor-alpha in serum of patients in various stages of HIV-1 infection. AIDS Res Hum Retroviruses. 1991 Apr;7(4):375–80.

214. Bosinger SE, Hosiawa KA, Cameron MJ, Persad D, Ran L, Xu L, et al. Gene expression profiling of host response in models of acute HIV infection. J Immunol. 2004 Dec 1;173(11):6858–63.

215. Ranganath N, Sandstrom TS, Fadel S, Côté SC, Angel JB. Type I interferon responses are impaired in latently HIV infected cells. Retrovirology. 2016 Sep 9;13(1):66.

216. Paludan SR, Bowie AG. Immune Sensing of DNA. Immunity. 2013 May;38(5):870–80.

217. Marié I, Smith E, Prakash A, Levy DE. Phosphorylation-induced dimerization of interferon regulatory factor 7 unmasks DNA binding and a bipartite transactivation domain. Molecular and Cellular Biology. 2000 Dec;20(23):8803–14.

218. Sato M, Suemori H, Hata N, Asagiri M, Ogasawara K, Nakao K, et al. Distinct and essential roles of transcription factors IRF-3 and IRF-7 in response to viruses for IFN-alpha/beta gene induction. Immunity. 2000 Oct;13(4):539–48.

219. Alexopoulou L, Holt AC, Medzhitov R, Flavell RA. Recognition of double-stranded RNA and activation of NF-κB by Toll-like receptor 3. Nature. 2001;413(6857):732–8.

220. Heil F, Hemmi H, Hochrein H, Ampenberger F, Kirschning C, Akira S, et al. Species-specific recognition of single-stranded RNA via toll-like receptor 7 and 8. Science. American Association for the Advancement of Science; 2004 Mar 5;303(5663):1526–9.

221. Hemmi H, Takeuchi O, Kawai T, Kaisho T, Sato S, Sanjo H, et al. A Toll-like receptor recognizes bacterial DNA. Nature. 2000 Dec 7;408(6813):740–5.

222. Martinelli E, Cicala C, Van Ryk D, Goode DJ, Macleod K, Arthos J, et al. HIV-1 gp120 inhibits TLR9-mediated activation and IFN-alpha secretion in plasmacytoid dendritic cells. Proc Natl Acad Sci U S A. National Acad Sciences; 2007 Feb 27;104(9):3396–401.

223. Lo CC, Schwartz JA, Johnson DJ, Yu M, Aidarus N, Mujib S, et al. HIV Delays IFN-α Production from Human Plasmacytoid Dendritic Cells and Is Associated with SYK Phosphorylation. Norris PJ, editor. PLoS One. 2012 May 31;7(5):e37052–11.

224. Martinson JA, Roman-Gonzalez A, Tenorio AR, Montoya CJ, Gichinga CN, Rugeles MT, et al. Dendritic cells from HIV-1 infected individuals are less responsive to toll-like receptor (TLR) ligands. Cellular Immunology. 2007 Nov;250(1-2):75–84.

225. Sachdeva N, Asthana V, Brewer TH, Garcia D, Asthana D. Impaired Restoration of Plasmacytoid Dendritic Cells in HIV-1-Infected Patients with Poor CD4 T Cell Reconstitution Is Associated with Decrease in Capacity to

Produce IFN-α but Not Proinflammatory Cytokines. J Immunol. 2008 Aug 6;181(4):2887–97.

226. Kaushik S, Teque F, Patel M, Fujimura SH, Schmidt B, Levy JA. Plasmacytoid Dendritic Cell Number and Responses to Toll-Like Receptor 7 and 9 Agonists Vary in HIV Type 1-Infected Individuals in Relation to Clinical State. AIDS Res Hum Retroviruses. 2013 Mar;29(3):501–10.

227. Hornung V, Ellegast J, Kim S, Brzózka K, Jung A, Kato H, et al. 5'-Triphosphate RNA is the ligand for RIG-I. Science. 2006 Nov 10;314(5801):994–7.

228. Kato H, Takeuchi O, Mikamo-Satoh E, Hirai R, Kawai T, Matsushita K, et al. Length-dependent recognition of double-stranded ribonucleic acids by retinoic acid–inducible gene-I and melanoma differentiation–associated gene 5. J Exp Med. 2008 Jul 7;205(7):1601–10.

229. Berg RK, Melchjorsen J, Rintahaka J, Diget E, Søby S, Horan KA, et al. Genomic HIV RNA induces innate immune responses through RIG-I-dependent sensing of secondary-structured RNA. Sommer P, editor. PLoS One. Public Library of Science; 2012;7(1):e29291.

230. Collins SE, Noyce RS, Mossman KL. Innate cellular response to virus particle entry requires IRF3 but not virus replication. J Virol. 2004 Feb;78(4):1706–17.

231. Honda K, Yanai H, Negishi H, Asagiri M, Sato M, Mizutani T, et al. IRF-7 is the master regulator of type-I interferon-dependent immune responses. Nature. 2005 Apr 7;434(7034):772–7.

232. Yoneyama M, Suhara W, Fukuhara Y, Fukuda M, Nishida E, Fujita T. Direct triggering of the type I interferon system by virus infection: activation of a transcription factor complex containing IRF-3 and CBP/p300. EMBO J. EMBO Press; 1998 Feb 16;17(4):1087–95.

233. Satoh T, Kato H, Kumagai Y, Yoneyama M, Sato S, Matsushita K, et al. LGP2 is a positive regulator of RIG-I- and MDA5-mediated antiviral responses. Proc Natl Acad Sci U S A. 2010 Jan 26;107(4):1512–7.

234. Solis M, Solis M, Nakhaei P, Nakhaei P, Jalalirad M, Jalalirad M, et al. RIG-I-mediated antiviral signaling is inhibited in HIV-1 infection by a protease-mediated sequestration of RIG-I. J Virol. 2011 Feb;85(3):1224–36.

235. Nissen SK, Højen JF, Andersen KLD, Kofod-Olsen E, Berg RK, Paludan SR, et al. Innate DNA sensing is impaired in HIV patients and IFI16 expression correlates with chronic immune activation. Clin Exp Immunol. 2014 Jun 9;177(1):295–309.

236. Iwasaki A. Innate Immune Recognition of HIV-1. Immunity. 2012 Sep;37(3):389–98.

237. Unterholzner L, Keating SE, Baran M, Horan KA, Jensen SB, Sharma S, et al. IFI16 is an innate immune sensor for intracellular DNA. Nat Immunol. 2010 Oct 3;11(11):997–1004.

238. Lahaye X, Satoh T, Gentili M, Cerboni S, Conrad C, Hurbain I, et al. The capsids of HIV-1 and HIV-2 determine immune detection of the viral cDNA by the innate sensor cGAS in dendritic cells. Immunity. 2013 Dec 12;39(6):1132–42.

239. Yan N, Regalado-Magdos AD, Stiggelbout B, Lee-Kirsch MA, Lieberman J. The cytosolic exonuclease TREX1 inhibits the innate immune response to human immunodeficiency virus type 1. Nat Immunol. 2010 Sep 26;11(11):1005–13.

240. Wheeler LA, Trifonova RT, Vrbanac V, Barteneva NS, Liu X, Bollman B, et al. TREX1 Knockdown Induces an Interferon Response to HIV that Delays Viral Infection in Humanized Mice. Cell Reports. 2016 May;15(8):1715–27.

241. Vermeire J, Roesch F, Sauter D, Rua R, Hotter D, Van Nuffel A, et al. HIV Triggers a cGAS-Dependent, Vpu- and Vpr-Regulated Type I Interferon Response in CD4+ T Cells. Cell Reports. ElsevierCompany; 2016 Oct 4;17(2):413–24.

242. Hou F, Sun L, Zheng H, Skaug B, Jiang Q-X, Chen ZJ. MAVS forms functional prion-like aggregates to activate and propagate antiviral innate immune response. Cell. 2011 Aug 5;146(3):448–61.

243. Paz S, Vilasco M, Werden SJ, Arguello M, Joseph-Pillai D, Zhao T, et al. A functional C-terminal TRAF3-binding site in MAVS participates in positive and negative regulation of the IFN antiviral response. Nat Rev Cancer. 2011 Jun;21(6):895–910.

244. Sanchez DJ, Miranda D, Marsden MD, Dizon TMA, Bontemps JR, Davila SJ, et al. Disruption of Type I Interferon Induction by HIV Infection of T Cells. Nevels M, editor. PLoS One. 2015 Sep 16;10(9):e0137951–17.

245. Sirois M, Robitaille L, Allary R, Shah M, Woelk CH, Estaquier J, et al. TRAF6 and IRF7 control HIV replication in macrophages. PLoS One. 2011;6(11):e28125–.

246. Cao Z, Xiong J, Takeuchi M, Kurama T, Goeddel DV. TRAF6 is a signal transducer for interleukin-1. Nature. 1996 Oct;383(6):443–6.

247. Häcker H, Redecke V, Blagoev B, Kratchmarova I, Hsu L-C, Wang GG, et al. Specificity in Toll-like receptor signalling through distinct effector functions of TRAF3 and TRAF6. Nature. 2006 Jan 12;439(7073):204–7.

248. Harman AN, Harman AN, Nasr N, Nasr N, Feetham A, Feetham A, et al. HIV Blocks Interferon Induction in Human Dendritic Cells and Macrophages by Dysregulation of TBK1. J Virol. 2015 Jul;89(13):6575–84.

249. Pomerantz JL, Baltimore D. NF-kappaB activation by a signaling complex containing TRAF2, TANK and TBK1, a novel IKK-related kinase. EMBO J. 1999 Dec 1;18(23):6694–704.

250. Fitzgerald KA, McWhirter SM, Faia KL, Rowe DC, Latz E, Golenbock DT, et al. IKKepsilon and TBK1 are essential components of the IRF3 signaling pathway. Nat Immunol. 2003 May;4(5):491–6.

251. Sharma S, tenOever BR, Grandvaux N, Zhou G-P, Lin R, Hiscott J. Triggering the interferon antiviral response through an IKK-related pathway. Science. 2003 May 16;300(5622):1148–51.

252. Pathak S, De Souza GA, Salte T, Wiker HG, Åsjö B. HIV induces both a down-regulation of IRAK-4 that impairs TLR signalling and an up-regulation of the antibiotic peptide dermcidin in monocytic cells. Scand J Immunol. 2009 Sep;70(3):264–76.

253. Jensen LE, Whitehead AS. IRAK1b, a novel alternative splice variant of interleukin-1 receptor-associated kinase (IRAK), mediates interleukin-1 signaling and has prolonged stability. J Biol Chem. American Society for Biochemistry and Molecular Biology; 2001 Aug 3;276(31):29037–44.

254. Koziczak-Holbro M, Joyce C, Glück A, Kinzel B, Müller M, Tschopp C, et al. IRAK-4 kinase activity is required for interleukin-1 (IL-1) receptor- and toll-like receptor 7-mediated signaling and gene expression. J Biol Chem. American Society for Biochemistry and Molecular Biology; 2007 May 4;282(18):13552–60.

255. Li S, Strelow A, Fontana EJ, Wesche H. IRAK-4: a novel member of the IRAK family with the properties of an IRAK-kinase. Proc Natl Acad Sci U S A. National Acad Sciences; 2002 Apr 16;99(8):5567–72.

256. Dhamija N, Choudhary D, Ladha JS, Pillai B, Mitra D. Tat predominantly associates with host promoter elements in HIV-1-infected T-cells - regulatory basis of transcriptional repression of c-Rel. FEBS J. 2015 Feb;282(3):595–610.

257. Lin R, Heylbroeck C, Pitha PM, Hiscott J. Virus-dependent phosphorylation of the IRF-3 transcription factor regulates nuclear translocation,

transactivation potential, and proteasome-mediated degradation. Molecular and Cellular Biology. 1998 May;18(5):2986–96.

258. Wathelet MG, Lin CH, Parekh BS, Ronco LV, Howley PM, Maniatis T. Virus infection induces the assembly of coordinately activated transcription factors on the IFN-beta enhancer in vivo. Molecular Cell. 1998 Mar;1(4):507–18.

259. Izaguirre A, Barnes BJ, Amrute S, Yeow W-S, Megjugorac N, Dai J, et al. Comparative analysis of IRF and IFN-alpha expression in human plasmacytoid and monocyte-derived dendritic cells. Journal of Leukocyte Biology. Society for Leukocyte Biology; 2003 Dec;74(6):1125–38.

260. Kerkmann M, Rothenfusser S, Hornung V, Towarowski A, Wagner M, Sarris A, et al. Activation with CpG-A and CpG-B Oligonucleotides Reveals Two Distinct Regulatory Pathways of Type I IFN Synthesis in Human Plasmacytoid Dendritic Cells. J Immunol. 2003 May 1;170(9):4465–74.

261. Kawai T, Sato S, Ishii KJ, Coban C, Hemmi H, Yamamoto M, et al. Interferon-alpha induction through Toll-like receptors involves a direct interaction of IRF7 with MyD88 and TRAF6. Nat Immunol. 2004 Oct;5(10):1061–8.

262. Chehimi J, Papasavvas E, Tomescu C, Gekonge B, Abdulhaqq S, Raymond A, et al. Inability of plasmacytoid dendritic cells to directly lyse HIV-infected autologous CD4+ T cells despite induction of tumor necrosis factor-related apoptosis-inducing ligand. J Virol. 2010 Mar;84(6):2762–73.

263. Geng W, Li S. Decreased IRF7 Expression Contributes to Deficient IFN-α Production of Plasmacytoid Dendritic Cells in Chronic HIV-1 Infected Men who have Sex with Men. J AIDS Clin Res. OMICS International; 2016;07(02).

264. Doehle BP, Hladik F, McNevin JP, McElrath MJ, Gale M. Human Immunodeficiency Virus Type 1 Mediates Global Disruption of Innate Antiviral Signaling and Immune Defenses within Infected Cells. J Virol. 2009 Sep 23;83(20):10395–405.

265. Okumura A, Alce T, Lubyova B, Ezelle H, Strebel K, Pitha PM. HIV-1 accessory proteins VPR and Vif modulate antiviral response by targeting IRF-3 for degradation. Virology. 2008 Mar 30;373(1):85–97.

266. Doehle BP, Chang K, Fleming L, McNevin J, Hladik F, McElrath MJ, et al. Vpu-deficient HIV strains stimulate innate immune signaling responses in target cells. J Virol. American Society for Microbiology; 2012 Aug;86(16):8499–506.

267. Hotter D, Kirchhoff F, Sauter D. HIV-1 Vpu does not degrade interferon regulatory factor 3. J Virol. American Society for Microbiology; 2013 Jun;87(12):7160–5.

268. Manganaro L, de Castro E, Maestre AM, Olivieri K, García-Sastre A, Fernandez-Sesma A, et al. HIV Vpu interferes with NF-κB activity but not with Interferon Regulatory Factor 3. J Virol. American Society for Microbiology; 2015 Jul 15;:JVI.01596–15.

269. Lau AS, Read SE, Williams BR. Downregulation of interferon alpha but not gamma receptor expression in vivo in the acquired immunodeficiency syndrome. Journal of Clinical Investigation. American Society for Clinical Investigation; 1988 Oct 1;82(4):1415–21.

270. Hardy GAD, Sieg SF, Rodriguez B, Jiang W, Asaad R, Lederman MM, et al. Desensitization to type I interferon in HIV-1 infection correlates with markers of immune activation and disease progression. Blood. American Society of Hematology; 2009 May 28;113(22):5497–505.

271. Yadav A, Fitzgerald P, Sajadi MM, Gilliam B, Lafferty MK, Redfield R, et al. Increased expression of suppressor of cytokine signaling-1 (SOCS-1): A mechanism for dysregulated T helper-1 responses in HIV-1 disease. Virology. 2009 Mar 1;385(1):126–33.

272. Akhtar LN, Qin H, Muldowney MT, Yanagisawa LL, Kutsch O, Clements JE, et al. Suppressor of cytokine signaling 3 inhibits antiviral IFN-beta signaling to enhance HIV-1 replication in macrophages. The Journal of Immunology. 2010 Aug 15;185(4):2393–404.

273. Song MM, Shuai K. The suppressor of cytokine signaling (SOCS) 1 and SOCS3 but not SOCS2 proteins inhibit interferon-mediated antiviral and antiproliferative activities. J Biol Chem. 1998 Dec 25;273(52):35056–62.

274. Reddy K, Winkler CA, Werner L, Mlisana K, Abdool Karim SS, Ndung'u T, et al. APOBEC3G expression is dysregulated in primary HIV-1 infection and polymorphic variants influence CD4+ T-cell counts and plasma viral load. AIDS. 2010 Jan 16;24(2):195–204.

275. Wie S-H, Wie S-H, Du P, Du P, Luong TQ, Luong TQ, et al. HIV downregulates interferon-stimulated genes in primary macrophages. J Interferon Cytokine Res. 2013 Feb;33(2):90–5.

276. Caldwell RL, Egan BS, Shepherd VL. HIV-1 Tat Represses Transcription from the Mannose Receptor Promoter. J Immunol. 2000 Dec 15;165(12):7035–41.

277. Howcroft TK, Palmer LA, Brown J, Rellahan B, Kashanchi F, Brady JN, et al. HIV Tat represses transcription through Sp1-like elements in the basal promoter. Immunity. 1995 Jul;3(1):127–38.

278. Howcroft TK, Strebel K, Martin MA, Singer DS. Repression of MHC class I gene promoter activity by two-exon Tat of HIV. Science. 1993 May 28;260(5112):1320–2.

279. Weissman JD, Brown JA, Howcroft TK, Hwang J, Chawla A, Roche PA, et al. HIV-1 Tat binds TAFII250 and represses TAFII250-dependent transcription of major histocompatibility class I genes. Proc Natl Acad Sci U S A. National Acad Sciences; 1998 Sep 28;95(20):11601–6.

280. Sauter D, Hotter D, Van Driessche B, Stürzel CM, Kluge SF, Wildum S, et al. Differential regulation of NF-κB-mediated proviral and antiviral host gene expression by primate lentiviral Nef and Vpu proteins. Cell Reports. 2015 Feb 3;10(4):586–99.

281. Gabuzda DH, Lawrence K, Langhoff E, Terwilliger E, Dorfman T, Haseltine WA, et al. Role of vif in replication of human immunodeficiency virus type 1 in CD4+ T lymphocytes. J Virol. 1992 Nov;66(11):6489–95.

282. Gillick K, Pollpeter D, Phalora P, Kim E-Y, Wolinsky SM, Malim MH. Suppression of HIV-1 infection by APOBEC3 proteins in primary human CD4(+) T cells is associated with inhibition of processive reverse transcription as well as excessive cytidine deamination. J Virol. 2013 Feb;87(3):1508–17.

283. Cobos Jiménez V, Booiman T, de Taeye SW, van Dort KA, Rits MAN, Hamann J, et al. Differential expression of HIV-1 interfering factors in monocyte-derived macrophages stimulated with polarizing cytokines or interferons. Sci Rep. 2012;2(1):763.

284. Mohanram V, Sköld AE, Bächle SM, Pathak SK, Spetz A-L. IFN-α induces APOBEC3G, F, and A in immature dendritic cells and limits HIV-1 spread to CD4+ T cells. The Journal of Immunology. American Association of Immunologists; 2013 Apr 1;190(7):3346–53.

285. Sheehy AM, Gaddis NC, Malim MH. The antiretroviral enzyme APOBEC3G is degraded by the proteasome in response to HIV-1 Vif. Nat Med. 2003 Nov;9(11):1404–7.

286. Kao S, Khan MA, Miyagi E, Plishka R, Buckler-White A, Strebel K. The Human Immunodeficiency Virus Type 1 Vif Protein Reduces Intracellular Expression and Inhibits Packaging of APOBEC3G (CEM15), a Cellular Inhibitor of Virus Infectivity. J Virol. 2003 Oct 13;77(21):11398–407.

287. Marin M, Rose KM, Kozak SL, Kabat D. HIV-1 Vif protein binds the editing enzyme APOBEC3G and induces its degradation. Nat Med. 2003 Oct 5;9(11):1398–403.

288. Giese S, Marsh M. Tetherin can restrict cell-free and cell-cell transmission of HIV from primary macrophages to T cells. Aiken C, editor. PLoS Pathog. Public Library of Science; 2014 Jul;10(7):e1004189.

289. Apps R, del Prete GQ, Chatterjee P, Lara A, Brumme ZL, Brockman MA, et al. HIV-1 Vpu Mediates HLA-C Downregulation. Cell Host Microbe. 2016 May 11;19(5):686–95.

290. Brand SR, Kobayashi R, Mathews MB. The Tat protein of human immunodeficiency virus type 1 is a substrate and inhibitor of the interferon-induced, virally activated protein kinase, PKR. J Biol Chem. 1997 Mar 28;272(13):8388–95.

291. Cai R, Carpick B, Chun RF, Jeang K-T, Williams BRG. HIV-I TAT Inhibits PKR Activity by Both RNA-Dependent and RNA-Independent Mechanisms. Archives of Biochemistry and Biophysics. 2000 Jan;373(2):361–7.

292. McMillan NA, Chun RF, Siderovski DP, Galabru J, Toone WM, Samuel CE, et al. HIV-1 Tat directly interacts with the interferon-induced, double-stranded RNA-dependent kinase, PKR. Virology. 1995 Nov 10;213(2):413–24.

293. Lemaire PA, Anderson E, Lary J, Cole JL. Mechanism of PKR Activation by dsRNA. J Mol Biol. 2008 Aug 29;381(2):351–60.

294. Maitra RK, McMillan NA, Desai S, McSwiggen J, Hovanessian AG, Sen G, et al. HIV-1 TAR RNA has an intrinsic ability to activate interferon-inducible enzymes. Virology. Academic Press; 1994 Nov 1;204(2):823–7.

295. Clerzius G, Clerzius G, Shaw E, Shaw E, Daher A, Daher A, et al. The PKR activator, PACT, becomes a PKR inhibitor during HIV-1 replication. Retrovirology. 2013 Sep 11;10(1):96.

296. Sanghvi VR, Steel LF. The Cellular TAR RNA Binding Protein, TRBP, Promotes HIV-1 Replication Primarily by Inhibiting the Activation of Double-Stranded RNA-Dependent Kinase PKR. J Virol [Internet]. 2011 Oct 27;85(23):12614–21. Available from: http://www-ncbi-nlm-nih-gov.proxy1.lib.umanitoba.ca/pmc/articles/PMC3209364/pdf/zjv12614.pdf

297. Cribier A, Descours B, Valadão ALC, Laguette N, Benkirane M. Phosphorylation of SAMHD1 by Cyclin A2/CDK1 Regulates Its Restriction Activity toward HIV-1. Cell Reports. The Authors; 2013 Apr 25;3(4):1036–43.

298. White TE, Brandariz-Nunez A, Valle-Casuso JC, Amie S, Nguyen LA, Kim B, et al. The retroviral restriction ability of SAMHD1, but not its deoxynucleotide

triphosphohydrolase activity, is regulated by phosphorylation. Cell Host Microbe. 2013 Apr 17;13(4):441–51.

299. Fricke T, White TE, Schulte B, de Souza Aranha Vieira DA, Dharan A, Campbell EM, et al. MxB binds to the HIV-1 core and prevents the uncoating process of HIV-1. Retrovirology. 2014 Aug 14;11(1):68.

300. Wei W, Guo H, Ma M, Markham R, Yu X-F. Accumulation of MxB/Mx2-resistant HIV-1 Capsid Variants During Expansion of the HIV-1 Epidemic in Human Populations. EBioMedicine. 2016 Jun;8:230–6.

301. Stojdl DF, Stojdl DF, Lichty BD, Lichty BD, tenOever BR, tenOever BR, et al. VSV strains with defects in their ability to shutdown innate immunity are potent systemic anti-cancer agents. Cancer Cell. 2003 Oct;4(4):263–75.

302. Dock G. THE INFLUENCE OF COMPLICATING DISEASES UPON LEUKÆMIA.*. The American Journal of the Medical Sciences. 1904 Apr;127(4):563–92.

303. Bierman HR, Crile DM, Dod KS, Kelly KH, Petrakis NL, White LP, et al. Remissions in leukemia of childhood following acute infectious disease: staphylococcus and streptococcus, varicella, and feline panleukopenia. Cancer. 1953 May;6(3):591–605.

304. Moore AE. The destructive effect of the virus of Russian Far East encephalitis on the transplantable mouse sarcoma 180. Cancer. 1949 May;2(3):525–34.

305. Moore AE, O'Connor S. Further studies on the destructive effect of the virus of Russian Far East encephalitis on the transplantable mouse sarcoma 180. Cancer. 1950 Sep;3(5):886–90.

306. Moore AE. Inhibition of growth of five transplantable mouse tumors by the virus of Russian Far East encephalitis. Cancer. 1951 Mar;4(2):375–82.

307. Kelly E, Russell SJ, Russell SJ. History of oncolytic viruses: genesis to genetic engineering. Mol Ther. 2007 Apr;15(4):651–9.

308. Hoster HA, Zanes RP, Haam von E. Studies in Hodgkin“s syndrome; the association of viral hepatitis and Hodgkin”s disease; a preliminary report. Cancer Res. 1949 Aug;9(8):473–80.

309. Southam CM, Moore AE. Clinical studies of viruses as antineoplastic agents with particular reference to Egypt 101 virus. Cancer. 1952 Sep;5(5):1025–34.

310. Georgiades J, Zielinski T, Cicholska A, Jordan E. Research on the oncolytic effect of APC viruses in cancer of the cervix uteri; preliminary report. Biul Inst Med Morsk Gdansk. 1959;10:49–57.

311. Asada T. Treatment of human cancer with mumps virus. Cancer. 1974 Dec;34(6):1907–28.

312. Southam CM. Homotransplantation of human cell lines. Bull N Y Acad Med. 1958 Jun;34(6):416–23.

313. Lerner BH. Sins of omission--cancer research without informed consent. N Engl J Med. 2004 Aug 12;351(7):628–30.

314. Moore AE, Southam CM, Rhoads CP. Homotransplantation of Human Cell Lines. Science. 1957 Jan 25;125(3239):158–60.

315. Rampling R, Cruickshank G, Papanastassiou V, Nicoll J, Hadley D, Brennan D, et al. Toxicity evaluation of replication-competent herpes simplex virus (ICP 34.5 null mutant 1716) in patients with recurrent malignant glioma. Gene Ther. 2000 May;7(10):859–66.

316. Papanastassiou V, Rampling R, Fraser M, Petty R, Hadley D, Nicoll J, et al. The potential for efficacy of the modified (ICP 34.5(-)) herpes simplex virus HSV1716 following intratumoural injection into human malignant glioma: a proof of principle study. Gene Ther. 2002 Mar;9(6):398–406.

317. Garber K. China approves world's first oncolytic virus therapy for cancer treatment. Journal of the National Cancer Institute. 2006 Mar 1;:298–300.

318. Liang M. Oncorine, the World First Oncolytic Virus Medicine and its Update in China. Curr Cancer Drug Targets. 2018;18(2):171–6.

319. Pol J, Kroemer G, Galluzzi L. First oncolytic virus approved for melanoma immunotherapy. OncoImmunology. 2016;5(1):e1115641.

320. Lawler SE, Speranza M-C, Cho C-F, Chiocca EA. Oncolytic Viruses in Cancer Treatment: A Review. JAMA Oncol. American Medical Association; 2017 Jun 1;3(6):841–9.

321. Clemens MJ, McNurlan MA. Regulation of cell proliferation and differentiation by interferons. 1985 Mar 1;226(2):345–60.

322. Hertzog PJ, Hwang SY, Kola I. Role of interferons in the regulation of cell proliferation, differentiation, and development. Mol Reprod Dev. John Wiley & Sons, Ltd; 1994 Oct;39(2):226–32.

323. Colamonici OR, Domanski P, Platanias LC, Blood MD, 1992. Correlation between interferon (IFN) alpha resistance and deletion of the IFN alpha/beta genes in acute leukemia cell lines suggests selection against the IFN system. Blood. 1992 Aug 1;80(3):744–9.

324. Wong LH, Krauer KG, Hatzinisiriou I, Estcourt MJ, Hersey P, Tam ND, et al. Interferon-resistant human melanoma cells are deficient in ISGF3 components, STAT1, STAT2, and p48-ISGF3gamma. J Biol Chem. 1997 Nov 7;272(45):28779–85.

325. Matin SF, Rackley RR, Sadhukhan PC, Kim MS, Novick AC, Bandyopadhyay SK. Impaired alpha-interferon signaling in transitional cell carcinoma: lack of p48 expression in 5637 cells. Cancer Res. 2001 Mar 1;61(5):2261–6.

326. Tsuno T, Mejido J, Zhao T, Schmeisser H, Morrow A, Zoon KC. IRF9 is a key factor for eliciting the antiproliferative activity of IFN-alpha. J Immunother. 2009 Oct;32(8):803–16.

327. Zhang K-X, Matsui Y, Hadaschik BA, Lee C, Jia W, Bell JC, et al. Down-regulation of type I interferon receptor sensitizes bladder cancer cells to vesicular stomatitis virus-induced cell death. Int J Cancer. John Wiley & Sons, Ltd; 2010 Aug 15;127(4):830–8.

328. Lu R, Au WC, Yeow WS, Hageman N, Pitha PM. Regulation of the promoter activity of interferon regulatory factor-7 gene. Activation by interferon snd silencing by hypermethylation. J Biol Chem. American Society for Biochemistry and Molecular Biology; 2000 Oct 13;275(41):31805–12.

329. Li Q, Tainsky MA. Epigenetic silencing of IRF7 and/or IRF5 in lung cancer cells leads to increased sensitivity to oncolytic viruses. Katoh M, editor. PLoS One. Public Library of Science; 2011;6(12):e28683.

330. Diaz MO, Ziemin S, Le Beau MM, Pitha P, Smith SD, Chilcote RR, et al. Homozygous deletion of the alpha- and beta 1-interferon genes in human leukemia and derived cell lines. Proc Natl Acad Sci U S A. 1988 Jul;85(14):5259–63.

331. Carpten J, Nupponen N, Isaacs S, Sood R, Robbins C, Xu J, et al. Germline mutations in the ribonuclease L gene in families showing linkage with HPC1. Nat Genet. 2002 Feb;30(2):181–4.

332. Dhar D, Spencer JF, Toth K, Wold WSM. Effect of preexisting immunity on oncolytic adenovirus vector INGN 007 antitumor efficacy in immunocompetent and immunosuppressed Syrian hamsters. J Virol. 2009 Mar;83(5):2130–9.

333. Schulick AH, Vassalli G, Dunn PF, Dong G, Rade JJ, Zamarron C, et al. Established immunity precludes adenovirus-mediated gene transfer in rat carotid arteries. Potential for immunosuppression and vector engineering to overcome barriers of immunity. J Clin Invest. 1997 Jan 15;99(2):209–19.

334. Thomas MA, Spencer JF, Toth K, Sagartz JE, Phillips NJ, Wold WSM. Immunosuppression enhances oncolytic adenovirus replication and antitumor efficacy in the Syrian hamster model. Mol Ther. 2008 Oct;16(10):1665–73.

335. Johnson KM, Vogel JE, Peralta PH. Clinical and serological response to laboratory-acquired human infection by Indiana type vesicular stomatitis virus (VSV). 1966 Mar;15(2):244–6.

336. Fields BN, Hawkins K. Human infection with the virus of vesicular stomatitis during an epizootic. N Engl J Med. 1967 Nov 9;277(19):989–94.

337. Travassos da Rosa AP, Tesh RB, Travassos da Rosa JF, Herve JP, Main AJ. Carajas and Maraba viruses, two new vesiculoviruses isolated from phlebotomine sand flies in Brazil. 1984 Sep;33(5):999–1006.

338. Stojdl DF, Lichty B, Knowles S, Marius R, Atkins H, Sonenberg N, et al. Exploiting tumor-specific defects in the interferon pathway with a previously unknown oncolytic virus. Nat Med. 2000 Jul;6(7):821–5.

339. Balachandran S, Barber GN. Vesicular stomatitis virus (VSV) therapy of tumors. IUBMB Life. 2000 Aug;50(2):135–8.

340. Ferran MC, Lucas-Lenard JM. The vesicular stomatitis virus matrix protein inhibits transcription from the human beta interferon promoter. J Virol. 1997 Jan;71(1):371–7.

341. Black BL, Lyles DS. Vesicular stomatitis virus matrix protein inhibits host cell-directed transcription of target genes in vivo. J Virol. 1992 Jul;66(7):4058–64.

342. Kobbe C von, van Deursen JM, Rodrigues JP, Sitterlin D, Bachi A, Wu X, et al. Vesicular stomatitis virus matrix protein inhibits host cell gene expression by targeting the nucleoporin Nup98. Mol Cell. 2000 Nov;6(5):1243–52.

343. Petersen JM, Her LS, Varvel V, Lund E, Dahlberg JE. The matrix protein of vesicular stomatitis virus inhibits nucleocytoplasmic transport when it is in the nucleus and associated with nuclear pore complexes. Molecular and Cellular Biology. American Society for Microbiology (ASM); 2000 Nov;20(22):8590–601.

344. Ahmed M, McKenzie MO, Puckett S, Hojnacki M, Poliquin L, Lyles DS. Ability of the matrix protein of vesicular stomatitis virus to suppress beta interferon gene expression is genetically correlated with the inhibition of host RNA and protein synthesis. J Virol. 2003 Apr;77(8):4646–57.

345. Lichty BD, Power AT, Stojdl DF, Bell JC. Vesicular stomatitis virus: re-inventing the bullet. Trends Mol Med. 2004 May;10(5):210–6.

346. Brun J, Brun J, McManus D, McManus D, Lefebvre C, Lefebvre C, et al. Identification of genetically modified Maraba virus as an oncolytic rhabdovirus. Mol Ther. 2010 Aug;18(8):1440–9.

347. Pol JG, Acuna SA, Yadollahi B, Tang N, Stephenson KB, Atherton MJ, et al. Preclinical evaluation of a MAGE-A3 vaccination utilizing the oncolytic Maraba virus currently in first-in-human trials. OncoImmunology. 2018 Oct 29;8(1):e1512329.

348. Clouse KA, Powell D, Washington I, Poli G, Strebel K, Farrar W, et al. Monokine regulation of human immunodeficiency virus-1 expression in a chronically infected human T cell clone. J Immunol. 1989 Jan 15;142(2):431–8.

349. Folks TM, Clouse KA, Justement J, Rabson A, Duh E, Kehrl JH, et al. Tumor necrosis factor alpha induces expression of human immunodeficiency virus in a chronically infected T-cell clone. Proc Natl Acad Sci U S A. 1989 Apr;86(7):2365–8.

350. Costiniuk CT, Salahuddin S, Farnos O, Olivenstein R, Pagliuzza A, Orlova M, et al. HIV persistence in mucosal CD4+ T-cells within the lungs of adults receiving long-term suppressive antiretroviral therapy. AIDS. 2018 Aug 14;:1.

351. Adachi A, Gendelman HE, Koenig S, Folks T, Willey R, Rabson A, et al. Production of acquired immunodeficiency syndrome-associated retrovirus in human and nonhuman cells transfected with an infectious molecular clone. J Virol. American Society for Microbiology (ASM); 1986 Aug;59(2):284–91.

352. Baer A, Kehn-Hall K. Viral concentration determination through plaque assays: using traditional and novel overlay systems. J Vis Exp. 2014 Nov 4;(93):e52065.

353. Zhang J, Tai L-H, Ilkow CS, Alkayyal AA, Ananth AA, de Souza CT, et al. Maraba MG1 virus enhances natural killer cell function via conventional dendritic cells to reduce postoperative metastatic disease. Mol Ther. 2014 Jul;22(7):1320–32.

354. Ranganath N, Sandstrom TS, Burke Schinkel SC, Côté SC, Angel JB. The Oncolytic Virus MG1 Targets and Eliminates Cells Latently Infected With HIV-1: Implications for an HIV Cure. J Infect Dis. 2018 Feb 14;217(5):721–30.

355. Saleh S, Solomon A, Wightman F, Xhilaga M, Cameron PU, Lewin SR. CCR7 ligands CCL19 and CCL21 increase permissiveness of resting memory CD4+ T cells to HIV-1 infection: a novel model of HIV-1 latency. Blood. American Society of Hematology; 2007 Dec 15;110(13):4161–4.

356. Vandergeeten C, Fromentin R, Merlini E, Lawani MB, DaFonseca S, Bakeman W, et al. Cross-clade ultrasensitive PCR-based assays to measure HIV persistence in large-cohort studies. J Virol. 2014 Nov;88(21):12385–96.

357. Imbeault M, Lodge R, Ouellet M, Tremblay MJ. Efficient magnetic bead-based separation of HIV-1-infected cells using an improved reporter virus system reveals that p53 up-regulation occurs exclusively in the virus-expressing cell population. Virology. 2009 Oct 10;393(1):160–7.

358. Deshiere A, Joly-Beauparlant C, Breton Y, Ouellet M, Raymond F, Lodge R, et al. Global Mapping of the Macrophage-HIV-1 Transcriptome Reveals that Productive Infection Induces Remodeling of Host Cell DNA and Chromatin. Sci Rep. 2017 Jul 12;7(1):5238.

359. Chomont N, El-Far M, Ancuta P, Trautmann L, Procopio FA, Yassine-Diab B, et al. HIV reservoir size and persistence are driven by T cell survival and homeostatic proliferation. Nat Med. 2009 Aug;15(8):893–900.

360. Sandstrom TS, Ranganath N, Angel JB. Impairment of the type I interferon response by HIV-1: Potential targets for HIV eradication. Cytokine and Growth Factor Reviews. 2017 Oct;37:1–16.

361. Chun TW, Carruth L, Finzi D, Shen X, DiGiuseppe JA, Taylor H, et al. Quantification of latent tissue reservoirs and total body viral load in HIV-1 infection. Nature. Nature Publishing Group; 1997 May 8;387(6629):183–8.

362. Vandergeeten C, Fromentin R, DaFonseca S, Lawani MB, Sereti I, Lederman MM, et al. Interleukin-7 promotes HIV persistence during antiretroviral therapy. Blood. 2013 May 23;121(21):4321–9.

363. Power D, Santoso N, Dieringer M, Yu J, Huang H, Simpson S, et al. IFI44 suppresses HIV-1 LTR promoter activity and facilitates its latency. Virology. Elsevier; 2015 Jul 1;481(C):142–50.

364. Yang F-C, Kuang W-D, Li C, Sun W-W, Qu D, Wang J-H. Toll-Interacting Protein Suppresses HIV-1 Long-Terminal-Repeat-Driven Gene Expression and Silences the Post-Integrational Transcription of Viral Proviral DNA. Kashanchi F, editor. PLoS One. 2015 Apr 27;10(4):e0125563.

365. Kaczmarek Michaels K, Natarajan M, Euler Z, Alter G, Viglianti G, Henderson AJ. Blimp-1, an Intrinsic Factor that Represses HIV-1 Proviral Transcription in Memory CD4+ T Cells. The Journal of Immunology. 2015 Mar 20;194(7):3267–74.

366. Lusic M, Giacca M. Regulation of HIV-1 Latency by Chromatin Structure and Nuclear Architecture. J Mol Biol. 2014 Jul.

367. Conrad RJ, Fozouni P, Thomas S, Sy H, Zhang Q, Zhou M-M, et al. The Short Isoform of BRD4 Promotes HIV-1 Latency by Engaging Repressive SWI/SNF Chromatin-Remodeling Complexes. Molecular Cell. 2017 Sep 21;67(6):1001–6.

368. Pace MJ, Agosto L, Graf EH, O'Doherty U. HIV reservoirs and latency models. Virology. 2011 Mar 15;411(2):344–54.

369. Zamborlini A, Lehmann-Che J, Clave E, Giron M-L, Tobaly-Tapiero J, Roingeard P, et al. Centrosomal pre-integration latency of HIV-1 in quiescent cells. Retrovirology. 2007 Sep 10;4(1):63.

370. Hamid FB, Kim J, Shin C-G. Distribution and fate of HIV-1 unintegrated DNA species: a comprehensive update. AIDS Res Ther. BioMed Central; 2017 Feb 16;14(1):9.

371. Lassen KG, Ramyar KX, Bailey JR, Zhou Y, Siliciano RF. Nuclear retention of multiply spliced HIV-1 RNA in resting CD4+ T cells. PLoS Pathog. Public Library of Science; 2006 Jul;2(7):e68.

372. Van Lint C, Bouchat S, Marcello A. HIV-1 transcription and latency: an update. Retrovirology. Retrovirology; 2013 Jun 26;10(1):1–1.

373. Imamichi H, Dewar RL, Adelsberger JW, Rehm CA, O'Doherty U, Paxinos EE, et al. Defective HIV-1 proviruses produce novel protein-coding RNA species in HIV-infected patients on combination antiretroviral therapy. Proc Natl Acad Sci U S A. 2016 Aug 2;113(31):8783–8.

374. Whitney JB, Hill AL, Sanisetty S, Penaloza-MacMaster P, Liu J, Shetty M, et al. Rapid seeding of the viral reservoir prior to SIV viraemia in rhesus monkeys. Nature. 2014 Aug 7;512(7512):74–7.

375. Persaud D, Gay H, Ziemniak C, Chen YH, Piatak M, Chun T-W, et al. Absence of detectable HIV-1 viremia after treatment cessation in an infant. N Engl J Med. 2013 Nov 7;369(19):1828–35.

376. Luzuriaga K, Gay H, Ziemniak C, Sanborn KB, Somasundaran M, Rainwater-Lovett K, et al. Viremic relapse after HIV-1 remission in a perinatally infected child. N Engl J Med. 2015 Feb 19;372(8):786–8.

377. Martínez-Bonet M, Puertas MC, Fortuny C, Ouchi D, Mellado MJ, Rojo P, et al. Establishment and Replenishment of the Viral Reservoir in Perinatally HIV-1-infected Children Initiating Very Early Antiretroviral Therapy. Clin Infect Dis. 2015 Oct 1;61(7):1169–78.

378. Meyerhans A, Vartanian JP, Hultgren C, Plikat U, Karlsson A, Wang L, et al. Restriction and enhancement of human immunodeficiency virus type 1

replication by modulation of intracellular deoxynucleoside triphosphate pools. J Virol. 1994 Jan;68(1):535–40.

379. Baldauf H-M, Pan X, Erikson E, Schmidt S, Daddacha W, Burggraf M, et al. SAMHD1 restricts HIV-1 infection in resting CD4(+) T cells. Nat Med. 2012 Nov;18(11):1682–7.

380. Descours B, Cribier A, Chable-Bessia C, Ayinde D, Rice G, Crow Y, et al. SAMHD1 restricts HIV-1 reverse transcription in quiescent CD4(+) T-cells. Retrovirology. 2012 Oct 23;9(1):87.

381. Donahue DA, Wainberg MA. Cellular and molecular mechanisms involved in the establishment of HIV-1 latency. Retrovirology. 2013;10:11.

382. Swiggard WJ, Baytop C, Yu JJ, Dai J, Li C, Schretzenmair R, et al. Human immunodeficiency virus type 1 can establish latent infection in resting CD4+ T cells in the absence of activating stimuli. J Virol. 2005 Nov 1;79(22):14179–88.

383. Agosto LM, Yu JJ, Dai J, Kaletsky R, Monie D, O'Doherty U. HIV-1 integrates into resting CD4+ T cells even at low inoculums as demonstrated with an improved assay for HIV-1 integration. Virology. 2007 Nov 10;368(1):60–72.

384. Cameron PU, Saleh S, Sallmann G, Solomon A, Wightman F, Evans VA, et al. Establishment of HIV-1 latency in resting CD4+ T cells depends on chemokine-induced changes in the actin cytoskeleton. Proc Natl Acad Sci U S A. 2010 Sep 28;107(39):16934–9.

385. Shan L, Deng K, Gao H, Xing S, Capoferri AA, Durand CM, et al. Transcriptional Reprogramming during Effector-to-Memory Transition Renders CD4+ T Cells Permissive for Latent HIV-1 Infection. Immunity. 2017 Oct 17;47(4):766–775.e3.

386. Iglesias-Ussel M, Vandergeeten C, Marchionni L, Chomont N, Romerio F. High Levels of CD2 Expression Identify HIV-1 Latently Infected Resting Memory CD4+ T Cells in Virally Suppressed Subjects. J Virol. 2013 Jul 26;87(16):9148–58.

387. Descours B, Petitjean G, López-Zaragoza J-L, Bruel T, Raffel R, Psomas C, et al. CD32a is a marker of a CD4 T-cell HIV reservoir harbouring replication-competent proviruses. Nat Rev Cancer. 2017 Mar 23;543(7646):564–7.

388. Fromentin R, Bakeman W, Lawani MB, Khoury G, Hartogensis W, DaFonseca S, et al. CD4+ T Cells Expressing PD-1, TIGIT and LAG-3 Contribute to HIV Persistence during ART. Douek DC, editor. PLoS Pathog. 2016 Jul;12(7):e1005761.

389. Gosselin A, Wiche Salinas TR, Planas D, Wacleche VS, Zhang Y, Fromentin R, et al. HIV persists in CCR6+CD4+ T cells from colon and blood during antiretroviral therapy. AIDS. 2017 Jan 2;31(1):35–48.

390. Chun TW, Carruth L, Finzi D, Shen X. Quantification of latent tissue reservoirs and total body viral load in HIV-1 infection. Nature. 1997;387(6629):183–8.

391. Pantaleo G, Graziosi C, Butini L, Pizzo PA, Schnittman SM, Kotler DP, et al. Lymphoid organs function as major reservoirs for human immunodeficiency virus. Proc Natl Acad Sci U S A. National Academy of Sciences; 1991 Nov 1;88(21):9838–42.

392. Pantaleo G, Graziosi C, Demarest JF, Butini L, Montroni M, Fox CH, et al. HIV infection is active and progressive in lymphoid tissue during the clinically latent stage of disease. Nature. Nature Publishing Group; 1993 Mar 25;362(6418):355–8.

393. Perreau M, Savoye A-L, De Crignis E, Corpataux J-M, Cubas R, Haddad EK, et al. Follicular helper T cells serve as the major CD4 T cell compartment for HIV-1 infection, replication, and production. Journal of Experimental Medicine. 2013 Jan 14;210(1):143–56.

394. Banga R, Procopio FA, Noto A, Pollakis G, Cavassini M, Ohmiti K, et al. PD-1(+) and follicular helper T cells are responsible for persistent HIV-1 transcription in treated aviremic individuals. Nat Med. 2016 Jul;22(7):754–61.

395. Khoury G, Fromentin R, Solomon A, Hartogensis W, Killian M, Hoh R, et al. Human Immunodeficiency Virus Persistence and T-Cell Activation in Blood, Rectal, and Lymph Node Tissue in Human Immunodeficiency Virus-Infected Individuals Receiving Suppressive Antiretroviral Therapy. J Infect Dis. 2017 Mar 15;215(6):911–9.

396. Evans VA, Kumar N, Filali A, Procopio FA, Yegorov O, Goulet J-P, et al. Myeloid dendritic cells induce HIV-1 latency in non-proliferating CD4+ T cells. PLoS Pathog. Public Library of Science; 2013;9(12):e1003799.

397. Okumura A, Lu G, Pitha-Rowe I, Pitha PM. Innate antiviral response targets HIV-1 release by the induction of ubiquitin-like protein ISG15. Proc Natl Acad Sci U S A. 2006 Jan 31;103(5):1440–5.

398. Berg RK, Rahbek SH, Kofod-Olsen E, Holm CK, Melchjorsen J, Jensen DG, et al. T cells detect intracellular DNA but fail to induce type I IFN responses: implications for restriction of HIV replication. Wu Y, editor. PLoS One. Public Library of Science; 2014;9(1):e84513.

399. Hara T. Human T cell activation. III. Rapid induction of a phosphorylated 28 kD/32 kD disulfide-linked early activation antigen (EA 1) by 12-o-

tetradecanoyl phorbol-13-acetate, mitogens, and antigens. Journal of Experimental Medicine. 1986;164(6):1988–2005.

400. Rea IM, McNerlan SE, Alexander HD. CD69, CD25, and HLA-DR activation antigen expression on CD3+ lymphocytes and relationship to serum TNF-alpha, IFN-gamma, and sIL-2R levels in aging. Exp Gerontol. 1999 Jan;34(1):79–93.

401. Dai J, Agosto LM, Baytop C, Yu JJ, Pace MJ, Liszewski MK, et al. Human immunodeficiency virus integrates directly into naive resting CD4+ T cells but enters naive cells less efficiently than memory cells. J Virol. American Society for Microbiology; 2009 May;83(9):4528–37.

402. Ranganath N. Oncolytic viruses as a potential approach to eliminate cells that constitute the latent HIV reservoir. 2018 Mar 22;:1–254.

403. Lamken P, Lata S, Gavutis M, Piehler J. Ligand-induced assembling of the type I interferon receptor on supported lipid bilayers. J Mol Biol. 2004 Jul 30;341(1):303–18.

404. Severa M, Remoli ME, Giacomini E, Ragimbeau J, Lande R, Uze G, et al. Differential responsiveness to IFN-alpha and IFN-beta of human mature DC through modulation of IFNAR expression. Journal of Leukocyte Biology. Society for Leukocyte Biology; 2006 Jun;79(6):1286–94.

405. Lewerenz M, Mogensen KE, Uzé G. Shared receptor components but distinct complexes for alpha and beta interferons. J Mol Biol. 1998 Sep 25;282(3):585–99.

406. Kadowaki N, Antonenko S, Lau JY, Liu YJ. Natural interferon alpha/beta-producing cells link innate and adaptive immunity. J Exp Med. 2000 Jul 17;192(2):219–26.

407. Yonezawa A, Morita R, Takaori-Kondo A, Kadowaki N, Kitawaki T, Hori T, et al. Natural Alpha Interferon-Producing Cells Respond to Human Immunodeficiency Virus Type 1 with Alpha Interferon Production and Maturation into Dendritic Cells. J Virol. 2003 Mar 15;77(6):3777–84.

408. Wathelet MG, Clauss IM, Content J, Huez GA. Regulation of two interferon-inducible human genes by interferon, poly(rI).poly(rC) and viruses. European Journal of Biochemistry. 1988 Jun 1;174(2):323–9.

409. Calvanese V, Chavez L, Laurent T, Ding S, Verdin E. Dual-color HIV reporters trace a population of latently infected cells and enable their purification. Virology. 2013 Nov;446(1-2):283–92.

410. Fenton-May AE, Dibben O, Emmerich T, Ding H, Pfafferott K, Aasa-Chapman MM, et al. Relative resistance of HIV-1 founder viruses to control by interferon-alpha. Retrovirology. BioMed Central Ltd; 2013;10(1):146.

411. Parrish NF, Gao F, Li H, Giorgi EE, Barbian HJ, Parrish EH, et al. Phenotypic properties of transmitted founder HIV-1. Proc Natl Acad Sci U S A. 2013 Apr 23;110(17):6626–33.

412. Bosque A, Famiglietti M, Weyrich AS, Goulston C, Planelles V. Homeostatic proliferation fails to efficiently reactivate HIV-1 latently infected central memory CD4+ T cells. Emerman M, editor. PLoS Pathog. 2011 Oct;7(10):e1002288.

413. Murray JM, Zaunders J, Emery S, Cooper DA, Hey-Nguyen WJ, Koelsch KK, et al. HIV dynamics linked to memory CD4+ T cell homeostasis. Kashanchi F, editor. PLoS One. 2017;12(10):e0186101.

414. Dondi E, Rogge L, Lutfalla G, Uze G, Pellegrini S. Down-modulation of responses to type I IFN upon T cell activation. J Immunol. 2003 Jan 15;170(2):749–56.

415. Balachandran S, Kim CN, Yeh WC, Mak TW, Bhalla K, Barber GN. Activation of the dsRNA-dependent protein kinase, PKR, induces apoptosis through FADD-mediated death signaling. EMBO J. 1998 Dec 1;17(23):6888–902.

416. Balachandran S, Roberts PC, Kipperman T, Bhalla KN, Compans RW, Archer DR, et al. Alpha/beta interferons potentiate virus-induced apoptosis through activation of the FADD/Caspase-8 death signaling pathway. J Virol. 2000 Feb;74(3):1513–23.

417. Gil J, Esteban M. The interferon-induced protein kinase (PKR), triggers apoptosis through FADD-mediated activation of caspase 8 in a manner independent of Fas and TNF-alpha receptors. Oncogene. 2000 Jul 27;19(32):3665–74.

418. Kotredes KP, Gamero AM. Interferons as inducers of apoptosis in malignant cells. J Interferon Cytokine Res. 2013 Apr;33(4):162–70.

419. Chavez L, Calvanese V, Verdin E. HIV Latency Is Established Directly and Early in Both Resting and Activated Primary CD4 T Cells. Emerman M, editor. PLoS Pathog. 2015 Jun 11;11(6):e1004955.

420. Dahabieh MS, Ooms M, Simon V, Sadowski I. A doubly fluorescent HIV-1 reporter shows that the majority of integrated HIV-1 is latent shortly after infection. J Virol. 2013 Apr;87(8):4716–27.

421. Abdel-Mohsen M, Kuri-Cervantes L, Grau-Exposito J, Spivak AM, Nell RA, Tomescu C, et al. CD32 is expressed on cells with transcriptionally active HIV but does not enrich for HIV DNA in resting T cells. Sci Transl Med. American Association for the Advancement of Science; 2018 Apr 18;10(437):eaar6759.

422. García M, Navarrete-Muñoz MA, Ligos JM, Cabello A, Restrepo C, López-Bernaldo JC, et al. CD32 Expression is not Associated to HIV-DNA content in CD4 cell subsets of individuals with Different Levels of HIV Control. Sci Rep. Nature Publishing Group; 2018 Oct 19;8(1):15541.

423. Martin GE, Pace M, Thornhill JP, Phetsouphanh C, Meyerowitz J, Gossez M, et al. CD32-Expressing CD4 T Cells Are Phenotypically Diverse and Can Contain Proviral HIV DNA. Front Immunol. 2018;9:928.

424. Noto A, Procopio FA, Banga R, Suffiotti M, Corpataux J-M, Cavassini M, et al. CD32+ and PD-1+ Lymph Node CD4 T Cells Support Persistent HIV-1 Transcription in Treated Aviremic Individuals. Silvestri G, editor. J Virol. American Society for Microbiology Journals; 2018 Oct 15;92(20):13193.

425. Tomalka AG, Resto-Garay I, Campbell KS, Popkin DL. In vitro Evidence That Combination Therapy With CD16-Bearing NK-92 Cells and FDA-Approved Alefacept Can Selectively Target the Latent HIV Reservoir in CD4+ CD2hi Memory T Cells. Front Immunol. 2018;9:2552.

426. Koppensteiner H, Brack-Werner R, Schindler M. Macrophages and their relevance in Human Immunodeficiency Virus Type I infection. Retrovirology. BioMed Central Ltd; 2012;9(1):82.

427. Hassan J, Browne K, De Gascun C. HIV-1 in Monocytes and Macrophages: An Overlooked Reservoir? Viral Immunol. 2016 Nov;29(9):532–3.

428. Xue J, Fu C, Cong Z, Peng L, Peng Z, Chen T, et al. Galectin-3 promotes caspase-independent cell death of HIV-1-infected macrophages. FEBS J. 2017 Jan;284(1):97–113.

429. Koenig S, Gendelman HE, Orenstein JM, Dal Canto MC, Pezeshkpour GH, Yungbluth M, et al. Detection of AIDS virus in macrophages in brain tissue from AIDS patients with encephalopathy. Science. 1986 Sep 5;233(4768):1089–93.

430. Bernard-Stoecklin S, Gommet C, Corneau AB, Guenounou S, Torres C, Dejucq-Rainsford N, et al. Semen CD4+ T cells and macrophages are productively infected at all stages of SIV infection in macaques. Silvestri G, editor. PLoS Pathog. 2013;9(12):e1003810.

431. Brown D, Mattapallil JJ. Gastrointestinal tract and the mucosal macrophage reservoir in HIV infection. Clin Vaccine Immunol. 2014 Nov;21(11):1469–73.

432. Fletcher CV, Staskus K, Wietgrefe SW, Rothenberger M, Reilly C, Chipman JG, et al. Persistent HIV-1 replication is associated with lower antiretroviral drug concentrations in lymphatic tissues. Proc Natl Acad Sci U S A. 2014 Feb 11;111(6):2307–12.

433. Lorenzo-Redondo R, Fryer HR, Bedford T, Kim E-Y, Archer J, Kosakovsky Pond SL, et al. Persistent HIV-1 replication maintains the tissue reservoir during therapy. Nature. 2016 Feb 4;530(7588):51–6.

434. Estes JD, Kityo C, Ssali F, Swainson L, Makamdop KN, del Prete GQ, et al. Defining total-body AIDS-virus burden with implications for curative strategies. Nat Med. 2017 Nov;23(11):1271–6.

435. Reinhart TA, Fallert BA, Pfeifer ME, Sanghavi S, Capuano S, Rajakumar P, et al. Increased expression of the inflammatory chemokine CXC chemokine ligand 9/monokine induced by interferon-gamma in lymphoid tissues of rhesus macaques during simian immunodeficiency virus infection and acquired immunodeficiency syndrome. Blood. 2002 May 1;99(9):3119–28.

436. Carr JM, Hocking H, Li P, Burrell CJ. Rapid and efficient cell-to-cell transmission of human immunodeficiency virus infection from monocyte-derived macrophages to peripheral blood lymphocytes. Virology. 1999 Dec 20;265(2):319–29.

437. DeLuca C, Kwon H, Pelletier N, Wainberg MA, Hiscott J. NF-kappaB protects HIV-1-infected myeloid cells from apoptosis. Virology. 1998 Apr 25;244(1):27–38.

438. Guillemard E, Jacquemot C, Aillet F, Schmitt N, Barré-Sinoussi F, Israël N. Human immunodeficiency virus 1 favors the persistence of infection by activating macrophages through TNF. Virology. 2004 Nov 24;329(2):371–80.

439. Olivetta E, Federico M. HIV-1 Nef protects human-monocyte-derived macrophages from HIV-1-induced apoptosis. Exp Cell Res. 2006 Apr 1;312(6):890–900.

440. Reynoso R, Wieser M, Ojeda D, Bönisch M, Kühnel H, Bolcic F, et al. HIV-1 induces telomerase activity in monocyte-derived macrophages, possibly safeguarding one of its reservoirs. J Virol. 2012 Oct;86(19):10327–37.

441. Crowe S, Zhu T, Muller WA. The contribution of monocyte infection and trafficking to viral persistence, and maintenance of the viral reservoir in HIV infection. Journal of Leukocyte Biology. 2003 Nov;74(5):635–41.

442. Crowe SM, Vardaxis NJ, Kent SJ, Maerz AL, Hewish MJ, McGrath MS, et al. HIV infection of monocyte-derived macrophages in vitro reduces phagocytosis of Candida albicans. Journal of Leukocyte Biology. 1994 Sep;56(3):318–27.

443. Cribbs SK, Lennox J, Caliendo AM, Brown LA, Guidot DM. Healthy HIV-1-infected individuals on highly active antiretroviral therapy harbor HIV-1 in their alveolar macrophages. AIDS Res Hum Retroviruses. 2015 Jan;31(1):64–70.

444. Gordon MA, Gordon SB, Musaya L, Zijlstra EE, Molyneux ME, Read RC. Primary macrophages from HIV-infected adults show dysregulated cytokine responses to Salmonella, but normal internalization and killing. AIDS. 2007 Nov 30;21(18):2399–408.

445. Ennen J, Seipp I, Norley SG, Kurth R. Decreased accessory cell function of macrophages after infection with human immunodeficiency virus type 1 in vitro. Eur J Immunol. 1990 Nov;20(11):2451–6.

446. Wonderlich ER, Wu W-C, Normolle DP, Barratt-Boyes SM. Macrophages and Myeloid Dendritic Cells Lose T Cell-Stimulating Function in Simian Immunodeficiency Virus Infection Associated with Diminished IL-12 and IFN-α Production. The Journal of Immunology. 2015 Oct 1;195(7):3284–92.

447. Kasper MR, Collins KL. Nef-mediated disruption of HLA-A2 transport to the cell surface in T cells. J Virol. American Society for Microbiology (ASM); 2003 Mar;77(5):3041–9.

448. Kasper MR, Roeth JF, Williams M, Filzen TM, Fleis RI, Collins KL. HIV-1 Nef disrupts antigen presentation early in the secretory pathway. J Biol Chem. American Society for Biochemistry and Molecular Biology; 2005 Apr 1;280(13):12840–8.

449. Nasr N, Maddocks S, Turville SG, Harman AN, Woolger N, Helbig KJ, et al. HIV-1 infection of human macrophages directly induces viperin which inhibits viral production. Blood. 2012 Jul 26;120(4):778–88.

450. Ryo A, Tsurutani N, Ohba K, Kimura R, Komano J, Nishi M, et al. SOCS1 is an inducible host factor during HIV-1 infection and regulates the intracellular trafficking and stability of HIV-1 Gag. Proc Natl Acad Sci U S A. National Acad Sciences; 2008 Jan 8;105(1):294–9.

451. Levy DE, Kessler DS, Pine R, Reich N, Darnell JE. Interferon-induced nuclear factors that bind a shared promoter element correlate with positive and negative transcriptional control. Genes Dev. 1988 Apr;2(4):383–93.

452. Levy DE, Kessler DS, Pine R, Darnell JE. Cytoplasmic activation of ISGF3, the positive regulator of interferon-alpha-stimulated transcription, reconstituted in vitro. Genes Dev. 1989 Sep 1;3(9):1362–71.

453. Kato H, Takeuchi O, Sato S, Yoneyama M, Yamamoto M, Matsui K, et al. Differential roles of MDA5 and RIG-I helicases in the recognition of RNA viruses. Nat Rev Cancer. 2006 May 4;441(7089):101–5.

454. Guerrero S, Batisse J, Libre C, Bernacchi S, Marquet R, Paillart J-C. HIV-1 replication and the cellular eukaryotic translation apparatus. Viruses. 2015 Jan 19;7(1):199–218.

455. Künzi MS, Pitha PM. Role of interferon-stimulated gene ISG-15 in the interferon-omega-mediated inhibition of human immunodeficiency virus replication. J Interferon Cytokine Res. 1996 Nov;16(11):919–27.

456. Pincetic A, Kuang Z, Seo EJ, Leis J. The interferon-induced gene ISG15 blocks retrovirus release from cells late in the budding process. J Virol. 2010 May;84(9):4725–36.

457. Clerzius G, Gélinas J-F, Gatignol A. Multiple levels of PKR inhibition during HIV-1 replication. Rev Med Virol. John Wiley & Sons, Ltd; 2011 Jan;21(1):42–53.

458. Gargan S, Ahmed S, Mahony R, Bannan C, Napoletano S, O'Farrelly C, et al. HIV-1 Promotes the Degradation of Components of the Type 1 IFN JAK/STAT Pathway and Blocks Anti-viral ISG Induction. EBioMedicine. 2018 Apr;30:203–16.

459. Yoneyama M, Kikuchi M, Natsukawa T, Shinobu N, Imaizumi T, Miyagishi M, et al. The RNA helicase RIG-I has an essential function in double-stranded RNA-induced innate antiviral responses. Nat Immunol. 2004 Jun 20;5(7):730–7.

460. Tian Q, Stepaniants SB, Mao M, Weng L, Feetham MC, Doyle MJ, et al. Integrated genomic and proteomic analyses of gene expression in Mammalian cells. Mol Cell Proteomics. 2004 Oct;3(10):960–9.

461. Haverland NA, Fox HS, Ciborowski P. Quantitative proteomics by SWATH-MS reveals altered expression of nucleic acid binding and regulatory proteins in HIV-1-infected macrophages. J Proteome Res. 2014 Apr 4;13(4):2109–19.

462. Nemeth J, Vongrad V, Metzner KJ, Strouvelle VP, Weber R, Pedrioli P, et al. In Vivo and in Vitro Proteome Analysis of Human Immunodeficiency Virus (HIV)-1-infected, Human CD4+ T Cells. Mol Cell Proteomics. 2017 Apr;16(4 suppl 1):S108–23.

463. Li C, Zhu Z, Du X, Cao W, Yang F, Zhang X, et al. Foot-and-mouth disease virus induces lysosomal degradation of host protein kinase PKR by 3C proteinase to facilitate virus replication. Virology. 2017 Sep;509:222–31.

464. Habjan M, Pichlmair A, Elliott RM, Overby AK, Glatter T, Gstaiger M, et al. NSs protein of rift valley fever virus induces the specific degradation of the double-stranded RNA-dependent protein kinase. J Virol. 2009 May;83(9):4365–75.

465. Ikegami T, Narayanan K, Won S, Kamitani W, Peters CJ, Makino S. Rift Valley fever virus NSs protein promotes post-transcriptional downregulation of protein kinase PKR and inhibits eIF2alpha phosphorylation. Gale M, editor. PLoS Pathog. 2009 Feb;5(2):e1000287.

466. Black TL, Safer B, Hovanessian A, Katze MG. The cellular 68,000-Mr protein kinase is highly autophosphorylated and activated yet significantly degraded during poliovirus infection: implications for translational regulation. J Virol. 1989 May;63(5):2244–51.

467. Chang Y-H, Lau KS, Kuo R-L, Horng J-T. dsRNA Binding Domain of PKR Is Proteolytically Released by Enterovirus A71 to Facilitate Viral Replication. Front Cell Infect Microbiol. 2017;7:284.

468. Ventoso I, Blanco R, Perales C, Carrasco L. HIV-1 protease cleaves eukaryotic initiation factor 4G and inhibits cap-dependent translation. Proc Natl Acad Sci U S A. 2001 Nov 6;98(23):12966–71.

469. Castelló A, Franco D, Moral-López P, Berlanga JJ, Alvarez E, Wimmer E, et al. HIV- 1 protease inhibits Cap- and poly(A)-dependent translation upon eIF4GI and PABP cleavage. PLoS One. 2009 Nov 24;4(11):e7997–.

470. Sharma A, Yilmaz A, Marsh K, Cochrane A, Boris-Lawrie K. Thriving under stress: selective translation of HIV-1 structural protein mRNA during Vpr-mediated impairment of eIF4E translation activity. Ross SR, editor. PLoS Pathog. 2012;8(3):e1002612.

471. Kleinman CL, Doria M, Orecchini E, Giuliani E, Galardi S, De Jay N, et al. HIV-1 infection causes a down-regulation of genes involved in ribosome biogenesis. Jan E, editor. PLoS One. 2014;9(12):e113908.

472. Okumura F, Okumura AJ, Uematsu K, Hatakeyama S, Zhang D-E, Kamura T. Activation of double-stranded RNA-activated protein kinase (PKR) by interferon-stimulated gene 15 (ISG15) modification down-regulates protein translation. J Biol Chem. 2013 Jan 25;288(4):2839–47.

473. Galabru J, Hovanessian AG. Two interferon-induced proteins are involved in the protein kinase complex dependent on double-stranded RNA. Cell. 1985 Dec;43(3 Pt 2):685–94.

474. de Haro C, Méndez R, Santoyo J. The eIF-2alpha kinases and the control of protein synthesis. FASEB J. 1996 Oct;10(12):1378–87.

475. Lichty BD, Stojdl DF, Taylor RA, Miller L, Frenkel I, Atkins H, et al. Vesicular stomatitis virus: a potential therapeutic virus for the treatment of hematologic malignancy. Human Gene Therapy. 2004 Sep;15(9):821–31.

476. Patel MR, Jacobson BA, Ji Y, Drees J, Tang S, Xiong K, et al. Vesicular stomatitis virus expressing interferon-β is oncolytic and promotes antitumor immune responses in a syngeneic murine model of non-small cell lung cancer. Oncotarget. 2015 Oct 20;6(32):33165–77.

477. Pol JG, Atherton MJ, Bridle BW, Stephenson KB, Le Boeuf F, Hummel JL, et al. Development and applications of oncolytic Maraba virus vaccines. Oncolytic Virother. 2018;7:117–28.

478. Kleijn A, Kloezeman J, Treffers-Westerlaken E, Fulci G, Leenstra S, Dirven C, et al. The therapeutic efficacy of the oncolytic virus Delta24-RGD in a murine glioma model depends primarily on antitumor immunity. OncoImmunology. 2014 Oct;3(9):e955697.

479. Jiang H, Clise-Dwyer K, Ruisaard KE, Fan X, Tian W, Gumin J, et al. Delta-24-RGD oncolytic adenovirus elicits anti-glioma immunity in an immunocompetent mouse model. Castro MG, editor. PLoS ONE. 2014;9(5):e97407.

480. Parker JN, Gillespie GY, Love CE, Randall S, Whitley RJ, Markert JM. Engineered herpes simplex virus expressing IL-12 in the treatment of experimental murine brain tumors. Proc Natl Acad Sci USA. National Academy of Sciences; 2000 Feb 29;97(5):2208–13.

481. Quiroz E, Moreno N, Peralta PH, Tesh RB. A human case of encephalitis associated with vesicular stomatitis virus (Indiana serotype) infection. 1988 Sep;39(3):312–4.

482. Sanjuán R, Moya A, Elena SF. The contribution of epistasis to the architecture of fitness in an RNA virus. Proc Natl Acad Sci U S A. 2004 Oct 26;101(43):15376–9.

483. Schubert M, Joshi B, Blondel D, Harmison GG. Insertion of the human immunodeficiency virus CD4 receptor into the envelope of vesicular stomatitis virus particles. J Virol. American Society for Microbiology (ASM); 1992 Mar;66(3):1579–89.

484. Schnell MJ, Johnson JE, Buonocore L, Rose JK. Construction of a novel virus that targets HIV-1-infected cells and controls HIV-1 infection. Cell. 1997 Sep 5;90(5):849–57.

485. Boritz E, GERLACH J, JOHNSON JE, Rose JK. Replication-competent rhabdoviruses with human immunodeficiency virus type 1 coats and green fluorescent protein: entry by a pH-independent pathway. J Virol. Am Soc Microbiol; 1999;73(8):6937–45.

486. Okuma K, Fukagawa K, Kohma T, Takahama Y, Hamaguchi Y, Ito M, et al. A recombinant vesicular stomatitis virus encoding CCR5-tropic HIV-1

receptors targets HIV-1-infected cells and controls HIV-1 infection. Microbes and Infection. 2017 Apr;19(4-5):277–87.

487. Bredow von B, Arias JF, Heyer LN, Gardner MR, Farzan M, Rakasz EG, et al. Envelope Glycoprotein Internalization Protects Human and Simian Immunodeficiency Virus-Infected Cells from Antibody-Dependent Cell-Mediated Cytotoxicity. Kirchhoff F, editor. J Virol. 2015 Oct;89(20):10648–55.

488. Costiniuk C. Oncolytic Viruses as a Potential Approach to Eliminate the HIV Reservoir. 2013.

489. Finkelshtein D, Werman A, Novick D, Barak S, Rubinstein M. LDL receptor and its family members serve as the cellular receptors for vesicular stomatitis virus. Proc Natl Acad Sci U S A. National Acad Sciences; 2013;110(18):7306–11.

490. Tong JG, Valdes YR, Barrett JW, Bell JC, Stojdl D, McFadden G, et al. Evidence for differential viral oncolytic efficacy in an in vitro model of epithelial ovarian cancer metastasis. Molecular Therapy - Oncolytics. 2015;2:15013.

491. Tong JG, Valdes YR, Sivapragasam M, Barrett JW, Bell JC, Stojdl D, et al. Spatial and temporal epithelial ovarian cancer cell heterogeneity impacts Maraba virus oncolytic potential. BMC Cancer. 2017 Aug 30;17(1):594.

492. Gaddy DF, Lyles DS. Vesicular stomatitis viruses expressing wild-type or mutant M proteins activate apoptosis through distinct pathways. J Virol. 2005 Apr;79(7):4170–9.

493. Oliere S, Arguello M, Mesplede T, Tumilasci V, Nakhaei P, Stojdl D, et al. Vesicular stomatitis virus oncolysis of T lymphocytes requires cell cycle entry and translation initiation. J Virol. 2008 Jun;82(12):5735–49.

494. Felt SA, Moerdyk-Schauwecker MJ, Grdzelishvili VZ. Induction of apoptosis in pancreatic cancer cells by vesicular stomatitis virus. Virology. 2015 Jan 1;474:163–73.

495. Beug ST, Tang VA, LaCasse EC, Cheung HH, Beauregard CE, Brun J, et al. Smac mimetics and innate immune stimuli synergize to promote tumor death. Nat Biotechnol. 2014 Jan 26;32(2):182–90.

496. Bourgeois-Daigneault M-C, St-Germain LE, Roy DG, Pelin A, Aitken AS, Arulanandam R, et al. Combination of Paclitaxel and MG1 oncolytic virus as a successful strategy for breast cancer treatment. Breast Cancer Res. BioMed Central; 2016 Aug 8;18(1):83.

497. Yu L, Alva A, Su H, Dutt P, Freundt E, Welsh S, et al. Regulation of an ATG7-beclin 1 program of autophagic cell death by caspase-8. Science.

American Association for the Advancement of Science; 2004 Jun 4;304(5676):1500–2.

498. Martinet W, Schrijvers DM, Herman AG, De Meyer GRY. z-VAD-fmk-induced non-apoptotic cell death of macrophages: possibilities and limitations for atherosclerotic plaque stabilization. Autophagy. 2006 Oct;2(4):312–4.

499. Sawai H. Differential effects of caspase inhibitors on TNF-induced necroptosis. Biochem Biophys Res Commun. 2013 Mar 15;432(3):451–5.

500. Degterev A, Huang Z, Boyce M, Li Y, Jagtap P, Mizushima N, et al. Chemical inhibitor of nonapoptotic cell death with therapeutic potential for ischemic brain injury. Nat Chem Biol. Nature Publishing Group; 2005 Jul;1(2):112–9.

501. Faber M, Faber M-L, Papaneri A, Bette M, Weihe E, Dietzschold B, et al. A single amino acid change in rabies virus glycoprotein increases virus spread and enhances virus pathogenicity. J Virol. 2005 Nov;79(22):14141–8.

502. Fang X, Zhang S, Sun X, Li J, Sun T. Evaluation of attenuated VSVs with mutated M or/and G proteins as vaccine vectors. Vaccine. 2012 Feb 8;30(7):1313–21.

503. Balachandran S, Porosnicu M, Barber GN. Oncolytic activity of vesicular stomatitis virus is effective against tumors exhibiting aberrant p53, Ras, or myc function and involves the induction of apoptosis. J Virol. 2001 Apr;75(7):3474–9.

504. Lin Y, Devin A, Rodriguez Y, Liu ZG. Cleavage of the death domain kinase RIP by caspase-8 prompts TNF-induced apoptosis. Genes Dev. 1999 Oct 1;13(19):2514–26.

505. Antoni BA, Sabbatini P, Rabson AB, virology EWJO, set. Inhibition of apoptosis in human immunodeficiency virus-infected cells enhances virus production and facilitates persistent infection. J Virol. 1995 Apr;69(4):2384–92.

506. Wagner RN, Reed JC, Chanda SK. HIV-1 protease cleaves the serine-threonine kinases RIPK1 and RIPK2. Retrovirology. 2015 Aug 22;12(1):74.

507. Heaton NS, Randall G. Dengue virus-induced autophagy regulates lipid metabolism. Cell Host Microbe. 2010 Nov 18;8(5):422–32.

508. Tallóczy Z, Jiang W, Virgin HW, Leib DA, Scheuner D, Kaufman RJ, et al. Regulation of starvation- and virus-induced autophagy by the eIF2 kinase signaling pathway. Proc Natl Acad Sci U S A. 2001;99(1):190–5.

509. Kyei GB, Dinkins C, Davis AS, Roberts E, Singh SB, Dong C, et al. Autophagy pathway intersects with HIV-1 biosynthesis and regulates viral yields in macrophages. J Cell Biol. 2009 Jul 27;186(2):255–68.

510. The HSV-2 mutant DeltaPK induces melanoma oncolysis through nonredundant death programs and associated with autophagy and pyroptosis proteins. Gene Ther. Nature Publishing Group; 2010 Mar;17(3):315–27.

511. Wang Q, Imamura R, Motani K, Kushiyama H, Nagata S, Suda T. Pyroptotic cells externalize eat-me and release find-me signals and are efficiently engulfed by macrophages. Int Immunol. 2013 Jun;25(6):363–72.

512. Guo ZS, Liu Z, Bartlett DL. Oncolytic Immunotherapy: Dying the Right Way is a Key to Eliciting Potent Antitumor Immunity. Front Oncol. 2014;4(Pt 1):74.

513. Batenchuk C, Le Boeuf F, Stubbert L, Falls T, Atkins HL, Bell JC, et al. Non-replicating rhabdovirus-derived particles (NRRPs) eradicate acute leukemia by direct cytolysis and induction of antitumor immunity. Blood Cancer Journal. Nature Publishing Group; 2013 Jul 1;3(7):e123–7.

514. Orzechowska B, Antoszków Z, immunologiae ISA, 2007. Cytokine production by human leukocytes with different expressions of natural antiviral immunity and the effect of antibodies against interferons and TNF-alpha. Arch Immunol Ther Exp (Warsz). 2007 Mar;55(2):111–7.

515. Chauhan VS, Furr SR, Sterka DG, Nelson DA, Moerdyk-Schauwecker M, Marriott I, et al. Vesicular stomatitis virus infects resident cells of the central nervous system and induces replication-dependent inflammatory responses. Virology. 2010 May 10;400(2):187–96.

516. Breitbach CJ, Paterson JM, Lemay CG, Falls TJ, McGuire A, Parato KA, et al. Targeted Inflammation During Oncolytic Virus Therapy Severely Compromises Tumor Blood Flow. Mol Ther. 2007 Jun 19;15(9):1686–93.

517. Han X, Becker K, Degen HJ, Jablonowski H, Strohmeyer G. Synergistic stimulatory effects of tumour necrosis factor alpha and interferon gamma on replication of human immunodeficiency virus type 1 and on apoptosis of HIV-1-infected host cells. Eur J Clin Invest. 1996 Apr;26(4):286–92.

518. Cassetta L, Kajaste-Rudnitski A, Coradin T, Saba E, Chiara Della G, Barbagallo M, et al. M1 polarization of human monocyte-derived macrophages restricts pre and postintegration steps of HIV-1 replication. AIDS. 2013 Jul 31;27(12):1847–56.

519. Cassol E, Cassetta L, Rizzi C, Alfano M, Poli G. M1 and M2a polarization of human monocyte-derived macrophages inhibits HIV-1 replication by distinct

mechanisms. The Journal of Immunology. American Association of Immunologists; 2009 May 15;182(10):6237–46.

520. Cassol E, Cassetta L, Alfano M, Poli G. Macrophage polarization and HIV-1 infection. J Leukoc Biol. 2010 Apr;87(4):599–608.

521. Wu L, Huang T-G, Meseck M, Altomonte J, Ebert O, Shinozaki K, et al. rVSV(M Delta 51)-M3 is an effective and safe oncolytic virus for cancer therapy. Human Gene Therapy. 2008 Jun;19(6):635–47.

522. Wollmann G, Rogulin V, Simon I, Rose JK, van den Pol AN. Some attenuated variants of vesicular stomatitis virus show enhanced oncolytic activity against human glioblastoma cells relative to normal brain cells. J Virol. 2010 Feb;84(3):1563–73.

523. Westcott MM, Liu J, Rajani K, D'Agostino R, Lyles DS, Porosnicu M. Interferon Beta and Interferon Alpha 2a Differentially Protect Head and Neck Cancer Cells from Vesicular Stomatitis Virus-Induced Oncolysis. Dermody TS, editor. J Virol. 2015 Aug;89(15):7944–54.

524. Obuchi M, Fernandez M, Barber GN. Development of recombinant vesicular stomatitis viruses that exploit defects in host defense to augment specific oncolytic activity. J Virol. 2003 Aug;77(16):8843–56.

525. Willmon CL, Saloura V, Fridlender ZG, Wongthida P, Diaz RM, Thompson J, et al. Expression of IFN-beta enhances both efficacy and safety of oncolytic vesicular stomatitis virus for therapy of mesothelioma. Cancer Res. American Association for Cancer Research; 2009 Oct 1;69(19):7713–20.

526. Bishnoi S, Tiwari R, Gupta S, Byrareddy SN, Nayak D. Oncotargeting by Vesicular Stomatitis Virus (VSV): Advances in Cancer Therapy. Viruses. 2018 Feb 23;10(2):90.

527. Betancourt D, Ramos JC, Barber GN. Retargeting Oncolytic Vesicular Stomatitis Virus to Human T-Cell Lymphotropic Virus Type 1-Associated Adult T-Cell Leukemia. Ross SR, editor. J Virol. 2015 Dec;89(23):11786–800.

528. Zalar A, Figueroa MI, Ruibal-Ares B, Baré P, Cahn P, de Bracco MM de E, et al. Macrophage HIV-1 infection in duodenal tissue of patients on long term HAART. Antiviral Res. 2010 Aug;87(2):269–71.

529. Yukl SA, Sinclair E, Somsouk M, Hunt PW, Epling L, Killian M, et al. A comparison of methods for measuring rectal HIV levels suggests that HIV DNA resides in cells other than CD4+ T cells, including myeloid cells. AIDS. 2014 Jan 28;28(3):439–42.

530. Asahchop EL, Meziane O, Mamik MK, Chan WF, Branton WG, Resch L, et al. Reduced antiretroviral drug efficacy and concentration in HIV-infected microglia contributes to viral persistence in brain. Retrovirology. BioMed Central; 2017 Oct 14;:1–17.

531. Castellano P, Prevedel L, Eugenin EA. HIV-infected macrophages and microglia that survive acute infection become viral reservoirs by a mechanism involving Bim. Sci Rep. 2017 Oct 9;7(1):12866.

532. O'Brien WA, Namazi A, Kalhor H, Mao SH, Zack JA, Chen IS. Kinetics of human immunodeficiency virus type 1 reverse transcription in blood mononuclear phagocytes are slowed by limitations of nucleotide precursors. J Virol. 1994 Feb;68(2):1258–63.

533. Sonza S, Maerz A, Deacon N, Meanger J, Mills J, Crowe S. Human immunodeficiency virus type 1 replication is blocked prior to reverse transcription and integration in freshly isolated peripheral blood monocytes. J Virol. 1996 Jun;70(6):3863–9.

534. Arfi V, Rivière L, Jarrosson-Wuillème L, Goujon C, Rigal D, Darlix J-L, et al. Characterization of the early steps of infection of primary blood monocytes by human immunodeficiency virus type 1. J Virol. 2008 Jul;82(13):6557–65.

535. MacLean JA, Xia W, Pinto CE, Zhao L, Liu HW, Kradin RL. Sequestration of inhaled particulate antigens by lung phagocytes. A mechanism for the effective inhibition of pulmonary cell-mediated immunity. Am J Pathol. American Society for Investigative Pathology; 1996 Feb;148(2):657–66.

536. Roth MD, Golub SH. Human pulmonary macrophages utilize prostaglandins and transforming growth factor beta 1 to suppress lymphocyte activation. Journal of Leukocyte Biology. 1993 Apr;53(4):366–71.

537. Martinez JA, King TE, Brown K, Jennings CA, Borish L, Mortenson RL, et al. Increased expression of the interleukin-10 gene by alveolar macrophages in interstitial lung disease. Am J Physiol. American Physiological Society Bethesda, MD; 1997 Sep;273(3 Pt 1):L676–83.

538. Coleman MM, Ruane D, Moran B, Dunne PJ, Keane J, Mills KHG. Alveolar macrophages contribute to respiratory tolerance by inducing FoxP3 expression in naive T cells. Am J Respir Cell Mol Biol. American Thoracic Society; 2013 Jun;48(6):773–80.

539. Schneider C, Nobs SP, Heer AK, Kurrer M, Klinke G, van Rooijen N, et al. Alveolar macrophages are essential for protection from respiratory failure and associated morbidity following influenza virus infection. Pekosz A, editor. PLoS Pathog. Public Library of Science; 2014 Apr;10(4):e1004053.

540. Hunninghake GW, Gadek JE, Szapiel SV, Strumpf IJ, Kawanami O, Ferrans VJ, et al. The human alveolar macrophage. Methods Cell Biol. 1980;21A:95–105.

541. Gomez Perdiguero E, Klapproth K, Schulz C, Busch K, Azzoni E, Crozet L, et al. Tissue-resident macrophages originate from yolk-sac-derived erythro-myeloid progenitors. Nature. 2015 Feb 26;518(7540):547–51.

542. van de Laar L, Saelens W, De Prijck S, Martens L, Scott CL, Van Isterdael G, et al. Yolk Sac Macrophages, Fetal Liver, and Adult Monocytes Can Colonize an Empty Niche and Develop into Functional Tissue-Resident Macrophages. Immunity. 2016 Apr 19;44(4):755–68.

543. Eguíluz-Gracia I, Schultz HHL, Sikkeland LIB, Danilova E, Holm AM, Pronk CJH, et al. Long-term persistence of human donor alveolar macrophages in lung transplant recipients. Thorax. 2016 Nov;71(11):1006–11.

544. Nayak DK, Zhou F, Xu M, Huang J, Tsuji M, Hachem R, et al. Long-Term Persistence of Donor Alveolar Macrophages in Human Lung Transplant Recipients That Influences Donor-Specific Immune Responses. Am J Transplant. 2016 Aug;16(8):2300–11.

545. Thomas ED, Ramberg RE, Sale GE, Sparkes RS, Golde DW. Direct evidence for a bone marrow origin of the alveolar macrophage in man. Science. 1976 Jun 4;192(4243):1016–8.

546. Misharin AV, Morales-Nebreda L, Reyfman PA, Cuda CM, Walter JM, McQuattie-Pimentel AC, et al. Monocyte-derived alveolar macrophages drive lung fibrosis and persist in the lung over the life span. Journal of Experimental Medicine. 2017 Aug 7;214(8):2387–404.

547. Chayt KJ, Harper ME, Marselle LM, Lewin EB, Rose RM, Oleske JM, et al. Detection of HTLV-III RNA in lungs of patients with AIDS and pulmonary involvement. JAMA. 1986 Nov 7;256(17):2356–9.

548. Salahuddin SZ, Rose RM, Groopman JE, Markham PD, Gallo RC. Human T lymphotropic virus type III infection of human alveolar macrophages. Blood. 1986 Jul;68(1):281–4.

549. Beck JM. Abnormalities in host defense associated with HIV infection. Clin Chest Med. 2013 Jun;34(2):143–53.

550. Elssner A, Carter JE, Yunger TM, Wewers MD. HIV-1 infection does not impair human alveolar macrophage phagocytic function unless combined with cigarette smoking. Chest. 2004 Mar;125(3):1071–6.

551. Matute-Bello G, Lee JS, Frevert CW, Liles WC, Sutlief S, Ballman K, et al. Optimal timing to repopulation of resident alveolar macrophages with donor

cells following total body irradiation and bone marrow transplantation in mice. J Immunol Methods. 2004 Sep;292(1-2):25–34.

552. Murphy J, Summer R, Wilson AA, Kotton DN, Fine A. The prolonged life-span of alveolar macrophages. Am J Respir Cell Mol Biol. 2008 Apr;38(4):380–5.

553. Costiniuk CT, Jenabian M-A. The lungs as anatomical reservoirs of HIV infection. Rev Med Virol. 2014 Jan;24(1):35–54.

554. Landay AL, Schade SZ, Takefman DM, Kuhns MC, McNamara AL, Rosen RL, et al. Detection of HIV-1 provirus in bronchoalveolar lavage cells by polymerase chain reaction. J Acquir Immune Defic Syndr. 1993 Feb;6(2):171–5.

555. Lamers SL, Rose R, Maidji E, Agsalda-Garcia M, Nolan DJ, Fogel GB, et al. HIV DNA Is Frequently Present within Pathologic Tissues Evaluated at Autopsy from Combined Antiretroviral Therapy-Treated Patients with Undetectable Viral Loads. Kirchhoff F, editor. J Virol. 2016 Oct 15;90(20):8968–83.

556. Horiike M, Iwami S, Kodama M, Sato A, Watanabe Y, Yasui M, et al. Lymph nodes harbor viral reservoirs that cause rebound of plasma viremia in SIV-infected macaques upon cessation of combined antiretroviral therapy. Virology. 2012 Feb 20;423(2):107–18.

557. Groot F, Russell RA, Baxter AE, Welsch S, Duncan CJ, Willberg C, et al. Efficient macrophage infection by phagocytosis of dying HIV-1 -infected CD4+T cells. Retrovirology. 2011;8(Suppl 2):O31.

558. Clarke JR, Gates AJ, Coker RJ, Douglass JA, Williamson JD, Mitchell DM. HIV-1 proviral DNA copy number in peripheral blood leucocytes and bronchoalveolar lavage cells of AIDS patients. Clin Exp Immunol. Wiley-Blackwell; 1994 May;96(2):182–6.

559. Azzoni L, Foulkes AS, Papasavvas E, Mexas AM, Lynn KM, Mounzer K, et al. Pegylated Interferon alfa-2a monotherapy results in suppression of HIV type 1 replication and decreased cell-associated HIV DNA integration. J Infect Dis. 2013 Jan 15;207(2):213–22.

560. Petravic J, Rasmussen TA, Lewin SR, Kent SJ, Davenport MP. Relationship between Measures of HIV Reactivation and Decline of the Latent Reservoir under Latency-Reversing Agents. Silvestri G, editor. J Virol. American Society for Microbiology; 2017 May 1;91(9):e02092–16.

561. Tomlinson GS, Booth H, Petit SJ, Potton E, Towers GJ, Miller RF, et al. Adherent human alveolar macrophages exhibit a transient pro-inflammatory

profile that confounds responses to innate immune stimulation. Chan MCW, editor. PLoS One. 2012;7(6):e40348.

562. Higham A, Lea S, Ray D, Singh D. Corticosteroid effects on COPD alveolar macrophages: dependency on cell culture methodology. J Immunol Methods. 2014 Mar;405:144–53.

563. Veckman V, Miettinen M, Matikainen S, Lande R, Giacomini E, Coccia EM, et al. Lactobacilli and streptococci induce inflammatory chemokine production in human macrophages that stimulates Th1 cell chemotaxis. Journal of Leukocyte Biology. 2003 Sep;74(3):395–402.

564. Benoit M, Desnues B, Mege J-L. Macrophage polarization in bacterial infections. The Journal of Immunology. 2008 Sep 15;181(6):3733–9.

565. Bayer C, Varani S, Wang L, Walther P, Zhou S, Straschewski S, et al. Human cytomegalovirus infection of M1 and M2 macrophages triggers inflammation and autologous T-cell proliferation. J Virol. 5 ed. 2013 Jan;87(1):67–79.

566. Campbell GM, Nicol MQ, Dransfield I, Shaw DJ, Nash AA, Dutia BM. Susceptibility of bone marrow-derived macrophages to influenza virus infection is dependent on macrophage phenotype. Journal of General Virology. 2015 Oct;96(10):2951–60.

567. Dutry I. The Effects of Macrophage Polarity on Influenza Virus Replication and Innate Immune Responses. J Clin Cell Immunol. 2015;06(01).

568. Kadioglu A, Andrew PW. The innate immune response to pneumococcal lung infection: the untold story. Trends Immunol. 2004 Mar;25(3):143–9.

569. Bazzan E, Turato G, Tinè M, Radu CM, Balestro E, Rigobello C, et al. Dual polarization of human alveolar macrophages progressively increases with smoking and COPD severity. Respir Res. BioMed Central; 2017 Feb 23;18(1):40.

570. Kumagai Y, Takeuchi O, Kato H, Kumar H, Matsui K, Morii E, et al. Alveolar macrophages are the primary interferon-alpha producer in pulmonary infection with RNA viruses. Immunity. 2007 Aug;27(2):240–52.

571. Schaefer TM, Fuller CL, Basu S, Fallert BA, Poveda SL, Sanghavi SK, et al. Increased expression of interferon-inducible genes in macaque lung tissues during simian immunodeficiency virus infection. Microbes and Infection. 2006 Jun;8(7):1839–50.

572. Alammar L, Gama L, Clements JE. Simian immunodeficiency virus infection in the brain and lung leads to differential type I IFN signaling during acute infection. The Journal of Immunology. 2011 Apr 1;186(7):4008–18.

573. Stojdl DF, Abraham N, Knowles S, Marius R, Brasey A, Lichty BD, et al. The murine double-stranded RNA-dependent protein kinase PKR is required for resistance to vesicular stomatitis virus. J Virol. 2000 Oct;74(20):9580–5.

574. Hummel J, Bienzle D, Morrison A, Cieplak M, Stephenson K, DeLay J, et al. Maraba virus-vectored cancer vaccines represent a safe and novel therapeutic option for cats. Sci Rep. 2017 Nov 16;7(1):15738.

575. Liu Y-P, Suksanpaisan L, Steele MB, Russell SJ, Peng K-W. Induction of antiviral genes by the tumor microenvironment confers resistance to virotherapy. Sci Rep. Nature Publishing Group; 2013;3(1):2375.

576. Denton NL, Chen C-Y, Scott TR, Cripe TP. Tumor-Associated Macrophages in Oncolytic Virotherapy: Friend or Foe? Biomedicines. Multidisciplinary Digital Publishing Institute; 2016 Jul 7;4(3):13.

577. Rose R, Nolan DJ, Maidji E, Stoddart CA, Singer EJ, Lamers SL, et al. Eradication of HIV from Tissue Reservoirs: Challenges for the Cure. AIDS Res Hum Retroviruses. 2018 Jan;34(1):3–8.

578. Martin NT, Bell JC. Oncolytic Virus Combination Therapy: Killing One Bird with Two Stones. Mol Ther. 2018 Jun 6;26(6):1414–22.

579. Kwok G, Yau TCC, Chiu JW, Tse E, Kwong Y-L. Pembrolizumab (Keytruda). Hum Vaccin Immunother. 2016 Nov;12(11):2777–89.

580. Diallo J-S, Le Boeuf F, Lai F, Cox J, Vaha-Koskela M, Abdelbary H, et al. A high-throughput pharmacoviral approach identifies novel oncolytic virus sensitizers. Mol Ther. 2010 Jun;18(6):1123–9.

581. Chang H-M, Paulson M, Holko M, Rice CM, Williams BRG, Marié I, et al. Induction of interferon-stimulated gene expression and antiviral responses require protein deacetylase activity. Proc Natl Acad Sci USA. 2004 Jun 29;101(26):9578–83.

582. Zobel K, Wang L, Varfolomeev E, Franklin MC, Elliott LO, Wallweber HJA, et al. Design, synthesis, and biological activity of a potent Smac mimetic that sensitizes cancer cells to apoptosis by antagonizing IAPs. ACS Chem Biol. American Chemical Society; 2006 Sep 19;1(8):525–33.

583. Hennessy EJ, Adam A, Aquila BM, Castriotta LM, Cook D, Hattersley M, et al. Discovery of a novel class of dimeric Smac mimetics as potent IAP antagonists resulting in a clinical candidate for the treatment of cancer (AZD5582). J Med Chem. American Chemical Society; 2013 Dec 27;56(24):9897–919.

584. Beug ST, Pichette SJ, St-Jean M, Holbrook J, Walker DE, LaCasse EC, et al. Combination of IAP Antagonists and TNF-α-Armed Oncolytic Viruses

Induce Tumor Vascular Shutdown and Tumor Regression. Molecular Therapy - Oncolytics. Elsevier; 2018 Sep 28;10:28–39.

585. Kim D-S, Dastidar H, Zhang C, Zemp FJ, Lau K, Ernst M, et al. Smac mimetics and oncolytic viruses synergize in driving anticancer T-cell responses through complementary mechanisms. Nat Commun. 2017 Aug 24;8(1):344.

586. Dyck L, Mills KHG. Immune checkpoints and their inhibition in cancer and infectious diseases. Eur J Immunol. John Wiley & Sons, Ltd; 2017 May;47(5):765–79.

587. Snell LM, McGaha TL, Brooks DG. Type I Interferon in Chronic Virus Infection and Cancer. Trends Immunol. 2017 Aug;38(8):542–57.

588. Day CL, Kaufmann DE, Kiepiela P, Brown JA, Moodley ES, Reddy S, et al. PD-1 expression on HIV-specific T cells is associated with T-cell exhaustion and disease progression. Nature. 2006 Sep 21;443(7109):350–4.

589. Petrovas C, Casazza JP, Brenchley JM, Price DA, Gostick E, Adams WC, et al. PD-1 is a regulator of virus-specific CD8+ T cell survival in HIV infection. J Exp Med. Rockefeller University Press; 2006 Oct 2;203(10):2281–92.

590. Trautmann L, Janbazian L, Chomont N, Said EA, Gimmig S, Bessette B, et al. Upregulation of PD-1 expression on HIV-specific CD8+ T cells leads to reversible immune dysfunction. Nat Med. 2006 Oct;12(10):1198–202.

591. Chew GM, Fujita T, Webb GM, Burwitz BJ, Wu HL, Reed JS, et al. TIGIT Marks Exhausted T Cells, Correlates with Disease Progression, and Serves as a Target for Immune Restoration in HIV and SIV Infection. Silvestri G, editor. PLoS Pathog. Public Library of Science; 2016 Jan;12(1):e1005349.

592. Ostios-Garcia L, Faig J, Leonardi GC, Adeni AE, Subegdjo SJ, Lydon CA, et al. Safety and Efficacy of PD-1 Inhibitors Among HIV-Positive Patients With Non-Small Cell Lung Cancer. J Thorac Oncol. 2018 Jul;13(7):1037–42.

593. Galanina N, Goodman AM, Cohen PR, Frampton GM, Kurzrock R. Successful Treatment of HIV-Associated Kaposi Sarcoma with Immune Checkpoint Blockade. Cancer Immunol Res. American Association for Cancer Research; 2018 Oct;6(10):1129–35.

594. Lee WS, Kristensen AB, Rasmussen TA, Tolstrup M, Østergaard L, Søgaard OS, et al. Anti-HIV-1 ADCC Antibodies following Latency Reversal and Treatment Interruption. Silvestri G, editor. J Virol. American Society for Microbiology Journals; 2017 Aug 1;91(15):728.

595. Keedy KS, Archin NM, Gates AT, Espeseth A, Hazuda DJ, Margolis DM. A limited group of class I histone deacetylases acts to repress human

immunodeficiency virus type 1 expression. J Virol. 2009 May;83(10):4749–56.

596. Cummins NW, Sainski AM, Dai H, Natesampillai S, Pang Y-P, Bren GD, et al. Prime, Shock, and Kill: Priming CD4 T Cells from HIV Patients with a BCL-2 Antagonist before HIV Reactivation Reduces HIV Reservoir Size. Silvestri G, editor. J Virol. American Society for Microbiology Journals; 2016 Apr;90(8):4032–48.

597. Hattori S-I, Matsuda K, Tsuchiya K, Gatanaga H, Oka S, Yoshimura K, et al. Combination of a Latency-Reversing Agent With a Smac Mimetic Minimizes Secondary HIV-1 Infection in vitro. Frontiers; 2018;9:2022.

598. Nakashima H, Nguyen T, Chiocca EA. Combining HDAC inhibitors with oncolytic virotherapy for cancer therapy. Oncolytic Virother. 2015;4:183–91.

599. Jammi NV, Whitby LR, Beal PA. Small molecule inhibitors of the RNA-dependent protein kinase. Biochem Biophys Res Commun. 2003 Aug 15;308(1):50–7.

600. Nguyên T, Abdelbary H, the MAPO, 2008. Chemical targeting of the innate antiviral response by histone deacetylase inhibitors renders refractory cancers sensitive to viral oncolysis. Proc Natl Acad Sci U S A. 2008 Sep 30;105(39):14981–6.

601. Shulak L, Beljanski V, Chiang C, Dutta SM, Van Grevenynghe J, Belgnaoui SM, et al. Histone deacetylase inhibitors potentiate vesicular stomatitis virus oncolysis in prostate cancer cells by modulating NF-κB-dependent autophagy. J Virol. 2014 Mar;88(5):2927–40.

602. McMillan NA, Chun RF, Siderovski DP, Galabru J, Toone WM, Samuel CE, et al. HIV-1 Tat directly interacts with the interferon-induced, double-stranded RNA-dependent kinase, PKR. Virology. 1995 Nov 10;213(2):413–24.

603. Cai R, Carpick B, Chun RF, Jeang KT, Williams BR. HIV-I TAT inhibits PKR activity by both RNA-dependent and RNA-independent mechanisms. Arch Biochem Biophys. 2000 Jan 15;373(2):361–7.

604. Gaddy DF, Lyles DS. Oncolytic vesicular stomatitis virus induces apoptosis via signaling through PKR, Fas, and Daxx. J Virol. 2007 Mar;81(6):2792–804.

605. Silverman RH, Sengupta DN. Translational regulation by HIV leader RNA, TAT, and interferon-inducible enzymes. J Exp Pathol. 1990;5(2):69–77.

606. Kukkonen S, Martinez-Viedma MDP, Kim N, Manrique M, Aldovini A. HIV-1 Tat second exon limits the extent of Tat-mediated modulation of interferon-

stimulated genes in antigen presenting cells. Retrovirology. BioMed Central Ltd; 2014;11(1):30.

607. McLaren PJ, Gawanbacht A, Pyndiah N, Krapp C, Hotter D, Kluge SF, et al. Identification of potential HIV restriction factors by combining evolutionary genomic signatures with functional analyses. Retrovirology. BioMed Central; 2015;12(1):41.

608. Tronel C, Page G, Bodard S, Chalon S, Antier D. The specific PKR inhibitor C16 prevents apoptosis and IL-1β production in an acute excitotoxic rat model with a neuroinflammatory component. Neurochem Int. 2014 Jan;64:73–83.

609. Xiao J, Tan Y, Li Y, Luo Y. The Specific Protein Kinase R (PKR) Inhibitor C16 Protects Neonatal Hypoxia-Ischemia Brain Damages by Inhibiting Neuroinflammation in a Neonatal Rat Model. Med Sci Monit. International Scientific Information, Inc; 2016 Dec 23;22:5074–81.

610. Farabaugh KT, Majumder M, Guan B-J, Jobava R, Wu J, Krokowski D, et al. Protein Kinase R Mediates the Inflammatory Response Induced by Hyperosmotic Stress. Mol Cell Biol. American Society for Microbiology Journals; 2017 Feb 15;37(4):173.

611. Jha BK, Dong B, Nguyen CT, Polyakova I, Silverman RH. Suppression of antiviral innate immunity by sunitinib enhances oncolytic virotherapy. Mol Ther. 2013 Sep;21(9):1749–57.

612. Archin NM, Espeseth A, Parker D, Cheema M, Hazuda D, Margolis DM. Expression of latent HIV induced by the potent HDAC inhibitor suberoylanilide hydroxamic acid. AIDS Res Hum Retroviruses. 2009 Feb;25(2):207–12.

613. Cummins NW, Sainski-Nguyen AM, Natesampillai S, Aboulnasr F, Kaufmann S, Badley AD. Maintenance of the HIV Reservoir Is Antagonized by Selective BCL2 Inhibition. Silvestri G, editor. J Virol. 2017 Jun 1;91(11):8869.

614. Valle-Casuso JC, Angin M, Volant S, Passaes C, Monceaux V, Mikhailova A, et al. Cellular Metabolism Is a Major Determinant of HIV-1 Reservoir Seeding in CD4+ T Cells and Offers an Opportunity to Tackle Infection. Cell Metab. 2018 Dec 19.

615. Campbell GR, Bruckman RS, Chu Y-L, Trout RN, Spector SA. SMAC Mimetics Induce Autophagy-Dependent Apoptosis of HIV-1-Infected Resting Memory CD4+ T Cells. Cell Host Microbe. 2018 Nov 14;24(5):689–702.e7.

616. Clerzius G, Gelinas JF, Daher A, Bonnet M, Meurs EF, Gatignol A. ADAR1 Interacts with PKR during Human Immunodeficiency Virus Infection of Lymphocytes and Contributes to Viral Replication. J Virol [Internet]. 2009

Sep 8;83(19):10119–28. Available from: http://www.ncbi.nlm.nih.gov/pmc/articles/PMC2747994/pdf/2457-08.pdf

617. Deleage C, Wietgrefe SW, Del Prete G, Morcock DR, Hao XP, Piatak M, et al. Defining HIV and SIV Reservoirs in Lymphoid Tissues. Pathog Immun. NIH Public Access; 2016;1(1):68–106.

618. Santangelo PJ, Rogers KA, Zurla C, Blanchard EL, Gumber S, Strait K, et al. Whole-body immunoPET reveals active SIV dynamics in viremic and antiretroviral therapy-treated macaques. Nat Methods. Nature Publishing Group; 2015 May;12(5):427–32.

619. Edén A, Fuchs D, Hagberg L, Nilsson S, Spudich S, Svennerholm B, et al. HIV-1 viral escape in cerebrospinal fluid of subjects on suppressive antiretroviral treatment. J Infect Dis. 2010 Dec 15;202(12):1819–25.

620. Damouche A, Lazure T, Avettand-Fènoël V, Huot N, Dejucq-Rainsford N, Satie A-P, et al. Adipose Tissue Is a Neglected Viral Reservoir and an Inflammatory Site during Chronic HIV and SIV Infection. Silvestri G, editor. PLoS Pathog. 2015 Sep;11(9):e1005153.

621. Nolan DJ, Rose R, Rodriguez PH, Salemi M, Singer EJ, Lamers SL, et al. The Spleen Is an HIV-1 Sanctuary During Combined Antiretroviral Therapy. AIDS Res Hum Retroviruses. 2018 Jan;34(1):123–5.

622. The National NeuroAIDS Tissue Consortium (NNTC) [Internet]. [cited 2018 Jun 17]. Available from: https://nntc.org

623. Morgello S, Gelman BB, Kozlowski PB, Vinters HV, Masliah E, Cornford M, et al. The National NeuroAIDS Tissue Consortium: a new paradigm in brain banking with an emphasis on infectious disease. Neuropathol Appl Neurobiol. 2001 Aug;27(4):326–35.

624. Gianella S, Taylor J, Brown TR, Kaytes A, Achim CL, Moore DJ, et al. Can research at the end of life be a useful tool to advance HIV cure? AIDS. 2017 Jan 2;31(1):1–4.

625. AIDS and Cancer Specimen Resource (ACSR) [Internet]. [cited 2018 Jun 17]. Available from: https://acsr.ucsf.edu/

626. Sandstrom TS, Burke Schinkel SC, Angel JB. Medical Assistance in Death as a Unique Opportunity to Advance HIV Cure Research. Clin Infect Dis. 2019 Jan 31.

627. Hashimoto D, Chow A, Noizat C, Teo P, Beasley MB, Leboeuf M, et al. Tissue-resident macrophages self-maintain locally throughout adult life with minimal contribution from circulating monocytes. Immunity. 2013 Apr 18;38(4):792–804.

628. Yona S, Kim K-W, Wolf Y, Mildner A, Varol D, Breker M, et al. Fate mapping reveals origins and dynamics of monocytes and tissue macrophages under homeostasis. Immunity. 2013 Jan 24;38(1):79–91.

629. Bain CC, Mowat AM. CD200 receptor and macrophage function in the intestine. Immunobiology. 2012 Jun;217(6):643–51.

630. Zigmond E, Varol C, Farache J, Elmaliah E, Satpathy AT, Friedlander G, et al. Ly6C hi monocytes in the inflamed colon give rise to proinflammatory effector cells and migratory antigen-presenting cells. Immunity. 2012 Dec 14;37(6):1076–90.

631. Zigmond E, Jung S. Intestinal macrophages: well educated exceptions from the rule. Trends Immunol. 2013 Apr;34(4):162–8.

632. Bain CC, Bravo-Blas A, Scott CL, Perdiguero EG, Geissmann F, Henri S, et al. Constant replenishment from circulating monocytes maintains the macrophage pool in the intestine of adult mice. Nat Immunol. Nature Publishing Group; 2014 Oct;15(10):929–37.

633. Epelman S, Lavine KJ, Beaudin AE, Sojka DK, Carrero JA, Calderon B, et al. Embryonic and adult-derived resident cardiac macrophages are maintained through distinct mechanisms at steady state and during inflammation. Immunity. 2014 Jan 16;40(1):91–104.

634. Molawi K, Wolf Y, Kandalla PK, Favret J, Hagemeyer N, Frenzel K, et al. Progressive replacement of embryo-derived cardiac macrophages with age. Journal of Experimental Medicine. 2014 Oct 20;211(11):2151–8.

635. Tamoutounour S, Guilliams M, Montanana Sanchis F, Liu H, Terhorst D, Malosse C, et al. Origins and functional specialization of macrophages and of conventional and monocyte-derived dendritic cells in mouse skin. Immunity. 2013 Nov 14;39(5):925–38.

636. Ginhoux F, Guilliams M. Tissue-Resident Macrophage Ontogeny and Homeostasis. Immunity. 2016 Mar 15;44(3):439–49.

637. Ganor Y, Real F, Sennepin A, Dutertre C-A, Prevedel L, Xu L, et al. HIV-1 reservoirs in urethral macrophages of patients under suppressive antiretroviral therapy. Nat Microbiol. 2019 Feb 4;48:872.

638. Matusali G, Dereuddre-Bosquet N, Le Tortorec A, Moreau M, Satie A-P, Mahé D, et al. Detection of Simian Immunodeficiency Virus in Semen, Urethra, and Male Reproductive Organs during Efficient Highly Active Antiretroviral Therapy. Silvestri G, editor. J Virol. 2015 Jun;89(11):5772–87.

639. Quayle AJ, Xu C, Mayer KH, Anderson DJ. T lymphocytes and macrophages, but not motile spermatozoa, are a significant source of human immunodeficiency virus in semen. J Infect Dis. 1997 Oct;176(4):960–8.

640. Deleage C, Moreau M, Rioux-Leclercq N, Ruffault A, Jégou B, Dejucq-Rainsford N. Human immunodeficiency virus infects human seminal vesicles in vitro and in vivo. Am J Pathol. 2011 Nov;179(5):2397–408.

641. Houzet L, Pérez-Losada M, Matusali G, Deleage C, Dereuddre-Bosquet N, Satie A-P, et al. Seminal Simian Immunodeficiency Virus in Chronically Infected Cynomolgus Macaques Is Dominated by Virus Originating from Multiple Genital Organs. Silvestri G, editor. J Virol. 2018 Jul 15;92(14):S622.

642. Vasquez JJ, Hussien R, Aguilar-Rodriguez B, Junger H, Dobi D, Henrich TJ, et al. Elucidating the Burden of HIV in Tissues Using Multiplexed Immunofluorescence and In Situ Hybridization: Methods for the Single-Cell Phenotypic Characterization of Cells Harboring HIV In Situ. J Histochem Cytochem. 2018 Feb 1;152(1):22155418756848.

643. Gobet R, Cerny A, Rüedi E, Hengartner H, Zinkernagel RM. The role of antibodies in natural and acquired resistance of mice to vesicular stomatitis virus. Exp Cell Biol. 1988;56(4):175–80.

644. Power AT, Wang J, Falls TJ, Paterson JM, Parato KA, Lichty BD, et al. Carrier cell-based delivery of an oncolytic virus circumvents antiviral immunity. Mol Ther. 2007 Jan;15(1):123–30.

645. Qiao J, Wang H, Kottke T, Diaz RM, Willmon C, Hudacek A, et al. Loading of oncolytic vesicular stomatitis virus onto antigen-specific T cells enhances the efficacy of adoptive T-cell therapy of tumors. Gene Therapy. Nature Publishing Group; 2008 Apr;15(8):604–16.

646. Roy DG, Power AT, Bourgeois-Daigneault MC, Falls T, Ferreira L, Stern A, et al. Programmable insect cell carriers for systemic delivery of integrated cancer biotherapy. J Control Release. 2015 Dec 28;220(Pt A):210–21.

647. Berlin C, Berg EL, Briskin MJ, Andrew DP, Kilshaw PJ, Holzmann B, et al. Alpha 4 beta 7 integrin mediates lymphocyte binding to the mucosal vascular addressin MAdCAM-1. Cell. 1993 Jul 16;74(1):185–95.

648. Erle DJ, Briskin MJ, Butcher EC, Garcia-Pardo A, Lazarovits AI, Tidswell M. Expression and function of the MAdCAM-1 receptor, integrin alpha 4 beta 7, on human leukocytes. J Immunol. 1994 Jul 15;153(2):517–28.

649. Fischer-Smith T, Croul S, Sverstiuk AE, Capini C, L'Heureux D, Régulier EG, et al. CNS invasion by CD14+/CD16+ peripheral blood-derived monocytes in HIV dementia: perivascular accumulation and reservoir of HIV infection. J Neurovirol. Springer-Verlag; 2001 Dec;7(6):528–41.

650. Williams KC, Corey S, Westmoreland SV, Pauley D, Knight H, deBakker C, et al. Perivascular macrophages are the primary cell type productively infected by simian immunodeficiency virus in the brains of macaques: implications for the neuropathogenesis of AIDS. J Exp Med. The Rockefeller University Press; 2001 Apr 16;193(8):905–15.

651. González-Scarano F, Martín-García J. The neuropathogenesis of AIDS. Nat Rev Immunol. 2005 Jan;5(1):69–81.

652. Avalos CR, Abreu CM, Queen SE, Li M, Price S, Shirk EN, et al. Brain Macrophages in Simian Immunodeficiency Virus-Infected, Antiretroviral-Suppressed Macaques: a Functional Latent Reservoir. Casadevall A, editor. MBio. American Society for Microbiology; 2017 Aug 15;8(4):2087.

653. Dey M, Yu D, Kanojia D, Li G, Sukhanova M, Spencer DA, et al. Intranasal Oncolytic Virotherapy with CXCR4-Enhanced Stem Cells Extends Survival in Mouse Model of Glioma. Stem Cell Reports. 2016 Sep 13;7(3):471–82.

654. Wollmann G, Drokhlyansky E, Davis JN, Cepko C, van den Pol AN. Lassa-vesicular stomatitis chimeric virus safely destroys brain tumors. Perlman S, editor. J Virol. 2015 Jul;89(13):6711–24.

655. Conant K, Garzino-Demo A, Nath A, McArthur JC, Halliday W, Power C, et al. Induction of monocyte chemoattractant protein-1 in HIV-1 Tat-stimulated astrocytes and elevation in AIDS dementia. Proc Natl Acad Sci U S A. National Academy of Sciences; 1998 Mar 17;95(6):3117–21.

656. Weiss JM, Nath A, Major EO, Berman JW. HIV-1 Tat induces monocyte chemoattractant protein-1-mediated monocyte transmigration across a model of the human blood-brain barrier and up-regulates CCR5 expression on human monocytes. J Immunol. 1999 Sep 1;163(5):2953–9.

657. Buckner CM, Calderon TM, Willams DW, Belbin TJ, Berman JW. Characterization of monocyte maturation/differentiation that facilitates their transmigration across the blood-brain barrier and infection by HIV: implications for NeuroAIDS. Cell Immunol. 2011;267(2):109–23.

658. Williams DW, Calderon TM, Lopez L, Carvallo-Torres L, Gaskill PJ, Eugenin EA, et al. Mechanisms of HIV entry into the CNS: increased sensitivity of HIV infected CD14+CD16+ monocytes to CCL2 and key roles of CCR2, JAM-A, and ALCAM in diapedesis. Buch SJ, editor. PLoS One. Public Library of Science; 2013;8(7):e69270.

659. Eugenin EA, Osiecki K, Lopez L, Goldstein H, Calderon TM, Berman JW. CCL2/monocyte chemoattractant protein-1 mediates enhanced transmigration of human immunodeficiency virus (HIV)-infected leukocytes across the blood-brain barrier: a potential mechanism of HIV-CNS invasion and NeuroAIDS. J Neurosci. 2006 Jan 25;26(4):1098–106.

660. Roberts TK, Eugenin EA, Lopez L, Romero IA, Weksler BB, Couraud P-O, et al. CCL2 disrupts the adherens junction: implications for neuroinflammation. Lab Invest. Nature Publishing Group; 2012 Aug;92(8):1213–33.

661. Mangus LM, Dorsey JL, Laast VA, Hauer P, Queen SE, Adams RJ, et al. Neuroinflammation and virus replication in the spinal cord of simian immunodeficiency virus-infected macaques. J Neuropathol Exp Neurol. 2015 Jan;74(1):38–47.

662. Hsu DC, Sunyakumthorn P, Wegner M, Schuetz A, Silsorn D, Estes JD, et al. Central Nervous System Inflammation and Infection during Early, Nonaccelerated Simian-Human Immunodeficiency Virus Infection in Rhesus Macaques. Simon V, editor. J Virol. American Society for Microbiology Journals; 2018 Jun 1;92(11):e00222–18.

663. Koppers-Lalic D, Hoeben RC. Non-human viruses developed as therapeutic agent for use in humans. Rev Med Virol. John Wiley & Sons, Ltd; 2011 Jul;21(4):227–39.

664. Velazquez-Salinas L, Naik S, Pauszek SJ, Peng K-W, Russell SJ, Rodriguez LL. Oncolytic Recombinant Vesicular Stomatitis Virus (VSV) Is Nonpathogenic and Nontransmissible in Pigs, a Natural Host of VSV. Hum Gene Ther Clin Dev. Mary Ann Liebert, Inc. 140 Huguenot Street, 3rd Floor New Rochelle, NY 10801 USA; 2017 Jun;28(2):108–15.

665. Egan MA, Chong SY, Rose NF, Megati S, Lopez KJ, Schadeck EB, et al. Immunogenicity of attenuated vesicular stomatitis virus vectors expressing HIV type 1 Env and SIV Gag proteins: comparison of intranasal and intramuscular vaccination routes. AIDS Res Hum Retroviruses. 2004 Sep;20(9):989–1004.

666. Johnson JE, Nasar F, Coleman JW, Price RE, Javadian A, Draper K, et al. Neurovirulence properties of recombinant vesicular stomatitis virus vectors in non-human primates. Virology. 2007 Mar 30;360(1):36–49.

667. Policicchio BB, Pandrea I, Apetrei C. Animal Models for HIV Cure Research. Front Immunol. Frontiers; 2016;7(8):12.

668. Lan P, Tonomura N, Shimizu A, Wang S, Yang Y-G. Reconstitution of a functional human immune system in immunodeficient mice through combined human fetal thymus/liver and CD34+ cell transplantation. Blood. American Society of Hematology; 2006 Jul 15;108(2):487–92.

669. Denton PW, Olesen R, Choudhary SK, Archin NM, Wahl A, Swanson MD, et al. Generation of HIV latency in humanized BLT mice. J Virol. American Society for Microbiology Journals; 2012 Jan;86(1):630–4.

670. Masse-Ranson G, Mouquet H, Di Santo JP. Humanized mouse models to study pathophysiology and treatment of HIV infection. Current Opinion in HIV and AIDS. 2018 Mar;13(2):143–51.

671. Halper-Stromberg A, Lu C-L, Klein F, Horwitz JA, Bournazos S, Nogueira L, et al. Broadly neutralizing antibodies and viral inducers decrease rebound from HIV-1 latent reservoirs in humanized mice. Cell. 2014 Aug 28;158(5):989–99.

672. Kessing CF, Nixon CC, Li C, Tsai P, Takata H, Mousseau G, et al. In Vivo Suppression of HIV Rebound by Didehydro-Cortistatin A, a "Block-and-Lock" Strategy for HIV-1 Treatment. Cell Reports. 2017 Oct 17;21(3):600–11.

673. Honeycutt JB, Wahl A, Archin N, Choudhary S, Margolis D, Garcia JV. HIV-1 infection, response to treatment and establishment of viral latency in a novel humanized T cell-only mouse (TOM) model. Retrovirology. BioMed Central; 2013 Oct 24;10(1):121.

674. Ling B, Veazey RS, Luckay A, Penedo C, Xu K, Lifson JD, et al. SIVmac pathogenesis in rhesus macaques of Chinese and Indian origin compared with primary HIV infections in humans. AIDS. 2002 Jul;16(11):1489–96.

675. Brainard DM, Seung E, Frahm N, Cariappa A, Bailey CC, Hart WK, et al. Induction of robust cellular and humoral virus-specific adaptive immune responses in human immunodeficiency virus-infected humanized BLT mice. J Virol. 2009 Jul;83(14):7305–21.

676. Veazey RS, Lackner AA. Nonhuman Primate Models and Understanding the Pathogenesis of HIV Infection and AIDS. ILAR J. 2017 Dec 1;58(2):160–71.

677. Hansen SG, Piatak M, Ventura AB, Hughes CM, Gilbride RM, Ford JC, et al. Immune clearance of highly pathogenic SIV infection. Nature. 2013 Oct 3;502(7469):100–4.

678. Barouch DH, Alter G, Broge T, Linde C, Ackerman ME, Brown EP, et al. Protective efficacy of adenovirus/protein vaccines against SIV challenges in rhesus monkeys. Science. 2015 Jul 17;349(6245):320–4.

679. Jenks N, Myers R, Greiner SM, Thompson J, Mader EK, Greenslade A, et al. Safety studies on intrahepatic or intratumoral injection of oncolytic vesicular stomatitis virus expressing interferon-beta in rodents and nonhuman primates. Human Gene Therapy. 2010 Apr;21(4):451–62.

680. Jonker DJ, Hotte SJ, Abdul Razak AR, Renouf DJ, Lichty B, Bell JC, et al. Phase I study of oncolytic virus (OV) MG1 maraba/MAGE-A3 (MG1MA3), with and without transgenic MAGE-A3 adenovirus vaccine (AdMA3) in incurable advanced/metastatic MAGE-A3-expressing solid tumours: CCTG IND.214. JCO. 2017 May 20;35(15_suppl):e14637–7.

Contributions of Collaborators

Several experiments included in this thesis would not have been possible without the generous efforts of others. These collaborations are as follows:

1. The optimization and validation of the $CD4^+$ T cell model of HIV latency used in Chapter 3 of this thesis was performed by Dr. Nischal Ranganath. Results pertaining to the optimization of this model were outlined in Figure 5, discussed in Chapter 3.3.1, and published in (354,402).

2. The oncolytic viruses used in Chapter 5-7 were provided through collaboration with Dr. John Bell and Dr. David Stojdl at the Ottawa Hospital Research Institute.

3. The alveolar macrophages and patient clinical data used in Chapter 6 of this thesis were obtained in collaboration with Dr. Cecilia Costiniuk (McGill University Health Centre) and Dr. Mohammad-Ali Jenabian (Université du Québec à Montréal). Sample processing and cell collection was performed by Syim Salahuddin (MSc conferred), Elaine Thomson (MSc student), and Dr. Oussama Meziane (Post-Doctoral Fellow).

Curriculum Vitae

Education

2016 – Present	**Doctor of Philosophy (PhD)**, University of Ottawa
2014 – 2016	**Master of Science (MSc)**, University of Ottawa
2010 – 2014	**Bachelor of Science (BSc Hon.)**, University of Manitoba

Research Experience

2014 – Present	**Regulation of type I interferon pathways during persistent HIV infection** Dr. Jonathan Angel, Ottawa Hospital Research Institute, Ottawa, Ontario
2013 – 2014	**Induction and monitoring of apoptosis in CHO cells within a bioprocess** Dr. Michael Butler, University of Manitoba, Winnipeg, Manitoba
2013	**Tigecycline Evaluation and Surveillance Trial** Dr. Marc Desjardins, The Ottawa Hospital, Ottawa, Ontario

Research Awards and Honours

2019	**New Investigator Award (Basic Sciences)** Awarded by The Canadian Association for HIV Research at the 28th Annual Canadian Conference on HIV/AIDS Research (May 8-12th, 2019)
2019	**Mark Wainberg Fund Grant** Awarded by The Canadian Association for HIV Research to cover travel and accommodations for the 28th Annual Canadian Conference on HIV/AIDS Research (May 8-12th, 2019)
2018	**CAHR Academic Scholarship** Awarded by The Canadian Association for HIV Research to cover travel, accommodations, and registration for the 27th Annual Canadian Conference on HIV/AIDS Research (April 26-29th, 2018)
2018	**1st place Oral Presentation (PhD category)** BMI Seminar Day. Ottawa, ON; Feb 22, 2018.
2017	**Oral Presentation Winner (Cancer and Transplantation Track)** Department of Medicine Research Day. Ottawa, ON; June 7, 2017.

2017	**Keystone Symposia Scholarship** Funded by: The National Institute of Allergy and Infectious Diseases (valued: $1,200); intended to defray travel and lodging expenses for the Keystone Symposium: Modeling Viral Infection and Immunity (May 1-4th, 2017)
2017	**Academic Scholarship in Vaccine Research** Awarded by The Canadian Association for HIV Research and The Canadian HIV Vaccine Initiative to cover travel, accommodations, and registration for the 26th Annual Canadian Conference on HIV/AIDS Research (April 6-9th, 2017)
2016	**Poster award (PhD category)** Canadian HIV Cure Enterprise (CanCURE) 3rd Annual Meeting. Montreal, QC; Nov 9-11, 2016.
2016 – 2019	**Frederick Banting and Charles Best Canada Graduate Scholarship (PhD)** Funding body: Canadian Institutes of Health Research (CIHR)
2016	**3rd place Oral Presentation (PhD category)** BMI Seminar Day. Ottawa, ON; March 8, 2016.
2015	**Microbiology and Immunology Program Award of Excellence** Awarded by the University of Ottawa Faculty of Medicine on the basis of extracurricular involvement and high academic standing.
2015 – 2016	**Frederick Banting and Charles Best Canada Graduate Scholarship (MSc)** Funding body: Canadian Institutes of Health Research (CIHR)
2014	**Ontario HIV Treatment Network Back to Basics Conference Travel Scholarship** Awarded by The Ontario HIV Treatment Network (Nov 25-26, 2014)
2014 – 2015	**Queen Elizabeth II Graduate Scholarship in Science and Technology** Funding body: The Ottawa Hospital Research Institute/The Ontario Government
2014 – 2018	**Excellence Scholarship** Award equivalent to tuition costs. Awarded by the University of Ottawa Faculty of Graduate and Postdoctoral Studies on the basis of academic standing.
2013	**University of Manitoba Student's Union Scholarship** Awarded by: The University of Manitoba Student's Union Awarded on the basis of high academic standing.

Publications

- **Sandstrom TS,** Ranganath N, Côté SC, Angel JB. Type I IFN impairment in HIV-infected macrophages facilitate their infection and killing by the IFN-sensitive oncolytic virus, MG1. *Manuscript in preparation.*
- **Sandstrom TS**, Burke Schinkel SC, Angel JB. Medical Assistance in Death as a Unique Opportunity to Advance HIV Cure Research. *Clinical Infectious Diseases*. 2018; epub. https://doi.org/10.1093/cid/ciz068
- **Sandstrom TS**, Angel JB. Introduction to the Special Issue: HIV Evasion of the Antiviral Response. *Cytokine & Growth Factor Reviews.* 2018;40:1-2. doi:10.1016/j.cytogfr.2018.03.011
- Ranganath N, **Sandstrom TS**, Burke Schinkel SC, Côté SC, Angel JB. The oncolytic virus, MG1, targets and eliminates latently HIV-1 infected cells: implications for an HIV cure. *Journal of Infectious Diseases*. 2017; 217(5): 721–730. doi: 10.1093/infdis/jix639
- **Sandstrom TS**, Ranganath N, Angel JB. Impairment of the type I interferon response by HIV-1: Potential targets for HIV eradication. *Cytokine & Growth Factor Reviews.* 2017;37:1-16. doi: 10.1016/j.cytogfr.2017.04.004
- Ranganath N, **Sandstrom TS**, Fadel S, Côté SC, Angel JB. Type I interferon responses are impaired in latently HIV infected cells. *Retrovirology*. 2016;13(1):66. doi:10.1186/s12977-016-0302-9.

Presentations (presenting author underlined)

- Sandstrom TS, Burke Schinkel SC, Ruiz MJ, Busman-Sahay K, Ponte R, Pagliuzza A, Cattin A, Wiche Salinas TR, Salahuddin S, Ancuta P, Power C, Routy J-P, Costiniuk C, Jenabian M-A, Estes JD, Cohen ÉA, Chomont N, Angel JB. "Post-Mortem Assessment of the HIV-1 Reservoir Following Medical Assistance in Death." Canadian Association of HIV Research 2019 Canadian Conference on HIV/AIDS. Saskatoon, SK, Canada; May 8-12, 2019.
- **Sandstrom TS**, Salahuddin S, Ranganath N, Côté SC, Costiniuk C, Jenabian M-A, Angel JB. "HIV-infected macrophages are selectively infected and killed by the oncolytic Rhabdovirus, MG1; a potential tool for viral eradication." Ottawa Hospital Research Institute 2018 Research Day. Ottawa, ON; Nov 8, 2018.
- **Sandstrom TS**, Salahuddin S**,** Ranganath N, Côté SC, Costiniuk C, Jenabian M-A, Angel JB. "HIV-infected macrophages are selectively infected and killed by the oncolytic Rhabdovirus, MG1; a potential tool for viral eradication." Canadian Association of HIV Research 2018 Canadian Conference on HIV/AIDS. Vancouver, BC, Canada; April 26-29, 2018.
- **Sandstrom TS**, Angel JB. "Type I interferon impairments facilitate oncolytic virus-mediated killing of HIV-infected macrophages." Department of

Biochemistry, Microbiology & Immunology Seminar Day. University of Ottawa. Ottawa, ON, Canada; February 22, 2018.

- **Sandstrom TS**, Ranganath N, Côté SC, Angel JB. "Altered IFN1 Signalling Facilitates Oncolytic Virus Infection of HIV-Infected Monocyte-Derived Macrophages." Department of Medicine Research Day. Ottawa, ON, Canada; June 7, 2017.
- **Sandstrom TS**, Ranganath N, Côté SC, Angel JB. "Altered IFN1 Signalling Facilitates OV Infection of HIV-Infected Monocyte-Derived Macrophages." Canadian Association of HIV Research 2017 Canadian Conference on HIV/AIDS. Montreal, QC, Canada; April 6-9, 2017.
- **Sandstrom TS**, Angel JB. "Regulation of type I interferon pathways during persistent HIV infection." Department of Biochemistry, Microbiology & Immunology Seminar Day. University of Ottawa. Ottawa, ON, Canada; March 8, 2016.

Abstracts and Posters (presenting author underlined)

- **Sandstrom TS**, Ranganath N, Côté SC, Angel JB. "Altered type I interferon signalling facilitates the eradication of HIV-Infected monocyte-derived macrophages by the oncolytic rhabdovirus, MG1." Ottawa Hospital Research Institute 2017 Research Day. Ottawa, ON; Nov 9, 2017. (Poster #44)
- **Sandstrom TS**, Ranganath N, Côté SC, Angel JB. "Altered type I interferon signalling facilitates the eradication of HIV-Infected monocyte-derived macrophages by the oncolytic rhabdovirus, MG1." Canadian HIV Cure Enterprise (CanCURE) 4th Annual Meeting. Montreal, QC; Oct 19-20, 2017. (Poster #B-11)
- **Sandstrom TS**, Ranganath N, Côté SC, Angel JB. "Altered IFN1 Signalling Facilitates Oncolytic Virus Infection of HIV-Infected Monocyte-Derived Macrophages." Department of Biochemistry, Microbiology and Immunology Poster Day. University of Ottawa. Ottawa, ON, Canada; May 11, 2017. (Poster #21)
- **Sandstrom TS**, Ranganath N, Côté SC, Angel JB. "Altered IFN1 Signalling Facilitates Oncolytic Virus Infection of HIV-Infected Monocyte-Derived Macrophages." Keystone Symposium: Modeling Viral Infections and Immunity. Estes Park, CO, USA; May 1-4, 2017. (Poster #2021)
- **Sandstrom TS**, Ranganath N, Côté SC, Angel JB. "Altered IFN-1 signalling facilitates OV infection of HIV-infected monocyte-derived macrophages." Canadian HIV Cure Enterprise (CanCURE) 3rd Annual Meeting. Montreal, QC; Nov 9-11, 2016. (Poster #B-19)
- **Sandstrom TS**, Ranganath N, Côté SC, Angel JB. "Characterizing the impaired type I interferon response in HIV-infected myeloid cells." Canadian Association of HIV Research 2016 Canadian Conference on HIV/AIDS. Winnipeg, MB, Canada; May 12-15, 2016. (Poster # BS3.7)

- **Sandstrom TS**, Ranganath N, Côté SC, Angel JB. "The type I interferon response is impaired during persistent HIV infection of myeloid cells." 29th Annual Canadian Society for Immunology Conference. Ottawa, ON, Canada; April 1-4, 2016. (Poster #108)
- **Sandstrom TS**, Ranganath N, Côté SC, Angel JB. "Latent HIV infection is associated with defects in the type I IFN response." Keystone Symposium: HIV Persistence. Olympic Valley, CA, USA; March 20-24, 2016. (Poster #4008)
- **Sandstrom TS**, Ranganath N, Côté SC, Angel JB. "Healthy human $CD4^+$ T cells are responsive to type I IFN stimulation, and are resistant to infection by MG1 and VSV-Δ51." Ottawa Hospital Research Institute 2015 Research Meeting. Ottawa, ON; Nov 18, 2015. (Poster #48)
- **Sandstrom TS**, Ranganath N, Côté SC, Angel JB. "Latent HIV infection is associated with defects in the type I IFN response." Canadian HIV Cure Enterprise (CanCURE) 2nd Annual Meeting. Montreal, QC; Nov 11-13, 2015. (Poster #B-4)
- **Sandstrom TS**, Côté SC, Ranganath N, Angel JB. "Human $CD4^+$ T cells, monocytes, and monocyte derived macrophages are resistant to infection by MG1 and VSV-Δ51." Canadian Association of HIV Research 2015 Canadian Conference on HIV/AIDS. Toronto, ON, Canada; April 30-May 3, 2015. (Poster #BS49)
- Saboktakin Rizi B, Braasch K, Salimi E, Mohammad K, Afshar Delkhah S, **Sandstrom T**, Butler M, Bridges GE, Thomson DJ. "Monitoring dielectric changes in Chinese hamster ovary cells during induction of apoptosis by oligomycin using a dielectrophoretic (DEP) cytometer." Miniaturized Systems for Chemistry and Life Sciences XVIII, San Antonio, TX, USA; October 26, 2014.
- Braasch K, Nikolic-Jaric M, Salimi E, **Sandstrom T**, Mohammad K, Bhide A, Rizi B, Thomson DJ, Bridges GE, Butler M. "Exploiting the dielectric properties of CHO cells to monitor apoptotic events in a bioprocess." Cell Culture Engineering XIV, Quebec-City, QC, Canada; May 4-9, 2014.

Teaching

2018	**Guest Lecturer for BIOC4009 (*Biochemistry of Disease*) at Carleton University,** Oct 9th, 2018 Prepare and provide 80min lecture on blood disorders (focusing on HIV); invited by Dr. Jennifer Bruin